Title
An Investigation of the Factors Controlling the Terrestrial Sulfur Cycle

Author
Yi-Balan, Simona Andreea

Publication Date
2013

Peer reviewed|Thesis/dissertation

An Investigation of the Factors Controlling the Terrestrial Sulfur Cycle

by

Simona Andreea Yi-Balan

A dissertation submitted in partial satisfaction of the
requirements for the degree of
Doctor of Philosophy

in

Environmental Science, Policy, and Management

in the

Graduate Division

of the

University of California, Berkeley

Committee in charge:

Professor Ronald Amundson, Chair
Professor Allen Goldstein
Professor John Coates

Fall 2013

An Investigation of the Factors Controlling the Terrestrial Sulfur Cycle

by Simona Andreea Yi-Balan

Abstract

An Investigation of the Factors Controlling the Terrestrial Sulfur Cycle

by

Simona Andreea Yi-Balan

Doctor of Philosophy in Environmental Science, Policy, and Management

University of California, Berkeley

Professor Ronald Amundson, Chair

Sulfur (S), like nitrogen (N), is an essential macronutrient for life on Earth. Its deficit in soils decreases primary productivity, but its excess can impair ecosystem health. Unlike N cycling however, for which both the natural and the human-impacted cycles have been well studied, most research on S has focused on S pollution. My thesis addressed S cycling in pristine terrestrial systems, to understand the potential effects of global change on these essential functions. I used chemical analyses and stable isotopes to investigate the impact of climate, vegetation, topography, parent material and landscape age on the natural terrestrial S cycle in comparison to that of N.

I examined the S content and isotopic composition (as $\delta^{34}S$ values) in soils and vegetation at 11 sites spanning broad gradients of climate globally. Soil S content generally increased with mean annual precipitation (MAP), but was uncorrelated with mean annual temperature (MAT). Soil and plant $\delta^{34}S$ values increased with increasing MAP and MAT. MAP and MAT together accounted for about half of the observed variability in folial $\delta^{34}S$ values, and for over a quarter of the observed variability in soil $\delta^{34}S$. These S patterns resembled those of soil N, known from previous studies. The difference between the $\delta^{34}S$ values of soils and atmospheric inputs increased significantly, but weakly, with MAP, suggesting greater biological S isotope fractionation in wetter climates.

To directly explore the impact of vegetation, topography and parent material on soil S biogeochemistry, I collected soil, plant, pore water and precipitation samples from the wet tropical Luquillo Experimental Forest, Puerto Rico. Topography impacted S cycling by influencing soil redox conditions, while vegetation and parent material had a minimal impact. Pore water data suggested the co-occurrence of at least three major S-fractionating processes: plant uptake, mineralization and dissimilatory bacterial sulfate reduction (DBSR). This complex biogeochemical cycling appeared to be driven by the high rainfall. I modeled soil isotopic fractionation assuming advective transport of organic matter through the soil profile. This model worked well for N, but failed to describe S transformations, revealing a decoupling of the N and S biogeochemical cycles in these soils due to biotic processes.

I found a similar decoupling of S from N cycling on a chronosequence of marine terraces in Santa Cruz, California, where I investigated the impact of landscape age. I propose that two factors account for this apparent greater redox sensitivity of S compared to N isotopes. First, S is in less biological demand, and thus more readily fractionated by redox reactions, unlike N, which might be fully consumed for plant and microbial cellular metabolism during biological processes. Second, S may experience several reduction-reoxidation cycles due to its retention in soils via adsorption on iron and aluminum oxides, unlike N, which is easily lost from soils once reduced to gaseous form. In the deeper soil layers, processes that deplete the heavy S isotope (such as DBSR) dominated in the youngest soils, while processes that enrich the soil in the heavy isotope (such as mineralization) dominated in the older soils. Furthermore, pore water data revealed a division in soil processes with depth in the older soils, with large fluctuations in sulfate concentration and isotope fractionation near the surface (likely due to DBSR), but little change below the well-developed argillic horizons. My data showed no significant effect of phosphorus limitation on S cycling in the older soils. Rather, age impacted soil S content and $\delta^{34}S$ values mostly due to changes in hydrology, including the development of a water restrictive argillic horizon, with increasing soil age.

In summary, my results showed that, of the factors examined, rainfall effects modified by landform characteristics are the most important controls on S biogeochemistry that dictate the types and rates of processes. S cycling should, therefore, most directly respond to the changes in rainfall predicted to occur due to global change. Specifically, a significant decrease in rainfall in many regions may reduce soil S content and the extent of its biological cycling.

Table of Contents

Acknowledgments

This labor of love and commitment would not have been possible without a wide network of people who have supported me, mentored me, and graciously gifted me their presence, attention, time and enthusiasm. I am grateful to all of you, including, though not limited to: my advisor, Ron Amundson, for inspiring me to be a good scientist and mentor, and for bearing the brunt of digging soil pits in the exhausting wet tropical heat; Professor Allen Goldstein, for believing in my potential, offering his steadfast support, and providing me with such a good example of excellent teaching; Professor John Coates, for his steadfast guidance, and for continuing to welcome me in his lab even though his ion chromatograph magically broke down almost every time I was there; Professor Whendee Silver, for sharing her knowledge of and passion for tropical rainforests; my collaborator Heather Buss, for all her timely and helpful advice, and for working side by side with me on everything from sampling soil cores, to publishing our joint manuscript; my collaborators from the USGS, Jorie Schulz and Corey Lawrence, for their help with my Santa Cruz chapter and their light-hearted company during field work; Kari Finstad, Mary Whelan and Steven Hall for keeping me in good company while getting soaking wet doing fieldwork in the rainforest; Justine Owen for being such a good role model, and for sharing with me the wonders of the Atacama Desert; Sarah Reed, for bravely traveling the winding path of dissertation-writing together with me; all my undergraduate students and mentees, particularly Ashley Kirk, for their enthusiasm and hard work; all the wonderful people who keep ESPM and UC Berkeley running, and who have supported me financially during my studies; my teammates on the ESPM Ultimate team, *Discus elegans*, for providing me with an avenue to run, play, laugh, and make fun of growing old as a grad student; all my yoga and meditation teachers and students, for helping me cultivate essential skills to remain grounded even during the most intense parts of my graduate studies; Hilary Snider, Natalie Sauvain, Hyojin Kim and Virginia Emery, for their true friendship; the Roots and Branches community, for putting up with me even during stressful periods; my family back in Romania, for their unconditional love and support wherever my journey takes me, despite their wishing I weren't so far away; my dear husband, Kelly Yi, for his loving understanding and lighthearted humor; and my beloved planet Earth, for having developed these amazingly intricate biogeochemical cycles that support our lives.

Chapter 1

Introduction

All life on Earth relies on geochemical cycling of elements, and living organisms mediate geochemical cycles, in a dynamic equilibrium between the biotic and the abiotic components of the Earth. As an essential macronutrient, sulfur (S) is biologically cycled in many ecosystems, thus the concentration and isotopic composition of S species can fluctuate in response to environmental change (van Stempvoort and Krouse, 1994).

S is the 5th most abundant (by weight) element in the universe, the 13th most abundant in the Earth's crust (~0.1%), and the second most abundant anion in seawater (~0.028 mol/l) (Likens et al., 2002). All organisms require S for growth, primarily as a component of the amino acids cysteine and methionine, as part of several enzyme cofactors (including biotin, coenzyme A, coenzyme M, thiamine and lipoic acid), and as an essential participant in many redox processes (Kertesz, 1999). S also plays a critical role on other planets. It has been suggested that SO_2 on early Mars enacted a climate feedback similar to that of CO_2 on Earth (Halevy et al., 2007), and that chemolithoautotrophic organisms could potentially use the redox gradients from the deposition of oxidized S species on the Martian regolith (Farquhar et al., 2000).

Despite its importance to life, S in terrestrial ecosystems has thus far been a somewhat "forgotten" element. Many studies have looked at its behavior in highly industrialized regions affected by anthropogenic S inputs (e.g. Likens et al., 2002), but little is known about what drives soil S cycling in more pristine ecosystems. Furthermore, there are no databases to access and compile information about soil or ecosystem S, like those available for carbon (C) (Post et al., 1982) and nitrogen (N) (Post et al., 1985). For this thesis project, I collected new S data for soil, vegetation, and atmospheric inputs, and studied what controls S cycling in pristine ecosystems using stable isotopes, comparing and contrasting the behavior of S with that of N and C. In particular, I investigated the effects on S biogeochemistry of the soil-forming factors identified by Jenny (1941): climate, organisms, relief, parent material and time.

1.1 S in Terrestrial Ecosystems

1.1.1 Stable Isotopes

S has four stable isotopes: ^{32}S, ^{33}S, ^{34}S and ^{36}S, with abundances of 95.0%, 0.75%, 4.20% and 0.017% respectively (Alexander et al., 2003). Isotopic compositions are measured using the δ notation, $\delta(‰) = (R_{sample}/R_{standard} - 1) \times 1000$, where R is the ratio of the less abundant to the most abundant isotope. For S, the international standard is troilite (FeS) from the Canyon Diablo meteorite, with a $^{34}S/^{32}S$ ratio of 1/22.22 (Thode et al., 1961).

S isotopes have been used extensively for source appointment (Szynkiewicz et al., 2009; Yuan and Mayer, 2012), and as indicators of paleo-limnological and paleo-

hydrological conditions (Rosen and Warren, 1990; Torfstein et al., 2008; Szynkiewicz et al., 2009). This is possible because of the high thermodynamic stability of sulfate molecules and low rate of isotopic exchange with other S compounds in aqueous solutions (Chiba and Sakai, 1985; Szynkiewicz et al., 2009); as a result, the isotope composition of a soil sulfate molecule reflects the source of that molecule and its formation and loss pathways.

1.1.2 Sulfur Sources to Terrestrial Systems

Nutrients in terrestrial ecosystems – defined here as the coupled soil-plant systems – originate from atmospheric deposition and weathering inputs. Soils and plants that derive their S from sedimentary rocks ($\delta^{34}S$ from -50 to +50‰) will have a similar S isotope composition to the parent material (Norman et al., 2004). The input from weathering however is generally negligible compared to that of atmospheric deposition (Bern and Townsend, 2008). The main natural sources of S in atmospheric deposition are marine seasalt and nonseasalt sources, volcanic emissions, dust from aeolian weathering, and reduced biogenic gases. Anthropogenic sources (including combustion and refining of fossil fuels, gypsum processing, ore smelting, etc.) dominate in many regions of the planet, particularly inland, where oceanic input is negligible.

Marine inputs are important near the coast. Marine sulfate aerosol is a mixture of sea salt aerosols produced by bursting bubbles at the ocean surface, and secondary non-seasalt (NSS) aerosols, formed by gas to particle conversion of reduced S compounds (O'Dowd et al. 1997; Wadleigh 2004). These reduced S compounds are naturally produced in surface ocean waters either biogenically, such as dimethyl sulfide (CH_3SCH_3, abbreviated DMS), carbon disulfide (CS_2), methanethiol (CH_3SH) and dimethyl disulfide (CH_3SSCH_3), or photochemically, such as hydrogen sulfide (H_2S) and carbonyl sulfide (COS) (Bates et al., 1992). COS is the most abundant atmospheric S gas in the remote troposphere, where it is relatively inert and commonly taken up by soils and vegetation (Liu et al., 2007). SO_2 is another abundant form of atmospheric S. Some of this SO_2 is anthropogenic, and some is derived from H_2S or DMS. SO_2 is then oxidized in the troposphere in gas- and aqueous-phase or on aerosol and dust surfaces (Liang and Jacobson, 1999; Seinfeld and Pandis, 1998; Jenkins and Bao, 2006). These different species have very different residence times in the atmosphere and are therefore mixed to different degrees: DMS and H_2S are transported over short-range distances (300 and 500 km, lifetime <1 day and 1 day respectively), SO_2 and SO_4^{2-} over medium-range (1,100 and 3,500 km, lifetime of 3 and 4 days respectively), and CS_2 and COS over long-range distances (35,000 and 650,000 km, lifetime 70 and 500 days respectively) (Newman et al., 1991). Thus, fluxes of DMS and H_2S from seas and continents mix only within a few hundred km of the coastline, but CS_2 and COS can mix over a longer distance inland.

The major S sources generally have distinctive $\delta^{34}S$ (and $\delta^{18}O$) values; it is thus possible to use stable isotopes of sulfate for source appointment. For instance, marine sulfate has a consistent $\delta^{34}S$ value of 21‰ (Rees et al., 1978; Bao and Reheis, 2003; Brimblecombe, 2003), whereas sulfate derived from DMS oxidation over the ocean ranges from 15 to 19‰ (Calhoun et al., 1991; Wadleigh, 2004). The isotopic composition of DMS overlaps with that of sea spray, but it can be distinguished mathematically by

assuming one or more conservative species like Na or Cl have been derived exclusively from sea salt (Mizutani and Rafter, 1969). Marine aerosols have a significantly lower isotope value due to the presence of reduced biogenic gasses. Compared to the continental atmosphere, the marine atmosphere is enriched by 5 to 10‰ on average (Newman et al., 1991). Continental sources over North America have a $\delta^{34}S$ around 4‰ (Wadleigh et al. 1994; 2001), due to a combination of volcanic, biogenic and especially anthropogenic sources. Volcanoes emit annually an estimated $28x10^6$ tons of S with an average $\delta^{34}S$ value of +4.7‰ (Nielsen et al., 1991). $\delta^{34}S$ of biogenic H_2S (from bacterial sulfate reduction) ranges from -28 to -15‰ in shallow marine regions, and from -22 to +12‰ in estuaries and coastal tidal zones (Newman et al., 1991). H_2S is also produced from biomass decay, in which case there should be little to no fractionation and the resulting $\delta^{34}S$ value should be close to the value of seawater (Kaplan and Rittenberg, 1964; Mekhtiyeva and Pankina, 1968). The $\delta^{34}S$ values of anthropogenic emissions differ among regions based on the type of coal used, but they are usually more negative than natural sources. $\delta^{34}S$ values of flue gas from coal combustion range from -0.5 to 20‰, but are mostly between -1 and 3‰ (Newman et al., 1991).

Throughfall and litterfall generally do not alter the $\delta^{34}S$ of precipitation in hardwood-forested watersheds (Stam et al., 1992; Andersson et al., 1992; Shanley et al., 2005), though some authors have found a 1‰ decrease (Novak et al., 2001) or increase (Zhang et al., 1998) in the $\delta^{34}S$ values of throughfall. Thus, generally, the isotopic composition of precipitation is a good measure for the integrative inputs to the soil-plant system.

1.1.3 Sulfur Pools, Transformations and Losses in Terrestrial Systems

Sulfate is the main form of inorganic S present in many soils, and the preferred form for plant uptake (Wang et al., 2006). The dominant S form in most soils however is organic, comprising C-bonded S, ester sulfate, sulfamates and sulfolipids (Likens et al., 2002). About 40% of the soil organic sulfur (SOS) is present as dissolved organic S (DOS) which, similarly to sulfate, can be readily leached from soils (Kaiser and Guggenberger, 2005).

Inside the soil-plant system, four main types of biologically-mediated processes occur: assimilation (conversion of inorganic S, usually sulfate, into organic S by plants or microorganisms), mineralization (conversion of organic S to sulfate), reduction (of sulfate to sulfide) and oxidation (of reduced S compounds to sulfate) (Fig. 1). Additionally, abiotic processes such as adsorption–desorption and dissolution–precipitation occur. S is lost from the soil-plant system through gaseous losses of reduced S compounds (under anoxic conditions), erosion, and aqueous leaching.

The abiotic and most of the biotic processes in the soil generally have only a minor effect on the $\delta^{34}S$ of soil sulfate (e.g. Van Stempvoort et al., 1990; Shanley et al., 2005). Dissimilatory bacterial sulfate reduction (DBSR) causes the most significant fractionation of S isotopes, since bacteria prefer to utilize the lighter ^{32}S isotope and therefore lead to an enrichment in ^{34}S in the remaining soil sulfate pool (Alewell et al., 1999; Shanley et al., 2005). All sulfate-reducing bacteria that release acetate as the final

product of organic substrate oxidation fractionate less than 18‰, whereas those that can enact complete oxidation to CO_2 usually fractionate more than 18‰ (Bruchert et al. 2001). Despite smaller fractionation factors, the other biotic processes (mineralization, assimilation and oxidation) can also significantly impact S isotope values because they operate in the same direction (Shanley et al., 2005). The small abiotic fractionation factors such as the dissolved sulfate to gypsum fractionation can also lead to large observed isotope variations in soils when Rayleigh-like processes operate (Ewing et al., 2008). In soils at steady state however, such abiotic effects are small, and thus the $\delta^{34}S$ values of soil S or pore water sulfate reflect the extent of biological cycling of the soil S pool. Additionally, soil $\delta^{34}S$ values can reflect whether assimilatory or dissimilatory S metabolism predominate (Alewell and Novak, 2001). Mineralization-assimilation cycles cause SOS to become enriched in ^{34}S since bacteria prefer to convert the lighter isotope into sulfate, which then may be leached away; this enrichment increases with soil depth, as the organic matter ages and becomes subjected to successive mineralization cycles (Novak et al., 1996). In contrast, DBSR enriches the soil solution in ^{34}S and, because generally the ^{34}S-depleted reduced inorganic S species are reoxidized and/or immobilized as organic material, the overall soil $\delta^{34}S$ value decreases (Alewell and Novak, 2001). The relative importance of the S transformation processes depends on soil T, pH, moisture, minerals, Al and Fe oxyhydroxide and clay content, and, as a result, changes with soil depth (Norman et al., 2002).

1.2 Anthropogenic Impact

Anthropogenic activities have greatly disturbed the biogeochemical S cycle in most regions of the planet (Wadleigh et al., 2001). Approximately two decades ago, an estimated 70% of total atmospheric S was anthropogenic (Seinfeld and Pandis, 1998). The percentage was higher (~92%) between 35 and 50°N, where most of the industrialized nations are located (Bates et al., 1992). Wadleigh et al. (2001) identified a North America continent-wide, well-mixed atmospheric reservoir of S, largely dominated by anthropogenic emissions (with $\delta^{34}S$ of +3.41±0.95‰). Many studies of ecosystem S have focused on responses to changes in acid deposition in temperate regions (e.g. Mayer et al., 1995; Alewell et al., 2000; Likens et al., 2002; Shanley et al., 2005). Soil acidification due to SO_2 emissions can deplete base cations such as Mg, Ca and K from the topsoil via exchange with H^+, reduce soil microbial activity (Reuss et al., 1987; Singh et al., 2004), and change the flora and fauna of the affected area (Schulze, 1989). For instance, at a site in India affected by emissions from a coal fired powerplant, Singh et al. (2004) found that higher pollutant concentrations reduced decomposition and nutrient turnover rates – except for the turnover of sulfate, which increased with increasing pollutant concentration. In polluted regions, direct assimilation of S by plants can cause a negative $\delta^{34}S$ shift since plants prefer the lighter isotope, leading to slightly lower $\delta^{34}S$ in throughfall compared to bulk precipitation (Zhang et al., 1998; Novak et al. 1995; 2001).

Since the implementation of the US Title IV of the 1990 Amendments to the US Clean Air Act (CAAA), anthropogenic emissions of SO_2 have significantly declined (Likens et al., 2002). However, ecosystem recovery after acidification is delayed for years or even decades by SOS mineralization (Morth et al., 2005) and the reversible

adsorption of inorganic sulfate (Mitchell et al., 1992; Alewell et al., 1997; Alewell, 1998). Nevertheless, the recent reduction in anthropogenic S emissions has exposed S-deficient soils in many regions of the planet, which is problematic for agriculture given the high demands for S of some crops, such as wheat, cereals and rape-seed (Brimblecombe, 2003). Typically, soils are considered S deficient if surface concentrations decrease below 6 ppm (Acquaye and Beringer). Soils with greater sulfate adsorption capacity and smaller proportion of residual S have greater resistance to S deficiency (Boye et al., 2010). Many agricultural soils are now S deficient, and S fertilizers are added as sulfate, elemental sulfur, ammonium thiosulfate, or ammonium polysulfide. Ultimately, these fertilizers, as well as the commonly used S-containing pesticides, are likely to appear in runoff water (Brimblecombe, 2003).

Land use change has also impacted the terrestrial S cycle (e.g. Rock and Mayer, 2009; Solomon et al., 2009; Yuan and Mayer, 2012). Agricultural activities can significantly enhance S cycling, particularly in fresh water systems, and change the S isotopic composition (Yuan and Mayer, 2012). Solomon et al. (2009) used XANES to determine the effects of land use change on speciation of soil S in three different ecoregions: tropical, subtropical and temperate. They found that in all regions land-use and land-cover changes resulted in net losses of total soil S, with highest losses in tropical (67-76%) followed by subtropical (48%) and lastly temperate (36-40%) ecoregions. Total S losses correlated significantly with MAT, due to higher decomposition rates at higher soil T. Intensive agricultural practices on soils prone to S deficiency can result in or exacerbate S deficit for crops. Lack of sufficient S reduces the protein and vitamin content and overall quality of fruits and vegetables (Brown, 1982).

1.3 Natural Controls on Soil S Cycling

The anthropogenic impacts on the terrestrial S cycle are much better known than the natural controls. Based on N studies (e.g. Austin and Vitousek, 1998; Amundson et al., 2003), it is likely that the soil formation factors identified by Jenny (1941) (climate, organisms, topography, parent material and time) play a role in the soil S cycle, however no previous research has addressed these controls systematically. Particularly, the effect of time has not been studied for S. A potential impact of topography was observed in Costa Rica, where Bern and Townsend (2008) found that hillslope soils had higher $\delta^{34}S$ values compared to alluvial soils. One study from Northern Ireland found no effect of parent material on soil $\delta^{34}S$ values, except for slightly lower values in gleyed soils and higher values in organic-rich soils; rather, the quantity and source (anthropogenic versus marine) of the atmospheric S inputs explained most of the observed geographical patterns in soil $\delta^{34}S$ values (Stack and Rock, 2011).

Limited research has been devoted to the relationship of soil S to climate, though climate should have considerable impacts on the rates and types of processes that occur in soils. Climate conditions drive the processes that control the form (and isotopic composition) of S that is lost from soil. Mean annual precipitation (MAP) impacts input and loss rates, and the dominant biological processes in the soil. Mean annual temperature (MAT) impacts the rates of biotic processes such as bacterial sulfate reduction (Bruchert et al., 2001; Canfield et al., 2006; Turchyn et al., 2010). Although no

study has attempted before to investigate S cycling on a broad climate gradient to evidence the effects of climate, several separate studies in different climatic regimes exist. Below I synthesize some of the main findings of previous studies in wet tropical, temperate, and arid/hyperarid ecosystems.

Wet tropical forest soils are known to emit H_2S due to DBSR (Delmas and Servant, 1983; Delmas et al., 1978; Newman et al., 1991), however previous research found that this was not an important process in Costa Rica (Bern et al., 2007; Bern and Townsend, 2008). Hillslope soils in Costa Rica depend exclusively on atmospheric S inputs, show only a slight decrease in S concentration and little S isotope variation with depth, and a slight enrichment in ^{34}S compared to the precipitation, which may be due to emissions of highly depleted biogenic S gases by vegetation, or due to mineralization of organic S (Bern et al., 2007; Bern and Townsend, 2008). Additionally, little to no fractionation was observed during plant uptake (Bern and Townsend, 2008).

Previous studies in temperate climates have focused on polluted regions and analyzed the factors impacting ecosystem recovery from acidification (e.g. Alewell and Novak, 2001; Mayer et al., 2001). Most of these studies found an increase in the $\delta^{34}S$ value of total soil S with depth (and a decrease in S%) due to the preferential mineralization and release of ^{32}S causing SOS to be isotopically heavier with increasing age (Giesemann et al., 1995; Mayer et al., 1995; Novak et al., 1996; Alewell and Novak, 2001; Norman et al., 2002; Novak et al., 2003; Marty et al., 2011). Decreasing $\delta^{34}S$ values with depth was also observed in eastern Bavaria, Germany, in soils where DBSR occurred (Alewell and Novak, 2001). Furthermore, in anthropogenically-impacted watersheds in Quebec, Canada, Marty et al. (2011) found a strong correlation between $\delta^{34}S$ and $\delta^{15}N$, suggesting that S and N must be strongly associated in SOM and undergoing the same processes with similar isotope effects.

For gypsiferous Aridisols in central Iran, Khademi et al. (1997) found that the $\delta^{34}S$ values of soil gypsum and dissolved sulfate (11.4 to 14.4‰) match that of marine sediments, confirming the absence of reduction or re-oxidation reactions; only dissolution and precipitation could explain the small fractionation observed. In Antarctica, within the individual soil profiles, $\delta^{34}S$ values generally decrease with depth by up to 3‰ (Bao and Marchant (2006)). Similarly, in the Atacama Desert, the $\delta^{34}S$ value of soil sulfate decreases with depth because the heavier isotopes concentrate in solid mineral phases, leaving the downward-percolating solution depleted (Ewing et al., 2008; Amundson et al., 2012). Ewing et al. (2008) explained these trends by abiotic fractionation alone using a Rayleigh-like fractionation model, with a fractionation factor $\alpha_{sulfate\text{-}gypsum}$ of 1.00165 as in Thode and Monster (1965). Moreover, Ewing et al. (2007; 2008) showed that, as rainfall declines to the point that vascular plants disappear, the soil N and S cycles lose fundamental processes, and become functionally abiotic.

These differences in S cycling processes among these individual studies suggest that climate may indeed drive S biogeochemistry. Teasing apart the effects of site differences from those of climate (MAP and MAT) requires researching these processes along a series of well-constrained climate gradients in minimally-disturbed soils at or near steady-state with respect to biogeochemical cycling.

1.4 Thesis outline

This thesis addresses the impact of soil-forming factors on the terrestrial S cycle in undisturbed soils. Each of the three main chapters (Chapter 2, 3 and 4) explores a different aspect of the S cycle, starting at a global scale in Chapter 2, then zooming in to the local scales in Chapters 3 and 4.

Chapter 2 is a large-scale overview of the impact of climate on the geographical variation of soil and plant sulfur concentration and stable isotopes, using a two-box mixing model approach. This research built upon a similar study done for N (Amundson et al., 2003), using some of the same soil and plant samples from archive, plus a series of newly collected samples from Puerto Rico, Santa Cruz (California), and the Chilean Andes. All soils studied were at or near steady state. Additionally, I compiled and mapped the growing set of isotopic measurements of S deposition in a variety of locations (e.g. Newman et al., 1991; Novak et al., 2001; Bao and Reheis, 2003; Norman et al., 2004; Novak et al., 2007), including my new measurements from several US locations, to constrain how the value of inputs varies across regions. I found a general depletion in soil ^{34}S compared to inputs, suggesting the influence of biological processes. The results also showed a significant impact of climate, particularly MAP, on soil and plant S content and isotopes, with over a quarter and about half of the observed variability in soil and plant $\delta^{34}S$ values respectively explained by multivariate regression on the climate variables MAP and MAT. Using these modeled linear regression parameters, I mapped the global distribution of soil and plant $\delta^{34}S$ values for steady state systems.

In Chapter 3, I explored S cycling at the wet end-member of the studied rainfall spectrum, in the Luquillo Experimental Forest in Puerto Rico. By analyzing soils on three topographic positions at two different sites with different parent material and forest type, I characterized the impact of topography, parent material and vegetation on S cycling in this environment. Only topography appeared to have an impact, by decreasing C, N and S content downslope and lowering soil $\delta^{34}S$ values due to DBSR closest to the stream. Using an advection model to describe the isotopic fractionation associated with the downward movement of organic matter, I found that N and S cycling in these soils are decoupled, with S being more impacted by redox variability. The underlining factor defining the characteristics of S cycling in this environment appeared to be the high rainfall, suggesting vulnerability of ecosystem S to any changes in rainfall patterns.

Chapter 4 targeted the impact of soil age along a chronosequence of well-preserved marine terraces in an annual grassland near Santa Cruz, California. This research built upon work by White et al. (e.g. 2008; 2009; 2012a; 2012b), and paralleled work done for N on another Californian chronosequence (Brenner et al., 2001). Landscape age appeared to impact S cycling primarily due changes in soil hydrology. I found a shift from processes that deplete the heavy S isotope in soil at greater depth on the youngest terrace (likely DBSR) to processes that enrich the soil in the heavy isotope on the oldest terraces. Pore water data also revealed a division in soil processes due to hydrologic changes with increased soil age: occasional large fluctuations in sulfate concentration and isotope fractionation (by up to 27‰ compared to the precipitation) near the surface in all soils, but little change below the well-developed argillic horizon in the older soils. Similar to the findings from Puerto Rico, S appeared to be more sensitive

than N to the redox fluctuations in the soils at Santa Cruz. I offered two possible explanations for this process: the greater biological demand for N, and the greater degree of recycling of S due to adsorption on iron and aluminum oxides.

Chapter 5 concludes the thesis by providing a synthesis of the findings, outlining the implications of this research, and suggesting possible directions for future work.

References

Acquaye D. K. and Beringer H. (1989) Sulfur in Ghanaian soils .1. Status and distribution of different forms of sulfur in some typical profiles. *Plant Soil* **113,** 197-203.

Alewell C. (1998) Investigating sulfate sorption and desorption of acid forest soils with special consideration of soil structure. *Z Pflanz. Bodenkunde* **161,** 73-80.

Alewell C., Bredemeier M., Matzner E. and Blanck K. (1997) Soil solution response to experimentally reduced acid deposition in a forest ecosystem. *J. Environ. Qual.* **26,** 658-665.

Alewell C., Manderscheid B., Gerstberger P. and Matzner E. (2000) Effects of reduced atmospheric deposition on soil solution chemistry and elemental contents of spruce needles in NE-Bavaria, Germany. *J Plant Nutr. Soil Sc.* **163,** 509-516.

Alewell C., Mitchell M. J., Likens G. E. and Krouse H. R. (1999) Sources of stream sulfate at the Hubbard Brook Experimental Forest: Long-term analyses using stable isotopes. *Biogeochemistry* **44,** 281-299.

Alewell C. and Novak M. (2001) Spotting zones of dissimilatory sulfate reduction in a forested catchment: the S-34-S-35 approach. *Environ. Pollut.* **112,** 369-377.

Amundson R., Austin A. T., Schuur E. A. G., Yoo K., Matzek V., Kendall C., Uebersax A., Brenner D. and Baisden W. T. (2003) Global patterns of the isotopic composition of soil and plant nitrogen. *Global Biogeochem. Cycles* **17**(1)**,** 1031, doi:10.1029/2002GB001903.

Amundson R., Barnes J. D., Ewing S., Heimsath A. and Chong G. (2012) The stable isotope composition of halite and sulfate of hyperarid soils and its relation to aqueous transport. *Geochim. Cosmochim. Acta* **99,** 271-286.

Andersson P., Torssander P. and Ingri J. (1992) Sulfur isotope ratios in sulfate and oxygen isotopes in water from a small watershed in Central Sweden. *Hydrobiologia* **235,** 205-217.

Austin A. T. and Vitousek P. M. (1998) Nutrient dynamics on a precipitation gradient in Hawai'i. *Oecologia* **113,** 519-529.

Bao H. M. and Reheis M. C. (2003) Multiple oxygen and sulfur isotopic analyses on water-soluble sulfate in bulk atmospheric deposition from the southwestern United States. *J. Geophys. Res.-Atmos.* **108,** D14, 4430, doi:10.1029/2002JD003022.

Bao H. and Marchant D. R. (2006) Quantifying sulfate components and their variations in soils of the McMurdo Dry Valleys, Antarctica. *J. Geophys. Res.-Atmos.* **111,** D16301, doi:10.1029/2005JD006669.

Bates T. S. and Lamb B. K. (1992) Natural sulfur emissions to the atmosphere of the continental United States. *Global Biogeochem. Cycles* **6,** 431-435.

Bern C. R., Porder S. and Townsend A. R. (2007) Erosion and landscape development decouple strontium and sulfur in the transition to dominance by atmospheric inputs. *Geoderma* **142,** 274-284.

Bern C. R. and Townsend A. R. (2008) Accumulation of atmospheric sulfur in some Costa Rican soils. *J Geophys Res-Biogeo.* **113,** G03001, doi:10.1029/2008JG000692.

Boye K., Eriksen J., Nilsson S. I. and Mattsson L. (2010) Sulfur flow in a soil-plant system-effects of long-term treatment history and soil properties. *Plant Soil* **334,** 323-334.

Brenner D. L., Amundson R., Baisden W. T., Kendall C. and Harden J. (2001) Soil N and 15N variation with time in a California annual grassland ecosystem. *Geochim. Cosmochim. Acta* **65(22),** 4171-4186.

Brimblecombe P. (2003) The global sulfur cycle. *Treatise on Geochemistry* **8,** 645-682.

Brown K. A. (1982) Sulfur in the environment - a Review. *Environ. Pollut. B* **3,** 47-80.

Bruchert V., Knoblauch C. and Jorgensen B. B. (2001) Controls on stable sulfur isotope fractionation during bacterial sulfate reduction in Arctic sediments. *Geochim. Cosmochim. Acta* **65,** 763-776.

Calhoun J. A., Bates T. S. and Charlson R. J. (1991) Sulfur isotope measurements of submicrometer sulfate aerosol-particles over the Pacific-Ocean. *Geophys. Res. Lett.* **18,** 1877-1880.

Canfield D. E., Olesen C. A. and Cox R. P. (2006) Temperature and its control of isotope fractionation by a sulfate-reducing bacterium. *Geochim. Cosmochim. Acta* **70,** 548-561.

Chiba H. and Sakai H. (1985) Oxygen isotope exchange-rate between dissolved sulfate and water at hydrothermal temperatures. *Geochim. Cosmochim. Acta* **49,** 993-1000.

Delmas R., Baudet J. and Servant J. (1978) Natural sources of sulfate in humid tropical environment. *Tellus* **30,** 158-168.

Delmas R. and Servant J. (1983) Atmospheric balance of sulfur above an equatorial forest. *Tellus B* **35,** 110-120.

Ewing S. A., Michalski G., Thiemens M., Quinn R. C., Macalady J. L., Kohl S., Wankel S. D., Kendall C., Mckay C. P. and Amundson R. (2007) Rainfall limit of the N cycle on Earth. *Global Biogeochem. Cycles* **21,** GB3009, doi:10.1029/2006GB002838.

Ewing S. A., Yang W., DePaolo D. J., Michalski G., Kendall C., Stewart B. W., Thiemens M. and Amundson R. (2008) Non-biological fractionation of stable Ca

isotopes in soils of the Atacama Desert, Chile. *Geochim. Cosmochim. Acta* **72,** 1096-1110.

Farquhar J., Savarino J., Jackson T. L. and Thiemens M. H. (2000) Evidence of atmospheric sulphur in the martian regolith from sulphur isotopes in meteorites. *Nature* **404,** 50-52.

Giesemann A., Jager H. J. and Feger K. H. (1995) Evaluation of sulfur cycling in managed forest stands by means of stable S-isotope analysis. *Plant Soil* **168,** 399-404.

Halevy I., Zuber M. T. and Schrag D. P. (2007) A sulfur dioxide climate feedback on early Mars. *Science* **318,** 1903-1907.

Jenkins K. A. and Bao H. M. (2006) Multiple oxygen and sulfur isotope compositions of atmospheric sulfate in Baton Rouge, LA, USA. *Atmos. Environ.* **40,** 4528-4537.

Jenny H. (1941) Factors of Soil Formation. McGraw-Hill, New York, 385 pp.

Kaiser K. and Guggenberger G. (2005) Dissolved organic sulphur in soil water under Pinus sylvestris L. and Fagus sylvatica L. stands in northeastern Bavaria, Germany - variations with seasons and soil depth. *Biogeochemistry* **72,** 337-364.

Kaplan I. R. and Rittenberg S. C. (1964) Microbiological fractionation of sulphur isotopes. *J. Gen. Microbiol.* **34,** 195-212.

Kertesz M. A. (2000) Riding the sulfur cycle – metabolism of sulfonates and sulfate esters in Gram-negative bacteria. *FEMS Microbiol. Rev.* **24,** 135-175.

Khademi H., Mermut A. R. and Krouse H. R. (1997) Sulfur isotope geochemistry of gypsiferous Aridisols from central Iran. *Geoderma* **80,** 195-209.

Liang J. Y. and Jacobson M. Z. (1999) A study of sulfur dioxide oxidation pathways over a range of liquid water contents, pH values, and temperatures. *J Geophys. Res.-Atmos.* **104,** 13749-13769.

Likens G. E., Driscoll C. T., Buso D. C., Mitchell M. J., Lovett G. M., Bailey S. W., Siccama T. G., Reiners W. A. and Alewell C. (2002) The biogeochemistry of sulfur at Hubbard Brook. *Biogeochemistry* **60,** 235-316.

Liu J., Mu Y., Geng C., Yu Y., He H. and Zhang Y. (2007) Uptake and conversion of carbonyl sulfide in a lawn soil. *Atmos. Environ.* **41,** 5697-5706.

Marty C., Houle D., Gagnon C. and Duchesne L. (2011) Isotopic compositions of S, N and C in soils and vegetation of three forest types in Quebec, Canada. *Appl. Geochem.* **26,** 2181-2190.

Mayer B., Fritz P., Prietzel J. and Krouse H. R. (1995) The use of stable sulfur and oxygen-isotope ratios for interpreting the mobility of sulfate in aerobic forest soils. *Appl. Geochem.* **10,** 161-173.

Mayer B., Prietzel J. and Krouse H. R. (2001) The influence of sulfur deposition rates on sulfate retention patterns and mechanisms in aerated forest soils. *Appl. Geochem.* **16,** 1003-1019.

Mekhtiyeva V. L. (1971) Isotopic composition of sulfur from plants and animals in water basins of various salinities. *Geochem. Int.* **8,** 461-&.

Mitchell M. J., David M. B. and Harrison R. B. (1992) *Sulphur dynamics of forest ecosystems.* In *Sulfur Cycling on the Continents* (eds. R. W. Howarth, J. W. B. Stewart and M. V. Ivanov). SCOPE, vol. 48, John Wiley and Sons Ltd, NY. pp. 215-254.

Mizutani Y. and Rafter T. A. (1969) Oxygen isotopic composition of sulphates .4. bacterial fractionation of oxygen isotopes in reduction of sulphate and in oxidation of sulphur. *New Zeal. J Sci.* **12,** 69-80.

Morth C. M., Torssander P., Kjonaas O. J., Stuanes A. O., Moldan F. and Giesler R. (2005) Mineralization of organic sulfur delays recovery from anthropogenic acidification. *Environ. Sci. Technol.* **39,** 5234-5240.

Newman L., Krouse H. R. and Grinenko V. A. (1991) Sulphur isotope variations in the atmosphere. In *Stable Isotopes in the Assessment of Natural and Anthropogenic Sulphur in the Environment* (eds. H. R. Krouse and V. A. Grinenko). SCOPE, vol. 43, John Wiley and Sons Ltd, Chichester. pp. 133-176.

Nielsen H., Pilot J., Grinenko L. N., Grinenko V. A., Lein A. Y., Smith J. W. and Pankina R. G. (1991) Lithospheric sources of sulfur. In *Stable Isotopes in the Assessment of Natural and Anthropogenic Sulphur in the Environment* (eds. H. R. Krouse and V. A. Grinenko). SCOPE, vol. 43, John Wiley and Sons Ltd, Chichester. pp. 65-132.

Norman A. L., Belzer W. and Barrie L. (2004) Insights into the biogenic contribution to total sulphate in aerosol and precipitation in the Fraser Valley afforded by isotopes of sulphur and oxygen. *J Geophys. Res.-Atmos.* **109,** D05311, doi:10.1029/2002JD003072.

Norman A. L., Giesemann A., Krouse H. R. and Jager H. J. (2002) Sulphur isotope fractionation during sulphur mineralization: Results of an incubation-extraction experiment with a Black Forest soil. *Soil Biol. Biochem.* **34,** 1425-1438.

Novak M., Bottrell S. H., Fottova D., Buzek F., Groscheova H. and Zak K. (1996) Sulfur isotope signals in forest soils of Central Europe along an air pollution gradient. *Environ. Sci. Technol.* **30,** 3473-3476.

Novak M., Bottrell S. H., Groscheova H., Buzek F. and Cerny J. (1995) Sulphur isotope characteristics of two North Bohemian forest catchments. *Water Air Soil Poll.* **85,** 1641-1646.

Novak M., Bottrell S. H. and Prechova E. (2001) Sulfur isotope inventories of atmospheric deposition, spruce forest floor and living Sphagnum along a NW-SE transect across Europe. *Biogeochemistry* **53,** 23-50.

Novak M., Buzek F., Harrison A. F., Prechova E., Jackova I. and Fottova D. (2003) Similarity between C, N and S stable isotope profiles in European spruce forest soils: implications for the use of delta S-34 as a tracer. *Appl. Geochem.* **18,** 765-779.

Novak M., Mitchell M. J., Jackova I., Buzek F., Schweigstillova J., Erbanova L., Prikryl R. and Fottova D. (2007) Processes affecting oxygen isotope ratios of atmospheric and ecosystem sulfate in two contrasting forest catchments in Central Europe. *Environ. Sci. Technol.* **41,** 703-709.

O'Dowd C. D., Lowe J. A., Smith M. H., Davison B., Hewitt N. and Harrison R. M. (1997) Biogenic sulphur emissions and inferred non-sea-salt-sulphate cloud condensation nuclei in and around Antarctica. *J Geophys. Res.-Atmos.* **102,** 12839-12854.

Post W. M., Emanuel W. R., Zinke P. J. and Stangenberger A. G. (1982) Soil carbon pools and world life zones. *Nature* **298,** 156-159.

Post W. M., Pastor J., Zinke P. J. and Stangenberger A. G. (1985) Global patterns of soil-nitrogen storage. *Nature* **317,** 613-616.

Rees C. E., Jenkins W. J. and Monster J. (1978) Sulfur isotopic composition of ocean water sulfate. *Geochim. Cosmochim. Acta* **42,** 377-381.

Reuss J. O., Cosby B. J. and Wright R. F. (1987) Chemical Processes Governing Soil and Water Acidification. *Nature* **329,** 27-32.

Rock L. and Mayer B. (2009) Identifying the influence of geology, land use, and anthropogenic activities on riverine sulfate on a watershed scale by combining hydrometric, chemical and isotopic approaches. *Chem. Geol.* **262,** 121-130.

Rosen M. R. and Warren J. K. (1990) The origin and significance of groundwater-seepage gypsum from Bristol Dry Lake, California, USA. *Sedimentology* **37,** 983-996.

Schulze E. D. (1989) Air-pollution and forest decline in a spruce (Picea-Abies) forest. *Science* **244,** 776-783.

Seinfeld J. H. and Pandis S. N. (1998) Atmospheric chemistry and physics: From air pollution to climate change. Wiley, New York, 1326 pp.

Shanley J. B., Mayer B., Mitchell M. J., Michel R. L., Bailey S. W. and Kendall C. (2005) Tracing sources of streamwater sulfate during snowmelt using S and O isotope ratios of sulfate and S-35 activity. *Biogeochemistry* **76,** 161-185.

Singh R. K., Dutta R. K. and Agrawal M. (2004) Litter decomposition and nutrient release in relation to atmospheric deposition of S and N in a dry tropical region. *Pedobiologia* **48,** 305-311.

Solomon D., Lehmann J., Kinyangi J., Pell A., Theis J., Riha S., Ngoze S., Amelung W., du Preez C., Machado S., Ellert B. and Janzen H. (2009) Anthropogenic and climate influences on biogeochemical dynamics and molecular-level speciation of soil sulfur. *Ecol. Appl.* **19,** 989-1002.

Stack P. and Rock L. (2011) A delta(34)S isoscape of total sulphur in soils across Northern Ireland. *Appl. Geochem.* **26,** 1478-1487.

Stam A. C., Mitchell M. J., Krouse H. R. and Kahl J. S. (1992) Stable Sulfur Isotopes of Sulfate in Precipitation and Stream Solutions in a Northern Hardwood Watershed. *Water Resour. Res.* **28,** 231-236.

Stempvoort D. R. v., Reardon E. J. and Fritz P. (1990) Fractionation of sulfur and oxygen isotopes in sulfate by soil sorption. *Geochim. Cosmochim. Acta* **54,** 2817-2826.

Szynkiewicz A., Moore C. H., Glamoclija M. and Pratt L. M. (2009) Sulfur isotope signatures in gypsiferous sediments of the Estancia and Tularosa Basins as indicators of sulfate sources, hydrological processes, and microbial activity. *Geochim. Cosmochim. Acta* **73,** 6162-6186.

Thode H. G. and Monster J. (1965) Sulfur-isotope geochemistry of petroleum, evaporates, and ancient seas. In *Fluids in Subsurface Environments* (eds. Young A. and J. E. Galley), *Mem. Am. Assoc. Petrol. Geol.* **4,** 367–377.

Thode H. G., Monster J. and Dunford H. B. (1961) Sulphur isotope geochemistry. *Geochim. Cosmochim. Acta* **25,** 159-174.

Torfstein A., Gavrieli I., Katz A., Kolodny Y. and Stein M. (2008) Gypsum as a monitor of the paleo-limnological-hydrological conditions in Lake Lisan and the Dead Sea. *Geochim. Cosmochim. Acta* **72,** 2491-2509.

Turchyn A. V., Bruchert V., Lyons T. W., Engel G. S., Balci N., Schrag D. P. and Brunner B. (2010) Kinetic oxygen isotope effects during dissimilatory sulfate reduction: A combined theoretical and experimental approach. *Geochim. Cosmochim. Acta* **74,** 2011-2024.

Vanstempvoort D. R. and Krouse H. R. (1994) Controls of delta-O-18 in sulfate - Review of experimental-data and application to specific environments. *Acs. Sym. Ser.* **550,** 446-480.

Wadleigh M. A. (2004) Sulphur isotopic composition of aerosols over the western North Atlantic Ocean. *Can. J. Fish. Aquat. Sci.* **61,** 817-825.

Wadleigh M. A., Schwarcz H. P. and Kramer J. R. (2001) Areal distribution of sulphur and oxygen isotopes in sulphate of rain over eastern North America. *J Geophys. Res.-Atmos.* **106,** 20883-20895.

Wadleigh M. A., Schwarcz H. P. and Kramer J. R. (1994) Sulfur isotope tests of seasalt correction factors in precipitation - Nova-Scotia, Canada. *Water Air Soil Poll.* **77,** 1-16.

Wang J. K., Solomon D., Lehmann J., Zhang X. D. and Amelung W. (2006) Soil organic sulfur forms and dynamics in the Great Plains of North America as influenced by long-term cultivation and. *Geoderma* **133,** 160-172.

White A. F., Schulz M. S., Stonestrom D. A., Vivit D. V., Fitzpatrick J., Bullen T. D., Maher K. and Blum A. E. (2009) Chemical weathering of a marine terrace chronosequence, Santa Cruz, California. Part II: Solute profiles, gradients and the comparisons of contemporary and long-term weathering rates. *Geochim. Cosmochim. Acta* **73,** 2769-2803.

White A. F., Schulz M. S., Vivit D. V., Blum A. E., Stonestrom D. A. and Anderson S. P. (2008) Chemical weathering of a marine terrace chronosequence, Santa Cruz, California I: Interpreting rates and controls based on soil concentration-depth profiles. *Geochim. Cosmochim. Acta* **72,** 36-68.

White A. F., Schulz M. S., Vivit D. V., Bullen T. D. and Fitzpatrick J. (2012) The impact of biotic/abiotic interfaces in mineral nutrient cycling: A study of soils of the Santa Cruz chronosequence, California. *Geochim. Cosmochim. Acta* **77,** 62-85.

White A. F., Vivit D. V., Schulz M. S., Bullen T. D., Evett R. R. and Aagarwal J. (2012) Biogenic and pedogenic controls on Si distributions and cycling in grasslands of the Santa Cruz soil chronosequence, California. *Geochim. Cosmochim. Acta* **94,** 72-94.

Yuan F. and Mayer B. (2012) Chemical and isotopic evaluation of sulfur sources and cycling in the Pecos River, New Mexico, USA. *Chem. Geol.* **291,** 13-22.

Zhang Y. M., Mitchell M. J., Christ M., Likens G. E. and Krouse H. R. (1998) Stable sulfur isotopic biogeochemistry of the Hubbard Brook Experimental Forest, New Hampshire. *Biogeochemistry* **41,** 259-275.

FIGURES

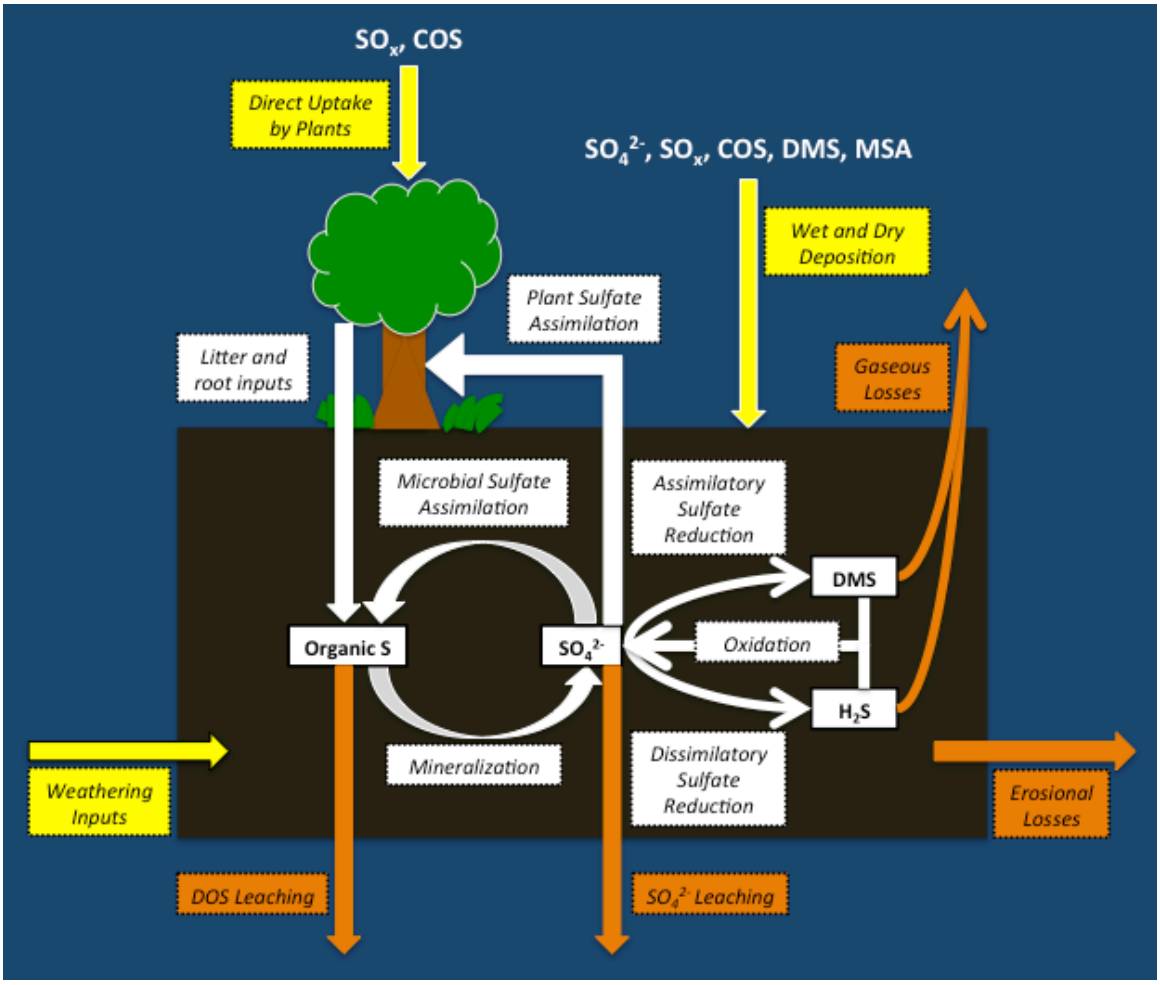

Figure 1: Schematic representation of the biotic terrestrial S cycle. Yellow arrows and boxes represent inputs, orange represents outputs, and white represents biologically-mediated transformations within the soil-plant system. (COS: carbonyl sulfide; DMS: dimethyl sulfide; DOS: dissolved organic sulfur; MSA: methanesulfonic acid; SO_x: sulfur oxides).

Chapter 2

The impact of climate on the geographical variation of soil and plant sulfur concentration and stable isotopes

Abstract

We examined how the average content and isotopic composition of sulfur (S) in soils and in dominant vegetation varied across broad gradients of climate. The patterns were evaluated with a 2-box mixing model, allowing us to calculate the apparent fractionation factors between plants and soil and between soil and atmospheric inputs. We discussed several differences in S patterns compared to those of the related soil nutrient nitrogen. Soil S content generally increased with mean annual precipitation (MAP), but did not correlate with mean annual temperature (MAT). MAP and MAT together accounted for almost half of the observed variability in folial $\delta^{34}S$ values, and for over a quarter of the observed variability in soil $\delta^{34}S$. Soil and plant $\delta^{34}S$ values increased with increasing MAP and MAT. Soils were generally depleted in ^{34}S compared to the inputs, on average by 6‰, likely due to assimilatory sulfate reduction by bacteria and plants followed by leaching of the isotopically heavier remaining sulfate pool (i.e. net immobilization). This difference between the $\delta^{34}S$ values of soils and atmospheric inputs was controlled by MAP, and to some extent by MAT. At the high end of the MAP spectrum studied, soils tended to be isotopically similar to or more enriched than the inputs, reflecting net mineralization. Using the calculated linear regression equation for $\delta^{34}S$ versus climate, we estimated and mapped the global distribution of soil and plant $\delta^{34}S$ for steady state systems.

1. Introduction

The behavior of sulfur (S) in highly industrialized regions subject to high deposition rates is well studied (e.g. Novak et al., 2001; Likens et al., 2002; Marty et al., 2011), but we still lack a basic understanding of how, in less perturbed environments, soil S varies with climate and other factors. Data compilations and analyses have been available for carbon (C) (Post et al., 1982) and nitrogen (N) (Post et al., 1985). A similar evaluation of S is necessary, for several reasons. First, S is an essential plant nutrient, one not abundant in rocks and minerals. Regions with sandy, low organic matter soils are, or may potentially become, S deficient for agriculture. Second, fossil fuel burning and anthropogenic emissions (while much reduced) continue to blanket the planet. While S deficiency is not commonly discussed due to inorganic fertilizers or additions of S from industrial emissions, as global energy availability declines, and as food demands increase, S will likely become part of a suite of more scarce and expensive nutrients underlining food security.

Climate controls biogeochemical cycles by affecting the rates and types of biological processes. The relationship between climate and elemental cycles has been

well documented for N, an element closely related to S. Soil organic C and N (Amundson et al., 1989; Austin and Vitousek, 1998; Miller et al., 2004) and total soil C and N (Post et al. 1982; 1985) increase with increasing mean annual precipitation (MAP) and decreasing mean annual temperature (MAT). Austin and Vitousek (1998) found that the concentration of soil extractable nitrate N and the $\delta^{15}N$ values of soil and vegetation, decreased with increasing mean annual precipitation (MAP) in five native forests in Hawai'i (MAP ranging from 500 mm to 5000 mm). Across a broad climate range, soil and plant $\delta^{15}N$ values decrease with increasing MAP and decreasing MAT, and the difference between the $\delta^{15}N$ values of plants and soils increases with decreasing MAT and, secondarily, increasing MAP (Amundson et al., 2003).

The existing literature also provides some evidence of how ecosystem S may vary with climate. At the very dry end of the climate spectrum, Ewing et al. (2007; 2008) showed that N and S accumulated in abiotic form. In the Great Plains of North America, Wang et al. (2006) found that soil organic S significantly decreased with increasing MAT in native grasslands and cultivated sites, while MAP affected only the cultivated sites, resulting in higher losses of organic S at higher MAP. In different climate regimes in Ghana total soil S decreased with decreasing MAP (Acquaye and Beringer, 1989). In a study of plant leaves in China, MAP explained more of the variability in S content than any other climate variable or than the effect of plant functional type, leading to a decrease in folial S content with increasing MAP (Han et al., 2011). While these studies are suggestive of S content and S isotope patterns that may mirror those of C and N, we lack a compilation of data to explain the patterns, and consider the underlining mechanisms. C, N and S share many characteristics, but differences in bonding and oxidation states should lead to differential processing in natural systems.

Here we use archived and new samples to begin to explore spatial patterns, and the relations between soil and plant S content and stable S isotopes. As we will discuss, many uncertainties remain in the nature of the patterns and the causes behind them, but the data provide a preliminary hypothesis of how this biologically–important element responds to global climate.

2. Theoretical Framework

Soil and plant S pools and pathways are illustrated in Fig. 1. We have considered the soil S cycle in more detail in Ch. 1. Briefly, in most ecosystems S is derived exclusively from atmospheric sources (Bern and Townsend, 2008). Biological and physical processes inside the soil partition S to various pools, and drive its removal to the external environment. These processes may also affect the S isotopic composition. Many of the fractionation factors associated with these processes are still unknown. In wet climates where soils become anaerobic, dissimilatory bacterial sulfate reduction (DBSR) depletes the total soil S pool in ^{34}S (Alewell et al., 1999; Shanley et al., 2005). In most climates, uptake by vegetation and mineralization of organic S can enrich the soil in ^{34}S (e.g. Novak et al., 2003). In hyperarid climates, large isotope changes can occur when dissolved sulfate precipitates as gypsum during Rayleigh-like processes (Ewing et al., 2008).

The isotopic composition of an element is expressed by the δ notation:

$$\delta(‰) = (\frac{R_{sample}}{R_{standard}} - 1) \cdot 1000, \quad (1)$$

where R is the ratio of the rare to common isotope. For $\delta^{34}S$ values, R is the ratio of ^{34}S to ^{32}S and the standard is Canon Diablo Troilite (CDT) (Thode et al., 1961). The isotope fractionation factor α is defined as:

$$\alpha = \frac{R_{product}}{R_{substrate}}, \quad (2)$$

and the Δ value:

$$\Delta = \delta_{product} - \delta_{substrate}. \quad (3)$$

To begin to understand ecosystem S, the soil-plant system can be represented as a 2-box model (Fig. 1). The change in total S in the soil pool is described in terms of in and out fluxes:

$$\frac{dS_{soil}}{dt} = I_{atm} - k_{loss}S_{soil} + k_{litter}S_{plant} - k_{uptake}S_{soil} \quad (4)$$

where I_{atm} represents the atmospheric input flux, S_{soil} and S_{plant} the concentration of S in the soil and plants respectively; k_{loss} is the loss constant of S from the soil to the environment; k_{litter} and k_{uptake} are constants describing the rate of litterfall and plant uptake of S from soil respectively. Here the first two terms correspond to additions and losses to and from the environment, while the last two terms reflect the uptake and input from plants. We can write a similar relationship for plants:

$$\frac{dS_{plant}}{dt} = k_{uptake}S_{soil} + I_{adsorption} - k_{litter}S_{plant} \quad (5)$$

where $I_{adsorption}$ is the flux of S directly adsorbed by plants from the atmosphere, and the other terms are as defined above. Except for in very polluted environments, $I_{adsorption}$ is negligible. Most of our study areas have minimal pollution inputs, and thus we excluded this term from the equation. At steady state (i.e. when flux in equals flux out) we can rearrange the equations to identify the parameters that control the content of S in soil and plants:

$$S_{soil} = \frac{I_{atm}}{k_{loss}} \quad (6)$$

$$S_{plant} = \frac{k_{uptake}}{k_{litter}}S_{soil} \quad (7)$$

I_{atm} depends on atmospheric deposition rates (and thus on MAP), and on the proximity and magnitude of S sources (mostly marine close to the ocean, or biogenic and anthropogenic further inland). k_{loss} depends on leaching rates, which vary with MAP. k_{litter} and k_{uptake} depend on both temperature and rain amount. Therefore, it is expected that S_{soil} and S_{plant} are also influenced by climate and the amount and type of S inputs.

Eqn. 6 and 7 can be assessed separately for the ^{32}S and ^{34}S isotopes, and the ratio (R) of these expressions is:

$$R_{soil} = \frac{^{34}S_{soil}}{^{32}S_{soil}} = \frac{\overline{R}_{inputs}}{\alpha_{loss}} \quad (8)$$

$$R_{plant} = \frac{^{34}S_{plant}}{^{32}S_{plant}} = \overline{\alpha}_{uptake} R_{soil} \quad (9)$$

where R_{soil} and R_{plant} are the isotope ratio of soil and plants, respectively, $\overline{R}_{inputs}$ is the average isotope value of the inputs to the system, and α_{uptake} and α_{loss} are the isotope fractionation factors associated with plant uptake from soil and with losses of S from the soil to the environment respectively.

These expressions show that, in a steady state system, deviations in soil $\delta^{34}S$ values from that of the inputs reflect the integrated fractionation factor for all soil S losses (after Amundson et al., (2003)). At a given site, using information on input values, we can calculate the apparent fractionation factors for all losses of S from soil. Similarly, from measurements of stable isotope ratios in plants and soils at various sites we can calculate α_{uptake}, the isotopic fractionation during plant uptake. We can then combine these factors with environmental variables to derive information on the climatic control of the S cycle. This model has previously been shown to be useful for interpreting N content and isotopes (Amundson et al., 2003).

3. Methods

3.1 Sample and data collection

Soil samples were collected from sites in Puerto Rico, Santa Cruz (California) and the Chilean Andes, and combined with archived samples from 8 other sites (Table 1). The sites were chosen because they span a very broad climate gradient: MAP from 40 to 4200 mm, MAT from 2.5 to 25.5 °C, and include several climosequences (all factors but climate constant). Furthermore, the archived samples were part of previous studies on N (Kelly, 1989; Brenner, 1999; Amundson et al., 2003), allowing us to directly compare the two elemental cycles. We also collected plant samples from Puerto Rico and Santa Cruz, and used archived plant samples when available. All samples were chosen on level or nearly level surfaces, to avoid departure from S steady state. Additionally, data on S isotopes in soils, vegetation and input was compiled from literature. To determine the isotopic value of the inputs, we analyzed rainwater samples from Puerto Rico and Santa Cruz and from the National Atmospheric Deposition Program (NADP) network at the other US locations that were available, and supplemented them with literature values. Where pertinent parameters for archived samples were unavailable, we used best estimates, deriving information from geological maps and publications.

3.2 Analytical measurements

For total soil S content and isotopes, splits of soil samples were dried at 60°C overnight, sieved to <2 mm, and ground with a mortar and pestle. Plant samples were kept frozen until they were freeze-dried and pulverized in a ball mill. Water samples (rain

and pore water) were shipped frozen, then filtered in the lab on 0.45 μm filters within a few days of sampling, and stored refrigerated until further use. Only water samples with a volume equal to or greater than 500 ml were processed for isotope measurements, to ensure large enough quantities of sulfate. In order to extract sulfate for isotope analysis, filtered water samples were heated in a warm water bath, and a 1M $BaCl_2$ solution was added in excess (in a quantity equal to approximately 10% of the sample volume). After 24 hours, the samples were acidified with a few drops of 1N HCl to dissolve carbonates, and then filtered again on a 0.45 μm filter to collect the $BaSO_4$ precipitate. Because the samples were low in S, it was impossible to collect the $BaSO_4$ precipitate off the filter; therefore, the entire surface of the filter was scraped off and used for analysis. The S content of blank filter samples was below detection limit. The total S concentration and $\delta^{34}S$ values of soils and plants, and the $\delta^{34}S$ value of sulfate in water samples, were determined using the SO_2 EA-combustion-IRMS method on a GV Isoprime isotope ratio mass spectrometer coupled with an Eurovector Elemental Analyzer (model EuroEA3028-HT). These measurements were performed at the Laboratory for Environmental and Sedimentary Isotope Geochemistry (LESIG), University of California at Berkeley. Briefly, a small amount of powdered sample containing a minimum of 2 μg S mixed with V_2O_5 catalyst was thermochemically decomposed with copper wires at 1020°C, and the isotopic composition of the resulting SO_2 gas was measured. Water vapor was removed with a $Mg(ClO_4)_2$ trap and CO_2 was eluted out using a dilutor. Several replicates of the international standard NBS127 and two lab standards (both pure $BaSO_4$) were run with each batch of samples. The long-term analytical precision of this method is better than 0.2‰. Soil N content (% dry weight) and $\delta^{15}N$ values were analyzed via elemental analyzer/continuous flow isotope ratio mass spectrometry using a CHNOS Elemental Analyzer (Vario ISOTOPE Cube, Elementar, Hanau, Germany) coupled with an IsoPrime100 IRMS (Isoprime, Cheadle, UK) at the Center for Stable Isotope Biogeochemistry, University of California, Berkeley. Long-term external precision for N isotope analyses is 0.15‰.

3.3 Data processing and calculations

We calculated the total S and $\delta^{34}S$ to 10, and 50 cm after *Brenner et al.* (2001):

$$S_d = \sum_{h=1}^{H} (\%S_h \cdot BD_h \cdot Z_h) \tag{10}$$

where S_d (in g/cm^2) is the amount of S per area in the soil to depth d, $\%S_h$, BD_h and Z_h are the percentage of S, the bulk density (adjusted for gravel content where necessary) and the thickness of horizon h respectively, and H is the total number of soil horizons down to depth d; and

$$\delta^{34}S_d = \sum_{h=1}^{H} \left(\frac{\%S_h \cdot BD_h \cdot Z_h}{S_d} \cdot \delta^{34}S_h \right) \tag{11}$$

where $\delta^{34}S_d$ is the average soil $\delta^{34}S$ to depth d, $\delta^{34}S_h$ is the $\delta^{34}S$ of horizon h, and the other symbols are as described above. If bulk density measurements were not available, we estimated a constant value for the entire profile. In our calculations, we used only

mineral soil horizons (no O horizons). Where more than one soil was analyzed per site, we averaged the values to avoid statistical overrepresentation.

All plant samples consisted of leaves of dominant vegetation. If more than one plant species was analyzed, the average isotope value is reported. This does not necessarily equal the average isotopic composition of the litter inputs to soil since different plant species occur in different proportions, and since other plant parts likely have different $\delta^{34}S$ values. Thus, this approach provides only a first-order approximation of the isotope value of the litter.

For some of the NADP sites, we only obtained one sample. For sites where several samples were collected, we computed volume-weighed concentrations and calculated the average isotope composition as:

$$\delta^{34}S_{average} = \frac{\sum_{i=1}^{n} \delta^{34}S_i \cdot [SO_4]_i \cdot V_i}{\sum_{i=1}^{n} [SO_4]_i \cdot V_i} \quad (12)$$

For statistical analysis we used only the sites that were at or near steady state (i.e. we excluded the two lowermost elevation samples from the Andean climosequence). Statistical analysis (univariate and multivariate regression) was performed in R, and the geospatial model in ArcGIS.

4. Results and Discussion

The factorial model of Jenny (1941) identifies five variables that play major roles in soil processes: climate, organisms, topography, parent material and time. The impacts of parent material, topography and landscape age were discussed elsewhere (Stack and Rock, 2011; Ch. 3 and 4 of this thesis). Here, we hypothesize that climate, driving oxidation states and rates of reactions, may have a first order control on the amounts and isotope composition of S. To begin, we consider the one factor besides climate that should most impact soil and plant S: input chemistry. Although the addition of latitude improves some of the models slightly, we do not consider it further, because it is not independent from climate, and because input chemical variability is not directly linked with latitude, as discussed below.

4.1 The impact of atmospheric inputs on soil and plant S

Since most ecosystems derive their S from atmospheric inputs (Bern and Townsend, 2008), the isotopic value of atmospheric S sets the baseline for the isotopic value of soil and plant S, and must be considered when discussing trends with climate. Amundson et al. (2003) explained the increasing soil and plant $\delta^{15}N$ values with decreasing MAP and increasing MAT by an increasing fraction of ^{15}N-depleted ecosystem N losses. For this reasoning to hold, the amount and isotopic values of the atmospheric inputs must be globally uniform, which is mostly true for N. For S however, due to the short lifetime of atmospheric S compounds, the amount and isotopic

composition of the inputs is geographically distinct (Fig. 2). For instance, sulfate ion wet deposition maps for the US created by the National Atmospheric Deposition Program (NADP) show that in the western half of the US inputs have consistently been below 8 kg SO_4^{2-} ha^{-1} yr^{-1}, while inputs in much of the eastern half of the US were >24 kg SO_4^{2-} ha^{-1} yr^{-1} up until the early 2000s, and only decreased to 16 kg SO_4^{2-} ha^{-1} yr^{-1} or less as of 2007 (*NADP*, 2007). This excess sulfate is anthropogenic, with $\delta^{34}S$ values close to 0‰ (Wadleigh et al. 2001).

Not only the amount, but also the form of S deposited to soils is spatially variable. Model simulations for 1990 (Chin et al., 2000) showed that SO_2 and sulfate aerosols were most abundant in eastern US, Europe and east Asia, originating mainly from anthropogenic emissions with low $\delta^{34}S$ values. Emissions of the high-$\delta^{34}S$ biogenic dimethyl sulfide (DMS) and its precursor methane sulfonic acid (MSA) were concentrated near the coast in western US, northern Europe, Peru, eastern Asia, as well as near the Great Lakes in North America (Chin et al., 2000). Thus, as Fig. 2 illustrates, inputs near the coast generally have high $\delta^{34}S$ values (>15‰), reflecting the seasalt sulfate value of 21‰ (Rees et al., 1978) and the 15.6±3.1‰ value of sulfate formed through the oxidation of biogenic DMS (Calhoun et al., 1991), while inputs inside continents have values closer to 0‰ (Wadleigh et al. 2001). However, we found no simple significant correlation between input $\delta^{34}S$ values and distance to ocean. Furthermore, input $\delta^{34}S$ values show a weak significant correlation with soil $\delta^{34}S$ values in the upper 10 cm (adjusted R^2 0.1936, $p<0.05$), but not in the upper 50 cm (adjusted R^2 0.0439, $p=0.1029$). This means that, although inputs set the basis for soil $\delta^{34}S$ values, the geographical variation in soil $\delta^{34}S$ values must be controlled by additional factors.

Nevertheless, the heterogeneity of S inputs adds a layer of complexity to Eqn. 6 and 8. To tease apart the variability in $\overline{R}_{inputs}$ from that in α_{loss}, it is helpful to consider the variations in the isotopic difference between inputs and soils ($\Delta_{soil\text{-}input}$), an equivalent and more intuitive measure for α_{loss}. In general, soils are depleted in the heavy isotope compared to our best estimates of atmospheric inputs (Table 1) by approximately 6‰ (Table 2). This suggests that S losses (which are mostly aqueous sulfate) are typically enriched in the heavy isotope compared to the soil. The soil sulfate pool could become isotopically heavier than the soils as a result of two main processes: (1) DBSR (Brunner and Bernasconi, 2005) and (2) sulfate immobilization or assimilatory sulfate reduction (Kaplan and Rittenberg, 1964). DBSR is unlikely to be a major process in most soils, since it requires prolonged anaerobic conditions to significantly impact soil isotopic composition. Assimilatory sulfate reduction, i.e. the assimilation of sulfate into organic S by microorganisms (also known as immobilization) (Kaplan and Rittenberg, 1964) and plants (Trust and Fry, 1992), occurs ubiquitously and is likely the main cause for the observed difference between soil and input $\delta^{34}S$. Previous studies found that assimilation by plants enriches the remaining soil sulfate pool by 1.5‰ on average (Fig. 1) (Trust and Fry, 1992). Additionally, microorganisms can fractionate by up to 2.8‰ during assimilatory sulfate reduction (Kaplan and Rittenberg, 1964). On the other hand, mineralization (conversion of organic S to sulfate by bacteria) depletes the soil sulfate pool and enriches the organic S pool relative to each other by 1±1‰ (Fig. 1) (Norman et al., 2002). For losses to be ^{34}S-enriched on average compared to the soil pool, the effect of assimilation must exceed that of mineralization in most soils, i.e. there must be net

immobilization of sulfate as organic S. The subsequent leaching of the remaining enriched sulfate pool can explain the resulting $\Delta_{soil\text{-}input}$ values. Sulfate reduction (assimilatory or dissimilatory) thus seems to be a dominant process in most pristine soils, causing a general depletion in the heavy isotope compared to inputs. Alternatively, the very low estimated $\Delta_{soil\text{-}input}$ values at some of the sites (Great Plains, Merced, Kyle Canyon, Sierra Nevada and the US East Coast) may be due to other factors, such as possible changes in the amount and isotope composition of atmospheric S due to reductions in industrial emissions. It is likely that input $\delta^{34}S$ values have increased over the past 20-30 years due to S pollution mitigation strategies.

There are also a few sites in our database where the soils are enriched compared to the measured inputs, by up to 3.2‰. These soils where the enrichment is significant are all in polluted regions (Quebec, Germany and Sweden), with low (<6‰) input $\delta^{34}S$ values. Multiple studies in such polluted temperate regions have shown that microbial decomposition and cycling of S increases the $\delta^{34}S$ value of soils compared to the inputs and decreases that of aqueous losses due to mineralization (e.g. Fuller et al., 1986; Novak et al., 1995; Zhang et al., 1998; Alewell and Gehre, 1999; Alewell et al., 1999). Two other sites in our database have small positive $\Delta_{soil\text{-}input}$ values, one on the marine terraces of Santa Cruz, and one in the rainforest of Puerto Rico. At both sites the soils reflect the isotopic value of the mostly marine inputs with minimal net fractionation, meaning that the effects of mineralization and immobilization are balanced.

Our results are consistent with a previous study of ten soils from the UK, China and New Zealand (Zhao et al., 2006), which found that more than half of the soils showed net immobilization (i.e. sulfate assimilation into organic sulfur) as opposed to net mineralization (i.e. conversion of organic S to sulfate). Immobilization rates did not correlate with the relative abundance of S species, but correlated negatively with the initial amount of sulfate present (Zhao et al., 2006). This suggests that soils in polluted regions with large anthropogenic S emissions or located near the coast with abundant marine sulfate inputs will tend to show net mineralization, whereas soils in more remote regions with small S input loads will experience net immobilization.

4.2 The impact of climate on soil and plant S

The impact of climate can be unambiguously distinguished from that of varying S input isotope values by using series of sites where climate varies significantly over short enough distances while inputs remain similar. Our data set included six such well-defined climosequences, i.e. series of sites for which MAP and/or MAT vary, but all other factors are nearly constant: Mt. Kilimanjaro, Sierra Nevada, Kyle Canyon, US Great Plains, Baja California and the Chilean Andes (Table 1). The close examination of these climosequences illustrates that the interactions between MAP and MAT at a local scale can lead to different trends in soil S content and stable isotopes (Fig. 3). Nevertheless, when combining the data, several trends become apparent. We report the results for both all data combined and the climosequences only (Table 3); the latter excludes the Chilean samples, because two of the sites in this climosequence were not at steady-state.

For all data, total soil S content increases significantly with MAP (Table 2), but shows no significant trend with MAT. The behavior of total soil S with MAP is similar to

that of N. As a result, soil N and S contents correlate significantly. The correlation is stronger when averaging over the top 10 cm, rather than the top 50 cm (adjusted R^2 of 0.66 versus 0.30) (Fig. 4), possibly suggesting differences in internal transport or decomposition processes for these two elements. When using only the climosequence data, the correlation between total soil S and climate improves and becomes significant with MAT as well. With increasing MAT, soil S content in the top 10 cm appears to decrease, but increases when averaged over the upper 50 cm (Table 3). Lower soil S content at higher MAT was also observed by Wang et al. (2006).

Soil $\delta^{34}S$ values increased significantly with MAT and MAP ($p<0.05$). MAP and MAT together account for over a quarter of the variability in soil $\delta^{34}S$ values globally, and for about half of the variability for the climosequence data only (Table 3). Although modest, these R^2 values are larger than those measured for N (Amundson et al., 2003), suggesting that despite greater input heterogeneity, climate plays a major role in regulating the terrestrial S cycle. The relationship of S with MAP is the opposite of that observed by Amundson et al. (2003) for N. This probably occurs because higher rainfall areas tend to be closer to the ocean and receive inputs with high $\delta^{34}S$. For the subset of sites studied here, $\delta^{15}N$ values decrease not only with increasing MAP like in Amundson et al. (2003), but also with increasing MAT. This is opposite the behavior of S (Fig. 5), and results in a lack of correlation between soil $\delta^{15}N$ and $\delta^{34}S$ values. The trends in soil $\delta^{34}S$ values with climate cannot be mechanistically interpreted, however, without considering the $\delta^{34}S$ values of the inputs.

Despite the limited input data available for this study, we observed a correlation between climate and $\Delta_{soil\text{-}input}$ values, which account to some extent for the heterogeneity in inputs. We found a significant, albeit weak (R^2 ~0.2), increase in $\Delta_{soil\text{-}input}$ values with MAP and decrease with MAT (Table 3). When using only data from well-designed climosequences, the correlation improves and $\Delta_{soil\text{-}input}$ values increase with both MAP and MAT (Table 3). Higher MAP, increasing the occurrence of anoxic events and microsites, is expected to increase the proportion of organic S species in reduced and intermediate oxidation states, which correlates with higher gross mineralization rates (Zhao et al., 2006). Thus, at high MAP, soils will more likely experience net mineralization, which creates ^{34}S-depleted losses, thus leading to positive $\Delta_{soil\text{-}input}$ values. At lower MAP, net immobilization leads to ^{34}S-enriched losses, thus to negative $\Delta_{soil\text{-}input}$ values.

Similar to the soil, plant $\delta^{34}S$ values increase with MAT and MAP ($p<0.05$), thought the correlation for plants is stronger than for soils, explaining 44% of the variation in plant stable S isotopes (Table 3). No significant correlation was found when using only the data from the climosequences, due to limited plant data availability at those sites. Plants act as both a source (via litterfall) and a sink (via uptake of soil water and nutrients) of soil S. In most locations, there is a large difference between soil and plant $\delta^{34}S$, as expressed by the $\Delta_{plant\text{-}soil}$ values. The $\Delta_{plant\text{-}soil}$ values vary from nearly -8 to +5‰ (Table 2), however, most commonly plants are slightly more depleted in ^{34}S compared to soils (~1‰ difference). These results are based on only 22 to 27 samples, depending on the depth to which the soil data were averaged. Despite sample size limitations, these data suggest that more variability may be present between plant and soil $\delta^{34}S$ values than reported in the current literature (Trust and Fry, 1992; Shanley et al.,

2005; Bern et al., 2007; Xiao et al., 2012), which is biased towards temperate regions in Europe and North America. Four factors could account for this variability. First, we used only folial tissue samples; isotope heterogeneity of plant tissues could lead to very different $\delta^{34}S$ values for the overall litter inputs. Second, plants take up S as sulfate from the soil, whereas most soil S is organic S; in-soil isotope fractionations can render the $\delta^{34}S$ of sulfate different from that of soil organic S, thus creating a difference between the isotope composition of plant-available and total S. Third, plants could create this difference either by discriminating against the heavier isotope during sulfate uptake from soil (Trust and Fry, 1992), or by fractionating during the conversion of sulfate to organic S inside the folial tissue. The magnitude of the fractionation could be plant species-specific. Fourth, isotope fractionation can occur during the conversion of plant litter to soil organic matter.

While it is difficult to determine from this study alone which factor dominates, the lack of a trend between $\Delta_{plant\text{-}soil}$ and climate hints that the main reason might be plant-related (heterogeneity among plant species and tissues or fractionation by plants). We found no significant correlations between $\Delta_{plant\text{-}soil}$ and MAT, MAP (univariate) or MAP+MAT (multivariate). The Amundson et al. (2003) study of N found that plants were also globally more depleted in ^{15}N than the soils (though those authors had no data on nitrate in soil pore waters, just total soil N). Furthermore, for N isotopes, $\Delta_{plant\text{-}soil}$ increases with decreasing MAT and secondarily with increasing MAP, which was explained by a systematic change in the source of plant-available N (organic/ammonia versus nitrate) with climate (Amundson et al., 2003). Such a shift however does not occur for S, since plants take up S mainly as sulfate in all climates. Isotopically variable sulfate inputs might also account for the differences in plant versus soil isotope values, as there is a very slight positive correlation between input and plant $\delta^{34}S$ values (R^2 0.117, $p<0.05$). Therefore, unlike for N, the S isotopic difference between soils and plant seems to be driven by plant type or site characteristics such as input chemistry, rather than by climate.

4.3 Global trends in soil and plant S isotopes

Using a 1950-2000 average global climate dataset from worldclim.org and the regression results in Table 3, we produced global maps of soil S content (Fig. 6), and $\Delta_{soil\text{-}input}$, soil $\delta^{34}S$ and plant $\delta^{34}S$ values (Fig. 7). All these maps were created using the linear regression results for all available data (rather than only the climosequences), to include a larger number of samples. The soil S content map (Fig. 6) uses only MAP data, since S content does not correlate significantly with MAT. The other maps are based on both MAP and MAT data.

The S content of soils in areas with <100 mm MAP is likely underestimated in this model, since previous studies found that S content increases at low rainfall due to passive accumulation of atmospheric sulfate (Ewing et al., 2008). Even if those areas are excluded, approximately half of the earth has soils with low S content, <1 g cm^{-2} summed over the upper 50 cm of the soil. The areas most predisposed to soil S deficiency are those with low rainfall, particularly most of N Africa, central Asia and southern Australia and New Zealand, as well as parts of the continental US. S deficiency in parts of Africa

and New Zealand is an already well-known problem (Acquaye and Beringer, 1989; Edmeades et al., 2005). The map thus pinpoints areas naturally low in S, most susceptible to S deficiency or to the effects of anthropogenic S additions.

In terms of isotopes (Fig. 7), the model predicts lowest $\Delta_{soil\text{-}input}$ values, i.e. soils most depleted compared to inputs, mainly in equatorial regions and in Australia. Lowest soil $\delta^{34}S$ values are predicted at high latitudes in the northern hemisphere, while southern hemisphere soils tend to have higher $\delta^{34}S$ values. Plants generally mirror the soil. Differences from the model could indicate significant departure from steady state due to anthropogenic influences, including pollution and fertilizer addition.

5. Conclusion

We performed an extensive analysis of stable sulfur (S) isotopes in soil and plants from a wide range of climates. Climate emerged as a major controller of S biogeochemistry, affecting both the amount of S in the soil, and the types of processes, and thus the $\delta^{34}S$ values. Like nitrogen (N), soil S content increased with increasing MAP, but, unlike N, it was not significantly affected by MAT. Soils were generally depleted in ^{34}S compared to the inputs, most likely due to net immobilization, i.e. assimilatory sulfate reduction by microorganisms and plants, followed by leaching of the isotopically heavier remaining sulfate pool. At higher MAP the $\Delta_{soil\text{-}input}$ values tended to be more positive, indicating a shift towards net mineralization. On average, plants were depleted in the heavy isotope compared to the soil, which may be due to heterogeneity in $\delta^{34}S$ of different plant tissues, or due to fractionation during assimilation by plants. Because $\Delta_{plant\text{-}soil}$ is climate-independent, in-soil processes are an unlikely cause for the observed isotope differences between plants and soil. Soil $\delta^{34}S$ and $\delta^{15}N$ values followed opposing trends with climate. Multivariate regression against MAP and MAT explained almost half of folial $\delta^{34}S$ and over a quarter of soil $\delta^{34}S$. The correlations improved when using only data from climosequences, which minimize the effects of input heterogeneity. Despite this input heterogeneity, we showed that it is possible to use global climate (MAP and MAT) data to successfully model soil and plant $\delta^{34}S$. Our climate-based map of global soil S content and $\delta^{34}S$ reflects what the values would be like in the absence of anthropogenic disturbance, and identifies soils susceptible to S deficiency. Overall, the dependence on climate of the terrestrial S cycle appears to be stronger than for the related soil nutrient, nitrogen. This means that S cycling is highly susceptible to the effects of climate change, particularly to changes in rainfall patterns.

Our results open up new opportunities to further tease apart the controls on the S cycle. These include: (1) measuring integrative litter inputs as opposed to folial $\delta^{34}S$ to determine if fractionation occurs during plant uptake of S; (2) adding long-term measurements of inputs to better characterize $\Delta_{soil\text{-}input}$; and (3) performing long-term measurements of $\delta^{34}S$ values in losses from soil. Such studies will continue to improve our understanding of the ecosystem S response to global change.

Acknowledgements. We thank M. Schulz, K. Finstad, S. Hall, M. Whelan and M. Rosario for technical assistance in the field, and C. Lehmann and B. Riney from the NADP, as well as M. C. Torrens, S. Moya, J. Carlos and J. Orlando for sample collection. We are also grateful to A. Kirk, A Laleian and A. Engelbrektson for laboratory assistance, and to J. Coates, W. Yang, P. Brooks and S. Mambelli for access to instruments and sample analysis.

References

Acquaye D. K. and Beringer H. (1989) Sulfur in Ghanaian soils .1. Status and distribution of different forms of sulfur in some typical profiles. *Plant Soil* **113,** 197-203.

Alewell C. and Gehre M. (1999) Patterns of stable S isotopes in a forested catchment as indicators for biological S turnover. *Biogeochemistry* **47,** 319-333.

Alewell C., Mitchell M. J., Likens G. E. and Krouse H. R. (1999) Sources of stream sulfate at the Hubbard Brook Experimental Forest: Long-term analyses using stable isotopes. *Biogeochemistry* **44,** 281-299.

Alewell C. and Novak M. (2001) Spotting zones of dissimilatory sulfate reduction in a forested catchment: the S-34-S-35 approach. *Environ. Pollut.* **112,** 369-377.

Amundson R. G., Chadwick O. A. and Sowers J. M. (1989) A comparison of soil climate and biological activity along an elevation gradient in the eastern Mojave Desert. *Oecologia* **83,** 395-400.

Amundson R., Francovizcaino E., Graham R. C. and Deniro M. (1994) The relationship of precipitation seasonality to the flora and stable-isotope chemistry of soils in the Vizcaino Desert, Baja-California, Mexico. *J. Arid Environ.* **28,** 265-279.

Amundson R., Austin A. T., Schuur E. A. G., Yoo K., Matzek V., Kendall C., Uebersax A., Brenner D. and Baisden W. T. (2003) Global patterns of the isotopic composition of soil and plant nitrogen. *Global Biogeochem. Cycles* **17**(1)**,** 1031, doi:10.1029/2002GB001903.

Andersson P., Torssander P. and Ingri J. (1992) Sulfur isotope ratios in sulfate and oxygen isotopes in water from a small watershed in Central Sweden. *Hydrobiologia* **235,** 205-217.

Astratov M. Y., Zaveryaeva I. I. and Ryaboshapko A. G. (1986) Variation of sulfate content in Arctic atmospheric precipitation during the last 90 years. *Soviet Meteorology and Hydrology* 38-42.

Austin A. T. and Vitousek P. M. (1998) Nutrient dynamics on a precipitation gradient in Hawai'i. *Oecologia* **113,** 519-529.

Baisden W. T., Amundson R., Brenner D. L., Cook A. C., Kendall C. and Harden J. W. (2002) A multiisotope C and N modeling analysis of soil organic matter turnover and transport as a function of soil depth in a California annual grassland soil chronosequence. *Global Biogeochem. Cycles* **16,** 1135.

Bao H. M. and Reheis M. C. (2003) Multiple oxygen and sulfur isotopic analyses on water-soluble sulfate in bulk atmospheric deposition from the southwestern United States. *J Geophys. Res.-Atmos.* **108,** D14, 4430, doi:10.1029/2002JD003022.

Bao H. M., Thiemens M. H. and Heine K. (2001) Oxygen-17 excesses of the Central Namib gypcretes: spatial distribution. *Earth Planet. Sci. Lett.* **192,** 125-135.

Bao H. and Marchant D. R. (2006) Quantifying sulfate components and their variations in soils of the McMurdo Dry Valleys, Antarctica. *J Geophys. Res.-Atmos.* **111,** D16301, doi:10.1029/2005JD006669.

Bern C. R., Porder S. and Townsend A. R. (2007) Erosion and landscape development decouple strontium and sulfur in the transition to dominance by atmospheric inputs. *Geoderma* **142,** 274-284.

Bern C. R. and Townsend A. R. (2008) Accumulation of atmospheric sulfur in some Costa Rican soils. *J Geophys Res-Biogeo.* **113,** G03001, doi:10.1029/2008JG000692.

Brenner D. L. (1999). Soil nitrogen isotopes along natural gradients: models and measurements. M.S. thesis, University of California, Berkeley, CA.

Brenner D. L., Amundson R., Baisden W. T., Kendall C. and Harden J. (2001) Soil N and N-15 variation with time in a California annual grassland ecosystem. *Geochim. Cosmochim. Acta* **65,** 4171-4186.

Brunner B. and Bernasconi S. M. (2005) A revised isotope fractionation model for dissimilatory sulfate reduction in sulfate reducing bacteria. *Geochim. Cosmochim. Acta* **69,** 4759-4771.

Buss H. L., Mathur R., White A. F. and Brantley S. L. (2010) Phosphorus and iron cycling in deep saprolite, Luquillo Mountains, Puerto Rico. *Chem. Geol.* **269,** 52-61.

Calhoun J. A., Bates T. S. and Charlson R. J. (1991) Sulfur Isotope Measurements of Submicrometer Sulfate Aerosol-Particles Over the Pacific-Ocean. *Geophys. Res. Lett.* **18,** 1877-1880.

Caron F., Tessier A., Kramer J. R., Schwarcz H. P. and Rees C. E. (1986) Sulfur and oxygen isotopes of sulfur in precipitation and lakewater, Quebec, Canada. *Appl. Geochem*. **1,** 601-606.

Chin M., Rood R. B., Lin S-J., Muller J-F. and Thompson A. M. (2000) Atmospheric sulfur cycle simulated in the global model GOCART: Model description and global properties. *J Geophys. Res.* **105**(D20), 24671-24687.

Chukhrov F. V., Churikov V. S., Ermilova L. P. and Nosik L. P. (1977) Isotope composition of atmospheric sulfur and its possible evolution in the history of the Earth (in Russian). *Izv. Akard Nauk SSSR, Ser. Geol.,* **7,** 5-13.

Chukhrov F. V., Ermilova L. P., Churikov V. S. and Nosik L. P. (1978) Phyto-geochemistry of sulfur isotopes. *Geokhimiya*1015-1031.

Cortecci G. and Longinel.a (1970) Isotopic Composition of Sulfate in Rain Water, Pisa, Italy. *Earth Planet. Sci. Lett.* **8,** 36-40.

Dosseto A., Buss H. L. and Suresh P. O. (2012) Rapid regolith formation over volcanic bedrock and implications for landscape evolution. *Earth Planet. Sci. Lett.* **337–338,** 47-55.

Edmeades D. C., Thorrold B. S. and Roberts A. H. C. (2005) The diagnosis and correction of sulfur deficiency and the management of sulfur requirements in New Zealand pastures: a review. *Aust. J. Exp. Agr.* **45,** 1205-1223.

Ewing S. A., Michalski G., Thiemens M., Quinn R. C., Macalady J. L., Kohl S., Wankel S. D., Kendall C., Mckay C. P. and Amundson R. (2007) Rainfall limit of the N cycle on Earth. *Global Biogeochem. Cycles* **21,** GB3009, doi:10.1029/2006GB002838.

Ewing S. A., Yang W., DePaolo D. J., Michalski G., Kendall C., Stewart B. W., Thiemens M. and Amundson R. (2008) Non-biological fractionation of stable Ca isotopes in soils of the Atacama Desert, Chile. *Geochim. Cosmochim. Acta* **72,** 1096-1110.

Finley J. B., Drever J. I. and Turk J. T. (1995) Sulfur isotope dynamics in a high-elevation catchment, West Glacier Lake, Wyoming. *Water Air Soil Poll.* **79,** 227-241.

Fuller R. D., Mitchell M. J., Krouse H. R., Wyskowski B. J. and Driscoll C. T. (1986) Stable sulfur isotope ratios as a tool for interpreting ecosystem sulfur dynamics. *Water Air Soil Poll.* **28,** 163-171.

Gavrishin A. I. and Rabinovich A. L. (1971) Sulfur isotopic composition of sulfate in natural waters from sulfide deposits in Middle Urals. *Geochem. Int.* **8,** 550-&.

Gu A., Gray F., Eastoe C. J., Norman L. M., Duarte O. and Long A. (2008) Tracing ground water input to base flow using sulfate (S, O) isotopes. *Ground Water* **46,** 502-509.

Han W. X., Fang J. Y., Reich P. B., Woodward F. I. and Wang Z. H. (2011) Biogeography and variability of eleven mineral elements in plant leaves across gradients of climate, soil and plant functional type in China. *Ecol. Lett.* **14,** 788-796.

Heartsill-Scalley T., Scatena F. N., Estrada C., McDowell W. H. and Lugo A. E. (2007) Disturbance and long-term patterns of rainfall and throughfall nutrient fluxes in a subtropical wet forest in Puerto Rico. *J Hydrol.* **333,** 472-485.

Heaton T. H. E., Spiro B., Madeline S. and Robertson C. (1997) Potential canopy influences on the isotopic composition of nitrogen and sulphur in atmospheric deposition. *Oecologia* **109,** 600-607.

Heaton T. H. E., Spiro B., Madeline S. and Robertson C. (1997) Potential canopy influences on the isotopic composition of nitrogen and sulphur in atmospheric deposition. *Oecologia* **109,** 600-607.

Hidy G. M. (2003) Snowpack and precipitation chemistry at high altitudes. *Atmos. Environ.* **37,** 1231-1242.

Jamieson R. E. and Wadleigh M. A. (2000) Tracing sources of precipitation sulfate in eastern Canada using stable isotopes and trace metals. *J Geophys. Res.-Atmos.* **105,** 20549-20556.

Jedrysek M. O. (2000) Oxygen and sulphur isotope dynamics in the SO_4^{2-} of an urban precipitation. *Water Air Soil Poll.* **117,** 15-25.

Jenkins K. A. and Bao H. M. (2006) Multiple oxygen and sulfur isotope compositions of atmospheric sulfate in Baton Rouge, LA, USA. *Atmos. Environ.* **40,** 4528-4537.

Jenny H. (1941) Factors of Soil Formation. McGraw-Hill, New York, 385 pp.

Jersak J. M. (1991) Quantification of chemical and physical changes occurring during the pedogenic process of podsolization: Examples from the northeastern United States. Ph.D. thesis, University of California, Berkeley, CA.

Jersak J., Amundson R. and Brimhall G. (1997) Trace metal geochemistry in spodosols of the northeastern United States. *J. Environ. Qual.* **26,** 511-521.

Jersak J., Amundson R. and Brimhall G. (1995) A Mass-Balance Analysis of Podzolization - Examples from the Northeastern United-States. *Geoderma* **66,** 15-42.

Ji Hongbing and Jiang Yongbin (2012) Carbon flux and C, S isotopic characteristics of river waters from a karstic and a granitic terrain in the Yangtze River system. *J Asian Earth Sci.* **57,** 38-53.

Kaplan I. R. and Rittenberg S. C. (1964) Microbiological fractionation of sulphur Isotopes. *J. Gen. Microbiol.* **34,** 195-212.

Kelly, E. F. (1989) A study of the influence of climate and vegetation on the stable isotope chemistry of soils in grassland ecosystems of the Great Plains. Ph.D. thesis, University of California, Berkeley, CA.

Kelly E. F., Amundson R. G., Marino B. D. and Deniro M. J. (1991) Stable carbon isotopic composition of carbonate in Holocene grassland soils. *Soil Sci. Soc. Am. J.* **55,** 1651-1658.

Khademi H., Mermut A. R. and Krouse H. R. (1997) Sulfur isotope geochemistry of gypsiferous Aridisols from central Iran. *Geoderma* **80,** 195-209.

Krouse H. R., Grinenko L. N., Grinenko V. A., Newman L., Forrest J., Nakai N., Tsuji Y., Yatsumimi T., Takeuchi U., Robinson B. W., Stewart, M. K., Gunatilaka A., Chambers L. A., Smith, J. W., Plumb L. A., Buzek F., Cerny J., Sramek J., Menon A. G., Iyer G. V. A., Venkatasubramanian V S., Egboka B. E. C., Irogbenachi M. M. and Eligwe C. A. (1991) Case Studies and Potential Applications. In *Stable Isotopes in the Assessment of Natural and Anthropogenic Sulphur in the Environment* (eds. H. R. Krouse and V. A. Grinenko). SCOPE, vol. 43, John Wiley and Sons Ltd, Chichester. pp. 307-425.

Kucera C. L. and Kirkham D. R. (1971) Soil respiration studies in tallgrass prairie in Missouri. *Ecology* **52,** 912-915.

Latorre C., Betancourt J. L., Rylander K. A., Quade J. and Matthei O. (2003) A vegetation history from the arid prepuna of northern Chile (22-23 degrees S) over the last 13,500 years. *Palaeogeogr. Palaeocl.* **194,** 223-246.

Lee C. C. W. and Thiemens M. H. (2001) The delta O-17 and delta O-18 measurements of atmospheric sulfate from a coastal and high alpine region: A mass-independent isotopic anomaly. *J Geophys. Res. –Atmos.* **106,** 17359-17373.

Likens G. E., Driscoll C. T., Buso D. C., Mitchell M. J., Lovett G. M., Bailey S. W., Siccama T. G., Reiners W. A. and Alewell C. (2002) The biogeochemistry of sulfur at Hubbard Brook. *Biogeochemistry* **60,** 235-316.

Longinelli A. and Bartelloni M. (1978) Atmospheric pollution in Venice, Italy, as indicated by isotopic analyses. *Water Air Soil Poll.* **10,** 335-341.

Ludwig F. L. (1976) Sulfur isotope ratios and origins of aerosols and cloud droplets in California stratus. *Tellus* **28,** 427-433.

Marty C., Houle D., Gagnon C. and Duchesne L. (2011) Isotopic compositions of S, N and C in soils and vegetation of three forest types in Quebec, Canada. *Appl. Geochem.* **26,** 2181-2190.

Matzek V. A. (1999) Differences in nutrient cycling and water availability in soils forming on different substrates: Evidence from coral and volcanic islands in tropical Pacific, M.S. thesis, University of California, Berkeley, CA.

Miller A. J., Amundson R., Burke I. C. and Yonker C. (2004) The effect of climate and cultivation on soil organic C and N. *Biogeochemistry* **67,** 57-72.

Mizutani Y. and Rafter T. A. (1969) Oxygen isotopic composition of sulphates .4. bacterial fractionation of oxygen isotopes in reduction of sulphate and in oxidation of sulphur. *New Zeal. J Sci.* **12,** 69-80.

Mukai H., Tanaka A., Fujii T., Zeng Y. Q., Hong Y. T., Tang J., Guo S., Xue H. S., Sun Z. L., Zhou J. T., Xue D. M., Zhao J., Zhai G. H., Gu J. L. and Zhai P. Y. (2001) Regional characteristics of sulfur and lead isotope ratios in the atmosphere at several Chinese urban sites. *Environ. Sci. Technol.* **35,** 1064-1071.

Murphy S. F. and Stallard R. F. (2012) Hydrology and climate of four watersheds in Eastern Puerto Rico. In *Water quality and landscape processes of four watersheds in Eastern Puerto Rico*: U.S. Geological Survey Professional Paper 1789 (eds. S. F. Murphy and R. F. Stallard). USGS, Reston, VA. pp 43-84.

National Atmospheric Deposition Program (NRSP-3) (2007) NADP Program Office, Illinois State Water Survey, 2204 Griffith Dr., Champaign, IL 61820.

Newman L., Krouse H. R. and Grinenko V. A. (1991) Sulphur isotope variations in the atmosphere. In *Stable Isotopes in the Assessment of Natural and Anthropogenic Sulphur in the Environment* (eds. H. R. Krouse and V. A. Grinenko). SCOPE, vol. 43, Ch. 5. John Wiley and Sons Ltd, Chichester. pp. 133-176.

Norman A. L. (1994) Isotope analysis of microgram quantities of sulfur: Applications to soil sulfur mineralization studies. PhD thesis, Univ. of Calgary, Canada.

Norman A. L., Giesemann A., Krouse H. R. and Jager H. J. (2002) Sulphur isotope fractionation during sulphur mineralization: Results of an incubation-extraction experiment with a Black Forest soil. *Soil Biol. Biochem.* **34,** 1425-1438.

Norman A. L., Belzer W. and Barrie L. (2004) Insights into the biogenic contribution to total sulphate in aerosol and precipitation in the Fraser Valley afforded by isotopes of sulphur and oxygen. *J Geophys. Res.-Atmos.* **109,** D05311, doi:10.1029/2002JD003072.

Novak M., Bottrell S. H., Groscheova H., Buzek F. and Cerny J. (1995) Sulphur isotope characteristics of two North Bohemian forest catchments. *Water Air Soil Poll.* **85,** 1641-1646.

Novak M., Bottrell S. H. and Prechova E. (2001) Sulfur isotope inventories of atmospheric deposition, spruce forest floor and living Sphagnum along a NW-SE transect across Europe. *Biogeochemistry* **53,** 23-50.

Novak M., Buzek F., Harrison A. F., Prechova E., Jackova I. and Fottova D. (2003) Similarity between C, N and S stable isotope profiles in European spruce forest soils: implications for the use of delta S-34 as a tracer. *Appl. Geochem.* **18,** 765-779.

Novak M., Mitchell M. J., Jackova I., Buzek F., Schweigstillova J., Erbanova L., Prikryl R. and Fottova D. (2007) Processes affecting oxygen isotope ratios of atmospheric and ecosystem sulfate in two contrasting forest catchments in Central Europe. *Environ. Sci. Technol.* **41,** 703-709.

Nriagu J. O., Rees C. E., Mekhtiyeva V. L, Lein A. Y., Fritz P., Drimmie R. J., Pankina R. W., Robinson R. W. and Krouse H. R. (1991) Hydrosphere. In *Stable Isotopes in the Assessment of Natural and Anthropogenic Sulphur in the Environment* (eds. H. R. Krouse and V. A. Grinenko). SCOPE, vol. 43, John Wiley and Sons Ltd, Chichester. pp. 177-265.

Ostlund G. (1959) Isotopic composition of sulfur in precipitation and sea water. *Tellus* **11,** 478-480.

Panettiere P., Cortecci G., Dinelli E., Bencini A. and Guidi M. (2000) Chemistry and sulfur isotopic composition of precipitation at Bologna, Italy. *Appl. Geochem.* **15,** 1455-1467.

Patris N., Cliff S. S., Quinn P. K., Kasem M. and Thiemens M. H. (2007) Isotopic analysis of aerosol sulfate and nitrate during ITCT-2k2: Determination of different formation pathways as a function of particle size. *J Geophys. Res.-Atmos.* **112,** D23301, doi:10.1029/2005JD006214.

Pichlmayer F., Schoner W., Seibert P., Stichler W. and Wagenbach D. (1998) Stable isotope analysis for characterization of pollutants at high elevation alpine sites. *Atmos. Environ.* **32,** 4075-4085.

Post W. M., Emanuel W. R., Zinke P. J. and Stangenberger A. G. (1982) Soil carbon pools and world life zones. *Nature* **298,** 156-159.

Post W. M., Pastor J., Zinke P. J. and Stangenberger A. G. (1985) Global patterns of soil-nitrogen storage. *Nature* **317,** 613-616.

Rech J. A., Quade J. and Hart W. S. (2003) Isotopic evidence for the source of Ca and S in soil gypsum, anhydrite and calcite in the Atacama Desert, Chile. *Geochim. Cosmochim. Acta* **67,** 575-586.

Rees C. E., Jenkins W. J. and Monster J. (1978) Sulfur isotopic composition of ocean water sulfate. *Geochim. Cosmochim. Acta* **42,** 377-381.

Romero A. B. and Thiemens M. H. (2003) Mass-independent sulfur isotopic compositions in present-day sulfate aerosols. *J Geophys. Res.-Atmos.* **108,** D16, doi:10.1029/2003JD003660.

Scatena F. N. (1989) An introduction to the physiography and history of the Bisley Experimental Watersheds in the Luquillo Mountains of Puerto Rico. *General Technical Report - Southern Forest Experiment Station,* USDA Forest Service.

Shanley J. B., Mayer B., Mitchell M. J., Michel R. L., Bailey S. W. and Kendall C. (2005) Tracing sources of streamwater sulfate during snowmelt using S and O isotope ratios of sulfate and S-35 activity. *Biogeochemistry* **76,** 161-185.

Stack P. and Rock L. (2011) A delta(34)S isoscape of total sulphur in soils across Northern Ireland. *Appl. Geochem.* **26,** 1478-1487.

Stam A. C., Mitchell M. J., Krouse H. R. and Kahl J. S. (1992) Stable Sulfur Isotopes of Sulfate in Precipitation and Stream Solutions in a Northern Hardwood Watershed. *Water Resour. Res.* **28,** 231-236.

Szynkiewicz A., Modelska M., Jedrysek M. O. and Mastalerz M. (2008) The effect of acid rain and altitude on concentration, delta S-14, and delta O-18 of sulfate in the water from Sudety Mountains, Poland. *Chem. Geol.* **249,** 36-51.

Thode H. G., Monster J. and Dunford H. B. (1961) Sulphur isotope geochemistry. *Geochim. Cosmochim. Acta* **25,** 159-174.

Tichomirowa M. and Heidel C. (2012) Regional and temporal variability of the isotope composition (O, S) of atmospheric sulphate in the region of Freiberg, Germany, and consequences for dissolved sulphate in groundwater and river water. *Isotopes Environ. Health Stud.* **48,** 118-143.

Trust B. A. and Fry B. (1992) Stable sulfur isotopes in plants - a review. *Plant Cell and Environ* **15,** 1105-1110.

Tye A. M. and Heaton T. H. E. (2007) Chemical and isotopic characteristics of weathering and nitrogen release in non-glacial drainage waters on Arctic tundra. *Geochim. Cosmochim. Acta* **71,** 4188-4205.

Uebersax A. (1996) The content and stable isotope systematics of carbon and nitrogen in soil organic matter from elevation transects in Hawaii (USA) and Mt. Kilimanjaro (Tanzania), M.S. thesis, University of California, Berkeley, CA.

van Stempvoort D. R. (1989) The use of stable isotope techniques to investigate the sulfur cycle in upland forests of Central and Southern Ontarion. Ph.D. thesis, University of Waterloo, Waterloo, Ontario, 254 p.

Wadleigh M. A., Schwarcz H. P. and Kramer J. R. (2001) Areal distribution of sulphur and oxygen isotopes in sulphate of rain over eastern North America. *J Geophys. Res.-Atmos.* **106,** 20883-20895.

Wakshal E. and Nielsen H. (1982) Variations of delta-S-34(SO_4), Delta-O-18(H_2O) and Cl. *Earth Planet. Sci. Lett.* **61,** 272-282.

Wang J. K., Solomon D., Lehmann J., Zhang X. D. and Amelung W. (2006) Soil organic sulfur forms and dynamics in the Great Plains of North America as influenced by long-term cultivation and. *Geoderma* **133,** 160-172.

White A. F., Blum A. E., Schulz M. S., Vivit D. V., Stonestrom D. A., Larsen M., Murphy S. F. and Eberl D. (1998) Chemical weathering in a tropical watershed, Luquillo mountains, Puerto Rico: I. Long-term versus short-term weathering fluxes. *Geochim. Cosmochim. Acta* **62,** 209-226.

White A. F., Schulz M. S., Vivit D. V., Blum A. E., Stonestrom D. A. and Anderson S. P. (2008) Chemical weathering of a marine terrace chronosequence, Santa Cruz, California I: Interpreting rates and controls based on soil concentration-depth profiles. *Geochim. Cosmochim. Acta* **72,** 36-68.

Xiao H., Wang Y., Tang C. and Liu C. (2012) Indicating atmospheric sulfur by means of S-isotope in leaves of the plane, osmanthus and camphor trees. *Environmental Pollution* **162,** 80-85.

Yang W. B., Spencer R. J. and Krouse H. R. (1996) Stable sulfur isotope hydrogeochemical studies using desert shrubs and tree rings, Death Valley, California, USA. *Geochim. Cosmochim. Acta* **60,** 3015-3022.

Zhang Y. M., Mitchell M. J., Christ M., Likens G. E. and Krouse H. R. (1998) Stable sulfur isotopic biogeochemistry of the Hubbard Brook Experimental Forest, New Hampshire*, Biogeochemistry* **41,** 259-275.

Zhao F. J., Lehmann J., Solomon D., Fox M. A. and McGrath S. P. (2006) Sulphur speciation and turnover in soils: evidence from sulphur XANES spectroscopy and isotope dilution studies. *Soil Biol. Biochem.* **38,** 1000-1007.

TABLES

Table 1: Study sites characteristics (with references) and isotope data (with references if not measured in this study).

Site	Vegetation	Altitude [masl]	km to coast	MAP [mm]	MAT [°C]	Input $\delta^{34}S$ ‰	g S cm^{-2} (10 cm)	g S cm^{-2} (50 cm)	$\delta^{34}S$ ‰ (10 cm)	$\delta^{34}S$ ‰ (50 cm)	Plant $\delta^{34}S$ ‰
Puerto Rico[1]	Colorado forest	680	12	4200	22	16.49	0.4805	1.5522	13.93	14.74	14.67
	Tabonuco forest	290	7.5	3500	25	16.49	0.6645	2.0698	16.42	17.30	15.41
French Polynesia[2]	Tropical moist forest	3	0.1	2035	25.5	15.30[19]	0.6101		14.29		14.44
Mt. Kilimanjaro[3]	Low montane forest	1829	263	1970	19.0	14.70[20]	0.4600	3.1213	8.45	8.68	
	Montane forest	2454	265	1670	15.0	14.70[20]	0.5426	2.1962	13.81	13.00	
	Tuft grasses	2545	265	1570	14.0	14.70[20]	0.3535	1.5928	14.70	14.31	10.26
	Grassland	2990	270	1320	12.0	14.70[20]	0.1248	1.3031	8.48	8.76	
	Heather	3505	275	1040	9.0	14.70[20]	0.2703		6.09		9.59
	Heather, grass, bare soil	3901	273	820	6.0	14.70[20]	0.3474		6.40		
US East Coast[4]	Deciduous forest	463	340	923	6.1	12.76	0.1612	0.4346	6.73	7.77	3.23
	Deciduous forest	448	295	834	6.8	12.69	0.1279	1.0068	5.65	5.89	3.05
	Deciduous forest	570	170	1064	7.5	14.40	0.0233	0.5912	5.58	6.10	2.00
Sierra Nevada, CA[5]	Oak grassland	470	223	310	17.8	18.26	0.1148		7.21		4.74
	Oak woodland	730	225	570	15.0	18.26	0.1178	0.5820	6.90	6.70	
	Mixed conifer	1240	226	910	11.7	18.26	0.1196	0.8832	7.40	2.71	5.80
	Mixed conifer	1950	233	1055	8.0	18.26	0.0800	0.1499	6.27	6.94	
	Mixed conifer	2890	247	1270	3.3	18.26	0.1399	0.2394	6.30	5.08	5.80
Santa Cruz, CA[6]	Grassland	10	0.7	400	13	14.80	0.3909	1.0402	11.67	11.79	
	Oak grassland	70	1.6	500	13	14.80	0.1426	0.5133	14.20	15.57	7.96
	Oak grassland	90	2.5	600	13	14.80	0.1780	0.5522	15.53	15.97	9.25
	Oak grassland	95	2.0	600	13	14.80	0.4689	1.0882	11.26	13.18	9.77
Kyle Canyon, NV[7]	Creosote	840	385	160	17.9	13.90	0.0881	0.1700	2.71	2.80	7.55
	Joshua Tree	1400	380	326	14.1	13.90	0.0619	0.3065	4.64	5.21	7.58
	Pinyon-Juniper	1750	375	436	11.6	13.90	0.1607	0.6486	5.27	6.15	7.09
	Ponderosa	2150	360	549	9.2	13.90	0.2506	0.9775	5.60	6.35	6.76
Merced, CA[8]	Grassland	320	140	300	16	17.26	0.3183	0.7817	4.23	3.25	3.51
	Grassland	315	132	300	16	17.26	0.1024	0.2702	2.92	1.75	5.23
	Grassland	400	136	300	16	17.26	0.1560	8.0370	3.21	1.24	5.27
	Grassland	270	145	300	16	17.26		0.4345		4.86	5.86
US Great Plains[9]	Native prairie	504	1800	404	6.1	9.39	0.2192	1.0950	-3.29	-1.95	
	Native prairie	439	1900	425	7.8	9.39	0.1963	0.9682	-4.92	-3.26	

Table 1 continued:

Site	Vegetation	Altitude [masl]	km to coast	MAP [mm]	MAT [°C]	Input $\delta^{34}S$ ‰	g S cm^{-2} (10 cm)	g S cm^{-2} (50 cm)	$\delta^{34}S$ ‰ (10 cm)	$\delta^{34}S$ ‰ (50 cm)	Plant $\delta^{34}S$ ‰
	Native prairie	632	1900	496	10.7	9.20	0.3462	1.3564	0.02	0.12	
	Native prairie	546	1900	625	11.7	9.20	0.2816	1.4164	2.61	1.17	
	Native prairie	781	1700	514	11.5	13.12	0.2833	1.2968	-0.12	-0.17	
	Native prairie	1308	1500	395	11.4	12.25	0.1781	0.8975	1.44	10.77	
Baja California, Mexico[10]	Succulents	59	40	141	18.6	13.10[21]	0.0467	0.1584	5.93	6.40	
	Succulents	-0.6	7	115	19.5	13.10[21]	0.0394	0.1005	5.16	5.16	
	Succulents	487	42	122	20.5	13.10[21]	0.0468	0.2085	5.38	4.64	
	Succulents	572	37	97	19.4	13.10[21]	0.1497	0.4216	9.91	8.14	
Andes, Chile[11]	Andean steppe	3370	106	120	3	5.40[22]	0.5099	2.6688	2.70	2.99	
	Submival	4190	138	150	2.5	5.40[22]	0.4196	1.4160	3.70	4.59	
Death Valley[12]	Desert	1000	370	38.1	24.2	3.5[23]					8.40[12]
Las Vegas[12]	Desert	1600	380	114.1	19	6.4[23]					8.66[12]
Costa Rica[13]	Tropical forest		5	5000	26	10.4[13]			12.38[13]		12.61[13]
Hawaii[14]	Tropical forest		5	2500	16	15.6[19]					20.6[14]
Quebec[15]	Sugar maple	330	375	1338	3.58	3.5[15]			5.3[15]	5.5[15]	4[15]
Quebec[15]	Balsam fir	800	400	1172	0.33	3.9[15]			7.1[15]	7.05[15]	3.8[15]
Quebec[15]	Black spruce	400	100	860	0.6	4.1[15]			6.9[15]	6.8[15]	3[15]
Czech Republic[16]	Norway spruce	775	645	900	5.9	9.3[24]			3.05[16]		
France[16]	Norway spruce	1050	465	1200	5.4	5.5[25]			2.7[16]		
Italy[16]	Norway spruce	950	35	1000	8.5	1.8[26]			0.6[16]		
Sweden[16]	Norway spruce	175	70	600	1	4.6[27]			6[16]		
Sweden[16]	Norway spruce	105	5	1200	7.6	5.9[28]			7.15[16]		
Germany[17]	Norway spruce	870	600	1030	5	5.5[25]			6.5[17]		3[17]
Germany[17]	Norway spruce	870	600	1030	5	5.5[25]			-3.75[17]		
Germany[17]	Norway spruce	870	600	1030	5	5.5[25]			4[17]		
China[18]	Urban	1100	700	1179	15.3	-0.2[18]			-3.73[18]		-3.11[18]

References: [1]*Scatena* [1989]; *White et al*. [1998]; *Heartsill-Scaley et al*. [2007]; *Buss et al.* [2010]; *Dosseto et al*. [2012]; *Murphy and Stallard* [2012]; [2]*Matzek* [1999]; [3]*Uebersax* [1996]; [4]*Jersak* [1991]; *Jersak et al*. [1995]; *Jersak et al*. [1997]; worldclimate.com; [5]*Brenner* [1999]; [6]*White et al*. [2008]; [7]*Brenner* [1999]; [8]*Baisden et al*. [2002]; *Brenner* [1999]; [9]*Kelly et al*. [1991]; [10]*Amundson et al*. [1994]; [11]*Latorre et al*. [2003]; worldclimate.com; [12]*Yang et al.* [1996]; [13]*Bern and Townsend* [2008]; [14]*Bern et al.* [2007]; [15]*Marty et al.* [2011]; [16]*Novak et al.* [2003]; [17]*Alewell and Novak* [2001]; [18]*Xiao et al*. [2012]; [19]*Calhoun et al*. [1991]; [20]*Newman et al*. [1991]; [21]*Chukhrov et al*. [1978]; [22]*Rech et al*. [2003]; [23]*Bao and Reheis* [2003]; [24]*Novak et al*. [1995]; [25]*Tichomirowa and Heidel* [2012]; [26]*Zuppi and Bortolami* [1982]; [27]*Andersson et al.* [1992]; [28]*Ostlund* [1959].

Table 2: Summary statistics for the box model results.

Ecosystem property	Minimum	Maximum	Average	Standard deviation	N
$\Delta_{Soil\text{-}Input}$ top 10 cm	-14.34	3.20	-5.79	5.16	53
$\Delta_{Soil\text{-}Input}$ top 50 cm	-16.02	3.15	-6.54	5.56	40
$\Delta_{Plant\text{-}Soil}$ top 10 cm	-6.28	4.83	-0.96	2.89	27
$\Delta_{Plant\text{-}Soil}$ top 50 cm	-7.61	4.75	-1.04	3.47	22

Table 3: Results of significant ($p<0.05$) univariate and multivariate regression analyses of ecosystem properties against climate variables.

Ecosystem property	Intercept	MAP [mm] coefficient	MAT [°C] coefficient	Adjusted R^2	N
All data					
g S cm^{-2} top 10 cm	0.1524	0.00011		0.3027	40
g S cm^{-2} top 50 cm	0.6750	0.00037		0.1894	37
Soil $\delta^{34}S$ ‰ top 10 cm	1.6473	0.0019	0.2208	0.2701	53
Soil $\delta^{34}S$ ‰ top 50 cm	2.3252	0.0029	0.1616	0.2875	41
$\Delta_{Soil\text{-}Input}$ top 10 cm	-5.8275	0.0029	-0.2358	0.2241	53
$\Delta_{Soil\text{-}Input}$ top 50 cm	-5.6819	0.0027	-0.2551	0.1508	40
Plant $\delta^{34}S$ ‰	1.6470	0.0016	0.2816	0.4398	31
Steady-state climosequences only					
g S cm^{-2} top 10 cm	0.1024	0.0001625	-0.001105	0.3773	25
g S cm^{-2} top 50 cm	-0.0835	0.001017	0.02268	0.4896	22
Soil $\delta^{34}S$ ‰ top 10 cm	-4.8258	0.0056	0.4858	0.5028	25
Soil $\delta^{34}S$ ‰ top 50 cm	-3.6137	0.0047	0.4358	0.3897	22
$\Delta_{Soil\text{-}Input}$ top 10 cm	-16.456	0.00359	0.4101	0.3962	25

FIGURES

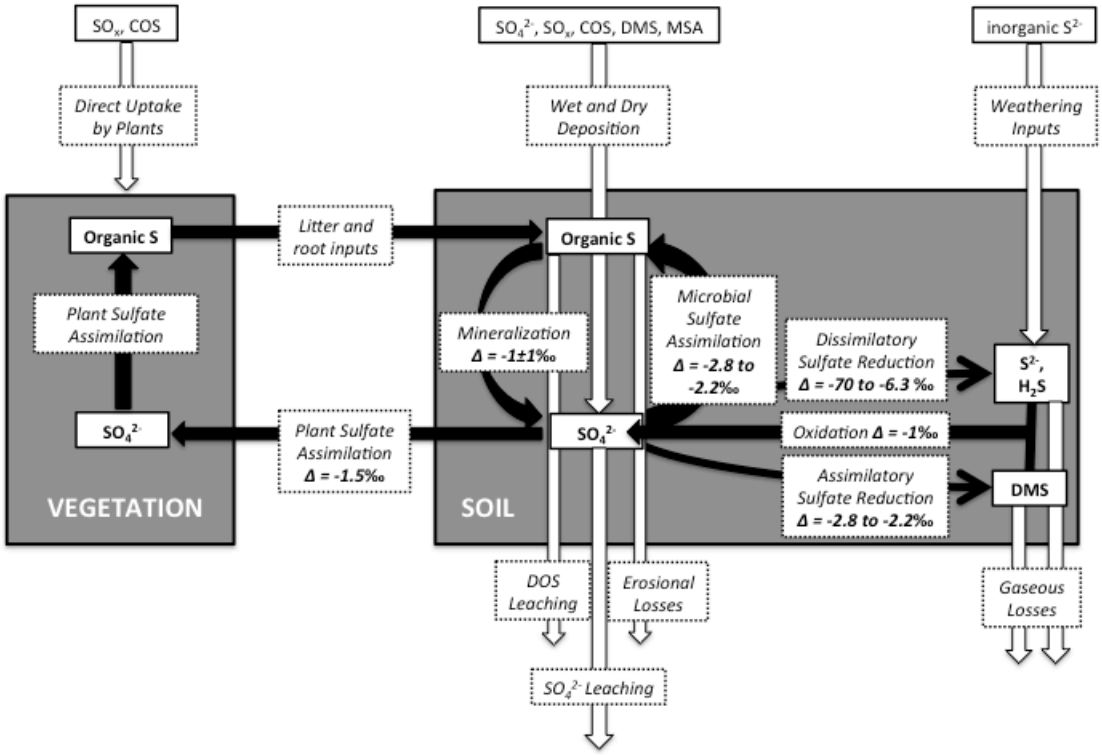

Figure 1: Schematic representation of the terrestrial S cycle, showing major inputs, outputs and in-soil biologically-mediated transformations, as well as the known fractionation factors (Kaplan and Rittenberg, 1964; Trust and Fry, 1992; Norman, 1994; Norman et al., 2002; Brunner and Bernasconi, 2005). White arrows represent inputs to and outputs from the coupled soil-vegetation system. Black arrows represent S transformations within the soil-vegetation system. (COS: carbonyl sulfide; DMS: dimethyl sulfide; DOS: dissolved organic sulfur; MSA: methanesulfonic acid).

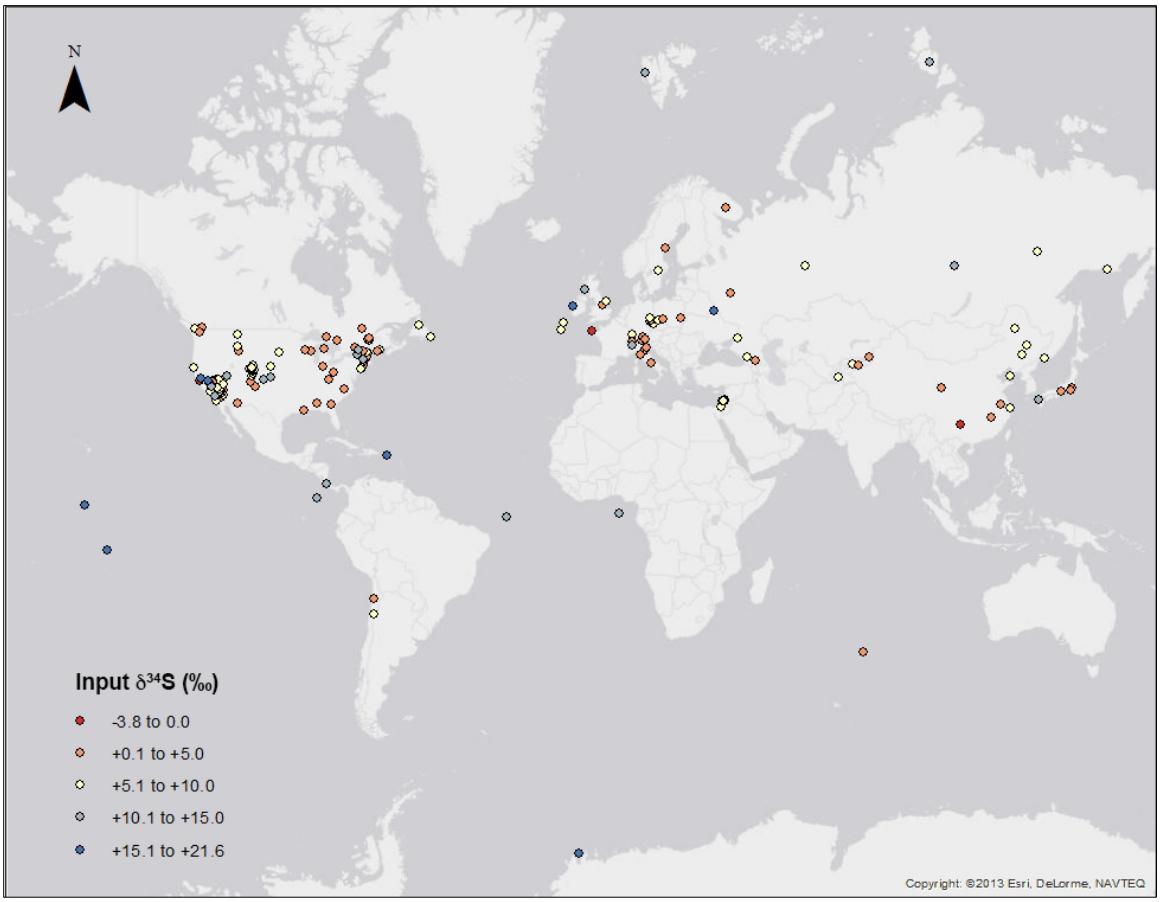

Figure 2: Variation in $\delta^{34}S$ of atmospheric inputs. Data used for making this map comes from this study (rainwater sulfate) and from literature (wet and dry deposition sulfate or SO_2); see Table A1 in the appendix for details and references.

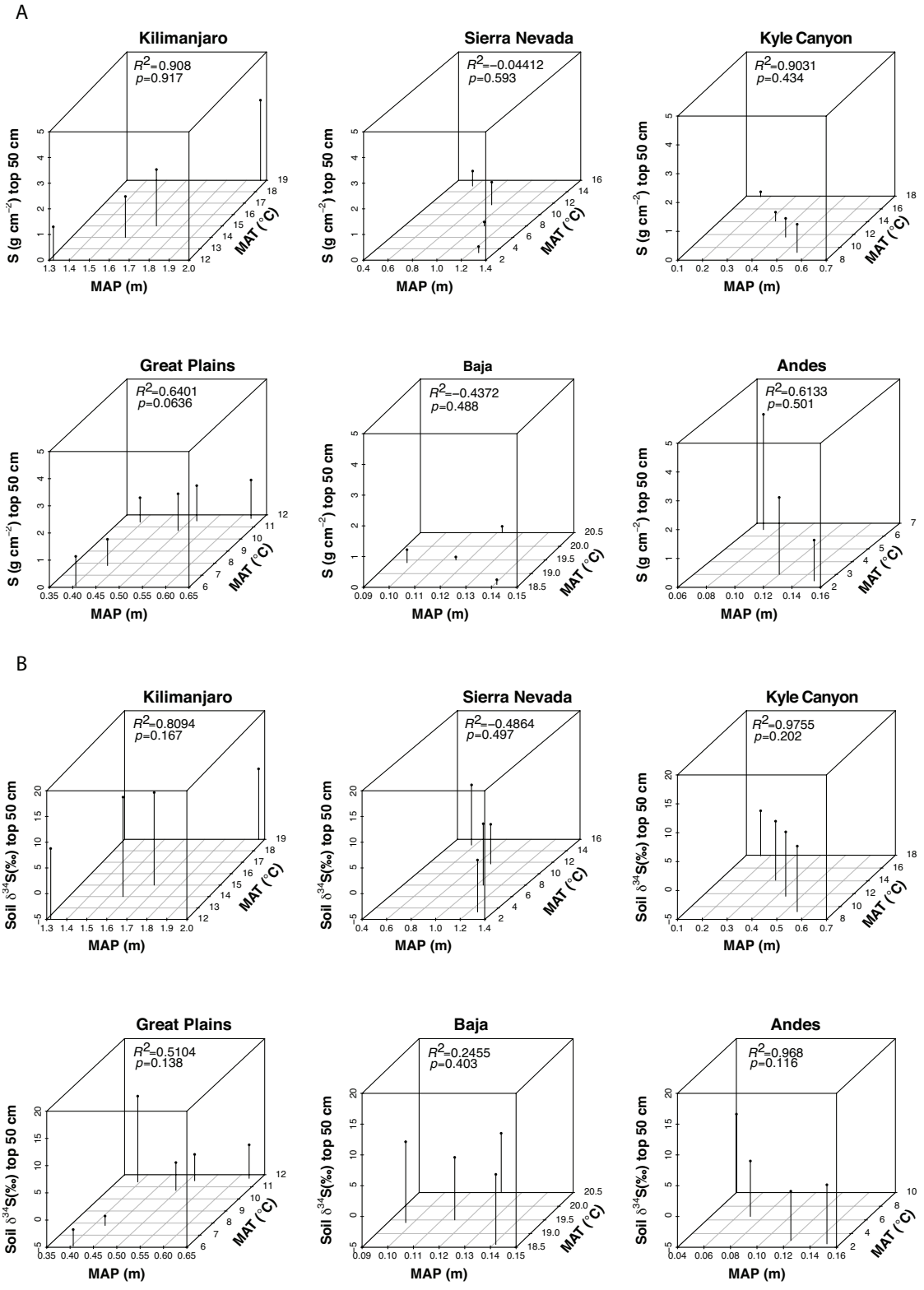

Figure 3 (a-b): Top 50 cm average soil S content (a) and δ^{34}S values (b) versus climate (MAT and MAP) for the six climosequences studied.

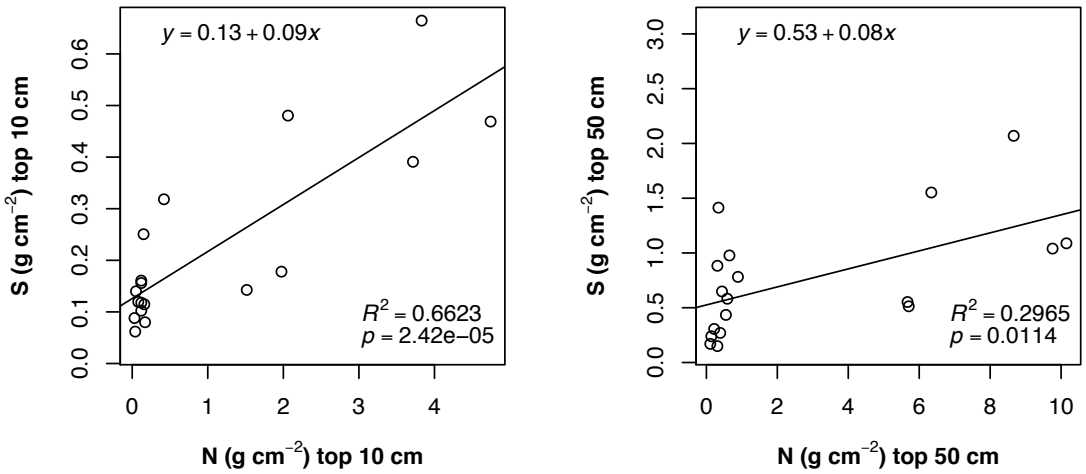

Figure 4: Soil S versus N content for the subset of sites where N data were available.

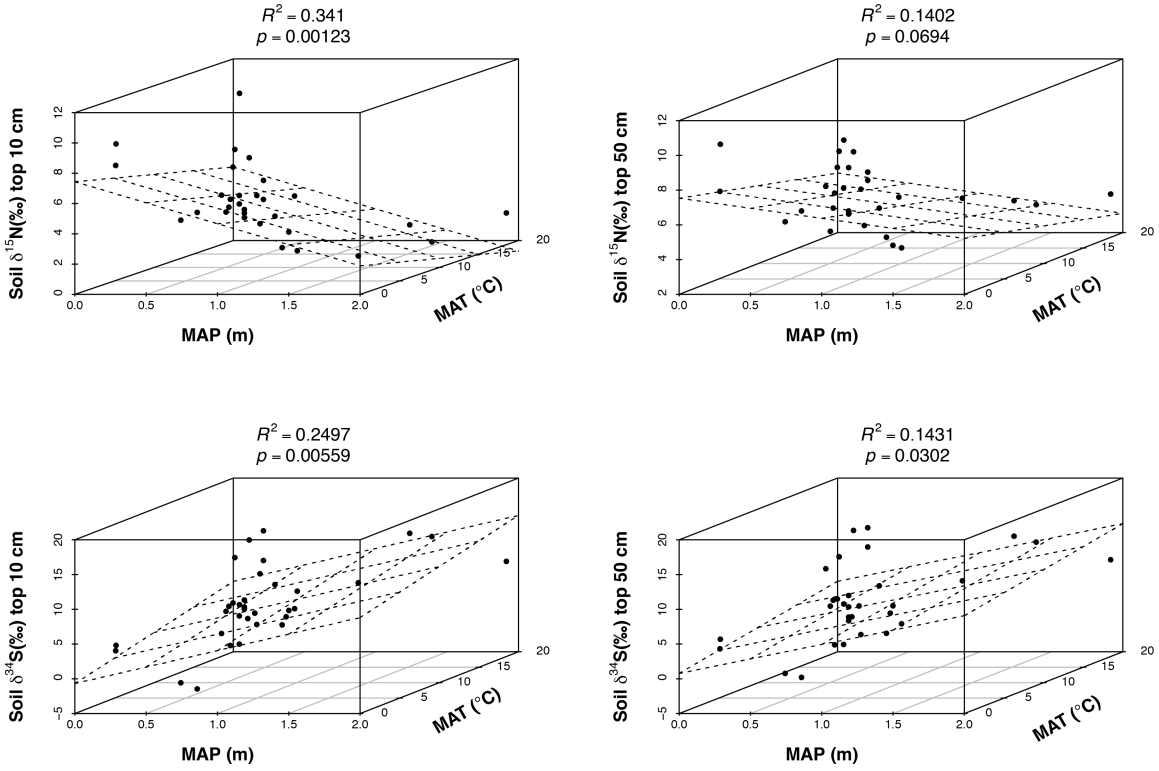

Figure 5: Comparison of soil $\delta^{15}N$ and $\delta^{34}S$ versus climate (MAT and MAP) for the Kilimanjaro, Kyle Canyon, Merced, Santa Cruz and Sierra Nevada sites. Note the different scales for N and S.

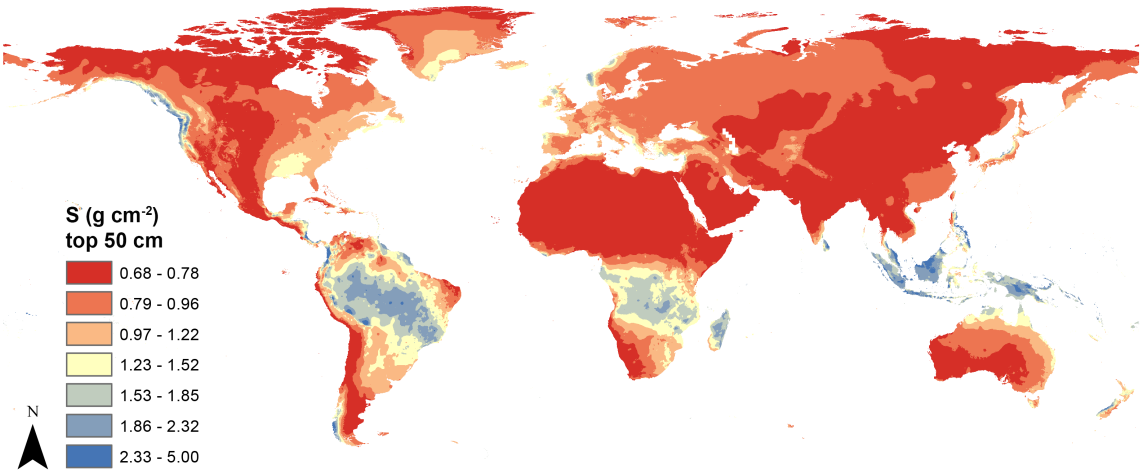

Figure 6: Modeled global distribution of the average soil S content in the upper 50 cm based on mean global temperature data. Model uses linear regression results for all data from Table 3. MAT data is 1950 to 2000 global average from WorldClim, www.worldclim.org/.

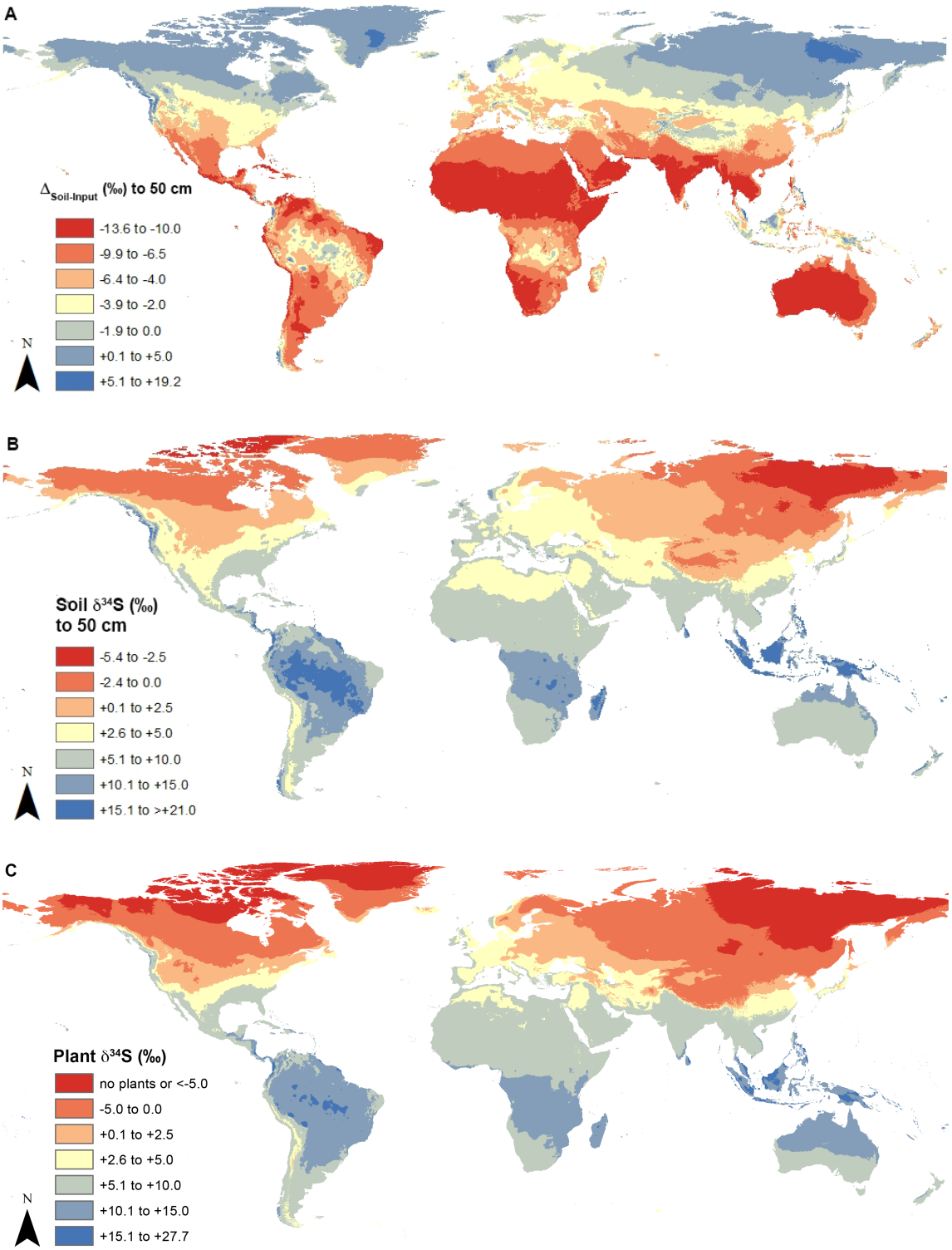

Figure 7 (a-c): Modeled global distribution of (a) $\Delta_{soil\text{-}input}$ in the top 50 cm, (b) total soil $\delta^{34}S$ values in the top 50 cm, and (c) plant (leaf) $\delta^{34}S$ values based on mean global temperature and precipitation data (1950 to 2000 global average from WorldClim, www.worldclim.org/). Model uses linear regression results for all data from Table 3.

APPENDIX

Table A1: $\delta^{34}S$ values of atmospheric inputs represented in the map in Fig. 2.

Location	°Latitude	°Longitude	Input $\delta^{34}S$ ‰	References
Antarctica, George-von-Neumeyer Station	-70.67	-8.27	17.00	*Newman et al* [1991]
Arctic, Severnaya Zemlya	79.50	97.50	10.70	*Astratov et al.* [1986]
Atlantic Ocean	0.00	-30.00	13.70	*Chukhrov et al.* [1978]
Austria, Hintereisferner	46.81	10.77	3.43	*Pichlmayer et al.* [1998]
Austria, Zugspitze	47.42	10.99	3.00	*Pichlmayer et al.* [1998]
Canada, Algoma	47.50	-84.25	2.10	*Wadleigh et al*. [2001]
Canada, British Columbia, Fraser Valley	49.35	-121.50	4.00	*Norman et al*. [2004]
Canada, central Ontario	45.42	-75.69	4.25	*van Stempvoort* [1989]
Canada, Quebec	46.82	-71.22	5.20	*Caron et al*. [1986]
Canada, Quebec, Lake Clair	46.95	-71.67	3.50	*Marty et al*. [2011]
Canada, Quebec, Lake Laflamme	47.28	-71.23	3.90	*Marty et al*. [2011]
Canada, Quebec, Lake Tirasse	49.20	-73.48	4.10	*Marty et al.* [2011]
Canada, Seal Cove, Newfoundland	49.93	-56.37	10.00	*Jamieson and Wadleigh* [2000]
Canada, St. John's, Newfoundland	47.57	-52.68	6.80	*Jamieson and Wadleigh* [2000]
Canada, Straight of Georgia, Saturna Island	49.29	-123.81	9.00	*Norman et al.* [2004]
Canada, Sudbury, Ontario	46.69	-81.01	4.70	*Nriagu and Coker* [1978]
Canada, Vancouver region	49.25	123.11	6.10	*Norman et al*. [2004]
Canada, Washington, Mt. Vernon	48.42	-122.33	2.00	*Norman et al*. [2004]
Caucasus mountains	42.50	45.00	0.70	*Chukhrov et al.* [1977]
Caucasus near Elbrus	43.36	42.44	10.00	*Chukhrov et al*. [1977]
Chile, Atacama Desert, Yungay	-24.00	-70.00	2.00	*Ewing et al.* [2008]
Chile, Atacama Desert	-28.00	-70.00	5.40	*Rech et al*. [2003]
China, Changchun	43.90	125.20	5.55	*Mukai et al*. [2001]
China, Dalian	39.03	121.77	5.80	*Mukai et al.* [2001]
China, Guiyang	26.65	106.63	-0.21	*Xiao and Liu* [2002]; *Xiao et al*. [2012]
China, Harbin	45.75	126.63	6.40	*Mukai et al*. [2001]
China, Nanchang	28.68	115.89	1.00	*Ji and Jiang* [2012]
China, Nanjing	32.05	118.77	3.85	*Mukai et al*. [2001]
China, Shanghai	31.20	121.50	5.35	*Mukai et al*. [2001]
China, Tsukuba	36.03	140.07	0.45	*Mukai et al*. [2001]
China, Waliguan	36.29	100.90	4.20	*Mukai et al*. [2001]
Costa Rica	9.92	-84.08	10.40	*Bern and Townsend* [2008]
Czech Rebublic, Rybarenska slat	49.05	-13.50	5.80	*Novak et al*. [2001]
Czech Republic, Cervena jama	50.63	13.48	8.10	*Novak et al.* [1995]
Czech Republic, Jezeri	50.63	13.48	7.70	*Novak et al.* [2007]

Table A1 continued:

Location	°Latitude	°Longitude	Input $\delta^{34}S$ ‰	References
Czech Republic, Nacetin	50.58	13.25	9.30	*Novak et al*. [1995]
Czech Republic, Ocean	50.35	-12.70	6.70	*Novak et al*. [2001]
Czech Republic, Prague	50.08	14.42	6.90	*Newman et al.* [1991]; *Krouse et al.* [1991]
England, Thorne Moors	53.70	-0.87	4.30	*Novak et al.* [2001]
England, Yorkshire	54.22	-0.10	5.06	*Heaton et al*. [1997]
France, Guisseny, Brittany	48.63	-4.41	-3.80	*Newman et al.* [1991]
Germany, Freiburg	48.00	7.85	5.13	*Tichomirowa and Heidel* [2012]
Germany, Oberbaerenburg	50.80	13.72	4.80	*Tichomirowa and Heidel* [2012]
Germany, Schmorren	51.22	13.13	5.50	*Tichomirowa and Heidel* [2012]
Gulf of Guinea	1.00	4.00	14.70	*Nriagu et al.* [1991]
Iran, Isfahan	52.50	32.50	21.61	*Khademi et al.* [1997]
Ireland, Connemara	53.40	-10.00	17.80	*Novak et al*. [2001]
Israel, central Upper Galilee, Mt. Kenaan	31.50	34.75	5.60	*Wakshal and Nielsen* [1982]
Israel, Nahariyya	33.01	35.10	9.50	*Wakshal and Nielsen* [1982]
Israel, Merom Golan	33.13	35.78	5.00	*Wakshal and Nielsen* [1982]
Israel, Kefar Hanasi	32.98	35.60	5.30	*Wakshal and Nielsen* [1982]
Israel, western Upper Galilee, Elon	33.06	35.22	6.80	*Wakshal and Nielsen* [1982]
Italy, Bologna	44.50	11.35	3.20	*Panetierre et al*. [2000]
Italy, central	42.00	13.55	1.80	*Zuppi and Bortolami* [1982]
Italy, Griesferner	46.99	11.71	3.53	*Pichlmayer et al.* [1998]
Italy, Pisa	43.72	10.40	1.10	*Cortecci and Longinelli* [1970]
Italy, Venice	45.43	12.32	3.00	*Longinelli and Bartelloni* [1978]
Japan, Kurume (rural)	33.18	130.33	12.80	*Newman et al.* [1991]
Japan, Nagoya	35.17	136.92	1.90	*Newman et al.* [1991]
Japan, Tokyo	35.68	139.77	1.70	*Newman et al.* [1991]
Kazakhstan mountains	43.35	79.08	4.10	*Chukhrov et al*. [1977]
Kirgizia mountains	41.76	74.25	6.90	*Chukhrov et al*. [1977]
New Amsterdam Island, Indian Ocean	-37.78	77.53	0.90	*Newman et al.* [1991]
New Zealand, Gracefield	-41.23	174.92	10.90	*Mizutani and Rafter* [1969]
Pacific Ocean, Coco Island	5.52	-87.07	13.10	*Chukhrov et al*. [1978]
Pacific Ocean, Southern hemisphere	-10.00	-150.00	15.60	*Calhoun et al.* [1991]
Poland, Lublin	51.23	22.57	3.70	*Newman et al.* [1991]
Poland, Sudety Mountains	50.74	15.74	4.69	*Szynkiewicz et al*. [2008]
Poland, Karkonosze Mountains	50.75	15.85	7.55	*Jedrysek et al*. [2002]
Poland, Wroclaw	51.12	17.03	3.40	*Gorka et al*. [2008]; *Jedrysek* [2000]
Russia, Kola Peninsula	67.69	35.94	4.00	*Chukhrov et al*. [1977]

Table A1 continued:

Location	°Latitude	°Longitude	Input $\delta^{34}S$ ‰	References
Russia, Magadan region	59.55	150.80	5.80	*Chukhrov et al*. [1977]
Russia, Moscow and Novgrod regions	55.75	37.62	4.00	*Chukhrov et al*. [1977]
Russia, Rostov region	47.23	39.70	7.10	*Gavrishin and Rabinovich* [1971]
Russia, Sakhalin and Vladivostok region	43.13	131.92	5.90	*Chukhrov et al*. [1977]
Russia, Siberia	60.00	105.00	10.60	*Chukhrov et al*. [1977]
Russia, Urals	60.00	60.00	5.40	*Chukhrov et al*. [1977]
Russia, Yakutia	62.04	129.75	6.60	*Chukhrov et al*. [1977]
Scotland, Mull	56.30	-6.28	13.70	*Novak et al*. [2001]
Svalbard, Ny-Alesund	78.90	11.88	12.35	*Tye et al*. [2007]
Sweden	59.27	15.76	5.90	*Ostlund* [1959]
Sweden, Lake Mjosjon watershed	62.65	17.77	4.58	*Andersson et al.* [1992]
Switzerland, Jungfraujoch	46.55	7.98	3.90	*Pichlmayer et al.* [1998]
Switzerland, Monte Rosa	45.94	7.87	11.50	*Pichlmayer et al.* [1998]
Tadhikistan mountains	38.70	70.00	7.20	*Chukhrov et al*. [1977]
US, Alabama, Selma	32.41	-87.02	4.60	Wadleigh et al. (2001)
US, Arizona, Tucson Basin	32.22	-110.93	4.00	*Gu et al.* [2008]
US, California, Bakersfield	35.37	-119.02	5.70	*Bao et al*. [2001]; *Romero and Thiemens* [2003]
US, California, La Jolla	32.84	-117.28	9.90	*Lee and Thiemens* [2001]; *Romero and Thiemens* [2003]
US, California, San Francisco Bay	37.78	-122.42	-1.30	*Ludwig* [1976]
US, California, White Mountain Research Station	37.50	-118.20	4.40	*Lee and Thiemens* [2001]; *Romero and Thiemens* [2003]
US, California, Trinidad Head	41.00	-124.00	5.65	*Patris et al*. [2007]
US, California, Kings River Experimental Watershed	37.06	-119.18	17.26	this study
US, California, Tanbark Flat	34.21	-117.76	13.46	this study
US, California, Sequoia National Park	36.57	-118.78	12.82	this study
US, California, Davis	38.54	-121.78	18.66	this study
US, California, Yosemite National Park	37.80	-119.86	18.26	this study
US, Californian, Death Valley	36.24	-116.83	6.57	*Yang et al.* [1996]
US, California	33.74	-115.93	5.50	*Bao and Reheis* [2003]
US, California	33.74	-115.93	4.50	*Bao and Reheis* [2003]
US, California	34.42	-115.29	6.30	*Bao and Reheis* [2003]
US, California	34.95	-115.61	6.30	*Bao and Reheis* [2003]
US, California	35.26	-115.73	5.00	*Bao and Reheis* [2003]
US, California	35.32	-116.12	1.70	*Bao and Reheis* [2003]

Table A1 continued:

Location	°Latitude	°Longitude	Input $\delta^{34}S$ ‰	References
US, California	35.31	-116.14	5.40	*Bao and Reheis* [2003]
US, California	35.82	-116.20	8.30	*Bao and Reheis* [2003]
US, California	35.97	-116.23	7.20	*Bao and Reheis* [2003]
US, California	36.56	-116.88	3.50	*Bao and Reheis* [2003]
US, California	36.58	-116.84	4.90	*Bao and Reheis* [2003]
US, California	36.36	-117.94	4.80	*Bao and Reheis* [2003]
US, California	36.22	-117.95	7.30	*Bao and Reheis* [2003]
US, California	36.03	-117.92	5.00	*Bao and Reheis* [2003]
US, California	36.97	-118.31	6.40	*Bao and Reheis* [2003]
US, California	37.02	-118.17	5.10	*Bao and Reheis* [2003]
US, Colorado, Wolf Creek	37.50	-106.80	4.00	*Hidy* [2003]
US, Colorado, Brumley	39.00	-106.50	5.70	*Hidy* [2003]
US, Colorado, Yampa Valley	40.50	-107.20	6.20	*Hidy* [2003]
US, Colorado, Fremont Pass	39.67	-106.20	5.30	*Hidy* [2003]
US, Colorado, Brooklyn Lake	40.17	-106.20	5.70	*Hidy* [2003]
US, Colorado, Phantom Valley	40.33	-105.80	5.60	*Hidy* [2003]
US, Colorado, Mt. Zirkel	40.30	-106.60	6.10	*Hidy* [2003]
US, Colorado, Mt. Zirkel Wilderness area	40.50	-106.60	6.00	*Hidy* [2003]
US, Colorado, Mt. Zirkel north	40.83	-106.60	6.30	*Hidy* [2003]
US, Colorado, Bent County	38.12	-103.12	12.25	this study
US, Connecticut, New Haven	41.31	-72.92	4.20	*Newman et al.* [1991]; *Krouse et al.* [1991]
US, Georgia, Uvalda	32.04	-82.51	4.30	*Wadleigh et al.* [2001]
US, Illinois, Rockport	41.13	-85.13	2.60	*Wadleigh et al.* [2001]
US, Indiana, Fort Wayne	41.08	-85.14	2.4	*Wadleigh et al.* [2001]
US, Kansas, Scott County	38.67	-100.91	13.12	this study
US, Kentucky, Morehead	38.18	-83.44	3.25	*Wadleigh et al.* [2001]
US, Louisiana, Baton Rouge	30.41	-90.82	1.10	*Jenkins and Bao* [2006]
US, Maine, Bear Brook Watershed	44.87	-68.11	5.9	*Stam et al*. [1992]
US, Maine, Winterport	44.66	-68.90	3.5	*Wadleigh et al.* [2001]
US, Massachusetts, Turner's Falls	42.60	-72.56	4.05	*Wadleigh et al.* [2001]
US, Michigan, Gaylord	45.03	84.67	3.00	*Wadleigh et al.* [2001]
US, Montana, west/central	45.67	-111.00	6.20	*Hidy* [2003]
US, Montanta, northwest	48.00	-111.00	5.30	*Hidy* [2003]
US, Nebraska, Lincoln County	41.06	-100.75	9.20	this study
US, Nevada, Great Basin National Park	39.01	-114.22	13.9	this study
US, Nevada	36.89	-116.36	6.30	*Bao and Reheis* [2003]
US, Nevada	36.89	-116.36	2.30	*Bao and Reheis* [2003]

Table A1 continued:

Location	°Latitude	°Longitude	Input $\delta^{34}S$ ‰	References
US, Nevada	36.89	-116.36	6.80	*Bao and Reheis* [2003]
US, Nevada	36.90	-116.36	7.80	*Bao and Reheis* [2003]
US, Nevada	36.89	-116.35	7.50	*Bao and Reheis* [2003]
US, Nevada	37.46	-116.35	4.50	*Bao and Reheis* [2003]
US, Nevada	37.46	-116.35	7.60	*Bao and Reheis* [2003]
US, Nevada	36.79	-116.46	3.80	*Bao and Reheis* [2003]
US, Nevada	36.52	-116.11	2.90	*Bao and Reheis* [2003]
US, Nevada	36.63	-116.74	4.40	*Bao and Reheis* [2003]
US, Nevada	36.64	-116.78	3.30	*Bao and Reheis* [2003]
US, Nevada	37.87	-116.62	5.20	*Bao and Reheis* [2003]
US, Nevada	36.38	-115.32	6.80	*Bao and Reheis* [2003]
US, Nevada	36.31	-115.44	6.50	*Bao and Reheis* [2003]
US, Nevada	36.31	-115.44	5.80	*Bao and Reheis* [2003]
US, Nevada	35.54	-115.07	5.00	*Bao and Reheis* [2003]
US, Nevada	37.04	-116.87	7.70	*Bao and Reheis* [2003]
US, Nevada	37.02	-117.01	6.50	*Bao and Reheis* [2003]
US, Nevada	37.69	-117.26	6.20	*Bao and Reheis* [2003]
US, Nevada	36.99	-117.34	6.50	*Bao and Reheis* [2003]
US, Nevada	38.09	-117.11	7.30	*Bao and Reheis* [2003]
US, Nevada	38.15	-116.63	10.70	*Bao and Reheis* [2003]
US, Nevada	38.18	-116.54	4.40	*Bao and Reheis* [2003]
US, Nevada	38.18	-116.42	6.20	*Bao and Reheis* [2003]
US, Nevada	36.99	-115.00	8.80	*Bao and Reheis* [2003]
US, Nevada	37.04	-115.05	5.50	*Bao and Reheis* [2003]
US, Nevada	37.87	-118.18	7.70	*Bao and Reheis* [2003]
US, New Hampshire, Hubbard Brook Experimental Forest	43.95	-71.72	4.20	*Alewell et al.* [1999]
US, New Hampshire, Sutton	43.33	-71.95	4.0	*Wadleigh et al.* [2001]
US, New Mexico, Gallegos Peak	36.50	-105.50	3.80	*Hidy* [2003]
US, New York, Moss Lake	43.79	-74.84	12.76	this study
US, New York, Akwesasne Mohawk-Fort Covington	44.92	-74.48	12.69	this study
US, New York, Eagle Bay	43.77	-74.82	2.60	*Wadleigh et al.* [2001]
US, New York, Long Island	40.80	-73.30	5.30	*Newman et al.* [1991]; *Krouse et al.* [1991]
US, New York City	40.67	-73.94	8.50	*Newman et al.* [1991]; *Krouse et al.* [1991]
US, North Carolina, Raleigh	35.82	-78.64	3.85	*Wadleigh et al.* [2001]
US, Ohio, Zanesville	39.95	-82.01	2.50	*Wadleigh et al.* [2001]
US, Pennsylvania, Tunkhannock	41.54	-75.95	3.30	*Wadleigh et al.* [2001]
US, Puerto Rico, Luquillo	18.27	-65.76	16.49	this study

Table A1 continued:

Location	°Latitude	°Longitude	Input $\delta^{34}S$ ‰	References
US, South Dakota, Beadle County	44.36	-98.29	9.39	this study
US, Vermont, Sleepers River Research Watershed	44.41	-72.02	5.60	*Shanley et al.* [2005]
US, Vermont, Underhill Center	44.51	-72.90	3.40	*Wadleigh et al.* [2001]
US, Vermont, Bennington County	42.88	-73.16	14.40	this study
US, Wisconsin, Clintonville	44.62	-88.76	2.00	*Wadleigh et al.* [2001]
US, Wisconsin, Longwoods	44.91	-90.61	2.50	*Wadleigh et al.* [2001]
US, Wyoming, West Glacier Lake	41.50	-106.20	5.6	*Finley and Drever* [1995]
US, Wyoming, Yellowstone	44.50	-110.5	5.00	*Hidy* [2003]

Chapter 3

Decoupling of sulfur and nitrogen cycling due to biotic processes in a tropical rainforest

Abstract

In this study, we examined the terrestrial ecosystem sulfur (S) cycle in the wet tropical Luquillo Experimental Forest (LEF), Puerto Rico. In two previously instrumented watersheds, we used chemical and isotopic measurements of carbon (C), nitrogen (N) and S to explore the inputs, in-soil processing, and losses of S through comparison to the N cycle. We found that ecosystem S originated mainly from atmospheric deposition, with a flux of 2.2 and 1.8 g S/m^2/yr at the two sites respectively. To examine the fate of the S once it enters the soil, we used an advection model to describe the isotopic fractionation associated with downward movement of organic matter. This model worked well for N, but the assumption of a constant fractionation factor α with depth failed to describe S transformations. This result reveals a fundamental difference between N and S cycling in these soils, indicating that different processes with different isotope fractionation factors drive S cycling. Pore water data suggest the co-occurrence of at least three major S-fractionating processes in these soils: plant uptake, mineralization and bacterial sulfate reduction. The rates and relative importance of these processes vary in time and space. The sites differ mostly with respect to two soil-forming factors: parent material (quartz diorite vs. volcaniclastics) and topography. Of these two, only topography appears to impact S cycling by influencing redox conditions: C, N and S content decrease downslope at all sites, and the Bisley lower slope shows evidence of bacterial sulfate reduction. S cycling, particularly the transport of S through soil, appears decoupled from that of C and N, and subsurface S concentrations increase with depth. S biogeochemistry in the LEF reflects mostly the high rainfall (which dictates the types and rates of processes), and will therefore directly respond to any changes in rainfall due to deforestation or climate change.

1. Introduction

Wet tropical ecosystems benefit from plentiful energy and water, but must adapt to the constraints of nutrient availability. Nutrients are commonly categorized as either rock-derived (e.g. P, Ca, K) or atmospherically-derived (e.g. N), but these distinctions become blurred in ecosystems downwind of dust sources, such as in Puerto Rico (McDowell et al., 1990; Pett-Ridge et al., 2009). Understanding the role and processing of atmospherically-derived nutrients is particularly important in the wet tropics, where depletion rates of rock and soil-derived nutrient pools are high, and ecosystem productivity largely depends on external inputs (Chadwick et al., 1999).

This paper addresses the geochemical cycling in a wet montane forest of one of the lesser-studied soil nutrients, sulfur (S), and compares it to the better-known cycles of carbon (C) and nitrogen (N). At the Luquillo Experimental Forest (LEF) in Puerto Rico, studies have focused on rates of chemical weathering and solute loss (e.g. White et al., 1998; Murphy et al., 1998; Schulz et al., 1999; Buss et al., 2008), and on the sources and cycling of nutrients such as N and P (e.g. Silver et al., 1994; Pett-Ridge et al., 2009; Buss et al., 2010). Sulfate and/or total S concentrations have been previously measured at the LEF in precipitation (Mcdowell et al., 1990; Asbury et al., 1994; White et al., 1998; Heartsill-Scalley et al., 2007), soil and saprolite (Cox et al., 2002; White et al., 1998; Stanko-Golden and Fitzgerald, 1991), and major streams (White et al., 1998; Mcdowell and Asbury, 1994; Bhatt and McDowell, 2007). Here, we integrate and expand on these previous studies and use stable S isotope measurements in the coupled precipitation-soil-vegetation system as tracers for sources and in-soil processes. Additionally, we present new C and N isotope data and discuss the interactions and differences between the C, N and S cycles.

2. Sulfur Cycling in Terrestrial Ecosystems

The geochemical balance of an element is driven by inputs and outputs, and its distribution within a system is driven by transformations occurring within the plant/soil cycle (e.g. Vitousek and Stanford, 1986). Like N, S has a complex geochemical cycle for two main reasons. First, S exists in a wide range of valence states (from -2 to +6), and can participate in intricate biochemical reactions, some of which are challenging to elucidate (Norman et al., 2002; Brunner and Bernasconi, 2005; Bradley et al., 2011; Sim et al., 2011). Second, S is an essential nutrient, but soils can suffer both from S deficiency (Acquaye and Beringer, 1989; Tabatabai, 1984), and from S excess (via pollution) (Likens et al., 2002).

Fig. 1 depicts the terrestrial ecosystem S cycle based on our current understanding (Trust and Fry, 1992; Likens et al., 2002; Norman et al., 2002; Brimblecombe, 2003; Goller et al., 2006). In most ecosystems, S originates from wet and dry deposition mainly as sulfate, but also as reduced S gases; rock weathering is rarely a significant source (Bern and Townsend, 2008). Within the soil, abiotic processes can affect soil S speciation (via abiotic oxidation), solubility and bioavailability (via adsorption/desorption, mineral precipitation/dissolution and hydration during wetting/drying cycles). S can also undergo microbially-mediated transformations such as: (1) dissimilatory sulfate reduction, (2) assimilatory sulfate reduction, (3) oxidation of reduced S, (4) sulfate assimilation, and (5) organic S mineralization (e.g. Norman et al., 2002). Plants preferentially take up soil S as sulfate (Trust and Fry, 1992; Brimblecombe, 2003) and assimilate it as organic S, which is then returned to the soil through litterfall and root exudates. Soil organic S (from microbial or plant assimilation) is the largest S reservoir in most soils, and includes arylsulfates, phenolic sulfates, sulfated polysaccharides and lipids, the amino acids methionine and cysteine, sulfoxides, sulfones, and sulfenic, sulfinic and sulfonic acids (Brimblecombe, 2003). The main S losses from the ecosystem include leaching of sulfate or dissolved organic S (DOS), emissions of reduced S gases such as dimethyl sulfide (DMS) or hydrogen sulfide (H_2S), and erosional losses. With respect to these combined

processes, the residence time for S in temperate hardwood forest soils is ~ 9 years (Likens et al., 2002).

Each step of the S cycle has the potential to fractionate the stable S isotopes, as reflected in $\delta^{34}S$ values:

$$\delta(‰) = (\frac{R_{Sample}}{R_{Standard}} - 1) \cdot 1000, \quad (1)$$

where R is the ratio of the less common to the more common isotope. For $\delta^{34}S$, R is the ratio of ^{34}S to ^{32}S and the standard is Canon Diablo Troilite (CDT) (Thode et al., 1961). Isotope fractionation is described by the fractionation factor α:

$$\alpha = \frac{R_{Product}}{R_{Substrate}}, \quad (2)$$

and the Δ value:

$$\Delta = \delta_{Product} - \delta_{Substrate}. \quad (3)$$

The rates and isotope values of the integrated inputs and losses determine the ecosystem S content and isotopic composition at steady state. For coastal environments, major sources of S are seasalt sulfate with a $\delta^{34}S$ value of 21‰ (Rees et al., 1978), and non-seasalt sulfate formed by the oxidation of reduced biogenic S compounds, with an average $\delta^{34}S$ of 15.6 ± 3.1‰ (Calhoun et al., 1991) (Table 1). The largest S isotope fractionations observed in nature occur during microbial dissimilatory sulfate reduction, which can deplete the sulfide products by up to 70‰ (Brunner and Bernasconi, 2005). Most other biotic and abiotic processes (Table 2) have α factors close to 1 (i.e. little to no fractionation). Despite their generally small magnitude, biological fractionations are significant because they all operate in the same direction: microbes and plants prefer the lighter isotope in their metabolic pathways, therefore $\delta^{34}S$ values tend to decrease in products of S cycling compared to the substrates. Lower $\delta^{34}S$ values in the soil and plant system compared to the atmospheric inputs thus identify in-soil biological processes.

3. Site Description

The Luquillo Experimental Forest (LEF) (18°18'N, 65°50'W, referenced to the NAD83 datum, encompassing the El Yunque National Forest and the El Toro Wilderness Area) is a Long-Term Ecological Research (LTER) and Critical Zone Observatory (CZO) site, with a long history of research (e.g. Scatena, 1989; McDowell et al., 1990; Silver et al., 1994; White et al., 1998). The LEF is a warm and humid tropical environment. Mean annual precipitation (MAP) increases with elevation, ranging from about 2500 mm to over 5000 mm at the highest elevation of 1074 m (Scatena, 1989; McDowell and Asbury, 1994). Rainfall is significant year round, although January through April, and especially March, are drier than the rest of the year (Heartsill-Scalley et al., 2007). The wettest months are May and August through November (McDowell and Estrada-Pinto, 1988; McDowell et al., 1990; McDowell and Asbury, 1994; Garcia-Martino et al., 1996). Most rainfall occurs as frequent, short, high intensity events (White et al., 1998; Scatena, 1989; Buss et al., 2010). Convective boundary layer storms with strong orographic effects dominate (White et al., 1998), but northeasterly trade winds, winter cold fronts, tropical storms, depressions and hurricanes also affect the region (Heartsill-Scalley et al., 2007).

Winds blow predominantly from the northeast in June through November, and northern cold fronts occasionally reach the island from December through May (Garcia-Martino et al., 1996). The human land use in the area is varied (Scatena, 1989; Bhatt and McDowell, 2007), and includes the introduction of non-native bamboo in the 1930s and 1940s for slope stabilization alongside roads, cattle grazing, coffee growing, timber extraction, subsistence farming, and charcoal production in the 1800s and 1900s (Murphy et al., 2012).

Our study focused on two LEF watersheds instrumented by the USGS (White et al., 1998; Buss et al., 2011; Buss and White, 2012): Icacos (mature Colorado forest on quartz diorite) and Bisley (mature Tabonuco forest on volcaniclastics) (Figure 2). Each site has installations in a transect from a hillslope nose downslope to the adjacent stream channel – a toposequence of sites. At the Icacos site, White et al. (1998) installed cup and plate tension lysimeters at three topographic locations on the Guaba Ridge: ridgetop, steep hillslope (~50% grade, downhill from the ridgetop) and ridge shoulder (moderate slope, ~25% grade, uphill from the ridgetop) – sites LG-1, LG-2 and LG-3, respectively. At the Bisley site, Buss et al. (2011) developed a similar installation on a ridgetop, upper slope and lower slope (riparian) (sites B1S1, B1S2 and B1S4 respectively). Additionally, ground water wells were installed at both sites (Buss and White, 2012). These two sites have similar depositional S source chemistry, as well as similar climatic and environmental histories.

The Icacos site (Fig. 3) is located on the shoulder of the Guaba ridge in the catchment of the Guaba stream, a tributary of Rio Icacos (see White et al., 1998, for a detailed description of the site). The site is above the average cloud condensation level of 600 m (Cox et al., 2002). The watershed is underlain by quartz diorite, a parent material rich in quartz and plagioclase, with moderate amounts of biotite, hornblende, K-feldspar, magnetite and apatite (Seiders, 1971; Murphy et al., 1998; White et al., 1998; Turner et al., 2003; Buss et al., 2005). Weathering rates are the highest ever measured for granitic terrains: long-term average physical denudation rates range from 25-50 m/Ma on relatively stable ridgetops (Brown et al., 1995) to 60-600 m/Ma on hill slopes affected by periodic landslides (Larsen, 1997); average chemical denudation rate estimates include 58 m/Ma (White et al., 1998), 65 m/Ma (Turner et al., 2003) and 75 m/Ma (McDowell and Asbury, 1994). Soils are somewhat poorly drained, and typically range in thickness from 50-100 cm, but can occasionally exceed 1.5 m (Murphy et al., 2012). Icacos soils are a mix of Ultisols (Boccheciamp, 1977) and Inceptisols (Huffaker, 2002; Soil Survey Staff, Web Soil Survey). The profile we investigated was a Plinthic Haplohumult, closely matching the Los Guineos series (very fine, kaolinitic, isothermic Humic Haplodox).

Bisley (Fig. 4) is located within the Rio Mameyes drainage system on volcaniclastic bedrock (Scatena, 1989), at an elevation below the average cloud condensation level. The terrain is generally steep, with slopes over 45% covering 50% of the drainage (Scatena, 1989). Soils are well drained on convex slopes, and somewhat poorly drained on concave slopes (Murphy et al., 2012). The soils are mapped as clay-rich Ultisols (Scatena, 1989; Johnston, 1992; Cox, et al, 2002; Soil Survey Staff, Web Soil Survey). The profile we investigated was a Typic Haplohumult, corresponding to the Humatus series.

4. Methods

4.1 Sample collection

Sampling began in June 2010. Field descriptions and sampling followed standard field methods (Schoeneberger et al., 2002). At the highest topographic position at each site, we excavated trenches to 2 m and sampled the soil by horizon, including the humus layer. At all hillslope positions, we collected two 1.5 m-deep hand-augered cores and fresh leaf litter from the forest floor. During the initial field campaign, we sampled all operational lysimeters. Subsequently, four lysimeters in the upper 2 m of the soil at each subsite were sampled monthly from February 2011 until February 2012, whenever water was present. The aim was to collect water at 15, 60, 150 and 180 cm; however, if functional lysimeters were unavailable at those depths at a site, we used the closest functional ones instead (Table 5).

Precipitation (openfall) was sampled monthly from June 2010 to March 2012, and then again in June 2012, at a station 2 km east of the Icacos site on Pico del Este (elevation 1051 m, MAP 4436 mm averaged over the period 1970-1994, Garcia-Martino et al. (1996)). The collectors were emptied weekly, thus each sample represents the average (i.e. combined wet and dry) deposition for the preceding week. Stream water was collected three times from the Guaba and Bisley streams at baseflow in February, March and June 2012, and a groundwater sample was collected in August 2012 from the groundwater well (LGW1) at the Icacos site. It was not possible to retrieve enough water for isotope analyses from the groundwater well at Bisley, which is frequently dry due to the fluctuating water table.

4.2 Sample processing and analysis

Soils were stored at room temperature in sealed bags. For total soil S isotope and geochemical analysis, splits of the soil samples were dried at 60°C overnight, sieved to <2 mm, and ground with a mortar and pestle. Plant-available sulfate was extracted from splits of the unprocessed samples by shaking the soils for a minimum of 4 hours in a 1:7 soil to deionized water mixture, centrifuging for 30 minutes at 3000 rpm, then filtering the supernatant to 0.45 μm glass microfiber filters. Plant samples were kept frozen then freeze-dried and pulverized in a ball mill.

Water samples (rain and pore water) were shipped frozen from Puerto Rico to Berkeley, then filtered in the lab to 0.45 μm within a few days of sampling, and stored refrigerated until further use. Only water samples with a volume equal to or greater than 500 ml were processed for isotope measurements, to ensure large enough quantities of sulfate. In order to extract sulfate for isotope analysis, filtered water samples were heated in a warm water bath, and a 1M $BaCl_2$ solution was added in excess (in a quantity equal to approximately 10% of the sample volume). After 24 hours, the samples were acidified with a few drops of 1N HCl to dissolve carbonates then filtered again on a 0.45 μm filter to collect the $BaSO_4$ precipitate. Because the samples were low in S, it was impossible to collect the $BaSO_4$ precipitate off the filter; therefore, the entire surface of the filter was scraped off and analyzed in the elemental analyzer/mass spectrometer. The S content of blank filter samples was below the detection limit.

Anion chemistry of the soil extracts and water samples was measured on a Dionex ICS-1500 ion chromatograph with an IonPac AS9-HC 4 mm column, a 9 mM sodium bicarbonate eluent at a flow rate of 1.0 mL/min and an international seven anion standard from Dionex. The analytical precision of the instrument in the range of values measured was ±10%.

Dry and ground soil and plant samples were analyzed for C and N contents (% dry weight) and stable isotope ratios ($\delta^{13}C$ and $\delta^{15}N$) via elemental analyzer/continuous flow isotope ratio mass spectrometry using a CHNOS Elemental Analyzer (Vario ISOTOPE Cube, Elementar, Hanau, Germany) coupled with an IsoPrime100 IRMS (Isoprime, Cheadle, UK). The reference material NIST SMR 1547 (peach leaves) was used as calibration standard. These isotope analyses were conducted at the Center for Stable Isotope Biogeochemistry, University of California, Berkeley. Long-term external precision for C and N isotope analyses is 0.10‰ and 0.15‰, respectively.

The total S concentration and $\delta^{34}S$ values of soils and plants, and the $\delta^{34}S$ value of sulfate in water samples, were determined using the SO_2 EA-combustion-IRMS method on a GV Isoprime isotope ratio mass spectrometer coupled with an Eurovector Elemental Analyzer (model EuroEA3028-HT). These measurements were performed at the Laboratory for Environmental and Sedimentary Isotope Geochemistry (LESIG), University of California at Berkeley. Briefly, a small amount of powdered sample containing a minimum of 2 μg S mixed with V_2O_5 catalyst was thermochemically decomposed with copper wires at 1020°C, and the isotopic composition of the resulting SO_2 gas was measured. Water vapor was removed with a $Mg(ClO_4)_2$ trap and CO_2 was eluted out using a dilutor. Several replicates of the international standard NBS127 and two lab standards (both pure $BaSO_4$) were run with each batch of samples. The long-term analytical precision of this method is better than 0.2‰.

Due to the lack of certified soil and organic material standards for S isotope analyses, we selected several different material types and cross-validated the results from the LESIG lab against measurements done by other labs. The results, displayed in Table A1 in the Appendix, show that the averages obtained by this lab agree well with those from other labs, and with good precision.

5. Results

5.1 Field observations

Both soil profiles we excavated had high clay contents, reddening and loss of rock structure (Tables 6 and 7). The granitic soil at Icacos had about 5% less clay than the volcanic-derived soil at Bisley. In addition, the clay content of the Icacos soil sharply declined below 111 cm, whereas it remained high to the depth of excavation (158 cm) at Bisley. In the upper 16-17 cm, both soils were rich in humus and highly mixed by earthworms. Below 17 cm, several significantly darker areas throughout the soil profile indicate that humus also accumulated in some subsurface horizons. Below the well-mixed biotic horizons, clay content increased and the soil color indicated gleying, suggesting at least periodic reducing conditions. The Rio Icacos soil had a prominent zone of plinthite (red areas enriched in Fe (III) oxide adjacent to gray, Fe (III)-depleted zones, formed in

response to fluctuating water tables and redox conditions) that lay above a 10 cm-thick layer displaying Mn oxide stains. In general, both soils showed evidence of reducing conditions due to periodic saturation, and adequate C for microbial metabolism and oxygen consumption.

5.2 Litter and humus chemistry

C, N and S contents and stable isotope values vary widely among vegetation types (Table 8). Palo Colorado (*Cyrilla racemiflora,* the dominant tree in the Icacos area) leaves have a C:N ratio twice that of Tabonuco (*Dacryodes excelsa,* the dominant tree in Bisley) leaves (54:1 versus 27:1), higher C:S (308:1 versus 253:1), but lower N:S (6:1 versus 9:1) (Table 8). The difference is even more pronounced in the O horizon (C:N ratio of 78:1 at Icacos versus 29:1 at Bisley, C:S ratio 522:1 versus 317:1, and N:S ratio 7:1 versus 11:1).

The $\delta^{13}C$ values of Palo Colorado leaves are slightly higher than those of Tabonuco (-33.2 versus -36.0‰), but the O horizon at both sites has a similar $\delta^{13}C$ value (-30‰). Despite higher $\delta^{15}N$ values in plant leaves at Icacos (0.97 compared to -0.51‰), $\delta^{15}N$ values of the O horizon are more negative at Icacos than at Bisley (-1.4 compared to -0.04‰). Similar to the N pattern, Palo Colorado leaves have higher $\delta^{34}S$ than Tabonuco leaves (15.4 versus 14.9‰), whereas O horizon $\delta^{34}S$ values are lower at Icacos than at Bisley (12.9 versus 13.3‰).

5.3 Mineral soil and saprolite chemistry

Soil C and N content declines exponentially with depth at all sites, from 0.9-4.3% C and 0.11-0.35% N at the surface to less than 0.2% C and 0.01% N at the bottom of the soil profiles (Fig. 5). C and N content also decreases downslope, with highest values on the ridges (surface values of 3.99±0.20% C and 0.22±0.01% N at Icacos, and 4.31±0.22% C and 0.35±0.02% N at Bisley). Assuming a homogeneous bulk density of 0.3 g/cm^3 for the O horizon and 1.2 g/cm^3 for the mineral soil, the total S content of the O horizon and mineral soil is 8.7 gS/m^2 and 374 gS/m^2 respectively at Icacos, and 6.2 gS/m^2 and 576 gS/m^2 respectively at Bisley.

Soil $\delta^{13}C$ values (Fig. 5) exceed those in plant litter and the O horizon (Table 8), and increase more with depth at Icacos than at Bisley (from ~-28 to ~-23‰ versus from ~-28 to ~-26‰). Surface $\delta^{13}C$ values are independent of topographic position.

Soil $\delta^{15}N$ values also exceed those in plant litter and the O horizon, and generally increase with depth in the mineral soil from as low as 3.8 to as high as 9.5‰ (Fig. 5). Surface $\delta^{15}N$ values are highest in Bisley soils. Surface soil $\delta^{15}N$ values increase downslope at Bisley (4.56±0.5‰ on the ridgetop, 6.45±0.6‰ on the upper slope and 6.8±0.8‰ on the lower slope), but are unaffected by topographic location at Icacos.

Total soil S and water extractable sulfate (Fig. 6) concentrations are highest in the surface horizons. Sulfate declines exponentially with depth, to <1 mg S/kg. In contrast, total S – largely in organic forms – decreases irregularly with soil depth, and has subsurface accumulations that correspond to the visual humus increases in some clay-rich

horizons. Total soil S concentrations decrease downslope on each toposequence. The highest S concentrations occurred in the Bisley ridgetop soil (625±27 mg S/kg in surface samples and 346±7 at the bottom of the profile), and the lowest in the Bisley lower slope soil (189±16 mg/kg at the surface, 12±3 mg/kg at the bottom).

C:S ratios decreased nearly exponentially with depth, from 130:1 to 3:1 at Icacos, and from 81:1 to 4:1 at Bisley (Fig. 6). The decrease is less pronounced in the Bisley lower slope site. Similarly, N:S ratios generally decrease with depth from 7.2:1 to 0.1:1 at Icacos, and from 9.2:1 to 0.5:1 at Bisley. N:S ratios are highest throughout at the Bisley lower slope site, and remain relatively constant with depth.

Compared to the O horizon, the mineral soil has a lower S content (between 12 and 625 mg S/kg), but is enriched in ^{34}S (depth-weighted average soil $\delta^{34}S$ values between 13.6 and 18.9‰, depending on the site) (Fig. 7). The difference between the $\delta^{34}S$ of plants and the top 10 cm of the soil ranges from -2.1 to 1.4‰.

5.4 Water chemistry

Precipitation chemistry integrates wet and dry inputs to the ecosystem. Total precipitation chemistry varied widely during the sampling period, with sulfate concentrations ranging from 4.6 to 38.8 μM, and $\delta^{34}S$ values from 10.7 to 20.5‰ (Table 9). Precipitation sulfate $\delta^{34}S$ values are uncorrelated with time of the year or sulfate concentration. The volume-weighted average precipitation $\delta^{34}S$ is 16.1±2.8‰ (see Table 9).

The Guaba and Bisley stream samples at baseflow show strikingly different chemistries (Table 10). The Guaba stream sulfate concentration (14.6±0.5 μM) resembles that of the volume-weighed precipitation average. The sulfate concentration of the Bisley stream (39.4±0.3 μM) is two and a half times greater than that of the Guaba, and just slightly larger than the precipitation maximum over the entire sampling period. Guaba $\delta^{34}S$ values (19.5±1.6‰) overlap with the precipitation average. The chemistry of the Icacos groundwater (Table 10) resembles the Guaba stream very closely. On the other hand, the Bisley stream $\delta^{34}S$ (1.6±0.7‰) is much closer to the $\delta^{34}S$ of volcanic or basalt S (Table 1).

Chloride (Cl) is a conservative tracer of precipitation and water flow. Cl concentrations in both streams exceed that of the volume-weighted precipitation average, but not the precipitation maximum. This Cl enrichment indicates evapotranspiration, as discussed by Murphy and Stallard (2012). At both sites, pore water Cl concentrations (Fig. 8) are generally highest in the shallowest samples and lowest in the deepest samples. Cl concentrations peak in the dry season, January through April, then decrease in May and stay low through the wetter months, until the following January when they begin to increase again. The only exception to this is the Bisley ridgetop site, where Cl is lowest in surface samples, and the increase during the drier months is less pronounced. Averaged over the sampling period, pore water Cl values only slightly exceed those of the volume-weighted precipitation average (Fig. 9). This suggests that, although evapotranspiration occurs at these sites, its impact on pore water chemistry averaged over the sampling period is minor.

Pore water sulfate concentrations (Fig. 10) and isotope ratios (Fig. 11) fluctuate with depth and season, though less so at Bisley than at Icacos. Averaged over the entire sampling period, the Icacos pore water sulfate concentrations resemble those in groundwater, Guaba stream and volume-weighted precipitation averages, except that they are higher near the soil surface (Fig. 12). The Bisley pore waters also resemble the precipitation average, except for higher sulfate concentrations at 183 cm, in the saprolite. All Bisley pore water samples contain significantly less sulfate than the Bisley stream (Fig. 12).

Average pore water sulfate $\delta^{34}S$ values (Fig. 13) show little variation with depth. The $\delta^{34}S$ values of the Icacos samples exceeded the volume-weighted rainfall average, but not the groundwater and baseflow values. The Bisley pore water samples are significantly enriched in the heavy isotope compared to the volume-weighted precipitation average and the Bisley stream.

Overall, we found no significant correlations between sulfate concentrations and $\delta^{34}S$ values, or between the S chemistry at the different sites in each given month. However, pore water $\delta^{34}S$ values increased in parallel at all sites after June 2011, mirroring changes in rain $\delta^{34}S$ (Fig. 11). At the same time, Cl concentrations decreased and remained low until January 2012 (Fig. 8), presumably due to more rainfall. Apparently, changes in input chemistry affect all topographic positions in parallel, and propagate quickly with soil depth.

6. Discussion

6.1 Major sources of S to the ecosystem

Our data confirm that atmospheric sources, as opposed to weathering, deliver the bulk of the S in this rainforest. The net fraction of pore water S from weathering (i.e. rock-derived) equals the amount measured in pore water minus the amount contributed by rainfall corrected for evapotranspiration (White et al., 2009):

$$S_{weathering} = S_{pore\ water} - S_{rainfall}\left[\frac{Cl_{pore\ water}}{Cl_{rainfall}}\right] \quad (4)$$

Utilizing the pore water S (Fig. 10) and precipitation S and Cl data (Table 9) with Eqn. 4 results in negative values for the average net weathering S input in all soils. Only deeper in the saprolite at Bisley do we find an indication of rock-derived S, where at 180 cm between 9 and 44% of the sulfate S is from weathering.

Our results based on pore water chemistry resemble those from stream chemistry collected between 1991 and 2005 (Stallard, 2012). The stream data show that sulfate inputs to the Icacos and Guaba watershed exceed river exports. This reflects little to no inputs from weathering and no storage of S in soil or gaseous losses (Stallard, 2012). In a wet tropical forest in Costa Rica, it has been shown that S inputs from basalt weathering are only significant in very young, minimally weathered soils (Bern et al., 2007; Bern and Townsend, 2008). The lack of significant rock-derived S in mature soils appears characteristic of highly-weathered, wet tropical systems.

Thus, the soil-vegetation system in the LEF contains atmospherically-derived S, which has five potential sources: seasalt, marine non-seasalt sulfate, volcanic ash input, Saharan dust, and anthropogenic emissions.

We used our Cl measurements (Table 9) to calculate the seasalt sulfate fraction:

$$seasalt\ SO_4 = 0.052 \cdot Cl \quad (5)$$

where 0.052 is the sulfate to chloride ratio in seasalt (Keene et al., 1986). We found that seasalt contributes an average of 37% of the precipitation sulfate, with a range from 12 to 74%. Conversely, between 26 and 88% of the precipitation sulfate (depending on the month) originates from a non-seasalt source with a volume-weighted average $\delta^{34}S$ of 13.4‰ (Table 9). In other words, in any given month, at least a quarter of the precipitation sulfate is of non-seasalt origin – assuming that S is as effectively transported as Cl.

Out of the 16 precipitation samples that were large enough for S isotope measurements, 6 have non-seasalt sulfate $\delta^{34}S$ values between 6.3 and 11.6‰ (Table 8), which is less than the typical range of 12.5 to 18.7‰ for sulfate produced by DMS oxidation (Calhoun et al., 1991). Three samples also have a total sulfate $\delta^{34}S$ value less than the average of precipitation over the Atlantic and Pacific Oceans (13.3‰) (Chukrov et al., 1980). The fact that seasalt and DMS fail to fully account for the total S indicates that there are significant non-marine sources at certain times of the year.

Volcanic sulfate (average $\delta^{34}S$ of 5‰) is an unlikely component given that the closest active volcano is Soufrière Hills on the Island of Montserrat (16°45'N, 62°12'W), about 500 km to the southeast, and no significant volcanic activity was reported over the study period.

Saharan mineral dust is known to deliver nutrients such as K, Mg (McDowell et al., 1990), Ca (Heartsill-Scalley, et al, 2007) and P (Pett-Ridge, 2009) to the LEF soils. While Saharan dust reaching Puerto Rico does contain measurable sulfate (Reid et al., 2003; Stallard, 2012), its quantitative importance is unclear. Heartsill-Scalley et al. (2007) found insignificant differences between sulfate fluxes during Saharan dust times (April-September) and the rest of the year at Bisley, concluding that dust contributes minimal sulfate. In this study, we observed only a slight increase in the sulfate concentrations (Table 9) during April-September compared to the rest of the year (volume-weighted average of 16.6 vs. 14.7 μM respectively). However, $\delta^{34}S$ values are slightly lower during April-September than the rest of the year (volume-weighted averages of 15.6 and 17.1‰ respectively). The reported $\delta^{34}S$ value of sulfate from Saharan marine evaporite deposits (17-19‰) is indistinguishable from that of the marine non-seasalt input (Brandmeier et al., 2011). In contrast, Saharan dust collected over the North Atlantic Ocean has lower $\delta^{34}S$ values that range between 11 and 13‰ (Gravenhorst, 1978). It has been suggested that this more depleted S in Saharan dust is probably not of Saharan soil origin, but rather anthropogenic SO_2 oxidized on the dust (Savoie et al., 1989; Harris et al., 2012), although Saharan soil $\delta^{34}S$ values have not been measured. It is therefore possible that at least some of the low $\delta^{34}S$ precipitation samples reflect inputs of long-range anthropogenic S via dust aerosols.

The low $\delta^{34}S$ values of samples collected during winter months (January and March) may also reflect anthropogenic inputs. Anthropogenic S (and N) can reach the LEF from North America via Northern cold fronts (McDowell et al., 1990), which deliver 5% of the rainfall at LEF (Scholl et al., 2009). Northern Hemisphere contaminant deposition peaks in January, April and May, when the cold fronts are strongest (Stallard, 2012). These cold fronts may explain the relatively low S isotope values.

In addition to sulfate, soils at LEF also take up carbonyl sulfide (COS) from the atmosphere, as indicated by flux chamber measurements (Whelan and Rhew, 2012). COS is the longest-lived (life time of ~500 days) and most abundant reduced S gas in the atmosphere, therefore it is relatively evenly distributed around the globe; although not directly measured, its $\delta^{34}S$ value has been estimated to be 11‰ (Newman et al., 1991). Its net uptake by the LEF soils indicates that the soils are predominantly oxic (Kettle et al., 2002; Whelan et al., 2013). However, this COS flux is three orders of magnitude smaller than the sulfate input, and therefore unlikely to significantly affect the isotopic composition of soil S.

In summary, the main source of S to the LEF soils is the steady influx of atmospheric sulfate, originating mostly from a mix of marine and anthropogenic sources. Multiplying the MAP times the average sulfate content of rain water (Table 9) suggests an atmospherically-derived S flux of 2.2 g S/m^2/yr at Icacos, and 1.8 g S/m^2/yr at Bisley. These values are consistent with the results of McDowell and Asbury (1994).

6.2 In-situ processes

6.2.1 Processes at the soil-plant interface

In addition to the atmospherically-derived S, soils also receive S from plants via litter. Litterfall rates average 680 g/m^2/yr in the Colorado forest (Icacos site) (Weaver et al., 1990). For the Tabonuco forest (Bisley site), published litterfall estimates range from 861 g/m^2/yr (Weaver et al., 1990) to 913 g/m^2/yr (Zou et al., 1995); for our calculations, we used an estimate of 890 g/m^2/yr. Multiplying these litterfall rates by the average S content of vegetation (Table 8) suggests an input from litter of approximately 2.2 and 2.8 g S/m^2/yr respectively for Icacos and Bisley.

The results show evidence of S isotope fractionation during plant uptake. Compared to the soil, plants are about 1‰ depleted in ^{34}S (Fig. 7). These differences between soil and vegetation $\delta^{34}S$ were also observed in Costa Rica (Bern et al., 2007), and have been reported for some temperate sites as well. This small difference between the $\delta^{34}S$ of total S in soils and plants might lead to an interpretation of little to no isotopic fractionation during plant uptake and assimilation. However, since plants take up S mostly as sulfate, plant $\delta^{34}S$ must be compared with rain and pore water $\delta^{34}S$ to evaluate this issue. Our data show that leaves are 3 to 5‰ depleted in ^{34}S compared to the average pore water (Fig. 7). This suggests that plants discriminate against the heavier isotope in the process of sulfate uptake and assimilation. A distinctive, albeit relatively small, fractionation during S assimilation is common also for other life forms. For instance, S metabolism studies with bacteria, algae and yeast (Table 2) found that assimilated S can be up to 2.8‰ depleted compared to its source (Kaplan and Rittenberg, 1964).

Plants also fractionate S isotopes via H_2S emissions, which can be 9.7 to 16.8‰ more negative than nutrient sources (Winner et al., 1981). Bern et al. (2007) calculated that this mechanism alone could elevate ecosystem S by 0.4-2.1‰ compared to atmospheric inputs at Rancho Mariposa, Costa Rica. Plants typically emit H_2S only when they are stressed by high S concentrations in inputs, such as in polluted regions (Trust and Fry, 1992). Since our sites have low S loading, we suspect H_2S emissions by plants are insignificant in this system.

6.2.2 Processes within the soil

The sites are likely near quasi-steady state with respect to the biogeochemical cycling of C, N, and S (e.g. Chestnut et al., 1999) because they have experienced minimal anthropogenic disturbance. C cycling rate constants have not been determined here, but from a meta-analysis, an organic matter turnover time of ~10 years (for the most rapidly cycling pool) is likely based on MAT (Sanderman et al., 2003). As a starting assumption, the S cycle in Puerto Rico likely resembles the one illustrated in Fig. 1. At steady state, the balance between the inputs losses will determine the $\delta^{34}S$ value of soil S.

We found that S content decreases with increasing depth and soil $\delta^{34}S$ values increase. This pattern is characteristic of biological decomposition and isotopic fractionation of downward moving organic matter pools in the soils. Isotopically-heavier organic residues remain behind as the isotopically-lighter S is lost to aqueous or gaseous phases. The N data show the same pattern (Fig. 5), suggesting some coupling of S and N cycling.

S mineralization rates have not been measured in the LEF, but a study of Bisley soils found high potential N mineralization rates in the top 10 cm of the soils, and virtually zero net mineralization potential between 35 and 100 cm, suggesting that C or N content in the deep soil might be too low or recalcitrant to support microbial N mineralization. (Bowden et al., 1992). Organic matter CNS ratios can help indicate whether N and S in these soils are more likely to undergo net immobilization (conversion of the inorganic form to organic form) or net mineralization (decomposition of the organic form into an inorganic form). Net mineralization of N or S occurs at C:N and C:S ratios below 20:1 and 200:1 respectively, while at C:N and C:S ratios above 30:1 and 400:1, net immobilization of N or S occurs (Stevenson and Cole, 1999, p. 68). Given the C:N and C:S values in the O horizon (Table 8), N and S immobilization should dominate at Icacos, but immobilization and mineralization are balanced at Bisley. Below the soil surface in both soils, however, C:S ratios become very low (<130 at Icacos and <85 at Bisley, Fig. 6), promoting S mineralization. In all soils except for the Bisley lower slope, C:S ratios drop to less than 10:1 below a depth of 60-100 cm. At such low C content and C:S ratios, microbial S metabolism may be C-limited. S mineralization, however, can occur even without microbial activity in the presence of extracellular enzymes (McGill and Cole, 1981).

The depth trends in solid phase S indicate that microbial decomposition and cycling of S may be releasing sulfate depleted in ^{34}S compared to the soil S. This has been observed in temperate regions, where the soil solution has lower sulfate $\delta^{34}S$ values than the precipitation (Fuller et al., 1986; Novak et al., 1995; Zhang et al., 1998; Alewell

and Gehre, 1999; Alewell et al., 1999). However, we found that during most months, aqueous phase sulfate at our sites is enriched in ^{34}S relative to the solids by up to 5.6‰ (Fig. 7). This suggests that, although soil $\delta^{34}S$ values do not decrease with depth, some dissimilatory sulfate reduction may be occurring in the aqueous phase. Plant uptake also increases pore water $\delta^{34}S$, however the plant roots are concentrated in the upper ~30 cm of the soils, and are unlikely to affect the deeper pore water samples. Other mechanisms such as the adsorption/desorption of sulfate (Table 2), produce significantly less isotopic fractionation and are likely not important here.

Our isotope data thus show evidence for both S mineralization and dissimilatory sulfate reduction. The co-occurrence of these two processes in LEF soils is supported by similar results for N (Pett-Ridge et al., 2006) and by other studies showing the co-occurrence of saturated and unsaturated processes due to spatial segregation in these soils (McSwiney et al., 2001).

6.2.3 Isotope fractionation during organic matter transport through the soil

Recent studies have examined the content and isotopic composition of organic matter with depth, assuming that transport occurs through advection (leaching of dissolved organic matter and colloidal transport) or diffusion (movement by burrowing fauna, earthworms, mesofauna, shrink/swell cycles, fungal hyphae activity, and dissolved organic matter transport during soil drying) (e.g. Brenner, 1999; Baisden et al., 2002; Sanderman and Amundson, 2008). Organic matter is physically moved downward by biological mixing and in dissolved or particulate forms by leaching. During transport, decomposition creates aqueous or gaseous products that leave the system.

At our sites, inputs are at or near the surface: roots are concentrated in the upper 16-17 cm (Tables 6 and 7), and plant litter is added to the O horizons. Biological mixing is accomplished mostly by earthworms, most commonly the exotic *Pontoscolex corethrurus* and the native *Pontoscolex spiralis* (Gonzalez et al., 2007). Although occasional earthworm tubes can be found even below 30 cm (McDowell et al., 1992), we found them only near the surface. Thus, advection is likely the main process responsible for downward moving organic matter in these soils. Below we consider the isotopic effects of this process.

Since aboveground inputs far exceed belowground inputs (Chestnut et al., 1999), the steady-state advection/decomposition equations for the abundant and rare isotopes are simply:

$$\frac{\delta[^{32}S]}{\delta t} = 0 = v\frac{\delta[^{32}S]}{\delta z} - k^{32}S \quad (5)$$

$$\frac{\delta[^{34}S]}{\delta t} = 0 = v\frac{\delta[^{34}S]}{\delta z} - k\alpha^{34}S \quad (6)$$

where ν is the advection coefficient (cm/yr), k is the decay constant (yr^{-1}) and α is the fractionation factor. In terms of the heavy to light isotope ratio R, the general solution becomes (after Brenner, 1999):

$$\frac{R(z)}{R(0)} = e^{-\frac{kz}{v}(\alpha-1)} \quad (7)$$

where R(z) and R(0) are the $^{34}S/^{32}S$ ratios of the soil at depth z and of the inputs respectively. Denoting the fraction of total S remaining at depth z compared to the surface inputs as *f*:

$$\frac{S(z)}{S(0)} = e^{-\frac{kz}{v}} = f \tag{8}$$

we can rewrite Eqn. 7 as:

$$\frac{R(z)}{R(0)} = f^{(\alpha-1)} \tag{9}$$

Converting from R to δ notation:

$$1000 \cdot ln\frac{R(z)}{R(o)} \cong \delta_z - \delta_0 \tag{10}$$

and substituting the enrichment factor instead of the fractionation factor:

$$\varepsilon = (\alpha - 1) \cdot 1000 \tag{11}$$

we can re-write Eqn. 9 as:

$$\delta_z = \varepsilon \cdot lnf + \delta_0 \tag{12}$$

The advection model thus implies a linear relationship between soil $\delta^{34}S$ and ln*f*, or equivalently, ln(*S%*). Fig. 14 shows that a linear relationship between $\delta^{15}N$ and ln(*N%*) exists, but not between $\delta^{34}S$ and ln(*S%*). This is a key difference between N and S biogeochemistry in these soils. Fig. 15 further confirms that $\delta^{15}N$ and $\delta^{34}S$ vary independently with depth in most of these soils. The fact that N conforms to the advection model signifies that the model assumptions – constant ν, k and α with depth (Baisden et al., 2003) – are met. On the other hand, one or more of these parameters must vary with depth for S. Since ν and k are parameters that should be similar for N and S, the S isotope fractionation factor α must be changing with depth due to changing processes.

We can therefore use an advection (or Rayleigh-like) model to compute the depth-insensitive fractionation factors for N. The A horizon appears to be heavily mixed by earthworms, and thus represents a well-mixed pool of organic N that then moves downward through the soil. The model is set up to describe aging of organic material in the A horizon (mineral soil surface) as it moves downward deeper in the soil. At fractionation factors α close to unity, Eqn. 9 can be converted to δ notation as follows (Ewing et al., 2008; Amundson et al., 2012):

$$\delta(z) = (\delta_i(z) + 1000) \cdot f(z)^{(\alpha-1)} - 1000, \tag{13}$$

where $\delta(z=0)$ equals the $\delta^{15}N$ value of the A horizon; for any subsequent horizons, $\delta_i(z) = \delta(z-1)$; and $f(z)$ equals the ratio of total soil N at depth *z* to the total soil N content of the uppermost horizon. We calculated the α values that best fit the data (Table 11). The best-fit α values are all smaller than 1, consistent with enrichment of the soil in the heavier isotope due to mineralization as the organic matter is leached down the soil profile.

For S, since α changes with depth, we computed the fractionation factor α between soil layers by applying Eqn. 13 to each layer using the layer above as the S input. The results show large variations in α with depth (Fig. 16), with both: (1) α values less than 1, indicative of mineralization, or successive cycles of mineralization and

immobilization, and (2) α values greater than 1, indicative of dissimilatory sulfate reduction, which leads to depleted reduced S compounds that are lost from the soil, thus enriching the soil in ^{34}S.

In sum, a simple advection model explains the movement and alteration of N in subsurface horizons, but the movement of S deviates from the simple model because the fractionation factor α varies with depth. This difference suggests a decoupling of the soil N and S cycles due to the prevalence of different biotic processes (mineralization-immobilization and dissimilatory sulfate reduction) driving S cycling at different depths.

6.2.4 Isotope fractionation during S movement in aqueous phase

Rainwater is the ultimate source of sulfate to the LEF soils. Rain infiltration rates in the surface soils are greater at Icacos (2-9 cm/min) than at Bisley (0.07-1.5 cm/min), and exceed typical rainfall intensity (0.013 cm/min) at both sites (McDowell et al., 1992). This suggests that, despite the high MAP, soil surfaces rarely become waterlogged. Once in the soil, the rainwater travels downwards mostly via macropores (White et al., 1998), and follows preferred drainage patterns downslope. At Icacos, subsurface water flow is generally deep, below the rooting zone (McDowell et al., 1992), typically along fractures at the saprolite-bedrock interface (White et al., 1998; Kurtz et al., 2011). On the other hand, soil water at Bisley flows within the rooting zone (McDowell et al., 1992). As a result, McDowell et al. (1992) proposed that mineralization, nitrification, plant uptake and denitrification are segregated in space at Icacos, but can coexist at Bisley due to highly variable redox conditions over only fractions of a cm.

We calculated the sulfate flux Q through the regolith (soil+saprolite) with the equation:

$$Q = q_h \Delta c \tag{14}$$

where q_h is the vertical infiltration rate or field flux density (product of the hydraulic conductivity and the hydraulic gradient), and $\Delta c = c_f - c_i$ is the change in concentration between two depths (White et al., 1998). White et al. (1998) first calculated a vertical infiltration rate of 1 m/yr at Icacos. Here we use the hydraulic field flux density values from Buss et al. (2011), which are corrected for evapotranspiration: 1.28 m/yr at Icacos and 1.62 m/yr at Bisley. We calculated sulfate fluxes to and from a given depth by multiplying q_h times the difference in the average sulfate concentration between the lysimeter sampled at that depth (c_f) and the one directly above it (c_i). For the topmost lysimeters sampled, the starting concentration c_i is the sulfate concentration in precipitation. We express the isotopic enrichment associated with these additions or losses in pore water as the difference between the $\delta^{34}S$ value of the two lysimeter samples (i.e. the Δ value, Eqn. 3) (Fig. 17).

Different processes occur at different depths (Fig. 17). All soils lose pore water sulfate near the surface (between 1.3 and 1.7 $gS/m^2/yr$), due to uptake by vegetation, and possibly due to sulfate reduction (thin dashed line in Fig. 17). This sulfate loss is associated with an enrichment in the heavier isotope in pore water by 1.1 to 3.2‰, which is consistent with biological sulfate uptake. This zone of apparent uptake is only 15 cm thick in the lower slope (riparian) soil at Bisley, but is approximately 60 cm thick for all

other soils. Below this is a zone of small losses or gains of sulfate with nearly no isotopic fractionation, consistent with mineralization. Our data suggest that mineralization, resulting in an influx of sulfate to the pore water with slightly lower $\delta^{34}S$ values, might occur all the way down to the saprolite. The soil-saprolite boundary was identified in the field, based on textural and color changes. For most of these soils, the saprolite acts as a net source of sulfate to pore water, likely due to cycles of adsorption/desorption. The net result is that as water travels through the soil, it loses sulfate and becomes enriched in the heavy isotopes of S. The net amount of sulfate lost over the entire soil depth (i.e. losses minus additions occurring above the soil-saprolite boundary) is similar for all soils on quartz diorite and for the volcaniclastic ridgetop soil (between 1.4 and 1.7 $gS/m^2/yr$). The slope sites on the volcaniclastic parent material lose significantly less sulfate (0.8-0.9 $gS/m^2/yr$). The net enrichment in heavier S isotopes is higher at the volcaniclastic sites (a $\delta^{34}S$ range of 2.3 to 3.2‰ compared to 1.1 to 2.8‰ on the quartz diorite) and decreases generally downslope. Lower enrichment on steeper slope sites may result from decreased plant uptake due to less dense vegetation on the steeper slopes.

The high MAP is a defining characteristic in this ecosystem, affecting the types and rates of processes. Bern et al. (2007) and Bern and Townsend (2008) examined S in similar ecosystems in Costa Rica and Hawaii. They found that dissimilatory sulfate reduction was not a major process despite the high MAP. The reasons for this remain unclear. In the LEF, S isotopes suggest that sulfate reduction occurs, but is spatially and temporally variable. The co-occurrence of mineralization and sulfate reduction makes interpretations ultimately complex.

6.3 S losses from the ecosystem

The main losses of S from soils occur in the aqueous, or possibly gaseous phase (Fig. 1). However, one-time flux chamber measurements could not detect any emissions of reduced S gases from soils (Whelan and Rhew, 2012). Therefore, the main loss pathway for S from this ecosystem must be aqueous.

Stream sulfate concentrations at baseflow (Table 10) reflect losses from soil. McDowell and Asbury (1994) found that N and S concentrations vary minimally with discharge, therefore our baseflow values are representative for S loss throughout the year. To estimate the net export of sulfate from the watershed, we multiplied the average stream sulfate concentration measured in this study by the average runoff estimates for the Guaba (3630 mm/yr) and Bisley (2007.5 mm/yr) streams from Stallard and Murphy (2012) and Schellekens et al. (2004) respectively. Our values, 1.7 g $S/m^2/yr$ at Icacos, and 2.5 g $S/m^2/yr$ at Bisley (Fig. 17), mirror the 2.4 g/m2/yr hydrologic export estimated by McDowell and Asbury (1994).

At Icacos, stream S export is 0.5 $g/m^2/yr$ less than the inputs, which means that S accumulated in soil organic matter and/or was released in gaseous form (Fig. 17). In contrast, the stream S export at Bisley exceeds atmospheric inputs by 0.7 $g/m^2/yr$, possibly indicating bedrock sources. Indeed, pyrite and other S-minerals, likely of hydrothermal origin, are present throughout drilled bedrock cores (to 37 m deep) from the Bisley watershed (Buss et al., 2013). Stream S export in the Mameyes stream, into which the Bisley stream drains, was also found to exceed atmospheric inputs (Stallard and

Murphy, 2012); rock weathering may thus be an important S source at Bisley. Additionally, Chestnut et al. (1999) found that N outputs exceed inputs at Bisley, suggesting unaccounted-for inputs or a slow depletion of soil organic N.

6.4 Controls on the tropical soil S cycle

Overall, climate is the driving force behind S cycling at these Puerto Rican sites. The high MAP quickly weathers rock and removes lithological sources of S, dictates the source and amounts of atmospheric inputs, and drives the fluxes through the soil. Here we examine the effects of the slight differences in MAP at the two sites, and two additional variables: lithology (parent material) and topography.

6.4.1 Climate

Given the higher elevation at the Icacos site, rainfall and dust deposition patterns are somewhat different than at Bisley (e.g. Scholl et al., 2009), resulting in higher sulfate input at Icacos. Icacos receives 700 mm more rainfall on average (Table 3), and derives ~5% of its total precipitation input from cloud water (Pett-Ridge et al., 2009). As a result, we observed higher extractable sulfate concentrations at the soil surface, and greater variability in Cl and sulfate concentrations in pore water. Because Cl and sulfate originate from atmospheric deposition, the differences in their concentrations between the two sites are due to differences in rainfall and dust deposition and/or in evapotranspiration rates. The slight differences in MAP also cause differences in vegetation, which impacts soil C, N and S.

6.4.2 Topography

Our sites were chosen to capture the topographic variation in weathering and pore waters from ridge to valley. Topography is known to impact N cycling in different climates (e.g. Robertson et al., 1988; Raghubanshi, 1992; Roy and Singh, 1994; Chestnut et al., 1999). In the LEF, previous studies have shown that changing redox conditions with topographic location affect N_2O production (McSwiney et al., 2001).

In this study, we found that the C, N and S content of the mineral soil decrease downslope at all sites, while soil surface $\delta^{15}N$ values decrease downslope at the Bisley site only. The lower slope site at Bisley has the lowest C, N and S content, as well as the highest $\delta^{15}N$ and lowest $\delta^{34}S$ values, indicating that reduction processes are important. Indeed, soils at this site are wetter and more gray in color than the soils at the other sites. At the other sites, $\delta^{34}S$ values seem unaffected by topography.

Similar trends with topographic position were observed in Costa Rica. Bern and Towsend (2008) found higher C, N and S content and higher $\delta^{34}S$ in the surface layer in hillslope soils compared to alluvial soils.

6.4.3 Lithology

According to our model, the stream water at baseflow should contain any rock-derived S. The Bisley baseflow $\delta^{34}S$ value (1.6±0.7‰) appears to indicate lithologic S inputs to the stream. The Icacos baseflow $\delta^{34}S$ value (19.5±1.6‰) is similar to that of atmospheric inputs, suggesting little lithologic input of S as expected (the Icacos bedrock does not contain substantial S-minerals, e.g., Buss et al., 2008). $\delta^{34}S$ values of the mineral

soil and pore waters are similar at both sites, indicating that any lithological S in the soil or shallow saprolite has been removed by weathering.

6.5 The tropical soil S cycle in the context of global change

In most ecosystems, the LEF included, S cycling depends entirely on the steady supply of sulfate from a variety of atmospheric sources. This Puerto Rican rainforest currently receives a portion of its S from anthropogenic sources in North America and the eastern side of the Atlantic. However, the system appears to be at steady state, and any changes in inputs have not greatly altered the ecosystem S balance. Inputs via rain at Icacos nearly equal outputs in stream water, while at Bisley stream sulfate outputs exceed rain inputs due to the lithologic inputs (Fig. 17). The volcaniclastic rock delivers S to the stream, but not to the soil, and therefore the soil-plant system depends exclusively on atmospheric inputs.

The ecosystem's dependence on atmospheric S inputs implies that any changes in the amount of rain or the amount of sulfate in rain will drive the system out of its present steady state. In the LEF, climate change and deforestation have already decreased orographic rains, which are responsible for 29-35% of the precipitation in this rainforest (Scholl et al., 2009). Eventually, such decreases in MAP could begin to deplete the soil organic S (and N) pool. In addition to changing rain patterns, deforestation also has a more direct effect on S cycling since vegetation assimilates and retains atmospheric sulfate in the soil. Disturbances in vegetation cover may thus accelerate S losses and decrease the soil organic S pool.

7. Conclusions

The biogeochemistry of S is not well known, especially in relation to the closely related elements C and N. Our study of S biogeochemistry in two Puerto Rican watersheds (Icacos and Bisley) combined a comparative analysis of stable C, N and S isotope measurements in the soil with S isotope measurements in atmospheric inputs, pore water, stream water at baseflow and groundwater. Atmospheric inputs ($\delta^{34}S$ values of 16.1±2.8‰), from a mixture of marine and anthropogenic sources, deliver on average 2.2 g S/m^2/yr at Icacos, and 1.8 g S/m^2/yr at Bisley. We estimated a hydrologic export of 1.7 g S/m^2/yr at Icacos, and 2.5 g S/m^2/yr at Bisley. The Bisley baseflow S isotope data suggest that rock weathering releases sulfate to the stream with a distinctive $\delta^{34}S$ of 1.6±0.7‰. Given the nearly balanced inputs and outputs, the system appears to be at or near steady state.

Total soil C and N contents, as well as extractable sulfate, decline exponentially with depth. Total soil S however decreases irregularly with depth, showing subsurface accumulations in areas visibly enriched in humus. Isotope fractionation occurs during biological processes. Plants are 3 to 5‰ depleted in ^{34}S compared to the average pore water, providing evidence for fractionation during uptake and assimilation. During most months, aqueous phase sulfate is enriched in ^{34}S relative to the solids by up to 5.6‰, suggesting that dissimilatory sulfate reduction may occur at least occasionally. Soil S content decreases with depth, while $\delta^{34}S$ values increase, a typical pattern for

mineralization. We used an advection model to describe the isotopic fractionation associated with downward movement of organic matter in this system. We found that although this model worked well for N, the assumption of a constant fractionation factor α with depth failed for S. This is a fundamental difference between N and S cycling in these soils, indicating that different processes with different fractionation factors affect soil S at different depths.

Both the advection model analysis and pore water data support the co-occurrence of three major S-fractionating processes in these soils: plant uptake, mineralization and dissimilatory bacterial sulfate reduction. The rate and importance of these processes vary in time and space, and their co-occurrence dampens their individual signals. However, the co-occurrence of mineralization and reduction has been previously noted also for N (Pett-Ridge et al., 2006).

We found no indication that parent material impacts S biogeochemistry within the soils. Topography, on the other hand, affected the S cycle through redox conditions. In particular, C, N and S contents decrease downslope at all sites, and the Bisley lower slope site shows the most evidence of bacterial sulfate reduction. Overall, climate is the driving force behind S cycling in the LEF. The high MAP is a defining characteristic of S cycling in this ecosystem, determining the types and rates of processes.

Acknowledgments

Logistical support and data were provided by the NSF-supported Luquillo Critical Zone Observatory (EAR-0722476) with additional support provided by the USGS Luquillo WEBB program and the USDA Forest Service International Institute of Tropical Forestry. We thank our collaborator H. Buss, as well as K. Finstad, S. Hall, M. Whelan and M. Rosario for technical assistance in the field, and M. C. Torrens, S. Moya, J. Carlos and J. Orlando for sample collection. We are also grateful to the late F. Scatena for his invaluable logistical support, to M. Leon for providing maps of the study area, to A. Kirk and A. Engelbrektson for laboratory assistance, and to J. Coates, W. Yang, P. Brooks and S. Mambelli for access to instruments and sample analysis.

References

Acquaye D. K. and Beringer H. (1989) Sulfur in Ghanaian soils .1. Status and distribution of different forms of sulfur in some typical profiles. *Plant Soil* **113,** 197-203.

Alewell C. and Gehre M. (1999) Patterns of stable S isotopes in a forested catchment as indicators for biological S turnover. *Biogeochemistry* **47,** 319-333.

Alewell C., Mitchell M. J., Likens G. E. and Krouse H. R. (1999) Sources of stream sulfate at the Hubbard Brook Experimental Forest: Long-term analyses using stable isotopes. *Biogeochemistry* **44,** 281-299.

Amundson R., Austin A. T., Schuur E. A. G., Yoo K., Matzek V., Kendall C., Uebersax A., Brenner D. and Baisden W. T. (2003) Global patterns of the isotopic composition

of soil and plant nitrogen. *Global Biogeochem. Cycles* **17***(1)***,** 1031, doi:10.1029/2002GB001903.

Amundson R., Barnes J. D., Ewing S., Heimsath A. and Chong G. (2012) The stable isotope composition of halite and sulfate of hyperarid soils and its relation to aqueous transport. *Geochim. Cosmochim. Acta* **99,** 271-286.

Asbury C. E., Mcdowell W. H., Trinidadpizarro R. and Berrios S. (1994) Solute deposition from cloud-water to the canopy of a Puerto-Rican montane forest. *Atmos. Environ.* **28,** 1773-1780.

Bern C. R., Porder S. and Townsend A. R. (2007) Erosion and landscape development decouple strontium and sulfur in the transition to dominance by atmospheric inputs. *Geoderma* **142,** 274-284.

Bern C. R. and Townsend A. R. (2008) Accumulation of atmospheric sulfur in some Costa Rican soils. *J Geophys Res-Biogeo* **113,** G03001, doi:10.1029/2008JG000692.

Bhatt M. P. and McDowell W. H. (2007) Controls on major solutes within the drainage network of a rapidly weathering tropical watershed. *Water Resour. Res.* **43,** W11402.

Boccheciamp R. A. (1977) Soil survey of the Humacao area of eastern Puerto Rico. *USDA Soil Conserv. Serv.*

Bradley A. S., Leavitt W. D. and Johnston D. T. (2011) Revisiting the dissimilatory sulfate reduction pathway. *Geobiology* **9,** 446-457.

Brandmeier M., Kuhlemann J., Krumrei I., Kappler A. and Kubik P. W. (2011) New challenges for tafoni research. A new approach to understand processes and weathering rates. *Earth Surf. Process. Landforms* **36,** 839-852.

Brenner D. L. (1999). Soil nitrogen isotopes along natural gradients: models and measurements. M.S. thesis, University of California, Berkeley, CA.

Brimblecombe P. (2003) The Global Sulfur Cycle. *Treatise on Geochemistry* **8,** 645-682.

Brown E. T., Stallard R. F., Larsen M. C., Raisbeck G. M. and Yiou F. (1995) Denudation rates determined from the accumulation of in situ-produced ^{10}Be in the Luquillo Experimental Forest, Puerto Rico. *Earth Planet. Sci. Lett.* **129**, 193-202.

Brunner B. and Bernasconi S. M. (2005) A revised isotope fractionation model for dissimilatory sulfate reduction in sulfate reducing bacteria. *Geochim. Cosmochim. Acta* **69,** 4759-4771.

Buss H. L., Bruns M. A., Schultz M. J., Moore J., Mathur C. F. and Brantley S. L. (2005) The coupling of biological iron cycling and mineral weathering during saprolite formation, Luquillo Mountains, Puerto Rico. *Geobiology* **3,** 247-260.

Buss H. L., Sak P. B., Webb S. M. and Brantley, S. L. (2008) Weathering of the Rio Blanco quartz diorite, Luquillo Mountains, Puerto Rico: Coupling oxidation, dissolution, and fracturing. *Geochim. Cosmochim. Acta* **72,** 4488-4507

Buss H. L., Mathur R., White A. F. and Brantley S. L. (2010) Phosphorus and iron cycling in deep saprolite, Luquillo Mountains, Puerto Rico. *Chem. Geol.* **269,** 52-61.

Buss H. L., White A. F., Blum A. E., Schulz M. S. and Vivit D. (2011) Long-term versus short-term weathering fluxes in contrasting lithologies at the Luquillo Critical Zone Observatory, Puerto Rico. *Mineral Mag.* **75**, p. 604.

Buss H. L. and White A. F. (2012) Weathering Processes in the Rio Icacos Watershed. In: Murphy S.F. and Stallard R.F., eds, *Water Quality and Landscape Processes of Four Watersheds in Eastern Puerto Rico:* U.S. Geological Survey Professional Paper 1789, pp. 249-262. http://pubs.usgs.gov/pp/1789/.

Buss H. L., Brantley S. L., Scatena F. N., Bazilievskaya E. A., Blum A., Schulz M., Jimenez R., White A. F., Rother G. and Cole D. (2013) Probing the deep critical zone beneath the Luquillo Experimental Forest, Puerto Rico. *Earth Surf. Proc. Land.* **38**, 1170-1186. DOI: 10.1002/esp.3409

Buss H. L., White A. F., Blum A. E., Schulz M. S. and Vivit D. (2011) Long-term versus short-term weathering fluxes in contrasting lithologies at the Luquillo Critical Zone Observatory, Puerto Rico. *Mineral Mag* **75**, p. 604.

Calhoun J. A., Bates T. S. and Charlson R. J. (1991) Sulfur isotope measurements of submicrometer sulfate aerosol-particles over the Pacific-Ocean. *Geophys. Res. Lett.* **18,** 1877-1880.

Chadwick O. A., Derry L. A., Vitousek P. M., Huebert B. J. and Hedin L. O. (1999) Changing sources of nutrients during four million years of ecosystem development. *Nature* **397,** 491-497.

Chestnut T. J., Zarin D. J., McDowell W. H. and Keller M. (1999) A nitrogen budget for late-successional hillslope tabonuco forest, Puerto Rico, *Biogeochemistry*, **46**, 85-108.

Chukrov F. V., Ermilova L. P., Chukirov V. S. and Nosik L. P. (1980) The isotopic composition of plant sulfur. *Org. Geochem.* **2**, 69 – 75.

Cox S. B., Willig M. R. and Scatena F. N. (2002) Variation in nutrient characteristics of surface soils from the Luquillo Experimental Forest of Puerto Rico: A multivariate perspective. *Plant Soil* **247,** 189-198.

Ewing S. A., Yang W., DePaolo D. J., Michalski G., Kendall C., Stewart B. W., Thiemens M. and Amundson R. (2008) Non-biological fractionation of stable Ca isotopes in soils of the Atacama Desert, Chile. *Geochim. Cosmochim. Acta* **72,** 1096-1110.

Fry B., Gest H. and Hayes J. M. (1988a) S-34/s-32 Fractionation in sulfur cycles catalyzed by anaerobic-bacteria. *Appl. Environ. Microbiol.* **54,** 250-256.

Fry B., Ruf W., Gest H. and Hayes J. M. (1988b) Sulfur isotope effects associated with oxidation of sulfide by O-2 in aqueous-solution. *Chem. Geol.* **73,** 205-210.

Fuller R. D., Mitchell M. J., Krouse H. R., Wyskowski B. J. and Driscoll C. T. (1986) Stable sulfur isotope ratios as a tool for interpreting ecosystem sulfur dynamics. *Water Air Soil Poll* **28,** 163-171.

Garcia-Martino A. R., Warner G. S., Scatena F. N. and Civco D. L. (1996) Rainfall, runoff and elevation relationships in the Luquillo Mountains of Puerto Rico. *Caribb J Sci* **32,** 413-424.

Goller R., Wilcke W., Fleischbein K., Valarezo C. and Zech W. (2006) Dissolved nitrogen, phosphorus, and sulfur forms in the ecosystem fluxes of a montane forest in ecuador. *Biogeochemistry* **77,** 57-89.

Gravenhorst G. (1978) Maritime Sulfate Over North-Atlantic. *Atmos. Environ.* **12,** 707-713.

Harris E., Sinha B., Foley S., Crowley J. N., Borrmann S. and Hoppe P. (2012) Sulfur isotope fractionation during heterogeneous oxidation of SO2 on mineral dust. *Atmos Chem Phys* **12,** 4867-4884.

Heartsill-Scalley T., Scatena F. N., Estrada C., McDowell W. H. and Lugo A. E. (2007) Disturbance and long-term patterns of rainfall and throughfall nutrient fluxes in a subtropical wet forest in Puerto Rico. *J Hydrol* **333,** 472-485.

Huffaker L. (2002) Soil Survey of Caribbean National Forest and Luquillo Experimental Forest, Commonwealth of Puerto Rico. USDA, NRCS, Washington, DC.

Johnston M. H. (1992) Soil-vegetation relationships in a Tabonuco forest community in the Luquillo Mountains of Puerto-Rico. *J. Trop. Ecol.* **8,** 253-263.

Kaplan I. R. and Rafter T. A. (1958) Fractionation of stable isotopes of sulfur by Thiobacilli. *Science* **127,** 517.

Kaplan I. R. and Rittenberg S. C. (1964) Microbiological fractionation of sulphur isotopes. *J. Gen. Microbiol.* **34,** 195-212.

Keene W. C., Pszenny A. A. P., Galloway J. N. and Hawley M. E. (1986) Sea-salt corrections and interpretation of constituent ratios in marine precipitation. *J Geophys Res-Atmos* **91,** 6647-6658.

Kettle A. J., Kuhn U., Von Hobe M., Kesselmeier J. and Andreae M. O. (2002) Global budget of atmospheric carbonyl sulfide: temporal and spatial variations of the dominant sources and sinks. *J Geophys. Res.* **107**, 4658-4674.

Kurtz A.C., Lugolobi F. and Salvucci G. (2011) Germanium-silicon as a flow path tracer: Application to the Rio Icacos watershed. *Water Resour. Res.* **47**, W06516. DOI: 10.1029/2010WR009853.

Larsen, M.C. (1997) A study of geomorphic processes and water budgets in the montaine humid-tropical and developed watersheds, Puerto Rico. PhD thesis, Univ. Colorado.

Likens G. E., Driscoll C. T., Buso D. C., Mitchell M. J., Lovett G. M., Bailey S. W., Siccama T. G., Reiners W. A. and Alewell C. (2002) The biogeochemistry of sulfur at Hubbard Brook. *Biogeochemistry* **60,** 235-316.

McDowell W. H. and Estrada Pinto A. (1988) Rainfall at the El Verde Field Station, 1964-1986. Univ. of Puerto Rico Center for Energy and Environment Research Technical Report **228**.

McDowell W. H. and Asbury C. E. (1994) Export of carbon, nitrogen, and major ions from 3 tropical montane watersheds. *Limnol. Oceanogr.* **39,** 111-125.

McDowell W. H., Sanchez C. G., Asbury C. E. and Perez C. R. R. (1990) Influence of sea salt aerosols and long-range transport on precipitation chemistry at El-Verde, Puerto-Rico. *Atmos Environ A-Gen* **24,** 2813-2821.

McDowell W. H., Bowden W. B. and Asbury C. E. (1992) Nitrogen dynamics in two geomorphologically distinct tropical rain forest watersheds: subsurface solute patterns. *Biogeochemistry* **18,** 53-75.

Murphy S. F., Brantley S. L., Blum A. E., White A. F. and Dong H. (1998) Chemical weathering in a tropical watershed, Luquillo Mountains, Puerto Rico: II Rate and mechanisms of biotite weathering. *Geochim. Cosmochim. Acta.* **62***(2)*, 227-243.

Murphy S. F. and Stallard R. F. (2012) Hydrology and climate of four watersheds in Eastern Puerto Rico. In *Water quality and landscape processes of four watersheds in Eastern Puerto Rico*: U.S. Geological Survey Professional Paper 1789 (eds. S. F. Murphy and R. F. Stallard). USGS, Reston, VA, pp. 43-84.

Murphy S. F., Stallard R. F., Larsen M. C. and Gould W. A. (2012) Physiography, geology and land cover of four watersheds in Eastern Puerto Rico. In *Water quality and landscape processes of four watersheds in Eastern Puerto Rico*: U.S. Geological Survey Professional Paper 1789 (eds. S. F. Murphy and R. F. Stallard). USGS, Reston, VA, pp. 1-24.

Newman L., Krouse H. R. and Grinenko V. A. (1991) Sulphur isotope variations in the atmosphere. In *Stable Isotopes in the Assessment of Natural and Anthropogenic Sulphur in the Environment* (eds. H. R. Krouse and V. A. Grinenko). SCOPE, vol. 43, John Wiley and Sons Ltd, Chichester. pp. 133-176.

Nielsen H., Pilot J., Grinenko L. N., Grinenko V. A., Lein A. Y., Smith J. W. and Paninka R. G. (1991) Lithospheric sources of sulfur. In *Stable Isotopes in the Assessment of Natural and Anthropogenic Sulphur in the Environment.* SCOPE, vol. 43, (eds. H. R. Krouse and V. A. Grinenko). John Wiley and Sons Ltd, Chichester. pp. 65-132.

Norman A. L. (1994) Isotope analysis of microgram quantities of sulfur: Applications to soil sulfur mineralization studies. PhD thesis, Univ. of Calgary, Canada.

Norman A. L., Giesemann A., Krouse H. R. and Jager H. J. (2002) Sulphur isotope fractionation during sulphur mineralization: Results of an incubation-extraction experiment with a Black Forest soil. *Soil Biol. Biochem.* **34,** 1425-1438.

Novak M., Bottrell S. H., Groscheova H., Buzek F. and Cerny J. (1995) Sulphur isotope characteristics of two North Bohemian forest catchments. *Water Air Soil Poll* **85,** 1641-1646.

Pett-Ridge J., Silver W. L. and Firestone M. K. (2006) Redox fluctuations frame microbial community impacts on N-cycling rates in a humid tropical forest soil. *Biogeochemistry* **81,** 95-110.

Pett-Ridge J. C. (2009) Contributions of dust to phosphorus cycling in tropical forests of the Luquillo Mountains, Puerto Rico. *Biogeochemistry* **94,** 63-80.

Pett-Ridge J. C., Derry L. A. and Kurtz A. C. (2009) Sr isotopes as a tracer of weathering processes and dust inputs in a tropical granitoid watershed, Luquillo Mountains, Puerto Rico. *Geochim. Cosmochim. Acta* **73,** 25-43.

Poulson S. R., Kubilius W. P. and Ohmoto H. (1991) Geochemical behavior of sulfur in granitoids during intrusion of the South Mountain Batholith, Nova-Scotia, Canada. *Geochim. Cosmochim. Acta* **55,** 3809-3830.

Prietzel J. and Mayer B. (2005) Isotopic fractionation of sulfur during formation of basaluminite, alunite, and natroalunite. *Chem. Geol.* **215,** 525-535.

Rees C. E., Jenkins W. J. and Monster J. (1978) Sulfur isotopic composition of ocean water sulfate. *Geochim. Cosmochim. Acta* **42,** 377-381.

Sakai H., Casadevall T. J. and Moore J. G. (1982) Chemistry and isotope ratios of sulfur in basalts and volcanic gases at Kilauea Volcano, Hawaii. *Geochim. Cosmochim. Acta* **46,** 729-738.

Sakai H., Desmarais D. J., Ueda A. and Moore J. G. (1984) Concentrations and isotope ratios of carbon, nitrogen and sulfur in ocean-floor basalts. *Geochim. Cosmochim. Acta* **48,** 2433-2441.

Savoie D. L., Prospero J. M. and Saltzman E. S. (1989) Non-sea-salt sulfate and nitrate in trade-wind aerosols at Barbados - evidence for long-range transport. *J Geophys Res-Atm* **94,** 5069-5080.

Scatena F. N. (1989) An introduction to the physiography and history of the Bisley Experimental Watersheds in the Luquillo Mountains of Puerto Rico. *General Technical Report - Southern Forest Experiment Station, USDA Forest Service.*

Schellekens J., Scatena F. N., Bruijnzeel L. A., van Dijk A. I. J. M, Groen M. M. A. and Hogezand R. J. P. (2004) Stormflow generation in a small rainforest catchment in the Luquillo Experimental Forest, Puerto Rico. *Hydrol. Process.* **18,** 505-530.

Schoeneberger P. J., Wysocki D. A., Benham E. C., and Broderson W. D. (eds.) (2002) Field book for describing and sampling soils, Version 2.0. NRCS, National Soil Survey Center, Lincoln, NE.

Scholl M. A., Shanley J. B., Zegarra J. P. and Coplen T. B. (2009) The stable isotope amount effect: New insights from NEXRAD echo tops, Luquillo Mountains, Puerto Rico. *Water Resour. Res.* **45,** W12407.

Seiders V. M. (1971) Cretaceous and lower Tertiary stratigraphy of the Gurabo and El Yunque Quadrangles, Puerto Rico. U.S. Geological Survey Bulletin. 58 p.

Silver W. L., Scatena F. N., Johnson A. H., Siccama T. G. and Sanchez M. J. (1994) Nutrient Availability in a Montane Wet Tropical Forest - Spatial Patterns and Methodological Considerations. *Plant Soil* **164,** 129-145.

Sim M. S., Bosak T. and Ono S. (2011) Large sulfur isotope fractionation does not require disproportionation. *Science* **333,** 74-77.

Soil Survey Staff, Natural Resources Conservation Service, United States Department of Agriculture. Web Soil Survey. Available online at: http://websoilsurvey.nrcs.usda.gov/. Accessed [05/15/2013].

Stallard R. F. (2012) Atmospheric inputs to watersheds of the Luquillo Mountains in Eastern Puerto Rico. In *Water quality and landscape processes of four watershed in eastern Puerto Rico*: U.S. Geological Survey Professional Paper 1789 (eds. S. F. Murphy and R. F. Stallard). USGS, Reston, VA, pp 85-112.

Stallard R. F. and Murphy S. F. (2012) Water quality and mass transport in four watersheds in Eastern Puerto Rico. In *Water quality and landscape processes of four watersheds in Eastern Puerto Rico*: U.S. Geological Survey Professional Paper 1789 (eds. S. F. Murphy and R. F. Stallard). USGS, Reston, VA, pp. 113-152.

Stanko-Golden K. M. and Fitzgerald J. W. (1991) Sulfur Transformations and pool sizes in tropical forest soils. *Soil Biol. Biochem* **23,** 1053-1058.

Stempvoort D. R. v., Reardon E. J. and Fritz P. (1990) Fractionation of sulfur and oxygen isotopes in sulfate by soil sorption. *Geochim. Cosmochim. Acta* **54,** 2817-2826.

Stevenson F. J. and Cole M. A. (1999) Cycles of Soil: Carbon, Nitrogen, Phosphorus, Sulfur, Micronutrients. Second Edition. John Wiley and Sons, Inc., Hoboken, NJ.

Tabatabai M. A. (1984) Importance of sulfur in crop production. *Biogeochemistry* **1,** 45-62.

Thode H. G. and Monster J. (1965) Sulfur-isotope geochemistry of petroleum, evaporates, and ancient seas. In *Fluids in Subsurface Environments* (eds. Young A. and J. E. Galley), *Mem. Am. Assoc. Petrol. Geol.* **4,** 367–377.

Trust B. A. and Fry B. (1992) Stable sulfur isotopes in plants - a review. *Plant Cell Environ* **15,** 1105-1110.

Turner B. F., Stallard R. F. and Brantley S. L. (2003) Investigation of in situ weathering of quartz diorite bedrock in the Rio Icacos basin, Luquillo Experimental Forest, Puerto Rico. *Chem. Geol.* **202,** 313-341.

Vitousek P. M. and Sanford R. L. (1986) Nutrient cycling in moist tropical forest. *Annu. Rev. Ecol. Syst.* **17,** 137-167.

Whelan M. and Rhew R. (2012) Effects of rainfall on terrestrial fluxes of global cooling gases: carbonyl sulfide (COS) and its precursor dimethyl sulfide (DMS). Abstract B44C-07, presented at 2012 Fall Meeting, AGU, San Francisco, Calif., 3-7 Dec.

Whelan M. E., Min D. H. and Rhew R. C. (2013) Salt marsh vegetation as a carbonyl sulfide (COS) source to the atmosphere. *Atmos. Environ.* **73**, 131-137.

White A. F., Blum A. E., Schulz M. S., Vivit D. V., Stonestrom D. A., Larsen M., Murphy S. F. and Eberl D. (1998) Chemical weathering in a tropical watershed, Luquillo mountains, Puerto Rico: I. Long-term versus short-term weathering fluxes. *Geochim. Cosmochim. Acta* **62,** 209-226.

White A. F., Schulz M. S., Stonestrom D. A., Vivit D. V., Fitzpatrick J., Bullen T. D., Maher K. and Blum A. E. (2009) Chemical weathering of a marine terrace

chronosequence, Santa Cruz, California. Part II: Solute profiles, gradients and the comparisons of contemporary and long-term weathering rates. *Geochim. Cosmochim. Acta* **73,** 2769-2803.

Winner W. E., Smith C. L., Koch G. W., Mooney H. A., Bewley J. D. and Krouse H. R. (1981) Rates of emission of H_2S from plants and patterns of stable sulfur isotope fractionation. *Nature* **289,** 672-673.

Zhang Y. M., Mitchell M. J., Christ M., Likens G. E. and Krouse H. R. (1998) Stable sulfur isotopic biogeochemistry of the Hubbard Brook Experimental Forest, New Hampshire. *Biogeochemistry* **41,** 259-275.

TABLES

Table 1: Isotopic values of some S sources relevant to the LEF.

Source	$\delta^{34}S$ [‰]	References
marine sulfate	21	Rees et al. (1987)
sulfate aerosol over the North Atlantic	2 to 15 (mean 11 ± 0.9)	Gravenhorst (1978)
Sahara dust collected over the North Atlantic	11 to 13	Gravenhorst (1978)
mean nss-sulfate aerosols (from DMS oxidation) over the South Pacific	15.6 ± 3.1	Calhoun et al. (1991)
mean precipitation over the Atlantic and Pacific	13.3	Chukrov et al. (1980)
mean volatile reduced biogenic S compounds	~0	Wakshal and Nielsen (1982)
mean volcanic SO_2 emissions	~5	Nielsen et al. (1991)
unaltered ocean-floor basalt	0.3 ± 0.5	Sakai et al. (1984)
basalt (Hawaii)	-0.8 ± 0.2	Sakai et al. (1982)
basalt (Costa Rica)	-16.4 ± 10.8	Bern et al. (2007)
granodiorite (Nova Scotia, Canada)	5.4 to 12.3	Poulson et al. (1991)
granite (Nova Scotia, Canada)	1.6 to 15	Poulson et al. (1991)
granite (New Brunswick, Canada)	-7.1 to 13 (mean 2.2 ± 5.0)	Yang and Lentz (2010)
coal combustion	-0.5 to 20 (typically -1 to 3)	Newman et al. (1991)
oil	-5 to 30 (typically 0 to 10)	Newman et al. (1991)

Table 2: Fractionation ($\alpha = \frac{R_{product}}{R_{substrate}}$) and enrichment ($\varepsilon = (\alpha - 1) \cdot 1000$) factors for some common S transformations.

Process	S fractions (substrate-product)	α	ε	References
Biotic (aquatic)				
organic S mineralization by *P. vulgaris* at 25°C	organic S-H_2S	0.9957	-4.3	Kaplan and Rittenberg (1964)
sulfate assimilation by bacteria (*E. coli*) at 30°C	SO_4^{2-}-SOS	0.9972 to 0.9978	-2.8 to -2.2	Kaplan and Rittenberg (1964)
sulfate assimilation by green algae (*Ankistrodesmus sp.*) at 30°C	SO_4^{2-}-SOS	0.9982 to 0.9991	-1.8 to -0.9	Kaplan and Rittenberg (1964)
sulfate assimilation by yeast (*S. cerevisiae*) at 30°C	SO_4^{2-}-SOS	0.9972	-2.8	Kaplan and Rittenberg (1964)
sulfate reduction by *D. desulfuricans* at 10-30°C	SO_4^{2-}-S^{2-}	0.954 to 0.9937	-46 to -6.3	Kaplan and Rittenberg (1964)
sulfate reduction by *D. vulgaris* and *C. vibrioforme* at 20-25°C	SO_4^{2-}-S^{2-}	0.9928	-7.2	Fry et al. (1988a)
sulfide oxidation by *T. concretivorus*	S^2-S^0	0.9975 to 1.0012	-2.5 to 1.2	Kaplan and Rittenberg (1964)
sulfide oxidation by *D. vulgaris* and *C. vibrioforme* at 20-25°C	S^2-S^0	1.0017	1.7	Fry et al. (1988a)
sulfur oxidation by *D. vulgaris* and *C. vibrioforme* at 20-25°C	S^0-SO_4^{2-}	0.9983	-1.7	Fry et al. (1988a)

Table 2 continued:

Process	S fractions (substrate-product)	α	ε	References
sulfide oxidation by *T. concretivorus*	S^{2-}-SO_4^{2-}	0.972 to 0.9895	-18 to -10.5	Kaplan and Rittenberg (1964)
sulfide oxidation by *Chromatium sp.* at 30°C	S^{2}-S^{0}	0.990 to 0.9949	-10 to -5.1	Kaplan and Rittenberg (1964)
sulfide oxidation by *Chromatium sp.* at 30°C	S^{2-}-SO_4^{2-}	0.9971 to 1.0009	-2.9 to 0.9	Kaplan and Rittenberg (1964)
assimilatory sulfate reduction by algae and aqueous rooted plants	SO_4^{2-}-org S^{2-}	0.998 to 0.999	-2 to -1	Mekhtiyeva (1971)
Biotic (soil/sediment)				
dissimilatory sulfate reduction	SO_4^{2-}-S^{2-}	≥ 0.93	≥ -70	Brunner and Bernasconi (2005)
oxidation of reduced S	S^{2-}-SO_4^{2-}		~-1	Norman, 1994
microbial SOS mineralization	SOS-SO_4^{2-}	0.999 ± 0.001	-1 ± 1	Norman et al. (2002)
assimilatory sulfate reduction by plants (average from several studies)	SO_4^{2-}-org S^{2-}	0.9985	-1.5	Trust and Fry (1992)
Abiotic (aquatic)				
abiotic oxidation of sulfide (aquatic media)	S^{2-}-SO_4^{2-}	0.997	-3	Kaplan and Rafter (1958)
abiotic oxidation of sulfide by oxygen (aquatic media)	S^{2-}-SO_4^{2-}	0.9948 ± 0.0014	-5.2 ± 1.4	Fry et al. (1988b)
wetting and drying cycles	solution SO_4^{2-}-gypsum	1.00165	1.65	Thode and Monster (1965)
Abiotic (soil)				
sorption/desorption of sulfate (in spodosols)	sorbed SO_4^{2-}-solution SO_4^{2-}	1.001 ± 0.001	1 ± 1	Stempvoort et al. (1990)
precipitation/dissolution of alunite	solution SO_4^{2-}-alunite	1.00084 ± 0.00034	0.84 ± 0.34	Prietzel and Mayer (2005)

Table 3: Study site characteristics.

Site Name:	Icacos	Bisley
Elevation range [m]	600-800[1]	265-456[2]
MAP [mm]	4200[3]	3500[2]
MAT [°C]	22[1]	23[4]
Forest Type	Colorado (*Cyrilla racemiflora)*[1]	Tabonuco (*Dacryodes excelsa*) [5]
Parent material	quartz diorite[6]	volcaniclastics[2]
Soil type	Inceptisols (Picacho and Utuado series)[7]	Ultisols (Humatus-Zarzal-Cristal complex)[8]

[1]White et al. (1998); [2]Scatena (1989); [3]Buss et al. (2010); [4]Murphy and Stallard (2012); [5]Heartsill-Scalley et al. (2007); [6]Seiders, 1971; [7]Huffaker, 2002; [8]Boccheicamp, 1977.

Table 4: Sampling locations.

Site code:	Topographic position	Elevation [masl]	Coordinates (datum: NAD83)
Icacos:			
LG-1	ridgetop	672	N18°16.903', W65°47.418'
LG-2	steep slope	664	N18°16.895', W65°47.409'
LG-3	ridge shoulder	681	N18°16.902', W65°47.441'
Bisley:			
B1S1	ridgetop	290	N18°18.956', W65°44.700'
B1S2	upper slope	288	N18°18.947', W65°44.705'
B1S4	lower slope	287	N18°18.937', W65°44.711'

Table 5: List of lysimeters sampled.

Location	Depth (in cm) of lysimeters sampled in May 2010	Depth (in cm) of lysimeters sampled from 02/2011 until 02/2012
LG-1	15, 31, 61, 91, 152, 183, 244, 548, 671, 853	15, 61, 91, 183
LG-2	15, 31, 61, 91, 122, 152, 183	15, 61, 152/122*, 183
LG-3	61, 91, 122, 152, 183, 213, 229	61, 91, 152, 183
B1S1	15, 31, 61, 91, 122, 152, 183, 427, 930	15, 61, 91, 183
B1S2	15, 31, 61, 91, 122, 152, 183, 213, 274	15, 61, 91, 183
B1S4	15, 31, 61, 91	15, 31, 61, 91

*The 152 cm lysimeter at LG-2 broke during the sampling period and delivered samples only until April 2011; as of August 2011 the 122 cm lysimeter was sampled instead.

Table 6: Field data for the Icacos soil from a pit dug at the ridge shoulder site. Nomenclature according to NRCS guidelines (Schoeneberger et al., 2002).

Horizon	Top [cm]	Bottom [cm]	Color	Text.	Clay %	Cons.	Structure	Roots	Features
O	3	0							
A1	0	7.5	10YR 4/6	cl	34	s, p	3 f,c sbk	2vf, 2f, 1m, 1c	
A2	7.5	16	10YR 5/6	cosc	37	vs, p	2 f,c sbk	1vf, 1f, 1c	
Btg1	16	30	10YR 7/2, 7/6; 7.5YR 6/8	cosc	40	vs, vp	3 c,vc sbk	1vf	
Btg2	30	45	10YR 7/2, 7/6; 7.5YR 5/8; 5YR 5/8	sc	>40	vs, vp	2 m,c sbk	1vf	
Btv	45	75	5YR 5/8; 10YR 6/8; 10YR 4/4	c (or vfsc)	>40	vs, vp	2 c,vc sbk	1vf	plinthite; dark spots with humus and Mn
Bt1	75	85	10YR 2/1; 7.5YR 6/4; 5YR 4/4; 2.5YR 4/6	cosc	35	vs, p	2 m,c sbk	0	Mn-rich zone
Bt2	85	102	2.5YR 4/6	cl	38	s, p	2 m,c sbk	0	white quartz and mica-rich; smooth
Btg3	102	111	5YR 8/1; 5YR 6/6	c	>40	s, p	2 m sbk	0	
Crt	111	127	2.5YR 3/4, 5YR 5/8, 7.5YR 7/5	grls	3	so, po	rock texture	0	oxidized saprolite with black Mn oxides

Table 7: Field data for the Bisley soil from a pit dug at the ridgetop site. Nomenclature according to NRCS guidelines (Schoeneberger et al., 2002).

Horizon	Top [cm]	Bottom [cm]	Color	Text.	Clay %	Cons.	Structure	Roots	Features
O	2	0	10YR 5/6					mat below litter	highly mixed
A1	0	10	10YR 5/6	cl	38-40	s, p	3 f,m sbk	3vf, 3f, 2m, 2c	highly mixed
A2	10	17	10YR 6/8, 5/6	c	45	s, p	3 f sbk	2vf, 2f, 1m, 1c	
Btg1	17	40	10YR 7/8; 7.5YR 6/8	c	>45	s, p	2 c abk	1vf, 1f, 1c	
Bt1	40	66	5YR 6/8; 10YR 5/6	c	>45	s, p	2 c abk → 2 f abk	1vf, 1f	
Bt2	66	95	2.5YR 6/8, 6/6; 10YR 7/8	c	>45	s, p	2 c sbk → 2 m sbk	1vf, 1f	white saprolite flakes mixed in; some reduced spots
Bt3	95	102	10R 5/6; 7.5YR 5/6	c	>45	s, p	2 m,c sbk	1vf	flakes of saprolite
Btg2	102	142	5YR 5/6; 10R 5/6; 7.5YR 6/8	c	40-45	s, p	2 m,c sbk	1vf	
Crt	142	158	10R 5/8	cl	36	s, p	2 c sbk	1vf	many white flakes of kaolinized grus

Table 8: The C, N and S composition of vegetation and O horizon (litter layer) at the Icacos and Bisley sites. All samples are whole leaves or leaf fragments collected from the forest floor in May 2010. Samples were run at least in duplicates. Analytical error is 0.1‰ for C and N isotopes and 5% of the value for C and N concentration; analytical error for S it is 0.6‰ for isotopes and 350 mg/kg for concentration.

Sample type	C %	$\delta^{13}C$ [‰]	N %	$\delta^{15}N$ [‰]	S [mg/kg]	$\delta^{34}S$ [‰]	C:N	C:S	N:S
Icacos:									
ground ferns	39.40	-32.9	1.37	-0.41	2266	13.9	29	174	6:1
Bromeliads (family Bromeliaceae)	45.63	-29.9	0.62	-2.5	1076	13.8	74	424	6:1
Heliconia (family Heliconiaceae)	48.01	-28.5	1.08	1.0	1018	13.2	45	471	11:1
ferns	44.90	-32.3	1.51	1.8	2078	13.8	30	216	7:1
Sierra Palm (*Prestoea Montana*)	45.18	-30.2	1.49	-2.9	7150	15.5	30	63	2:1
Colorado (*Cyrilla racemiflora*)	51.51	-33.2	0.95	0.97	1671	15.4	54	308	6:1
O horizon (3-0 cm)	50.41	-29.7	0.64	-0.63	965	12.9	78	522	7:1
Bisley:									
Tabonuco (*Dacryodes excelsa*)	45.38	-36.0	1.67	-0.51	1791	14.9	27	253	9:1
Sierra Palm (*Prestoea Montana*)	43.44	-31.7	1.41	-1.7	4354	16.0	31	100	3:1
O horizon (2-0 cm)	32.97	-30.0	1.13	-0.04	1040	13.3	29	317	11:1

Table 9: Anion chemistry of the East Peak precipitation samples. The non-seasalt fraction calculations assume all Cl is of marine origin and use the SO_4/Cl in seasalt ratio from Keene et al. (1986). The calculated non-seasalt sulfate $\delta^{34}S$ values assume linear mixing of seasalt and non-seasalt sulfate. Missing isotope values indicate samples that had insufficient S due to low sulfate concentration and/or low sample volume.

Sampling date	Cl [μM]	SO_4 [μM]	SO_4 $\delta^{34}S$ [‰]	% nss-SO_4	Calculated nss-SO_4 $\delta^{34}S$ [‰]
6/1/10	18	7.3		87	
7/6/10	46	11.1	12.6	78	10.3
8/3/10	164	19.4	18.3	56	16.1
9/7/10*	76	10.9	17.9	64	16.1
10/5/10*	35	12.4	15.8	85	14.9
11/2/10	110	13.6	16.6	58	13.5
12/14/10*	37	9.5		80	
1/25/11	118	26.2		77	
2/8/11	158	12.8		36	
3/8/11	148	10.4	18.5	26	11.1
4/5/11	226	38.8	10.7	70	6.3
5/17/11	18	5.4		83	
6/7/11	19	8.2	12.3	88	11.0
7/19/11	196	23.1	17.6	56	14.9
8/9/11	56	10.8	17.2	73	15.7
9/6/11	27	4.6	18.0	69	16.7
10/11/11	61	13.4		76	
11/8/11*	38	13.2	20.5	85	20.5
1/3/12	113	13.9	14.7	58	10.1
1/31/12	164	12.7	21.4	33	22.3
3/13/12*	125	14.4	15.8	55	11.6
6/26/12	166	24.5	16.0	65	13.2
average (volume-weighed)	***116 ± 65***	***15.9 ± 7.9***	***16.1 ± 2.8***	***63 ± 18***	***13.4 ± 4.0***

* These samples were not included in the volume-weighted averages due to missing volume information.

Table 10: Anion chemistry of the Guaba (tributary of Rio Icacos) and Bisley streams compared to groundwater sampled at the Icacos site. The streams were sampled at or near baseflow.

Sampling date	Cl [μM]	SO_4 [μM]	SO_4 $\delta^{34}S$ [‰]
Guaba stream:			
2/2/12	175	13.9	20.2
3/8/12	206	14.9	17.7
6/20/12	165	14.8	20.6
average	***182 ± 21***	***14.6 ± 0.5***	***19.5 ± 1.6***
Bisley stream:			
2/2/12	221	39.1	1.9
3/8/12	226	39.5	0.9
6/26/12	214	39.7	2.0
average	***220 ± 6***	***39.4 ± 0.3***	***1.6 ± 0.7***
Icacos groundwater:			
8/18/12	160	14.6	20.2

Table 11: The α values used in the advection model to best approximate measured depth profiles of total soil $\delta^{15}N$ for the Icacos and Bisley soils.

Location	α
Icacos ridge shoulder pit	0.9992
Icacos ridge shoulder	0.9992
Icacos steep slope	0.9986
Icacos	
Bisley ridgetop pit	0.9985
Bisley ridgetop	0.9997
Bisley upper slope	0.9995
Bisley lower slope	0.9990

FIGURES

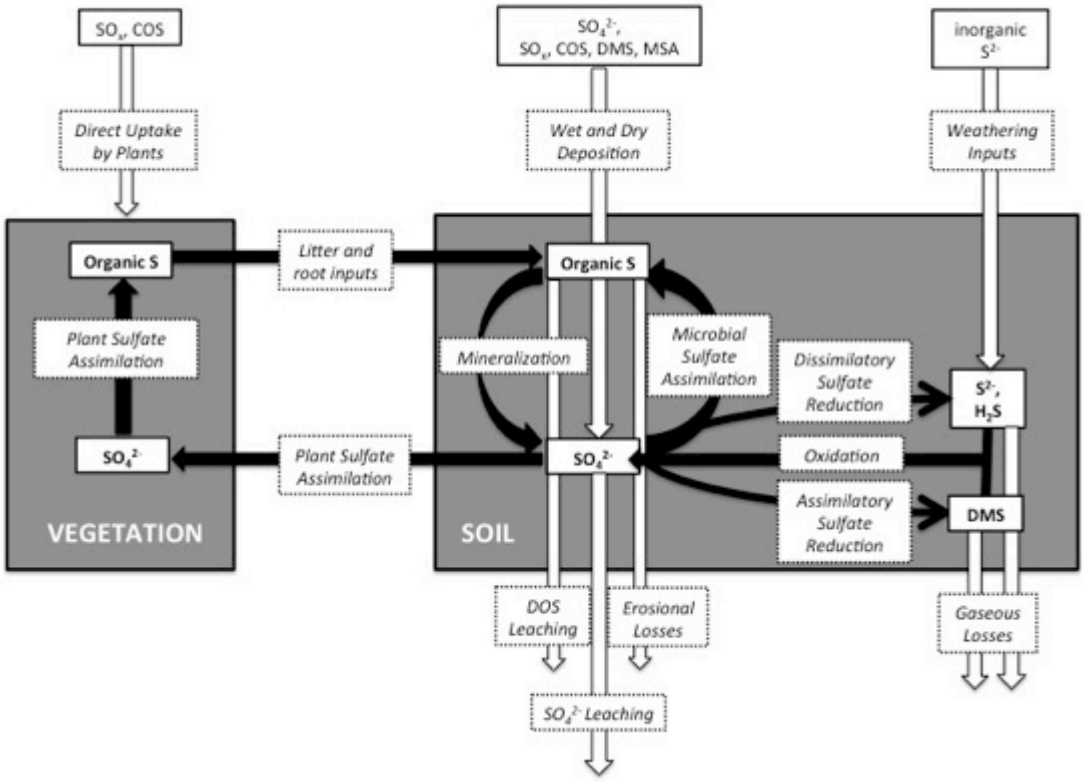

Figure 1: Schematic representation of the terrestrial S cycle, showing major inputs, outputs and in-soil biologically-mediated transformations. White arrows represent inputs to and outputs from the coupled soil-vegetation system. Black arrows represent S transformations within the soil-vegetation system. (COS: carbonyl sulfide; DMS: dimethyl sulfide; DOS: dissolved organic sulfur; MSA: methanesulfonic acid).

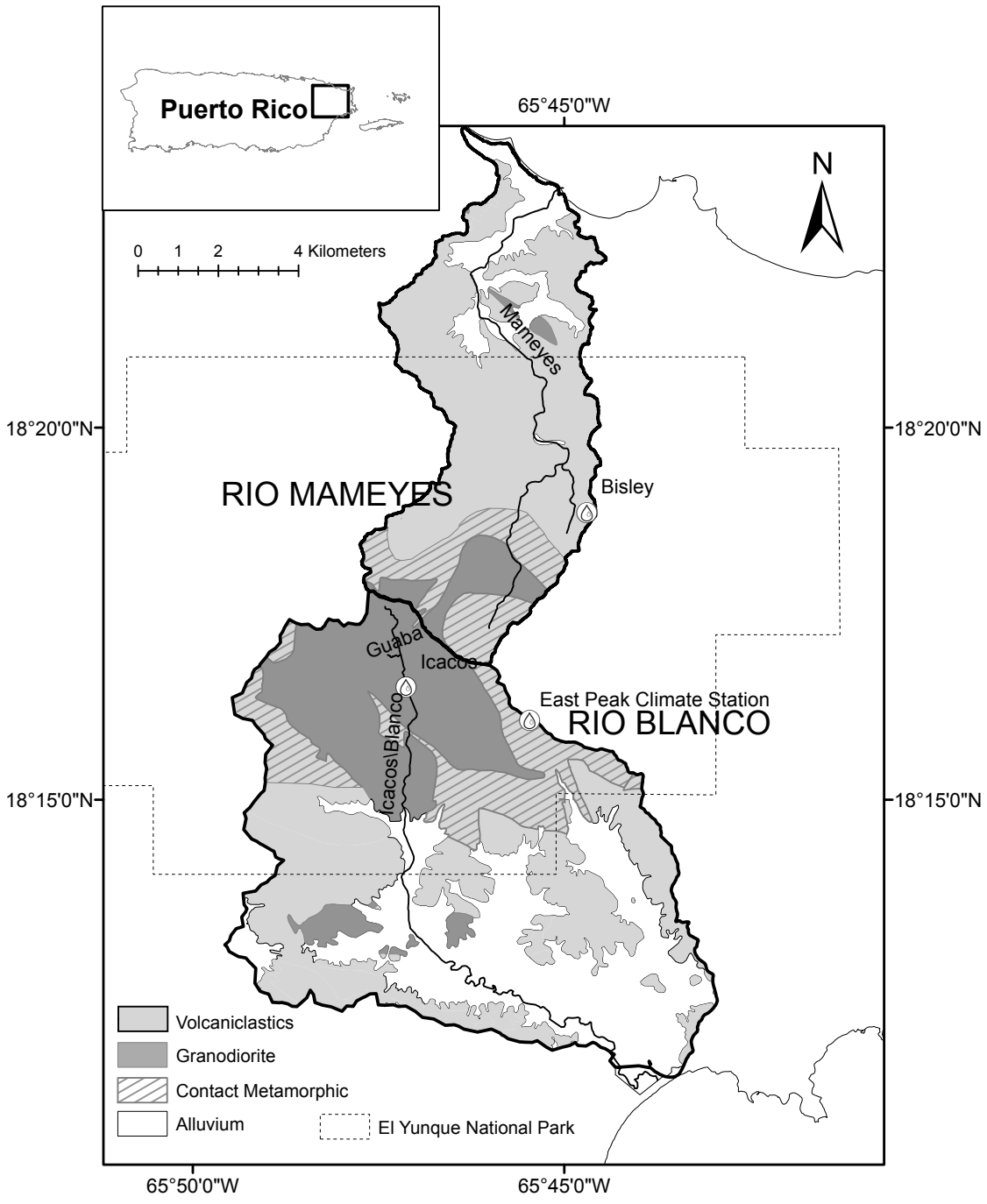

Figure 2: Map of the study area. Courtesy of Miguel Leon through the Luquillo Critical Zone Observatory (EAR-0722476).

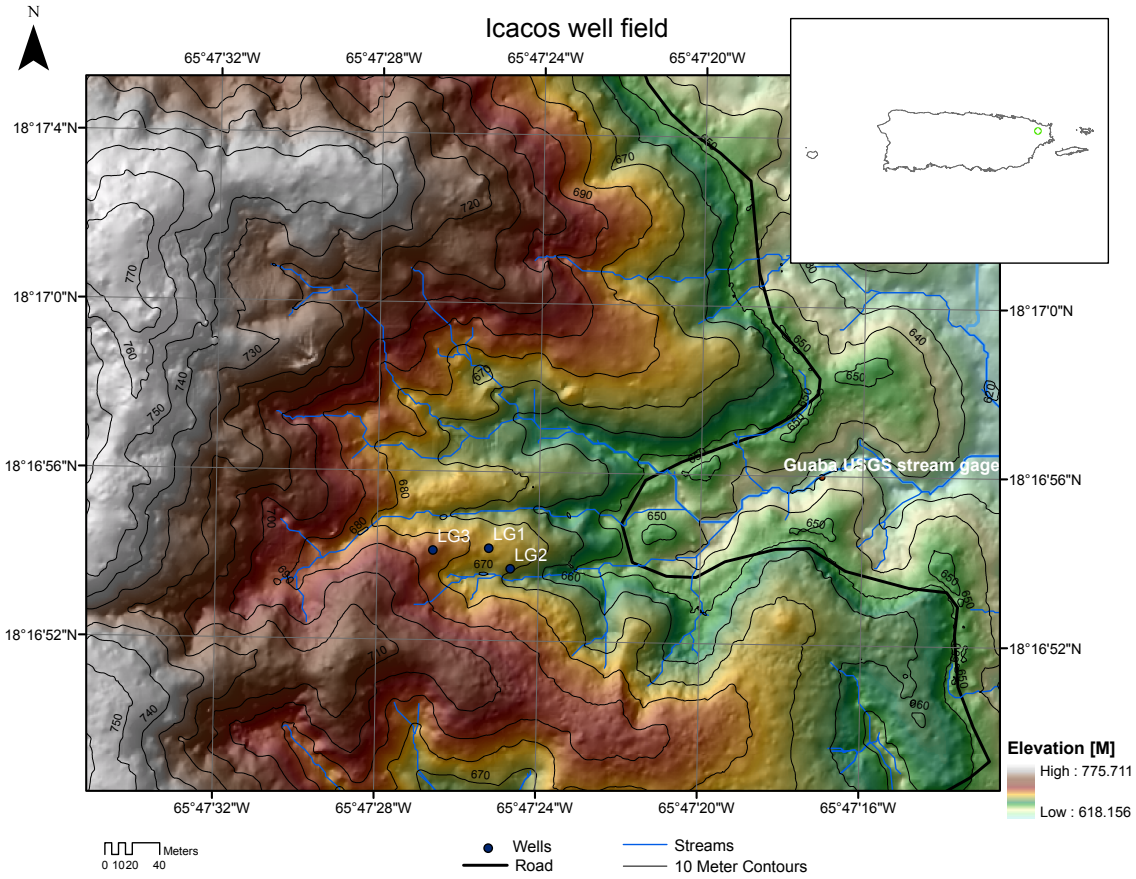

Figure 3: Map of the Icacos field site, showing the location of the three lysimeter fields, LG3 (ridge shoulder), LG1 (ridgetop) and LG2 (steep slope). Courtesy of Miguel Leon through the Luquillo Critical Zone Observatory (EAR-0722476).

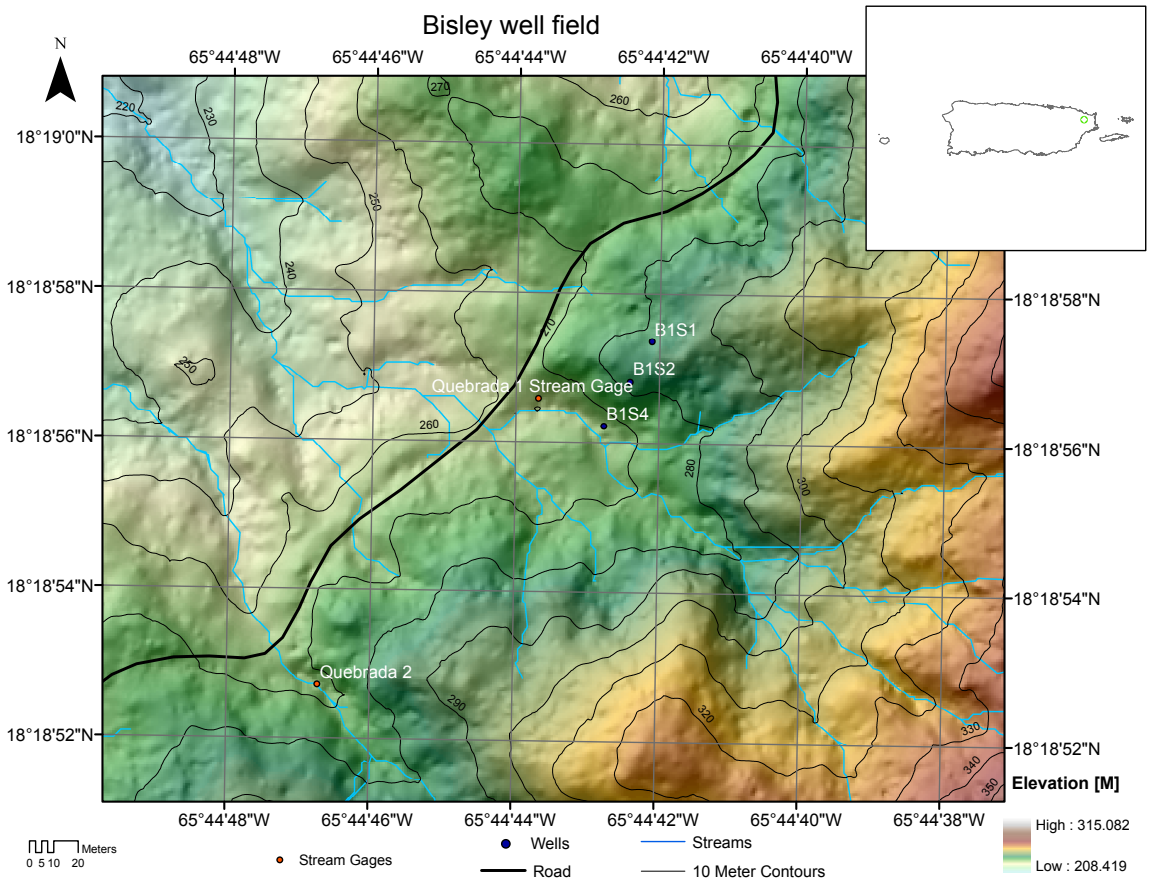

Figure 4: Map of the Bisley field site, showing the location of the three lysimeter fields, B1S1 (ridgetop), B1S2 (upper slope) and B1S4 (lower slope). Courtesy of Miguel Leon through the Luquillo Critical Zone Observatory (EAR-0722476).

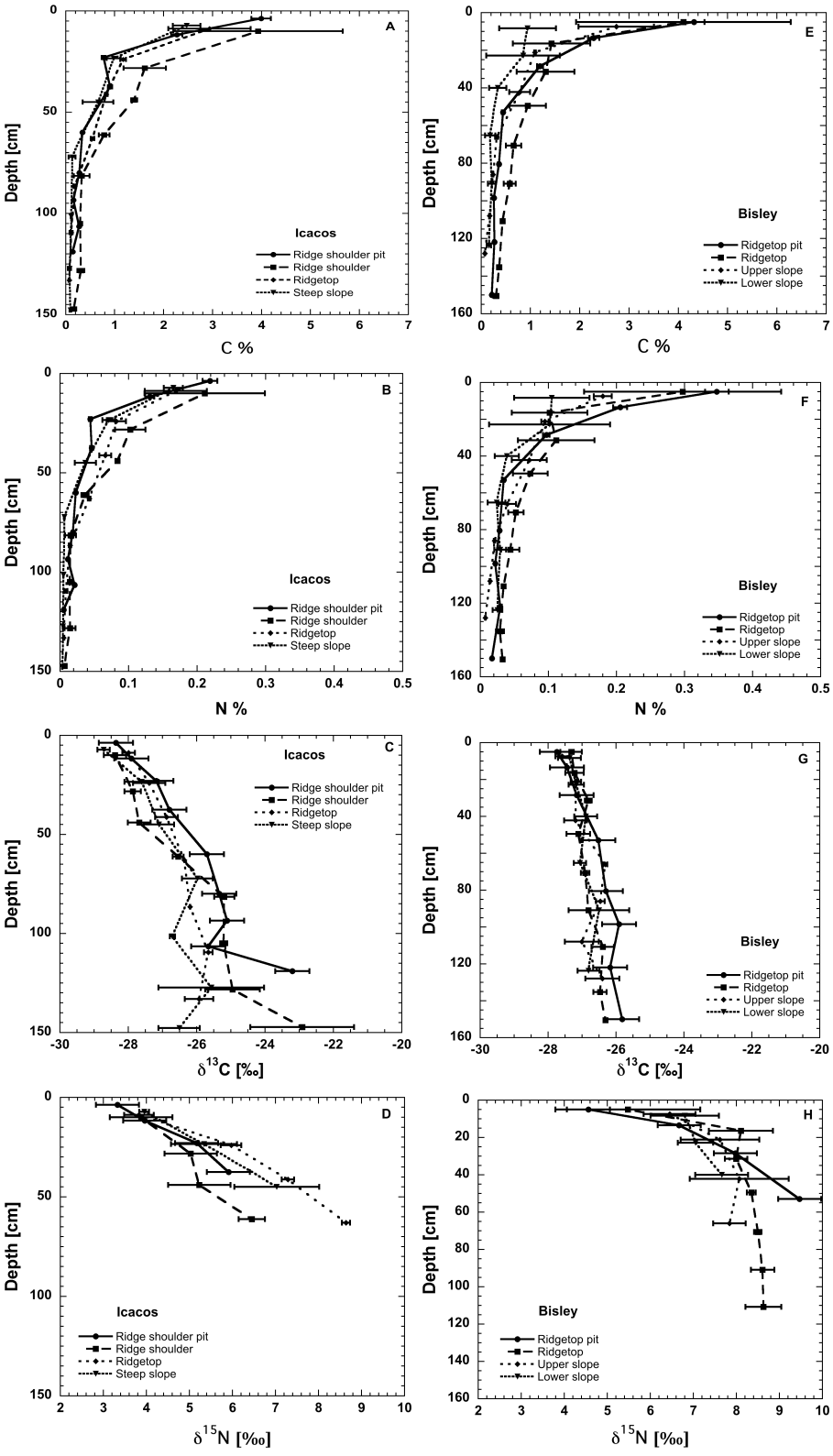

Figure 5 a-h: C and N concentration and stable isotopes for soil and plants at Icacos (a-d) and Bisley (e-h). Concentrations for litter and O horizon are off the scale and not

shown. Except for the pit soils, which were sampled according to horizon designation, all other data are averages of two soil cores, and the error bars represent the variability observed among the different core samples.

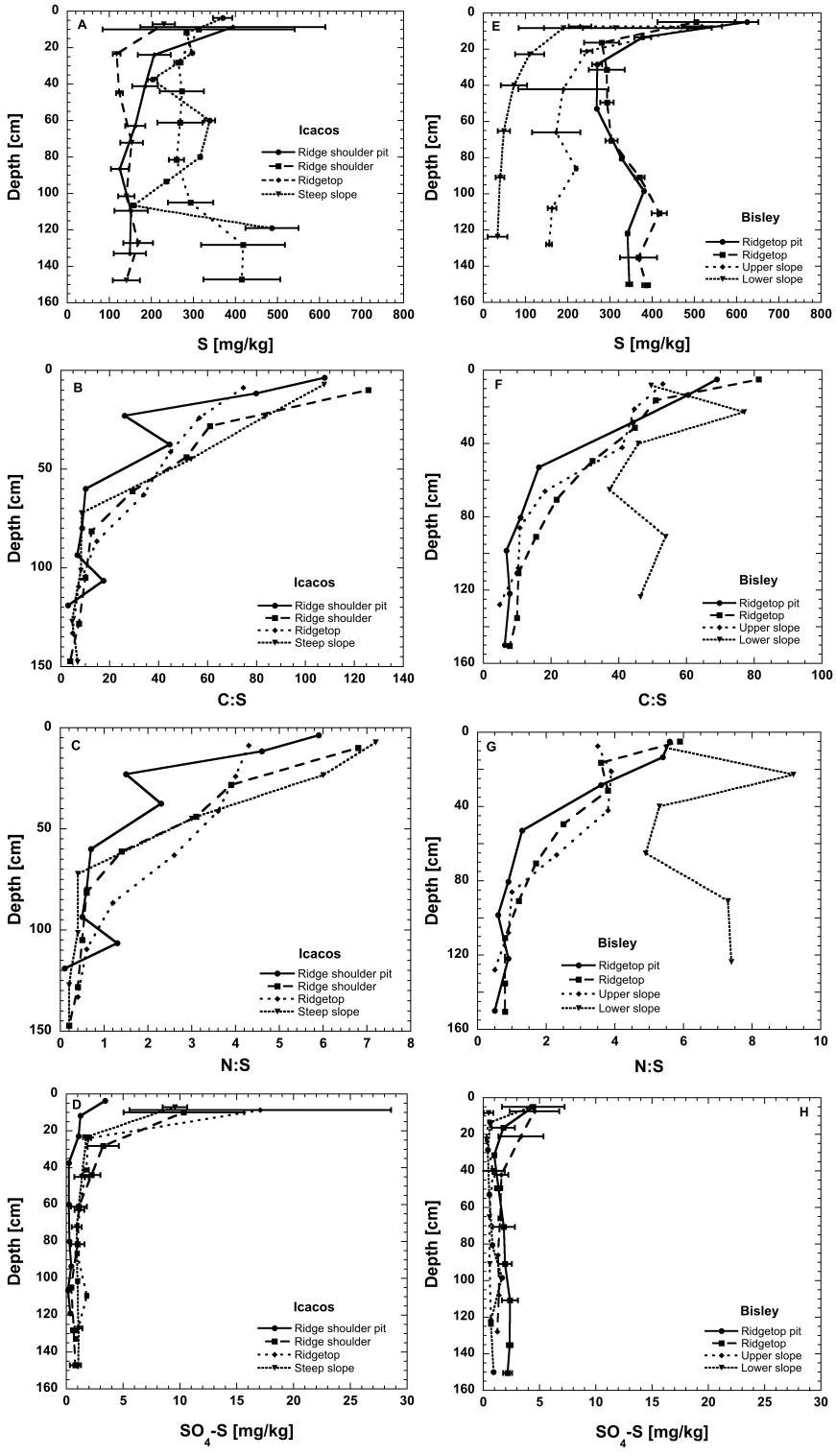

Figure 6 a-h: Depth trends in total S, C:S, N:S and sulfate S concentration for the Icacos (a-d) and Bisley (e-h) soils. Except for the pit soils, which were sampled according to horizon designation, all other data are averages of two soil cores, and the error bars represent the variability observed among the different core samples.

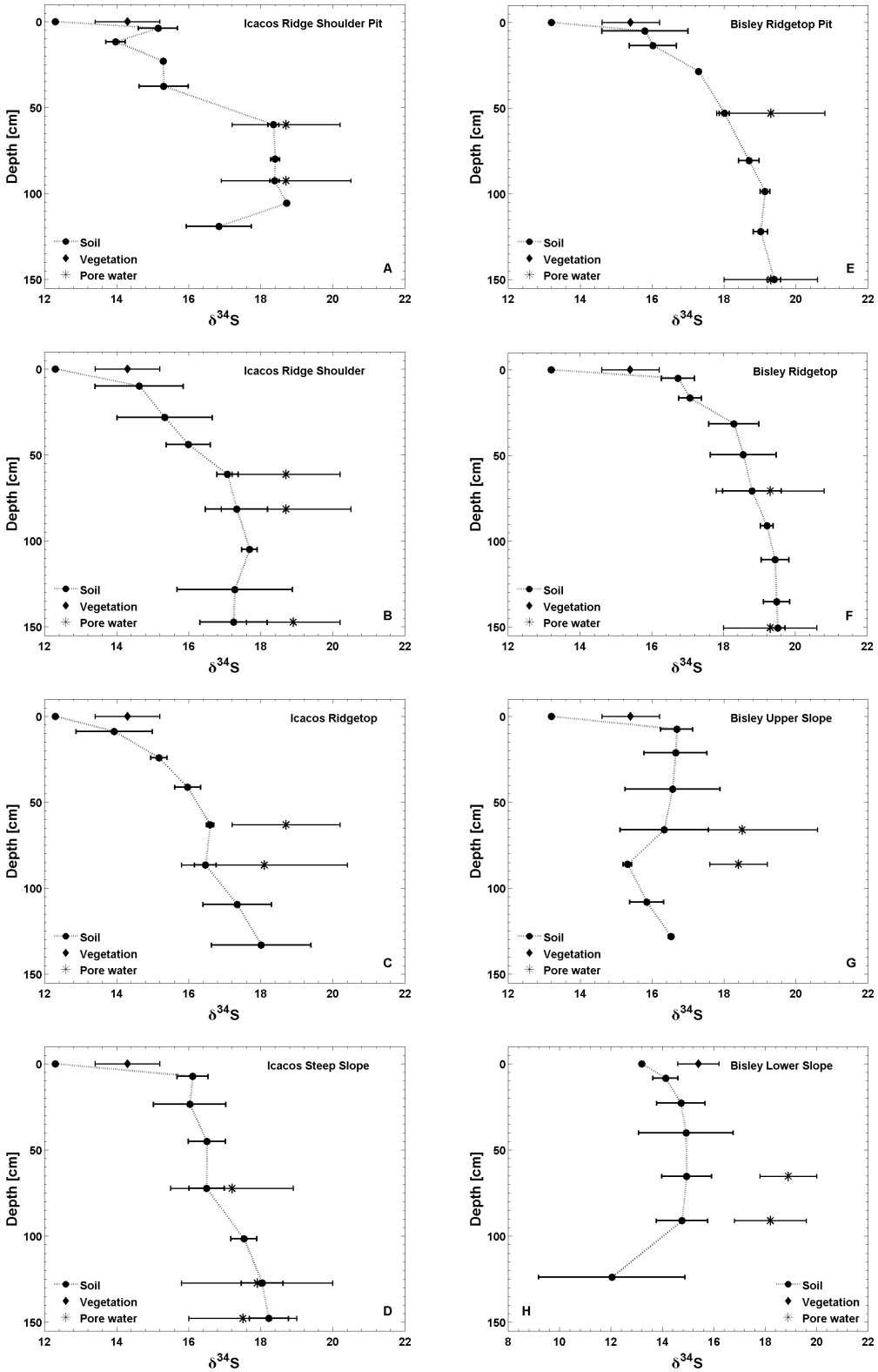

Figure 7 a-h: Soil S isotopes compared with vegetation and pore water averaged over the entire study period at Icacos (a-d) and Bisley (e-h). The sample at 0 cm is the O horizon.

Except for the pit soils, which were sampled according to horizon designation, all other data are averages of two soil cores, and the error bars represent the variability observed among the different core samples. The error bars for pore water values represent the variability seen in different months. Similarly, error bars in the plant value represent variability seen among different plant types.

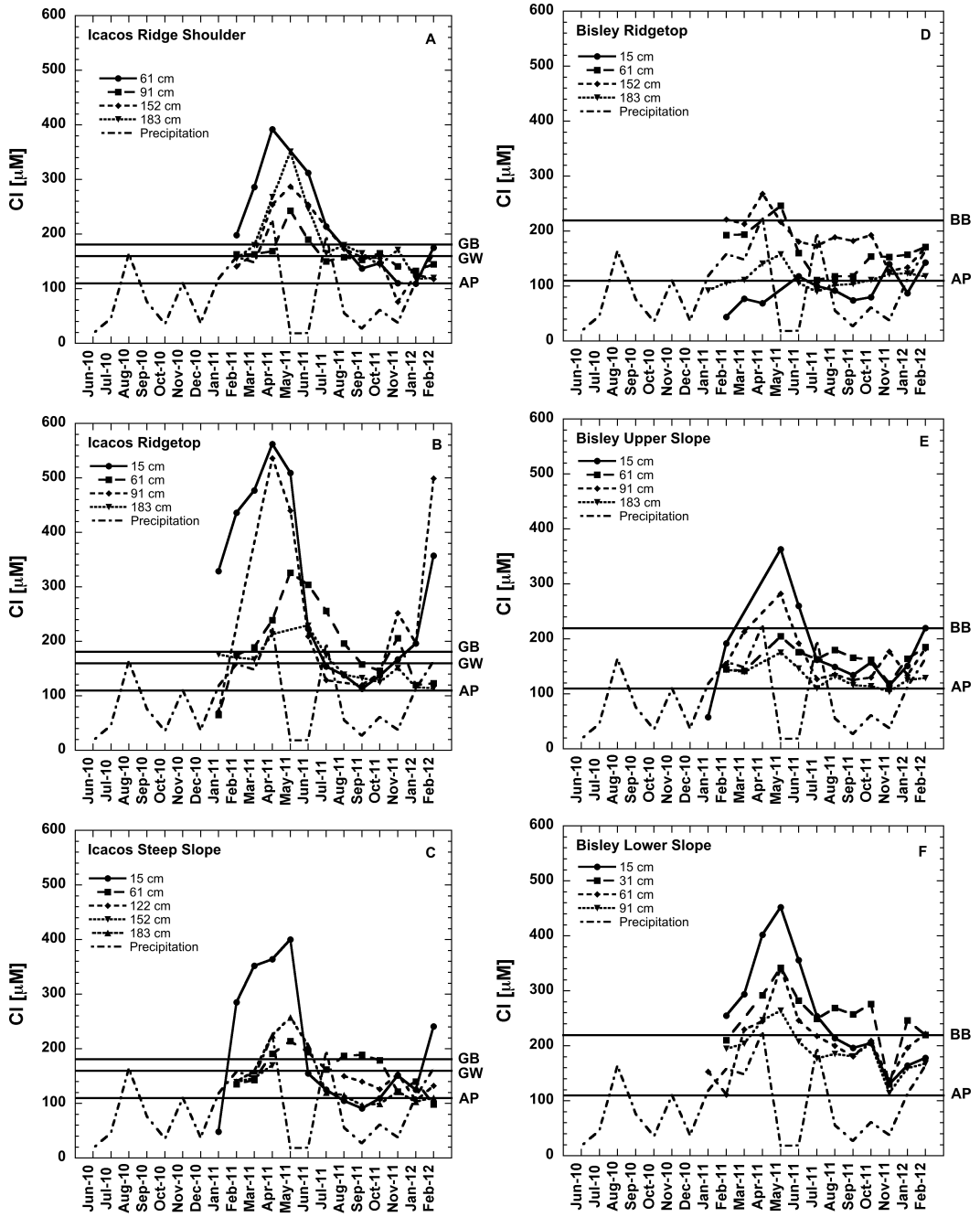

Figure 8 a-f: Temporal variations in pore water Cl concentration at different depths on the three topographic positions at Icacos (a-c) and Bisley (d-f). Horizontal lines represent the Cl concentrations of volume-weighed average precipitation (AP), groundwater (GW) at the Icacos site, Guaba baseflow (GB) and Bisley baseflow (BB). Precipitation data were included for comparison.

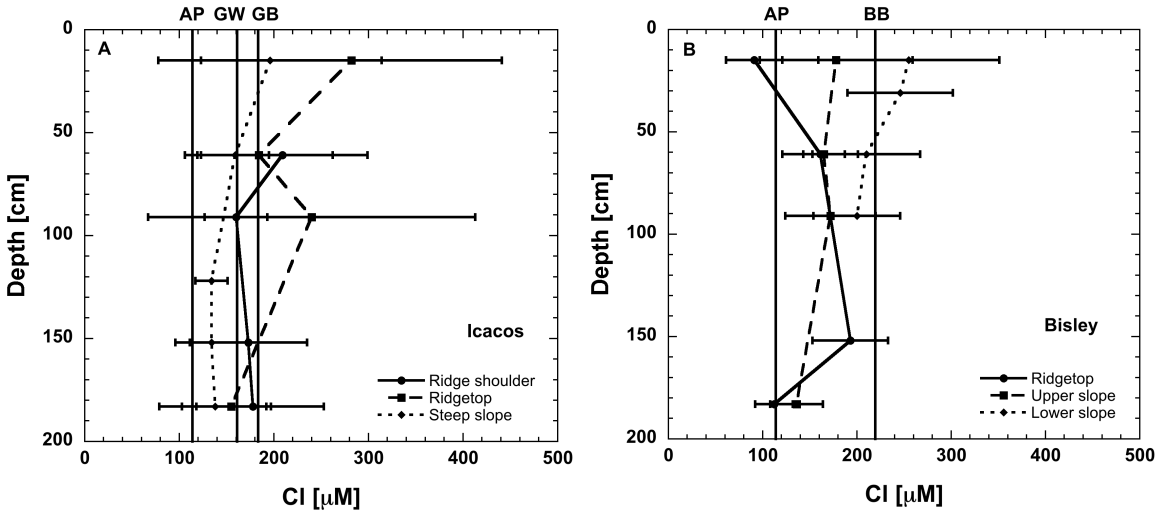

Figure 9 a-b: Depth trends in pore water Cl concentrations averaged over the entire sample period at Icacos (a) and Bisley (b). The error bars are standard deviations. Vertical lines represent the Cl concentration of volume-weighed average precipitation (AP), groundwater (GW) at the Icacos site, Guaba baseflow (GB) and Bisley baseflow (BB).

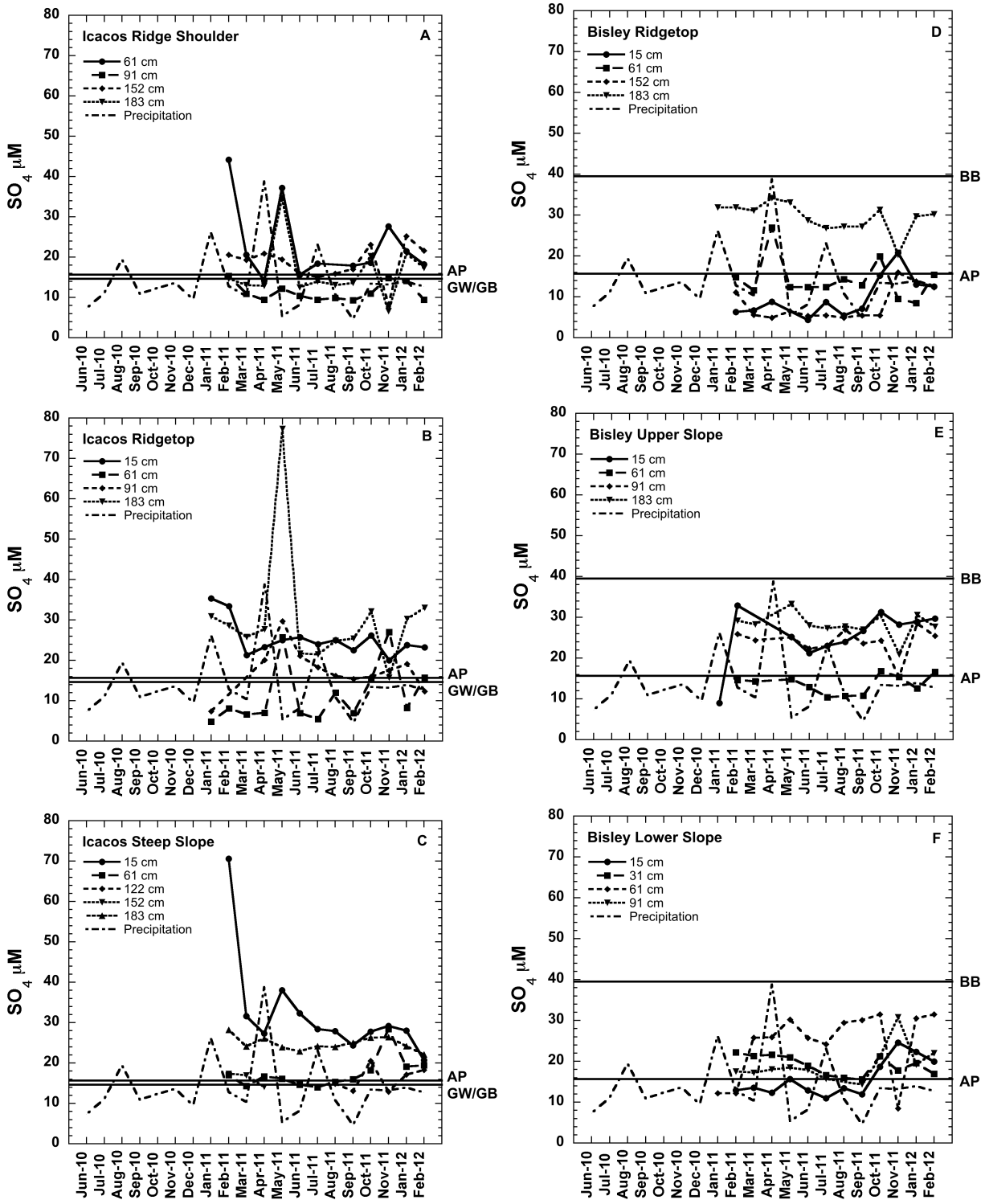

Figure 10 a-f: Temporal variations in pore water sulfate concentration at different depths on the three topographic positions at Icacos (left) and Bisley (right). Horizontal lines represent the Cl concentrations of volume-weighed average precipitation (AP), groundwater (GW) at the Icacos site, Guaba baseflow (GB) and Bisley baseflow (BB). Precipitation data were included for comparison.

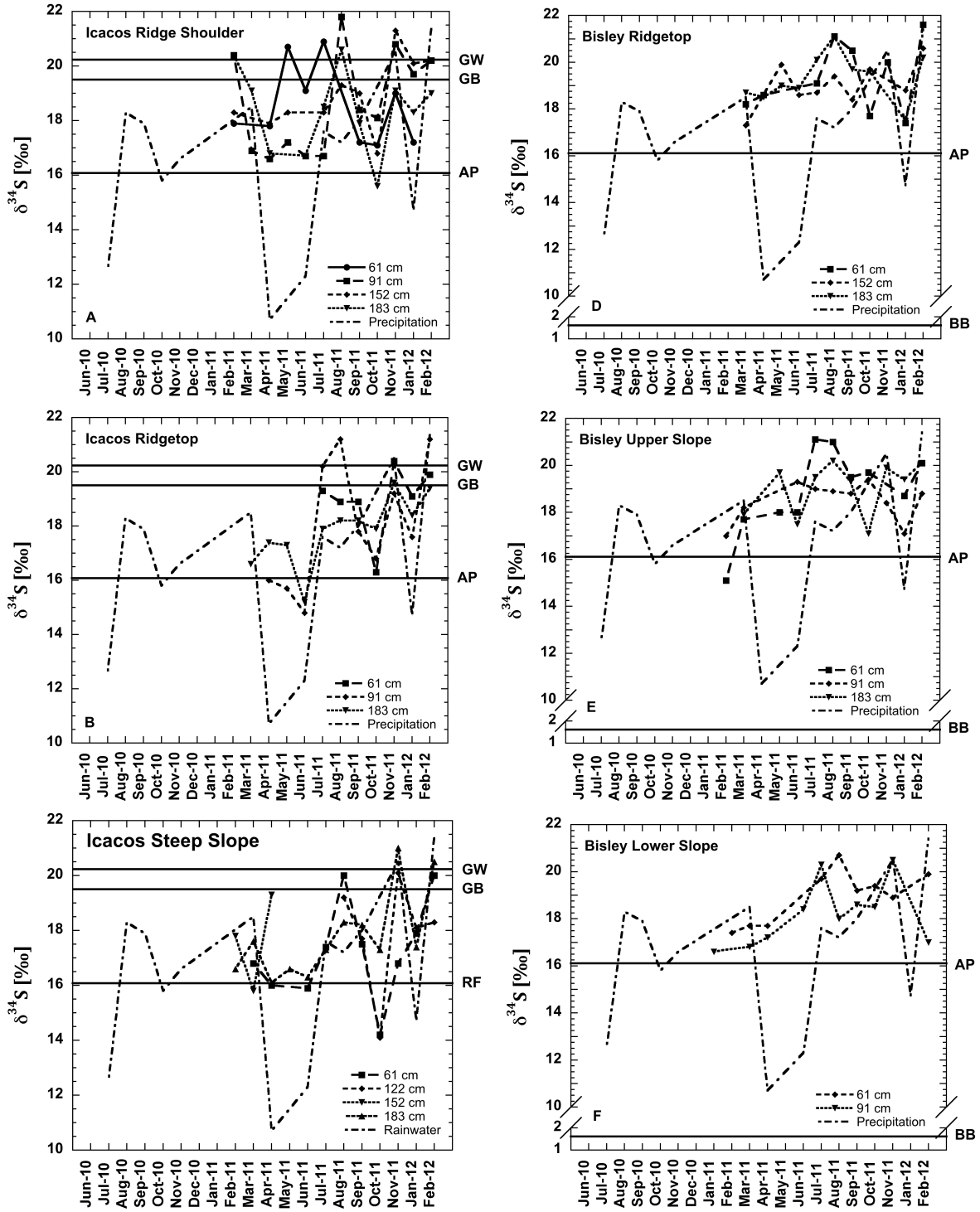

Figure 11 a-f: Temporal variations in pore water sulfate $\delta^{34}S$ at different depths on the three topographic positions at Icacos (a-c) and Bisley (d-f). Horizontal lines represent the Cl concentrations of volume-weighed average precipitation (AP), groundwater (GW) at the Icacos site, Guaba baseflow (GB) and Bisley baseflow (BB). Precipitation data were included for comparison.

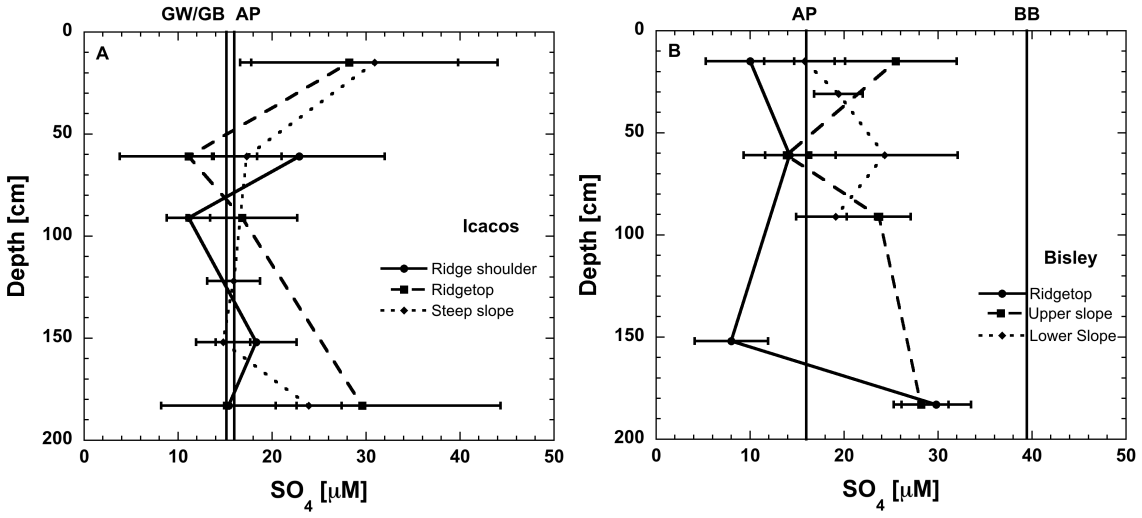

Figure 12 a-b: Depth trends in pore water sulfate concentrations averaged over the entire sample period at Icacos (a) and Bisley (b). The error bars are standard deviations. Vertical lines represent the sulfate concentration of volume-weighed average precipitation (AP), groundwater (GW) at the Icacos site, Guaba baseflow (GB) and Bisley baseflow (BB).

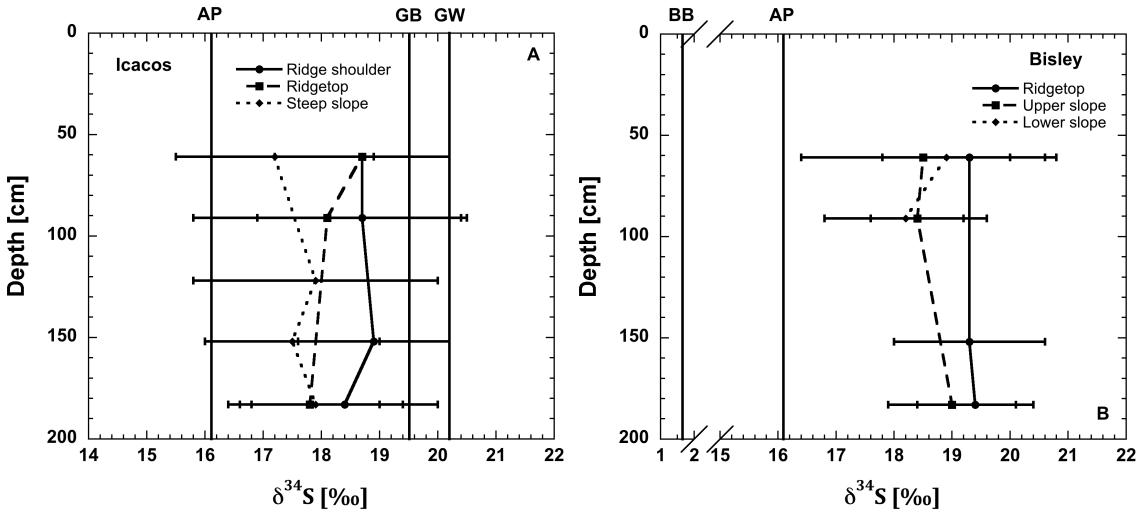

Figure 13 a-b: Depth trends in pore water sulfate $\delta^{34}S$ averaged over the entire sample period at the Icacos (a) and Bisley (b) sites. The error bars are standard deviations. Vertical lines represent the sulfate $\delta^{34}S$ of volume-weighed average precipitation (AP), groundwater (GW) at the Icacos site, Guaba baseflow (GB) and Bisley baseflow (BB).

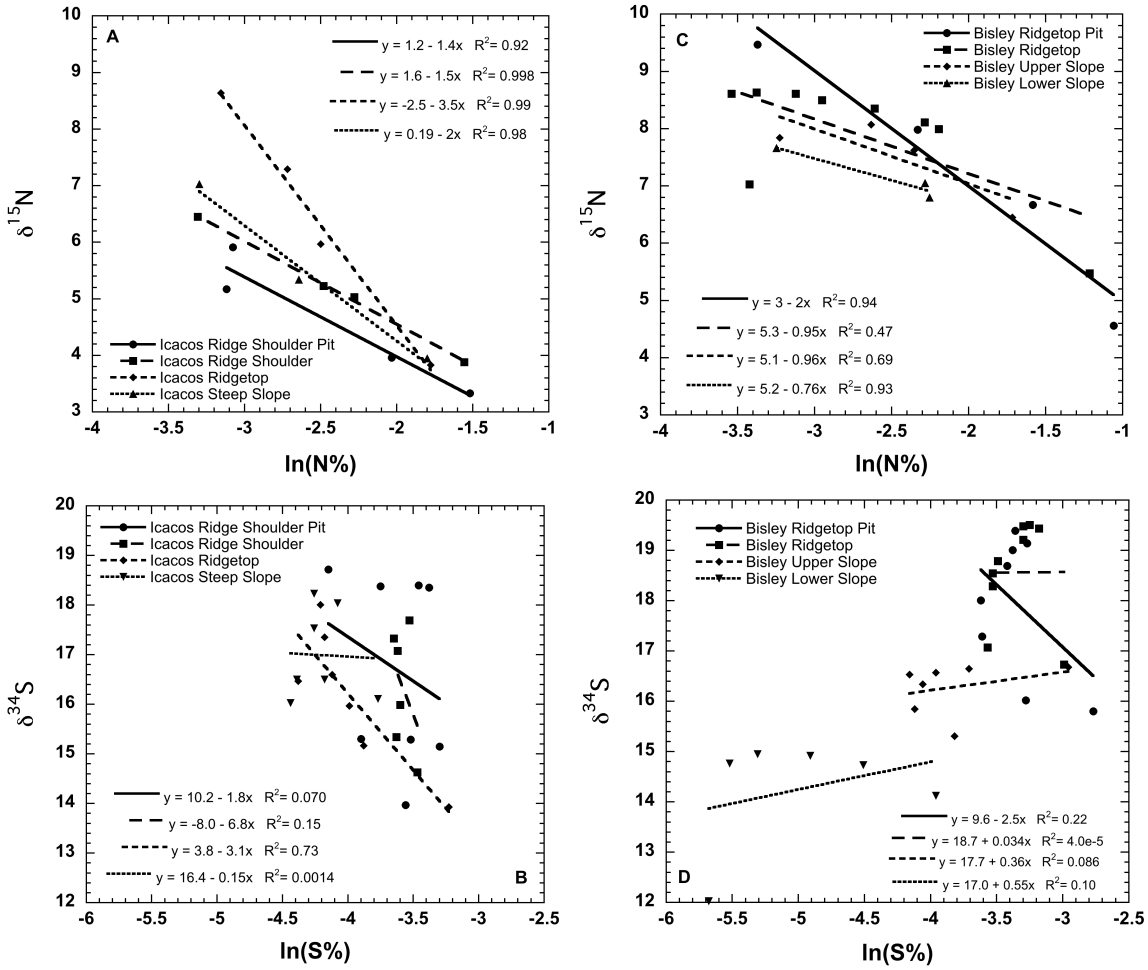

Figure 14 a-d: Linear regression between δ values and the natural logarithm of concentration for N and S at Icacos (a-b) and Bisley (c-d).

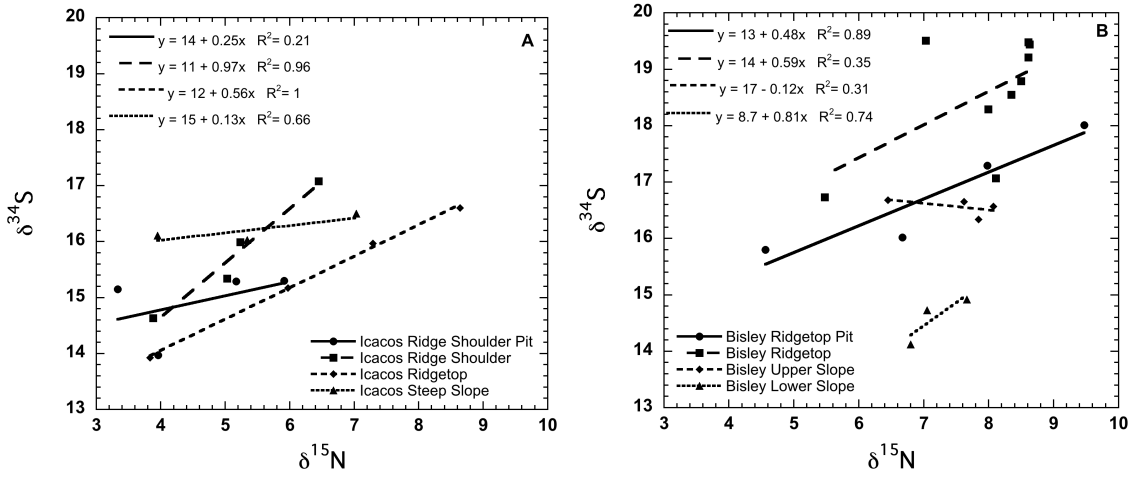

Figure 15 a-b: $\delta^{15}N$ versus $\delta^{34}S$ in the Icacos (a) and Bisley (b) soils.

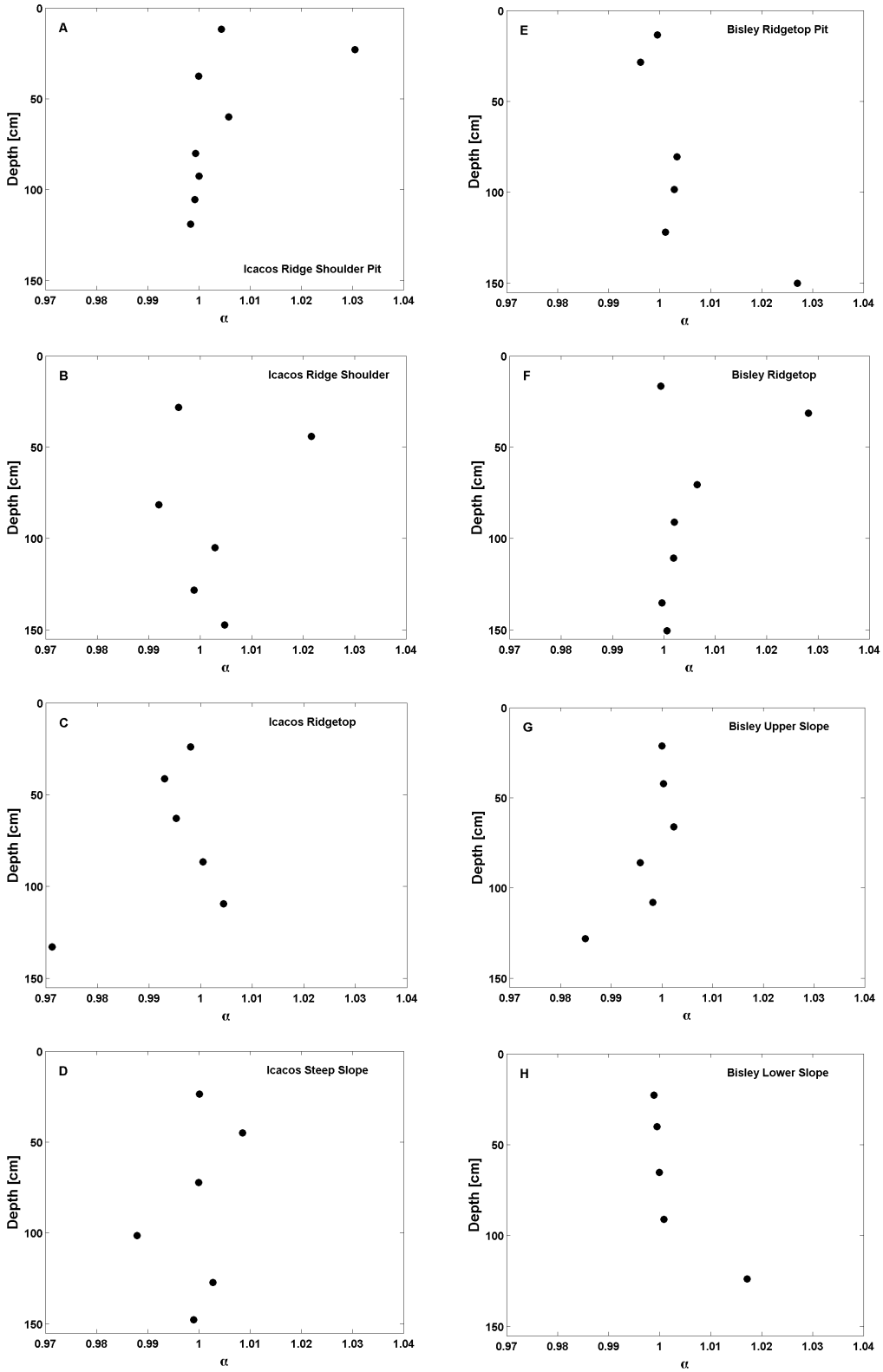

Figure 16 a-h: Variation in α values with depth for the Icacos (a-d) and Bisley (e-h) soils. Each horizon is assumed to be the source of S for the horizon immediately below.

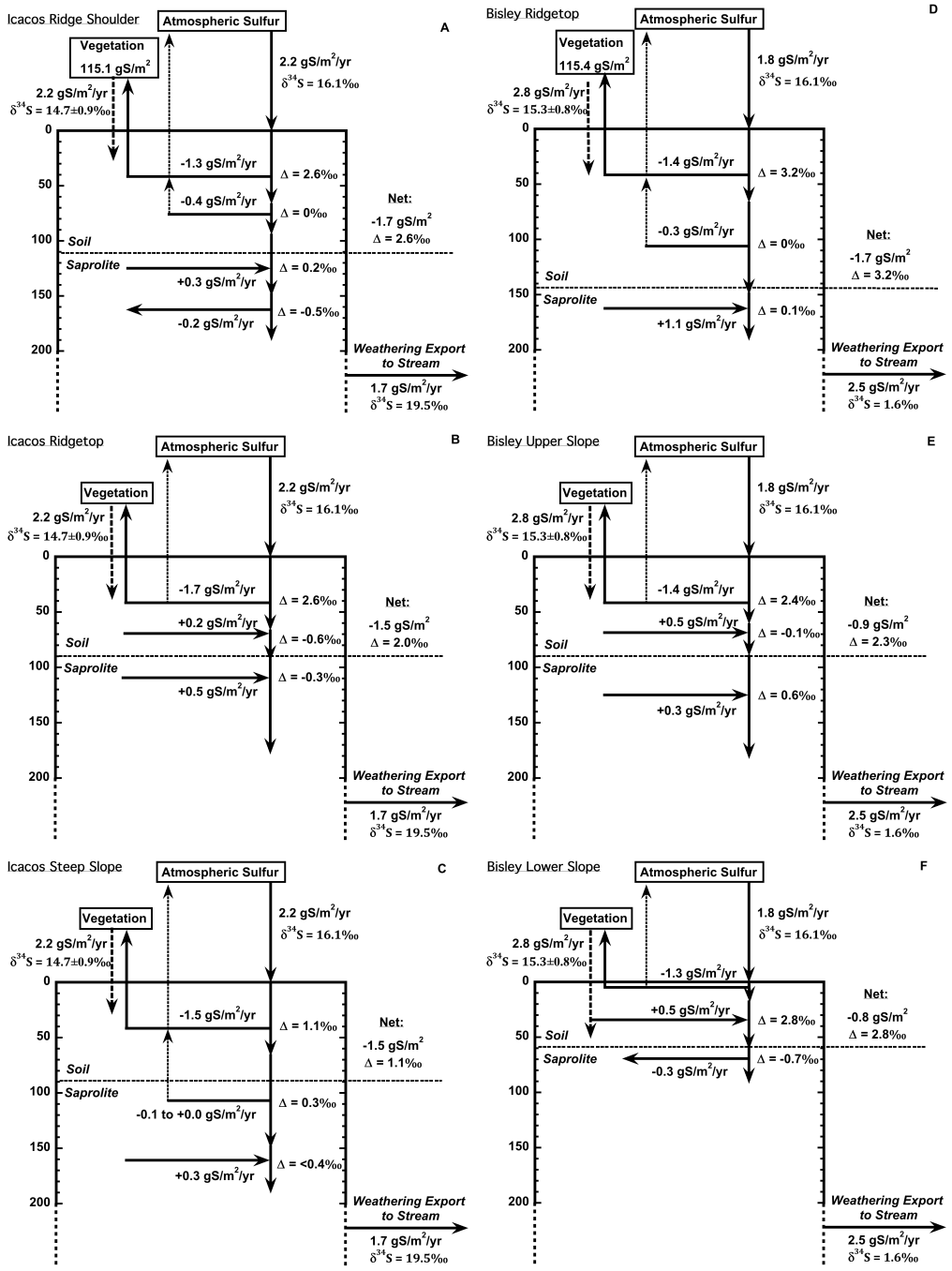

Figure 17 a-f: The fate of atmospheric S in the soils at Icacos (a-c) and Bisley (d-f). Arrows shown represent fluxes in and out of the pore water (not the bulk soil). Solid arrows represent fluxes of sulfate, dashed arrows represent fluxes of other S compounds (e.g. organic S from litterfall and reduced S gases). S in litterfall was calculated using mean litterfall values from Weaver et al. (1990) and Zou et al. (1995). S in vegetation uses aboveground biomass estimates from Gould et al. (2006). The hydrologic export calculations use average runoff estimates for the Guaba and Bisley streams from Stallard and Murphy (2012) and Schellekens et al. (2004) respectively. Hydraulic field flux densities for calculating downward S fluxes in pore water are from Buss et al. (2011).

APPENDIX

Table A1: S concentration and isotope data for several soil, sediment and organic matter samples run at the Laboratory for Environmental and Sedimentary Isotope Geochemistry (LESIG), UC Berkeley, compared to results from the Center for Stable Isotope Biogeochemistry (CSIB), UC Berkeley, and Elemental Microanalysis (EM). The low organic content soil (catalog no. B2153) and high organic content sediment (catalog no. B2151) are Elemental Microanalysis Ltd standards; their S values however are uncertified and given for information purposes only. The malachite lake mud is a calibration standard used by the IsoLab at the University of Washington, with a reported average $\delta^{34}S$ around 8‰.

	LESIG		CSIB		EM	
Sample	**$\delta^{34}S$ ‰**	**S %**	**$\delta^{34}S$ ‰**	**S %**	**$\delta^{34}S$ ‰**	**S %**
Low organic content soil	4.12±0.15	0.019±0.0004	4.63±0.11	0.024±0.001	4.94±1.4	0.022±0.004
High organic content sediment	5.29±0.17	0.701±0.046	4.35±0.16	0.74±0.02	4.2	0.69±0.04
Malachite lake mud	7.12±0.15	0.195±0.009	8.26±0.45	0.24±0.03		
Fishmeal	17.85±0.15	0.86±0.061	18.88±1.12			
Spirulina	2.29±0.032	0.698±0.007	2.31±0.54			
Bovine liver	7.73±0.081	0.796±0.011	8.25±0.41			

Chapter 4

Sulfur cycling along a Californian grassland chronosequence

Abstract

We tested the hypothesis that landscape age may drive the biological cycling of sulfur (S) and the related elements carbon (C) and nitrogen (N) along a relatively pristine ~ 250 kyr soil chronosequence on the marine terraces near Santa Cruz, California. We used an advection/decomposition model, a solute flux process-based approach, and a mass-balance approach to interpret the trends with age in mineral soil data, solute chemistry, and average values for total soil and vegetation chemistry respectively. Most of the variability in C and N isotopes with soil depth (decreasing concentration and increasing isotope values) could be explained by advective movement of organic matter downwards through the soil. The simple advection model, however, failed to explain the trends in S isotopes because the S isotope fractionation factor varied with depth. The isotope fractionation was greatest below the argillic horizon (~100 cm) on the oldest terrace. We observed a shift from processes that deplete the heavy S isotope from soils at depth on the youngest terrace (likely dissimilatory bacterial sulfate reduction (DBSR)) to processes that enrich the soil in the heavy isotope on the older terraces. Pore water data also revealed a division in soil processes above and below the argillic horizons, with large fluctuations in sulfate concentration and isotope fractionation (by up to 27‰ compared to the precipitation) due to DBSR near the surface in all soils, but little change below the well-developed argillic horizon in the older soils.

The mass balance approach revealed that the average soil S, N and C contents in the upper 50 cm varied similarly with soil age, with highest concentrations on the youngest, followed by the oldest, marine terrace. These trends in average soil S, N and C with age were uncorrelated with inputs (precipitation and plant litter). We found higher $\delta^{34}S$ values in the intermediate age soils compared to inputs, reflecting uptake by vegetation and mineralization of organic S, and lower $\delta^{34}S$ values in the youngest soils, consistent with DBSR. Sulfate from precipitation appeared to be transported through the oldest soil without fractionation, which could be due to a number of reasons, including co-occurring processes with opposite isotope effects. Plants were more depleted in the heavy C, N and S isotopes compared to the soils on all terraces. This depletion was nearly constant with age (around 3‰) for C, increased with soil age for N, from 2.1 to 4.7‰, and decreased with age for S, from 8.2 to 5.2‰. Plants were also depleted in the heavy S isotope compared to soil sulfate extracts, pore water and precipitation, reflecting significant fractionating during plant S uptake.

Overall, we found that landscape age impacts S cycling mostly due to changes in the degree of soil profile development and hydrologic conditions. Our data also provided preliminary evidence that S isotopes are more sensitive indicators of redox fluctuations than N isotopes in the soils at Santa Cruz. We proposed that this occurs due to a

combination of two factors that enhance isotopic effects during sulfate reduction compared to denitrification: (1) the greater biological demand for N than for S, which leads to the near complete consumption of the nitrate by any biological process and minimizes isotope fractionation; and (2) the adsorption of sulfate on iron and aluminum oxides, which recycles S during sulfate reduction, thus causing multiple reduction-oxidation cycles to be reflected in the $\delta^{34}S$ values.

1. Introduction

Sulfur (S), like nitrogen (N), is an essential macronutrient for all life on Earth, and its low abundance in rocks and minerals suggests that most ecosystems depend on atmospheric S inputs (Bern and Townsend, 2008). Limited research has been devoted to understanding the major controls of the S biogeochemical cycle in terrestrial systems with minimal anthropogenic influence (e.g. Bern et al., 2007; Bern and Townsend, 2008).

Soil age can impact biogeochemistry as follows. First, it has been shown that young (10^1 yrs old) soils are N limited, while older soils (10^4 to 10^5 yrs old) may have phosphorus (P) limitations due to chemical transformations and P losses (Vitousek et al., 1997). N is largely an atmospherically derived element, thus its concentration is low in young soils, while P is derived mostly from soil minerals, which become weathered and depleted with increasing soil age (Vitousek et al., 1997). Second, as soils on weatherable parent material age, clay content increases, permeability decreases, and in highly seasonal environments periodic reduction may occur in much of the soil profile, possibly driving N and S redox reactions.

The coast of California north of Santa Cruz is an ideal setting to examine the changes in soil biogeochemistry with age. A well-preserved suite of five marine terraces has been dated using terrestrial cosmogenic radionuclides (Perg et al., 2001). Research on these terraces has explored the rates of channel and hillslope evolution (Rosenbloom and Anderson, 1994), long-term chemical weathering rates (White et al., 2008), changes in soil hydrology and short-term solute weathering (White et al., 2009), reactive transport processes (Maher et al., 2009), microbiology (Moore et al., 2010), pedogenic Fe formation (Schulz et al., 2010), Mg isotope distribution (Tipper et al., 2010) and mineral nutrient cycling at the biotic/abiotic interface (White et al., 2012a; 2012b). This background work sets the context for the present study, which focuses specifically on S, N, and C. To test the hypothesis that soil age controls S biological cycling, we used: (1) an advection model approach to interpret depth trends in soil chemistry with age; (2) a process-based approach to interpret trends in solute chemistry with age; and (3) a mass-balance approach to interpret trends in average values for total soil and vegetation chemistry with age.

2. Study Site

The marine terraces along the coast north of Santa Cruz, California (Fig. 1) were formed due to steady coastal uplift combined with sea level changes (White et al., 2008). From youngest to oldest, the terraces are referred to as SCT 1 through SCT 5 (after White et al., 2008). Their ages (Table 1), as measured using cosmogenic isotopes, range from 58

to 212 kyr old (Perg et al., 2001). The soils on these terraces are Mollisols (Aniku and Singer, 1990), and have developed on marine sediments, sands and gravels rich in plagioclase, potassium feldspar, and quartz, which reflect a granitic source to the local coastal sediment supplies (White et al., 2008).

The area has a highly seasonal Mediterranean climate: cool wet winters and warm dry summers. The mean annual precipitation (MAP) and mean annual temperature (MAT) for the city of Santa Cruz are 850 mm and 13.4°C respectively (White et al., 2008). Because the orographic effect of nearby Ben Lomond Mountain influences the terraces, MAP increases with elevation (Table 1). Significant precipitation falls from November to May, and is essentially absent from June to October (White et al., 2009). During the dry season, moisture input derives from coastal fog (White et al., 2009). Due to their proximity to the ocean, the terraces receive continuous marine inputs, with chloride (Cl), sulfate and nitrate as the major anions. These solute fluxes from precipitation remain relatively constant along the terraces because MAP increases with elevation as the amount of marine solutes decreases with distance from coast (White et al., 2009).

From the late 1700s through the early 1970s the sites were used as rangelands (Wilder Ranch State Park, 2009). Since then, most of the terraces have become part of the Wilder Ranch State Park, and grazing has stopped. The current vegetation is coastal prairie, with non-native European annual grasses, and scattered shrubs and oaks (White et al., 2009; Schulz et al., 2011). Every 3-4 years the area is subjected to controlled fires to prevent encroachment of chaparral species (Moore et al., 2010). Much of the first terrace (SCT 1) is outside the park and used for intensive agriculture, and only a few pristine patches remain. SCT 4 has been disturbed by anthropogenic activities, particularly through the removal of the top 30 cm of the soil surface (White et al., 2008) and the making of charcoal on site (Schulz et al., 2011). Therefore, SCT 4 was excluded from this study.

All soils except for those on SCT 1 possess argillic horizons that become better defined with increasing age. The argillic horizons minimize seasonal moisture variations in the deep soil (Schulz et al., 2011), and impede percolation, producing perched ground water tables during the rainy season in all but the youngest terrace (White et al., 2009). Below ~2 m, the soils are generally unsaturated throughout the year (White et al., 2009). The permanent water table lies below 2.7, 11.52 and 9.45 m on SCT 1, 3 and 5 respectively; on SCT 2, the depth to ground water is greater than 15.34 m (White et al., 2008). Seasonal soil moisture variations occur at progressively shallower depths with increasing soil age (White et al., 2009). The labile nutrient pool accumulated from dead biomass during the dry season rapidly leaches into the pore water with the first rains (White et al., 2012a). Later in the spring, as storm frequency decreases and plant transpiration increases, unsaturated soil conditions retard pore water infiltration (Stonestrom et al., 1998). As a result, pore waters are relatively immobile and confined within separate soil horizons during much of the year (White et al., 2012a). Fluid residence times in the entire profile above the permanent water table were measured as 9.7, 21.6, 22.6 and 23.6 yrs for SCT 1, 2, 3 and 5 respectively (White et al., 2009).

3. Methods

3.1 Sampling

One soil profile per terrace was sampled in July 2011. The sampling sites were adjacent to the research sites established by White et al. (2008; 2009). Pits were dug and soils were sampled by horizon in the upper 100-150 cm, then auger samples were retrieved down to 200 cm. Bulk density cores were collected for every horizon. Horizon identification (Table 2) and sampling followed standard field methods (Schoeneberger et al., 2002). Pore water samples from unsaturated soils were collected as often as possible in 2011, 2012 and 2013 (Table 4) using previously installed nested porous-cup suction water samplers evacuated at ~80 cbars vacuum (White et al., 2009). Archived rainwater samples collected at SCT 2 and 5 from several rain events in April 2008 were combined to measure the S isotope composition of precipitation (Table 3).

3.2 Sample preparation

Soils were stored at room temperature in sealed bags. To measure bulk density and soil water content, the bulk density cores were weighed before and after drying at 105°C for 12 hours. Bulk density was calculated by dividing the dry mass of the soil by the core volume. The water content was measured gravimetrically as the difference between the wet and dry sample weights. For total soil S isotope and geochemical analysis, splits of the soil samples were dried at 60°C overnight, sieved to <2 mm, and ground with a mortar and pestle. Plant-available anions were extracted from splits of the unprocessed soil samples by shaking the soils for a minimum of 4 hours in a 1:7 soil to deionized water mixture, centrifuging for 30 minutes at 3000 rpm, then filtering the supernatant on 0.45 μm glass microfiber filters. Plant samples were stored frozen for a few days, then freeze-dried and pulverized in a ball mill. Water samples (precipitation and pore water) were shipped frozen from the field or from U.S. Geological Survey in Menlo Park to Berkeley, filtered in the lab on 0.45 μm glass microfiber filters within a few days of sampling, and stored refrigerated until further use.

In order to extract sulfate for isotope analysis, the filtered water samples and soil extracts were heated in a warm water bath, and a 1M $BaCl_2$ solution was added in excess (in a quantity equal to approximately 10% of the sample volume). After 24 hours, the samples were acidified with a few drops of 1N HCl to dissolve carbonates then filtered again on a 0.22 μm glass microfiber filter to collect the $BaSO_4$ precipitate. Because the samples were low in S, it was impossible to collect the $BaSO_4$ precipitate off the filter; therefore, the entire surface of the filter was scraped off and analyzed in the mass spectrometer. The S content of blank filter samples was below detection limit.

3.3 Geochemical analyses

The following analyses were performed: total soil C, N and S content and stable isotopes; anion chemistry (SO_4^{2-}, NO_3^-, Cl^-) and sulfate $\delta^{34}S$ of aqueous soil extracts, pore water and precipitation. Anion chemistry of the soil extracts and water samples was measured on a Dionex ICS-1500 ion chromatograph with an IonPac AS9-HC 4 mm column, a 9 mM sodium bicarbonate eluent at a flow rate of 1.0 mL min^{-1} and an

international seven anion standard from Dionex. The analytical precision of the instrument in the range of values measured was ±10%. Dry and ground soil and plant samples were analyzed for C and N contents (% dry weight) and stable isotope ratios ($\delta^{13}C$ and $\delta^{15}N$) via elemental analyzer/continuous flow isotope ratio mass spectrometry using a CHNOS Elemental Analyzer (Vario ISOTOPE Cube, Elementar, Hanau, Germany) coupled with an IsoPrime100 IRMS (Isoprime, Cheadle, UK). The reference material NIST SMR 1547 (peach leaves) was used as calibration standard. These isotope analyses were conducted at the Center for Stable Isotope Biogeochemistry, University of California, Berkeley. Long-term external precision for C and N isotope analyses is 0.10‰ and 0.15‰, respectively. The total S concentration and $\delta^{34}S$ values of soils and plants, and the $\delta^{34}S$ value of sulfate in water samples, were determined using the SO_2 EA-combustion-IRMS method on a GV Isoprime isotope ratio mass spectrometer coupled with an Eurovector Elemental Analyzer (model EuroEA3028-HT). These measurements were performed at the Laboratory for Environmental and Sedimentary Isotope Geochemistry (LESIG), University of California at Berkeley. Several replicates of the international standard NBS127 and two lab standards (both pure $BaSO_4$) were run with each batch of samples. The long-term analytical precision of this method is better than 0.2‰.

3.4 Data analysis

3.4.1 Isotopic relations

Isotope values are expressed using the δ notation:

$$\delta(‰) = \left(\frac{R_{Sample}}{R_{Standard}} - 1\right) \cdot 1000, \quad (1)$$

where R is the ratio of the less common to the more common isotope. For $\delta^{34}S$, R is the ratio of ^{34}S to ^{32}S and the standard is Canon Diablo Troilite (CDT) (Thode et al., 1961). Isotope fractionation is described by the fractionation factor α:

$$\alpha = \frac{R_{Product}}{R_{Substrate}}, \quad (2)$$

and the Δ value:

$$\Delta = \delta_{Product} - \delta_{Substrate} \cong 1000(\alpha - 1). \quad (3)$$

The soil extractable anion concentration in mg kg^{-1} ($c_{mg\ kg^{-1}}$) was calculated as follows:

$$c_{mg\ kg^{-1}} = c_{mg\ l^{-1}} \cdot \frac{(m_w + m_s \cdot \Theta_s)}{m_s \cdot (1 - \Theta_s)}, \quad (4)$$

where $c_{mg\ l^{-1}}$ is the concentration in soil extracts, m_w is the mass of water added for extraction, m_s is the mass of the soil used for extraction, and Θ_s is the soil water content.

We calculated the total S, N and C content and isotopes averaged to a depth of 50 cm after Brenner et al. (2001):

$$X_d = \sum_{h=1}^{H} (\%X_h \cdot BD_h \cdot Z_h), \tag{5}$$

where X_d (in g cm^{-2}) is the amount of S, N or C per area in the soil to depth d, $\%X_h$, BD_h and Z_h are the percentage of S, N or C, the bulk density and the thickness of horizon h respectively, and H is the total number of soil horizons down to depth d; and

$$\delta X_d = \sum_{h=1}^{H} (\frac{\%X_h \cdot BD_h \cdot Z_h}{X_d} \cdot \delta X_h), \tag{6}$$

where δX_d is the average soil $\delta^{34}S$, $\delta^{15}N$ or $\delta^{13}C$ to depth d, δX_h is the $\delta^{34}S$, $\delta^{15}N$ or $\delta^{13}C$ of horizon h, and the other symbols are as described above.

3.5.3 Soil S advection model

We examine in-soil processes using an advection/reaction model that we have previously used for soil N. If aboveground inputs dominate, the general solution of the steady-state advection/decomposition equations for the abundant and rare isotopes of some element X is (after Brenner, 1999):

$$\frac{R_z}{R_0} = e^{-\frac{kz}{v}(\alpha-1)} = {f_z}^{(\alpha-1)}, \tag{7}$$

where R_z and R_0 are the ratio of the heavy to the light isotopes of X in the soil at depth z and in the inputs respectively, v is the advection coefficient (in cm yr^{-1}), k is the decay constant (in yr^{-1}), α is the fractionation factor, and f_z is the fraction of total X remaining at depth z compared to the surface inputs.

Converting from R to δ notation:

$$1000 \cdot ln\frac{R_z}{R_0} \cong \delta_z - \delta_0, \tag{8}$$

Eqn. 7 can be rearranged to become (Ewing et al., 2008; Amundson et al., 2012):

$$\delta_z = (\delta_{i,z} + 1000) \cdot {f_z}^{(\alpha-1)} - 1000, \tag{9}$$

where δ_z is the isotope value of the soil layer at depth z, and $\delta_{i,z}$ is the isotope value of the inputs to the soil layer at depth z. The parameters in Eqn. 9 were estimated as follows: δ_0 equals the $\delta^{13}C$, $\delta^{15}N$ or $\delta^{34}S$ of the topmost mineral horizon; for any subsequent horizons, $\delta_{i,z} = \delta_{z-1}$; and f_z equals the ratio of total soil C, N or S at depth z to the total soil C, N or S content of the uppermost mineral horizon.

This expression can also be rewritten as:

$$\delta_z = (\alpha - 1) \cdot 1000 \cdot lnf_z + \delta_0. \tag{10}$$

Thus, if the downward transport and decomposition of a given element is constant with depth, there should be a linear relationship between the isotope values in the soil and lnf_z, or equivalently, the natural logarithm of the percent concentration at depth z, ln($\%X_z$). A

significant deviation from this relationship would signify that either more processes are involved, or the rates of processes are depth dependent.

3.5.4 Solute flux calculations

The sulfate flux Q [gS m^{-2} yr^{-1}] through the soil is given by:

$$Q = q_h \Delta c, \tag{11}$$

where q_h is the hydraulic flux that describes the rate of pore water movement through the profile, and $\Delta c = c_f - c_i$ is the change in a solute's concentration between two depths, in g S m^{-3} (White et al., 1998; 2008). We calculated the change in concentration as the difference in the sulfate concentration between adjacent lysimeter samples. We assumed that the average precipitation values from White et al. (2009) represented the source of solutes in the shallowest pore water samples. The q_h values are from White et al. (2009), calculated from Cl solute mass balances: 0.062, 0.173, 0.170 and 0.088 m yr^{-1} for SCT 1, 2, 3 and 5 respectively.

3.4.2 The mass-balance model

A mass balance box model of soil S (or N) accounts for the cumulative effects of the inputs to and outputs from the soil-vegetation system (Fig. 2) (e.g. Brenner et al., 2001). While a box model lacks the ability to describe processes within the soil, it is amenable for interpreting large-scale variations with age. For steady state soil systems, the isotopic fractionation factor (the α value) can be determined:

$$\alpha_{loss} = \frac{\bar{R}_{inputs}}{R_{soil}}, \tag{12}$$

$$\alpha_{uptake} = \frac{R_{plant}}{R_{soil}}, \tag{13}$$

where R_{soil} and R_{plant} are the isotope ratio of soil and plants respectively, $\bar{R}_{inputs}$ is the average isotope value of the inputs to the system, and α_{uptake} and α_{loss} are the isotope fractionation factors associated with plant uptake from soil and with losses of S from the soil to the environment respectively. The fractionation factor can alternatively be reported as $\Delta_{Plant\text{-}Soil}$ and $\Delta_{Soil\text{-}Input}$ values (per Eqn. 3), which are larger numbers and more intuitive to interpret.

4. Results and Discussion

4.1 Input chemistry

White et al. (2009) studied atmospheric input chemistry (Table 3). In addition, we measured sulfate S isotopes in archived samples from SCT 2 and 5 from several rain events in April 2008. Cl is the dominant anion in precipitation. Sulfate inputs are an order of magnitude smaller than Cl and approximately twice greater than nitrate inputs. Sulfate

and nitrate fluxes increase slightly from SCT 1 to SCT 3, then decrease at SCT 5. The sulfate to chloride ratio in precipitation exceeds the seasalt ratio 0.052 (Keene et al., 1986), suggesting significant non-seasalt sources of sulfate. These sources are likely marine, because the $\delta^{34}S$ values fall within the 15.6 ± 3.1‰ range of non-seasalt sulfate formed by the oxidation of reduced marine biogenic S compounds (Calhoun et al., 1991).

4.2 Depth trends in soil chemistry with age: an advection model approach

The total soil pool of C, N and S integrates the systematic changes in both concentration and stable isotope distributions with depth. We used the advection/decomposition model (Eqn. 9) to interpret the mineral soil data (Fig. 3). For well-drained soils with depth-independent processes, this advection model predicts a linear relationship between isotope values and the natural logarithm of concentration (Eqn. 10).

Soil C and N are associated in organic matter, and as a result show similar trends with depth in both content and stable isotopes. Total soil C and N (Fig. 3a and c), as well as C:N (not shown) and C:S ratios (Fig. 4a), decrease with depth on all terraces, while N:S ratios (Fig. 4b) decrease with depth on the older terraces, but peak below 100 cm depth on SCT 1. Soil $\delta^{13}C$ and $\delta^{15}N$ values (Fig. 3b and d) increase with depth by up to 6 and 12‰ respectively. The increase in $\delta^{13}C$ and $\delta^{15}N$ with depth is consistent with the occurrence of soil organic matter mineralization. The advection model explains most of the variation in C isotopes and concentration on all terraces, as can be seen in the good linear correlation between $\delta^{13}C$ and ln(%C), especially on the relatively uncomplicated SCT 2 (Fig. 5a). The model also works well for N, except for SCT 1, where redox conditions are likely most variable (Fig. 5b). The higher redox sensitivity of N implies other processes occur in addition to mineralization, thus complicating the depth independent relationship in Eqn. 10.

For S, constant processes with depth fail to explain most of the observed trends (Fig. 5c), a relationship also observed in the tropical soils of the Luquillo Experimental Forest, Puerto Rico (Ch. 3). Mineralization of soil organic S progressively enriches the organic soil S pool in the heavy isotope as organic matter ages and is transported downwards (Novak et al., 2003). Total soil S (Fig. 3e) however does not shows the typical exponential decrease with depth reflective of mineralization. In the older soils, S content has a local minimum at ~50 cm that corresponds to the argillic horizon, and is higher at depth compared to the surface. On SCT 1, the minimum occurs around 125 cm. Total soil $\delta^{34}S$ values are lower on SCT 1 than at all other sites (Fig. 3f), and decrease strongly below 150 cm (down to 4.3‰). These low values at depth are likely due to sulfides in the underlining mudstone, as we reached soft bedrock at the bottom of the profile. In general, soil $\delta^{34}S$ values reflect the marine inputs near the surface (Fig. 3f), and on the older terraces increase slightly with depth, suggesting that mineralization occurs to some extent. Highest $\delta^{34}S$ values in the deep horizons occur on SCT 3 and 5 (approaching 19‰). Increased biological cycling due to the higher moisture content of these soils (White et al., 2008) could explain these results. In particular, mineralization produces ^{34}S-depleted sulfate and thus enriches the remaining soil organic S pool in ^{34}S. However, if mineralization were the only process leading to the increase in $\delta^{34}S$ values

with depth we would expect a significant correlation between $\delta^{34}S$ and ln(%S) in these soils, which does not occur (Fig. 5c). Cycles of sulfate adsorption-desorption on iron and aluminum oxides followed by assimilatory or dissimilatory reduction may also occur, complicating the trend.

Dissimilatory bacterial sulfide reduction (DBSR), i.e. the reduction of sulfate to sulfide (with hydrogen sulfide, H_2S, as the typical end-product), occurs under anoxic conditions and causes the largest S isotope fractionations observed in nature, depleting the sulfide product in ^{34}S compared to the substrate by up to 70‰ (Brunner and Bernasconi, 2005). Small amounts of this isotopically light hydrogen sulfide may be lost from soils, or may react with iron to produce solid sulfides. However, in fresh-water systems and soils, the long-term dominant product of DBSR is organic S, because the inorganic reduced S species (such as hydrogen sulfide or iron sulfides) are eventually reoxidized and/or immobilized as organic material (Giblin and Wieder, 1992; Alewell and Novak, 2001). The isotopic discrimination during DBSR greatly exceeds that during reoxidation (which enriches the reduced fraction by ~1‰ if mediated by biota (Norman, 1994) or by up to 5.2‰ if it occurs abiotically (Fry et al., 1988). Immobilization of inorganic S into organic matter further depletes the organic product compared to the inorganic substrate by up to 2.8‰ (Kaplan and Rittenberg, 1964), thus leading to an overall depletion in ^{34}S of the soil organic matter. The sulfate fraction that doesn't undergo DBSR thus becomes isotopically enriched, and the loss through leaching of this sulfate results in a net decrease in ecosystem soil $\delta^{34}S$ values. This process seems to be most pronounced on SCT 1, but likely occurs to some degree on the other terraces as well.

To better understand the heterogeneity in S-cycling processes, we calculated the variation in the isotope fractionation factor with depth by applying Eqn. 9 to each soil layer considering the layer above as the source of S. The results, converted to Δ notation (Fig. 6), show that both the variability in isotope fractionation with depth and the magnitude of the fractionation increase with soil age. Above 100 cm (the lower boundary of the argillic horizon in the older soils), Δ values on all terraces are close to 0, indicating minimal fractionation. Below 100 cm, Δ values are negative on the youngest terrace, corresponding to a depletion in ^{34}S of the total soil pool, consistent with DBSR. On the older terraces, particularly on SCT 5, the Δ values become very positive, indicating enrichment of the soil S in the heavy isotope, which is consistent with mineralization.

This abrupt increase in variability of the fractionation factor in the deeper soils coincides with the "biotic/abiotic boundary" identified by White et al., (2012a and b). In the older soils, particularly on SCT 5, these authors argue that the argillic horizon development causes a clear distinction between biological nutrient cycling in the upper meter, and geochemically-driven cycling coupled with active weathering below (Moore et al., 2010; White et al., 2012a). However, although biomass is low below the top meter, biological reactions still occur, as evidenced by the continuous mineralization of the C and N in the downward moving organic matter (Fig. 5). S is in greater excess compared to N, as reflected in the very low N:S ratios, below 5:1 (Fig. 4). The fractionations associated with biological S cycling might become more prominent at this depth because the biologically-produced isotopically depleted sulfate is leached more quickly from the

soil. As we discuss in Section 4.3 below, pore water data show losses of sulfate below 100 cm on SCT 5, consistent with this interpretation.

Aqueous soil extracts provide strong evidence for differences in processes with age. Cl content has a minimum right above the argillic horizon, and increases greatly at depth on SCT 1 (Fig. 7a). Soil extractable nitrate (Fig. 7b) generally decreases with depth. Soil extractable sulfate (Fig. 7c) is nearly constant and low at the surface (1-2 mg kg^{-1}), and increases below 50 cm in all soils, with another concentration minimum around 125 cm on SCT 1. Extractable sulfate $\delta^{34}S$ values vary widely with depth. SCT 2, 3 and 5 reflect the value of the inputs (14.8‰, Table 3); higher values below 1 m depth on SCT 1 are consistent with DBSR.

4.3 Redox sensitivity of S and N at Santa Cruz

One surprising finding of the advection model is that S seems to be impacted more by the fluctuating redox conditions than N. Both N and S are redox-sensitive elements, thus they are expected to display variability in isotope values as a result of biological processes in both oxic and anoxic conditions. Denitrification should be thermodynamically favored compared to DBSR, since it has a higher Gibbs free energy yield (Zehnder and Stumm, 1988). Despite thermodynamic considerations, previous studies have found that soils can harbor several reduction processes simultaneously in different microhabitats (Alewell et al., 2006; Paul et al., 2006). However, our data seem to suggest that not only do sulfate reduction and denitrification co-occur in these soils, but also S is more strongly impacted by redox conditions than N. One possible explanation is that denitrification is inhibited to some degree in these soils. The presence of sulfides has been found to inhibit denitrification and stimulate dissimilatory nitrate reduction to ammonia and incomplete denitrification to nitrogen oxides (Brunet and Garcia-Gil, 1996). However, sulfides are yet to be found in these soils. XANES (X-ray Absorption Near Edge Structure) analysis of soil samples from SCT 2 did not detect sulfides (Schulz, unpublished data). High nitrate concentrations can also inhibit denitrification (Glass and Silverstein, 1998). However, nitrate concentrations never reach the 2700 mg l^{-1} NO_3-N concentration used in the study done by Glass and Silverstein (1999) that caused inhibition. In fact, measurements in permeable marine sediments have shown that denitrification rates increase with nitrate concentration following Michaelis-Menten kinetics, at concentrations up to 4000 μM nitrate (Evrard et al., 2013), which is the range found in the Santa Cruz soils.

An alternative explanation is that the isotope fractionation effects associated with S reduction are enhanced compared to those of denitrification. Two factors support this explanation. First, S is in greater excess than N in these soils, as evidenced by the generally low N:S ratios (Fig. 4). If N becomes limiting, the observable fractionation will be greatly reduced due to near complete consumption of the nitrate by any biological fractionating process, unless reduced N trace gasses that leave the system are formed. Because S is less biologically demanded, it is less likely to be completely consumed by any process, and therefore the observed isotope effects will be greater. Second, sulfate adsorbs on iron and aluminum oxides, which are abundant in these soils (White et al., 2008; Schulz et al., 2010). Furthermore, instead of being lost in gaseous form, reduced S

species are generally reoxidized and/or immobilized into organic matter (Alewell and Novak, 2001), and can subsequently re-experience mineralization and reduction. In contrast, nitrate is poorly absorbed in soils, and reduced N species easily leave the soil as gaseous losses. Adsorption/desorption of sulfate acts as a buffer to decreasing sulfate concentrations in soil solution (Alewell et al., 2006). This means that S isotopes reflect an integrative view of multiple cycles of reduction and oxidation processes. In sum, the greater apparent redox sensitivity of S compared to N isotopes is likely not due to an inhibition of denitrification, but due to the combined isotope effects associated with the greater relative biological demand for N than for S, and the greater in situ recycling of soil S via to adsorption-desorption processes.

4.4 Trends in pore water solute chemistry with age

Lysimeters were available only on SCT 2, 3 and 5. Although we sampled after several rain events (Table 4), only on 3 dates were enough samples available for comparison among terraces (Fig. 8). Our results parallel those of White et al. (2009), who also found that Cl and nitrate in shallow pore waters vary by more than an order of magnitude. This occurs much more markedly on SCT 2. Because Cl and nitrate are not derived from chemical weathering, their variability reflects the seasonality of precipitation and evapotranspiration and, in the case of nitrate, microbial activity (White et al., 2009). The trend of decreasing surface pore water nitrate concentrations with soil age (Fig. 8) suggests a possible increase in denitrification rates with soil age that would result in greater N gas losses (as N_2O or N_2) at the oldest site. The reason for this shift is likely due to changes in hydrology with increasing soil age. In general, later in the rain season (which begins in late October and ends in May), after the soils have experienced wet, and possibly saturated, conditions, the ratios of nitrate and sulfate to Cl show greater variability (Fig. 9). This suggests that nitrate and sulfate are produced in excess of immediate biological utilization from mineralization after significant rainfall, particularly on SCT 2 and 3.

Isotope data show strong redox effects on S cycling, especially on the youngest terrace. Pore water $\delta^{34}S$ values (Fig. 8 d, h and l) exceed the seawater sulfate value at the surface by up to nearly 28‰, then generally decrease with depth, approaching the seawater value of 21‰. Pore water can become enriched in ^{34}S due to the preferential uptake of isotopically light sulfate by plants, especially during periods of high moisture availability. However, the high increase in pore water $\delta^{34}S$ values after some rain events compared to the ~15‰ of the precipitation S suggest that DBSR may occur occasionally on all terraces, if the period of saturation is long enough to drive this process.

For a mechanistic understanding of S cycling in these soils, we calculated the sulfate fluxes in pore water using Eqn. 11 and the short-term contemporary solute fluxes from White et al. (2009). We expressed the isotopic enrichment associated with these additions or losses in pore water as the difference between the $\delta^{34}S$ of the two adjacent lysimeter samples (i.e. the Δ value, Eqn. 3). Precipitation was considered to be the input value for the shallowest lysimeter sampled on any given date, using the average sulfate concentration values from White et al. (2009) and the average of the $\delta^{34}S$ values measured in this study (Table 3).

Pore water sulfate reflects the balance between production and loss mechanisms. The results suggest the soils on SCT 2 experience net additions of sulfate, particularly near the surface and below 200 cm depth, with some losses between 50 and 150 cm (Fig. 10a). The intermediate-aged soils (Fig. 10c) also experience mostly net additions, particularly near the surface, but sulfate production becomes negligible below the argillic horizon (~150 cm). The oldest soils (Fig. 10e) experience net additions in the upper 150 cm, with minimal losses below. The fact that net additions of sulfate to pore waters dominate near the surface means that sulfate production through mineralization generally exceeds the combined effects of sulfate assimilation by plants and microbes, DBSR, and leaching. Nevertheless, the high $\delta^{34}S$ values in surface pore waters compared to inputs (Fig. 10 and 14) suggest significant DBSR near the soil surface.

Overall, the pore water data reveals large fluctuations in sulfate concentration and isotope fractionation due to mineralization and DBSR in the biotic soil zone of all soils, but little change below the well-developed argillic horizons of the SCT 3 and 5 soils, which restrict hydrologic flow. In contrast, the less developed argillic horizon of the SCT 2 soil results in greater variability in pore water sulfate concentration and isotope values at depth.

4.4 Total soil and vegetation chemistry

The total soil S, N and C contents (Fig.11 a, c and e) all varied similarly in a U-shaped pattern with age: highest contents on the youngest terrace (0.82, 7.7 and 66.0 g cm^{-2} respectively), followed by the oldest terrace (0.81, 6.9 and 65.8 g cm^{-2} respectively), while the intermediate age terraces had lower storage (0.45-0.49, 5.1-4.5 and 44.9-46.4 g cm^{-2} respectively). This trend is the opposite of that in precipitation deposition rates (Table 3), and differs from the trend in vegetation S inputs. Multiplying the net primary productivity (NPP) (White et al., 2012a) by the %S in grasses (Fig. 12a) results in S inputs from vegetation of 60, 24 and 26 g S m^{-2} for SCT 2, 3 and 5 respectively. Similarly for N, the input from vegetation is 342, 165 and 322 g S m^{-2} for SCT 2, 3 and 5 respectively. The lack of correlation between soil S (and N) and inputs (precipitation and plant litter) suggests that S (and N) variation with age is largely driven by in-soil processes and losses.

C:S ratios (Fig. 11g) increase from SCT 1 to 2, then decrease with age. C:N ratios increase from 8.6 on SCT 1 to 10.4 on SCT 3, and decrease to 9.5 on SCT 5. The C:N and C:S ratios remained below 20:1 and 200:1, indicating that net mineralization (as opposed to net immobilization) of N and S occurs in all these soils (Stevenson and Cole, 1999, p. 68). N:S ratios (Fig. 11h) follow the same trend as C:S, suggesting that S is in greater excess with respect to N on the older terraces.

S, N and C isotope values all show different patterns with age. $\delta^{34}S$ (Fig. 11b) values increase from SCT 1 (12.0‰) to SCT 3 (16.2‰), then decrease slightly on SCT 5 (15.0‰). In contrast, soil $\delta^{15}N$ values (Fig. 11d) decrease from SCT 1 (8.7‰) to SCT 3 (7.5‰), then increase again on SCT 5 (9.2‰). Soil $\delta^{13}C$ values (Fig. 11f) show little variation with age, remaining around -26‰ on all terraces. Compared to the inputs, soils are depleted in ^{34}S on the youngest terrace (by 2.8‰), enriched on SCT 2 and 3 (by 1.4‰), and neither significantly enriched nor depleted on SCT 5 (Fig. 13a). Comparisons

of soil $\delta^{34}S$ values to those of the inputs reflect biological processes inside the soil. The higher $\delta^{34}S$ values on SCT 2 and 3 soils versus inputs reflect uptake by vegetation and mineralization of organic S, two processes that enrich the soil in ^{34}S (e.g. Novak et al., 2003). The lower $\delta^{34}S$ values on SCT 1 can be explained by DBSR (e.g. Alewell et al., 1999), and/or by more rapid leaching of ^{34}S-enriched compounds (e.g. the sulfate fraction that hasn't yet undergone DBSR). SCT 5 soils have been previously shown to support higher rates of microbial respiration than the younger terrace soils (Schulz et al., 2011) due to their slightly higher soil moisture content (White et al., 2009). The apparent lack of fractionation relative to the inputs on SCT 5 might be due to co-occurring processes with opposite isotope effects.

Plant $\delta^{34}S$ values (Fig. 12b) increase with landscape age, from 8.0‰ on SCT 2 to 9.8‰ on SCT 5. Plant $\delta^{15}N$ values (Fig. 12d) follow the same trend with age as the soil. Also similar to the soil, plant $\delta^{13}C$ values (Fig. 12f) show no significant trend with age. Plants are more depleted in the heavy C, N and S isotopes compared to the soils on all terraces. This depletion is nearly constant with age (around 3‰) for C, increases with soil age for N, from 2.1 to 4.7‰, and decreases with age for S, from 8.2 to 5.2‰ (Fig. 13b and c). The decreasing difference between plant and soil $\delta^{34}S$ values with increasing soil age signifies reduced fractionation during plant uptake of soil sulfate, during decomposition of plant litter, and/or during mineralization of organic S to sulfate inside the soil.

Although most of the soil S is organic, plants take up soil S as sulfate and assimilate it internally into organic S, which is then returned to the soil as litter and converted back to sulfate through the process of mineralization (Fig. 2). Fig. 14 integrates S isotope data for all the pools measured during this study. Plants are significantly depleted in ^{34}S compared to the bulk soil, soil extractable sulfate (by 1 to 12‰), pore water (by 2 to 15), and precipitation (by 5 to 7‰). Surface soil horizons are similar to the inputs in precipitation. Soil extractable sulfate is isotopically depleted compared to the total soil near the surface on SCT 1 and 3, and enriched at depth on SCT 1 and near the surface on SCT 5. Total soil values resemble those of pore water sulfate below 100 cm (though no pore water data was available for SCT 1). This suggests that little fractionation occurs in the "abiotic zone". However, in the zone of the argillic horizon and immediately above, where the seasonally perched water table resides, pore water is enriched compared to the total soil S, likely due to preferential uptake of isotopically light sulfate by plants, and perhaps also due to occasional DBSR resulting in the conversion of pore water sulfate to ^{34}S-depleted reduced S forms.

5. Conclusion

We presented results of S, N and C concentration and stable isotope analysis of the soils on the marine terrace chronosequence near Santa Cruz, California. The changes in soil physical and hydrological properties with time led to a seasonal wet zone above the argillic horizon and a permanent unsaturated zone below. Several lines of evidence showed that, particularly due to its impact on hydrology, soil age impacted C, N and S biochemistry, but the response of S to these conditions differed from that of N and C. S isotopes appeared to be more affected by fluctuating redox conditions than N. This may

have occurred because: (1) N was in greater biological demand than S, and therefore biota discriminated less against the heavier isotope, and (2) the adsorption of S on iron and aluminum oxides enabled S to possibly undergo several reduction-reoxidation cycles, thus magnifying the isotope effects. Alternatively, denitrification could have been inhibited by various factors, such as the presence of sulfides.

Although S was not derived from the parent material, the degree of development of the soil influenced S transport, and thus S transformations in the soil, as well as the availability of water for microbial S cycling. Our data suggest that, due to the greater extent of pedogenesis, older soils are better at retaining S for biological cycling, and are thus less susceptible to S deficiency than intermediate-aged soils. This is in contrast to previous research on the impact of landscape age on N on a chronosequence near Merced, CA, which found a decline in total N storage with time, concomitant with an increase in the fraction of inorganic (as opposed to organic) N losses, due to phosphorus (P) limitations in the older soils (Brenner et al., 2001). The Merced chronosequence however is significantly longer, spanning 3000 kyrs. It is possible that P limitations could become important on older soils, however our data show minimal impact of P availability along the ~250 kyr Santa Cruz chronosequence.

Acknowledgments

We would like to thank our collaborators M. Schulz and C. Lawrence from the USGS; the California State Park at Wilder Ranch for enabling access to the sampling sites; Chloe Lewis, Mary Whelan and Ashley Kirk for assistance with sampling; J. Coates, W. Yang, P. Brooks and S. Mambelli for access to instruments and sample analysis. The research was supported by a grant from NSF Geobiology and Low Temperature Geochemistry.

References

Adam D. P., Byrne R. and Luther E. (1981) A late Pleistocene and Holocene pollen record from Laguna de Las Tancas, northern coastal Santa Cruz County, California. *Madrono* **28,** 255-272.

Alewell C. and Novak M. (2001) Spotting zones of dissimilatory sulfate reduction in a forested catchment: the S-34-S-35 approach. *Environ. Pollut.* **112,** 369-377.

Alewell C., Mitchell M. J., Likens G. E. and Krouse H. R. (1999) Sources of stream sulfate at the Hubbard Brook Experimental Forest: Long-term analyses using stable isotopes. *Biogeochemistry* **44,** 281-299.

Alewell C., Paul S., Lischeld G., Kuesel K. and Gehre M. (2006) Characterizing the redox status in three different forested wetlands with geochemical data. *Environ. Sci. Technol.* **40,** 7609-7615.

Amundson R., Barnes J. D., Ewing S., Heimsath A. and Chong G. (2012) The stable isotope composition of halite and sulfate of hyperarid soils and its relation to aqueous transport. *Geochim. Cosmochim. Acta* **99,** 271-286.

Aniku J. R. F. and Singer M. J. (1990) Pedogenic iron oxide trends in a marine terrace chronosequence. *Soil Sci. Soc. Am. J.* **54,** 147-152.

Bern C. R., Porder S. and Townsend A. R. (2007) Erosion and landscape development decouple strontium and sulfur in the transition to dominance by atmospheric inputs. *Geoderma* **142,** 274-284.

Bern C. R. and Townsend A. R. (2008) Accumulation of atmospheric sulfur in some Costa Rican soils. *J Geophys Res-Biogeo* **113,** G03001.

Brenner D. L. (1999). Soil nitrogen isotopes along natural gradients: models and measurements. M.S. thesis, University of California, Berkeley, CA.

Brenner D. L., Amundson R., Baisden W. T., Kendall C. and Harden J. (2001) Soil N and 15N variation with time in a California annual grassland ecosystem. *Geochim. Cosmochim. Acta* **65(22),** 4171-4186.

Brunet R. C. and Garcia-Gil L. J. (1996) Sulfide-induced dissimilatory nitrate reduction to ammonia in anaerobic freshwater sediments. *FEMS Microbiol. Ecol.* **21,** 131-138.

Brunner B. and Bernasconi S. M. (2005) A revised isotope fractionation model for dissimilatory sulfate reduction in sulfate reducing bacteria. *Geochim. Cosmochim. Acta* **69,** 4759-4771.

Calhoun J. A., Bates T. S. and Charlson R. J. (1991) Sulfur isotope measurements of submicrometer sulfate aerosol-particles over the Pacific-Ocean. *Geophys. Res. Lett.* **18,** 1877-1880.

Evrard V., Glud R. N. and Cook P. L. M. (2013) The kinetics of denitrification in permeable sediments. *Biogeochemistry* **113,** 563-572.

Ewing S. A., Yang W., DePaolo D. J., Michalski G., Kendall C., Stewart B. W., Thiemens M. and Amundson R. (2008) Non-biological fractionation of stable Ca isotopes in soils of the Atacama Desert, Chile. *Geochim. Cosmochim. Acta* **72,** 1096-1110.

Fry B., Ruf W., Gest H. and Hayes J. M. (1988) Sulfur isotope effects associated with oxidation of sulfide by O-2 in aqueous-solution. *Chem. Geol.* **73,** 205-210.

Giblin A. E. and Wieder R. K. (1992) *Sulphur cycling in marine and freshwater wetlands.* In *Sulfur Cycling on the Continents* (eds. R. W. Howarth, J. W. B. Stewart and M. V. Ivanov). SCOPE, vol. 48, John Wiley and Sons Ltd, NY.

Glass C. and Silverstein J. (1998) Denitrification kinetics of high nitrate concentration water: pH effect on inhibition and nitrite accumulation. *Wat. Res.* **32,** 831-839.

Kaplan I. R. and Rittenberg S. C. (1964) Microbiological fractionation of sulphur isotopes. *J. Gen. Microbiol.* **34,** 195-212.

Keene W. C., Pszenny A. A. P., Galloway J. N. and Hawley M. E. (1986) Sea-salt corrections and interpretation of constituent ratios in marine precipitation. *J Geophys Res-Atmos* **91,** 6647-6658.

Maher K., Steefel C. I., White A. F. and Stonestrom D. (2009) The role of reaction affinity and secondary minerals in regulating chemical weathering rates at the Santa Cruz marine terrace chronosequence, California. *Geochim. Cosmochim. Acta* **73,** 2804-2831.

Moore J., Macalady J. L., Schulz M. S., White A. F. and Brantley S. L. (2010) Shifting microbial community structure across a marine terrace grassland chronosequence, Santa Cruz, California. *Soil Biol. Biochem.* **42,** 21-31.

Norman A. L. (1994) Isotope analysis of microgram quantities of sulfur: Applications to soil sulfur mineralization studies. PhD thesis, Univ. of Calgary, Canada.

Novak M., Buzek F., Harrison A. F., Prechova E., Jackova I. and Fottova D. (2003) Similarity between C, N and S stable isotope profiles in European spruce forest soils: implications for the use of $\delta^{34}S$ as a tracer. *Appl. Geochem.* **18,** 765-779.

Paul S., Kusel K. and Alewell C. (2006) Reduction processes in forest wetlands: Tracking down heterogeneity of source/sink functions with a combination of methods. *Soil Biology & Biochemistry* **38,** 1028-1039.

Perg L. A., Anderson R. S. and Finkel R. C. (2001) Use of a new ^{10}Be and ^{26}Al inventory method to date marine terraces, Santa Cruz, California, USA. *Geology* **29,** 879-882.

Rosenbloom N. A. and Anderson R. S. (1994) Hillslope and channel evolution in a marine terraced landscape, Santa Cruz, California. *J. Geophys. Res.* **99(B7),** 14013-14029.

Schoeneberger P. J., Wysocki D. A., Benham E. C., and Broderson W. D. (eds.) (2002) Field book for describing and sampling soils, Version 2.0. NRCS, National Soil Survey Center, Lincoln, NE.

Schulz M. S., Vivit D. V., Schulz C., Fitzpatrick J. and White A. F. (2010) Biologic origin of iron nodules in a marine terrace chronosequence, Santa Cruz California. *Soil Sci. Am. J.* **74,** 550-564.

Schulz M., Stonestrom D., Von Kiparski G., Lawrence C., Masiello C., White A. and Fitzpatrick J. (2011) Seasonal dynamics of CO_2 profiles across a soil chronosequence, Santa Cruz, California. *Appl. Geochem.* **26,** S132-S134.

Stevenson F. J. and Cole M. A. (1999) Cycles of Soil: Carbon, Nitrogen, Phosphorus, Sulfur, Micronutrients. Second Edition. John Wiley & Sons, Inc., Hoboken, NJ.

Thode H. G., Monster J. and Dunford H. B. (1961) Sulphur isotope geochemistry. *Geochim. Cosmochim. Acta* **25,** 159-174.

Tipper E. T., Gallardet J., Louvat P., Capmas F. and White A. F. (2010) Mg isotope constraints on soil pore-fluid chemistry: evidence from Santa Cruz, California. *Geochim. Cosmochim. Acta* **74,** 3883-3896.

Vitousek P. M., Chadwick O. A., Crews T. E., Fownes J. H., Hendricks D. M. and Herbert D. (1997) Soil and ecosystem development across the Hawaiian Islands. *GSA Today* **7,** 1-10.

Wilder Ranch State Park, 2009. California State Parks, Sacramento, CA.

White A. F., Blum A. E., Schulz M. S., Vivit D. V., Stonestrom D. A., Larsen M., Murphy S. F. and Eberl D. (1998) Chemical weathering in a tropical watershed, Luquillo mountains, Puerto Rico: I. Long-term versus short-term weathering fluxes. *Geochim. Cosmochim. Acta* **62,** 209-226.

White A. F., Schulz M. S., Stonestrom D. A., Vivit D. V., Fitzpatrick J., Bullen T. D., Maher K. and Blum A. E. (2009) Chemical weathering of a marine terrace chronosequence, Santa Cruz, California. Part II: Solute profiles, gradients and the comparisons of contemporary and long-term weathering rates. *Geochim. Cosmochim. Acta* **73,** 2769-2803.

White A. F., Schulz M. S., Vivit D. V., Bullen T. D., Fitzpatrick J. and Tipper E. T. (2012a) The impact of biotic/abiotic interfaces on mineral nutrient cycling in a soil chronosequence, Santa Cruz, California. *Geochim. Cosmochim. Acta* **55,** 62-85.

White A. F., Vivit D. V., Schulz M. S., Bullen T. D., Evett R. R. and Aagarwal J. (2012b) Biogenic and pedogenic controls on Si distribution and cycling in grasslands of the Santa Cruz soil chronosequence, California. *Geochim. Cosmochim. Acta* **94,** 72-94.

Zehnder A. J. B. and Stumm W. (1988) Geochemistry and biogeochemistry of anaerobic habitats. In *Biology of Anaerobic Microorganisms* (ed. A. J. N. Zehnder). Wiley, New York, pp 469-585.

TABLES

Table 1: Location and characteristics of the study sites.

Terrace	Age (kyr)[1]	Coordinates	Elevation (m)	Distance to coast (km)	MAP (mm)[2]
SCT 1	65	N36.9588°, W122.0807°	18	0.7	390
SCT 2	90	N36.9679°, W122.0862°	70	1.6	520
SCT 3	137	N36.9763°, W122.0788°	107	2.5	596
SCT 5	226	N36.9945°, W122.1343°	187	2	586

[1]Perg et al. (2001); [2]White et al. (2009).

Table 2: Field description of the soils sampled by horizon.

Terrace	Horizon	Top depth (cm)	Bottom depth (cm)	Water content (%)	Bulk density (g/cm^3)	Notes
SCT 1	O	0	7			
	-	7	21	6.69	1.10	
	-	21	39	6.22	0.96	
	-	39	53	7.04	1.02	
	-	53	75	9.20	1.13	
	-	75	87	9.48	1.18	
	-	87	105	6.59	1.08	
SCT 2	O	0	5			
	A1	5	35	10.90	0.81	
	A2	35	47	10.74	0.90	
	AB	47	56	8.18	1.01	
	Bt1	56	84	7.82	0.95	
	Bt2	84	93	15.57	1.08	
	Bt3	93	119	16.86	1.10	bioturbation by gophers
	Bg	119	130	22.45	0.91	
	Btgk	130	141	17.10	1.20	
SCT 3	O	0	7			
	A1	7	16	9.05	0.95	
	A2	16	30	10.89	0.93	
	AB	30	45	8.72	1.13	
	Bt1	45	59	11.25	1.10	
	Bt2	59	70	15.26	1.11	
	Btg1	70	79	15.94	1.06	
	Btg2	79	100	18.56	1.12	
SCT 5	O	0	5			
	A1	5	14	8.38	0.97	bioturbation by gophers
	A2	14	25	8.23	1.07	bioturbation by gophers
	AB	25	38	8.50	0.97	bioturbation by gophers
	Bt1	38	53	11.49	1.08	bioturbation by gophers
	Bt2	53	72	19.03	0.91	bioturbation by gophers
	Bt3	72	105	18.95	1.01	

Table 3: Volume-weighted average anion concentration and fluxes in precipitation from White et al. (2009), and stable S isotope composition of precipitation sulfate from April 2008 samples measured in this study.

Terrace	Cl		NO_3		SO_4		$\delta^{34}S\text{-}SO_4$ (‰)
	µM	mmol m^{-2}	µM	mmol m^{-2}	µM	mmol m^{-2}	
SCT 1	273	106.4	8.12	3.32	18.44	7.19	
SCT 2	265	133.1	8.72	4.53	18.79	9.77	14.7
SCT 3	162	96.6	12.7	7.57	19.25	11.47	
SCT 5	171	100.2	8.28	4.85	13.71	8.03	14.9

Table 4: Pore water chemistry.

Terrace	Depth (cm)	Sampling date	Cl (µM)	NO_3 (µM)	SO_4 (µM)	$\delta^{34}S\text{-}SO_4$ (‰)
SCT 2	15	12/16/11	719	1613	33	22.4
SCT 2	60	3/21/12	1003	63	21	39.7
SCT 2	91	3/21/12	262	24	63	13.1
SCT 2	122	3/21/12	237	90	179	12.6
SCT 2	152	3/21/12	318	62	77	18.6
SCT 2	183	3/21/12	269	166	150	13.6
SCT 2	244	3/21/12	276	109	205	14.1
SCT 2	549	3/21/12	548	326	430	17.5
SCT 2	30	12/14/12	5337	990	393	13.5
SCT 2	549	12/14/12	527	313	650	17.3
SCT 2	15	1/10/13	3556	-	57	11.1
SCT 2	60	1/10/13	2168	895	103	14.3
SCT 2	61	1/10/13	3166	5947	21	20.0
SCT 2	91	1/10/13	1076	1224	46	15.8
SCT 2	122	1/10/13	1056	1040	144	13.8
SCT 2	152	1/10/13	337	393	36	17.2
SCT 2	183	1/10/13	928	1411	73	15.2
SCT 2	244	1/10/13	1040	959	125	14.7
SCT 2	15	2/6/13	2658	3993	211	14.1
SCT 2	30	2/6/13	1277	639	174	14.9
SCT 2	91	2/6/13	1154	1092	135	16.3
SCT 2	122	2/6/13	1105	1144	192	14.2
SCT 2	152	2/6/13	885	1018	160	14.8
SCT 2	183	2/6/13	1133	1256	180	13.9
SCT 2	244	2/6/13	1197	1197	181	15.6
SCT 2	305	2/6/13	586	247	398	15.3
SCT 3	91	1/25/12	205	34	55	17.8
SCT 3	122	1/25/12	291	222	53	19.4
SCT 3	152	1/25/12	277	95	54	23.3
SCT 3	549	1/25/12	471	249	56	17.6
SCT 3	91	2/6/12	219	17	58	15.2
SCT 3	91	3/5/12	205	13	58	17.2
SCT 3	549	3/5/12	477	239	56	20.2
SCT 3	60	3/21/12	161	132	22	29.8
SCT 3	91	3/21/12	256	8.5	49	20.0
SCT 3	152	3/21/12	322	67	75	19.3

Table 4 continued: Pore water chemistry.

Terrace	Depth (cm)	Sampling date	Cl (µM)	NO_3 (µM)	SO_4 (µM)	$\delta^{34}S\text{-}SO_4$ (‰)
SCT 3	183	3/21/12	209	4.5	57	17.9
SCT 3	122	12/14/12	357	777	248	18.5
SCT 3	183	12/14/12	224	5.5	248	18.6
SCT 3	30	1/10/13	725	2436	14	27.0
SCT 3	91	1/10/13	210	371	17	21.0
SCT 3	122	1/10/13	503	693	29	19.3
SCT 3	183	1/10/13	449	231	34	20.1
SCT 3	192	1/10/13	375	317	56	19.9
SCT 3	549	1/10/13	492	268	56	20.3
SCT 3	15	2/6/13	249	712	167	17.9
SCT 3	152	2/6/13	515	657	128	21.2
SCT 3	549	2/6/13	498	264	158	20.3
SCT 5	183	1/25/12	498	50	66	19.4
SCT 5	244	1/25/12	340	116	56	20.5
SCT 5	120	2/6/12	342	20	69	15.4
SCT 5	183	3/5/12	495	41	69	18.7
SCT 5	30	3/21/12	220	-	5.7	42.8
SCT 5	150	3/21/12	748	7.0	151	17.2
SCT 5	180	3/21/12	503	41	72	19.1
SCT 5	90	5/7/12	510	7.7	108	14.1
SCT 5	150	5/7/12	655	3.2	155	17.4
SCT 5	180	5/7/12	508	39	75	18.2
SCT 5	244	5/7/12	367	45	89	19.4
SCT 5	152	12/14/12	686	18	368	17.4
SCT 5	183	12/14/12	484	32	266	18.7
SCT 5	244	12/14/12	627	50	232	20.1
SCT 5	365	12/14/12	829	60	249	21.7
SCT 5	30	1/10/13	783	19	26	28.4
SCT 5	61	1/10/13	534	32	137	25.8
SCT 5	91	1/10/13	900	12	199	16.4
SCT 5	122	1/10/13	983	7.9	145	17.7
SCT 5	152	1/10/13	683	5.0	232	17.5
SCT 5	183	1/10/13	552	27	167	19.3
SCT 5	152	2/6/13	689	2.8	248	17.4
SCT 5	183	2/6/13	572	20	178	19.1
SCT 5	244	2/6/13	706	10	162	19.3
SCT 5	365	2/6/13	889	61	126	22.2

FIGURES

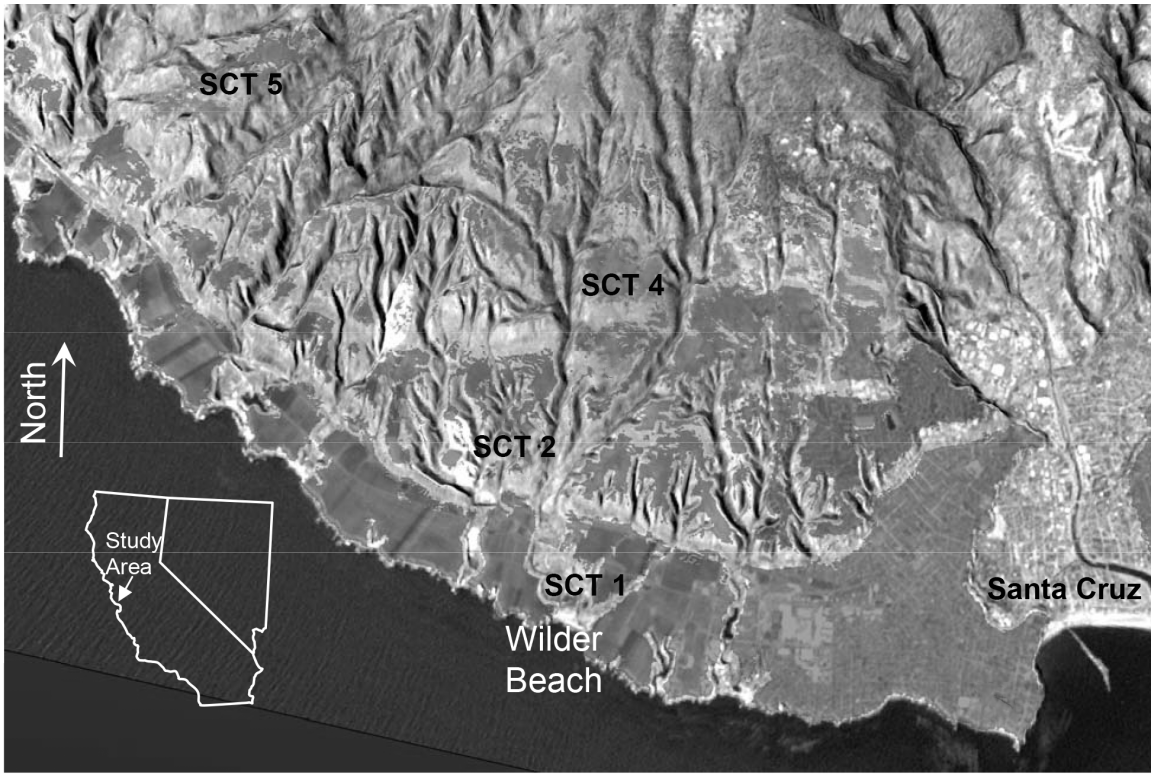

Figure 1: Map of the Santa Cruz area, showing the location of the soil sampling sites. The lysimeter fields are located near SCT 2, 3 and 5. Adapted, with permission, from White et al. (2008).

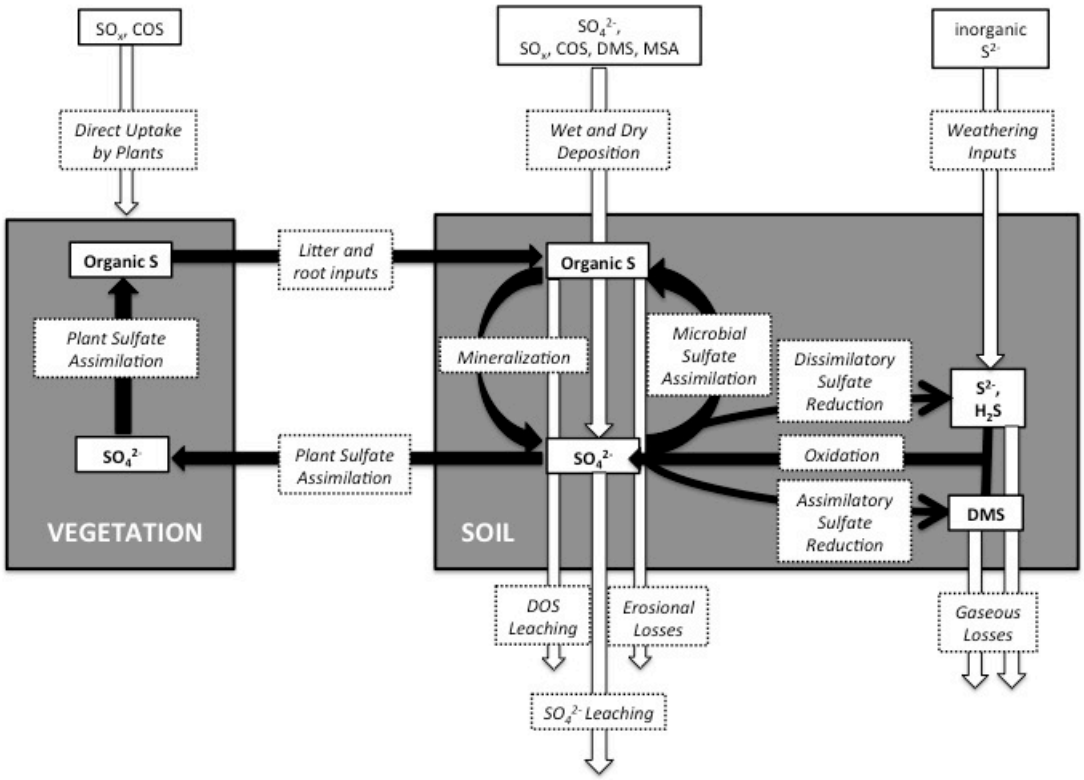

Figure 2: Schematic representation of the terrestrial S cycle, showing major inputs, outputs and in-soil biologically-mediated transformations. White arrows represent inputs to and outputs from the coupled soil-vegetation system. Black arrows represent S transformations within the soil-vegetation system. (COS: carbonyl sulfide; DMS: dimethyl sulfide; DOS: dissolved organic sulfur; MSA: methanesulfonic acid).

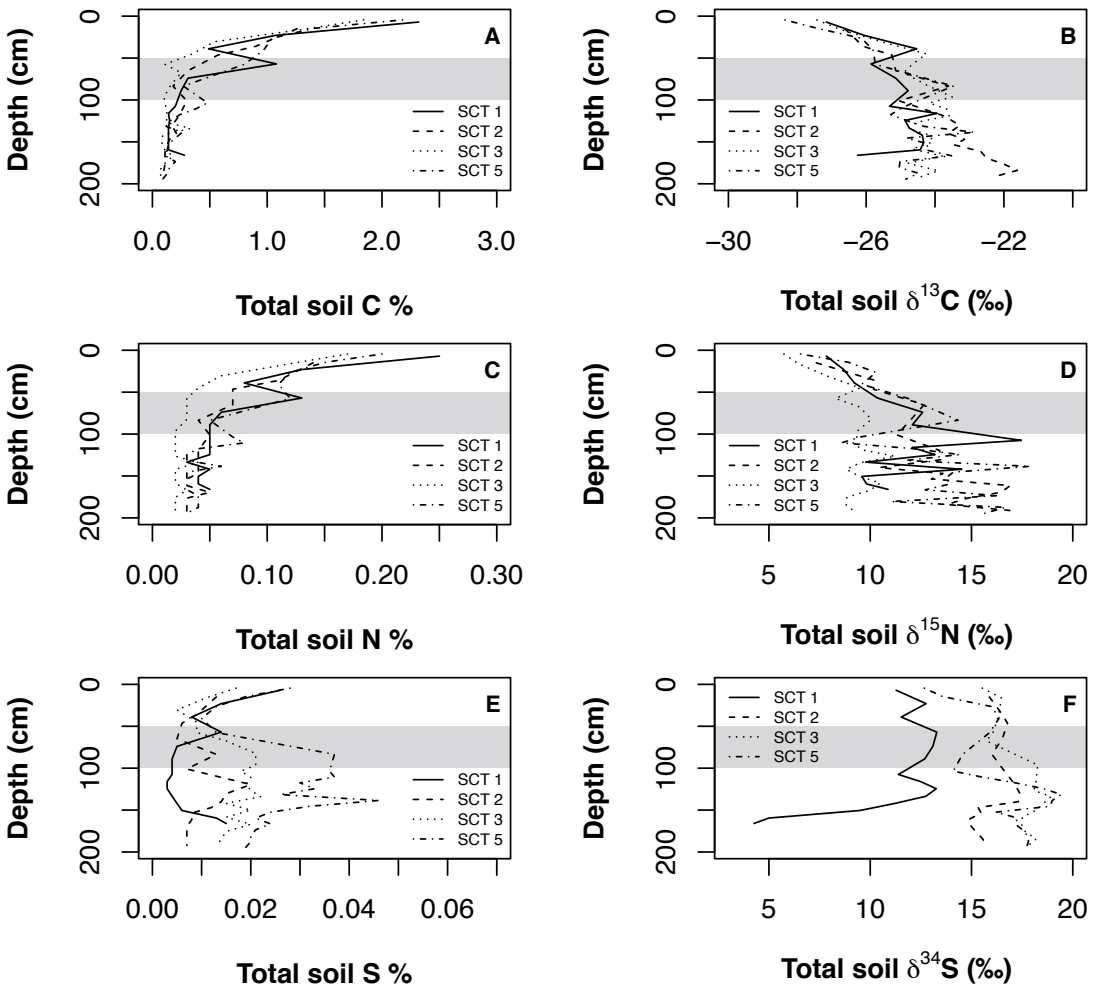

Figure 3 (a-f): Total soil C (a), N (c) and S (e) content and stable isotopes (b, d, and f respectively) with depth on the Santa Cruz terraces. The light gray areas indicate the location of the seasonal perched water table, after White et al. (2009).

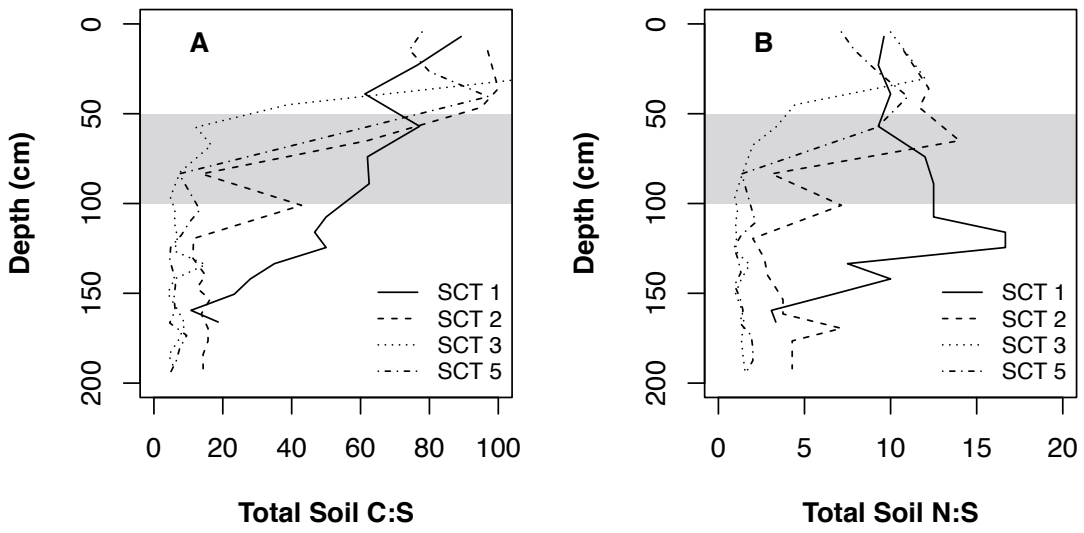

Figure 4 (a-b): Total soil C:S (a) and N:S (b) with depth on the Santa Cruz terraces. The light gray areas indicate the location of the seasonal perched water table, after White et al. (2009).

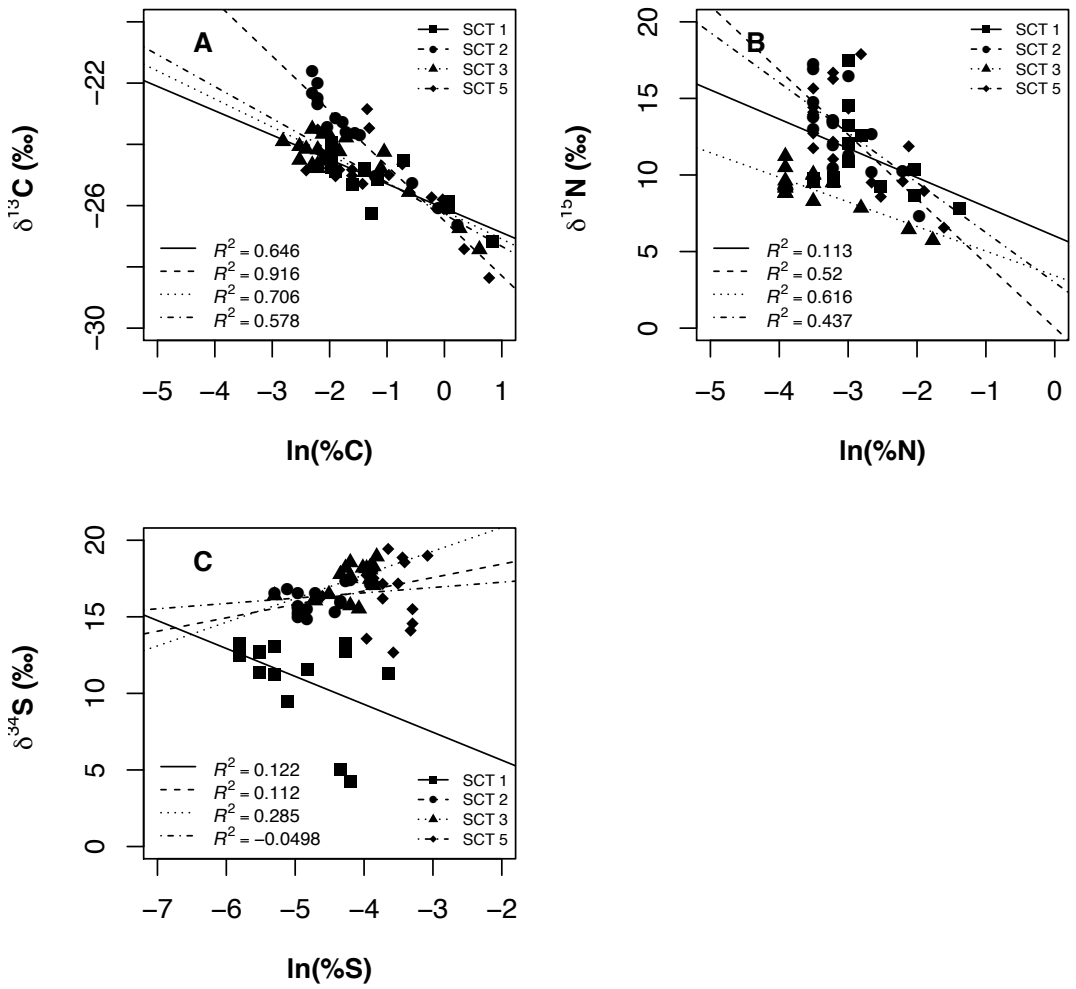

Figure 5 (a-c): Linear regression between δ values and the natural logarithm of concentration for C (a), N (b) and S (c).

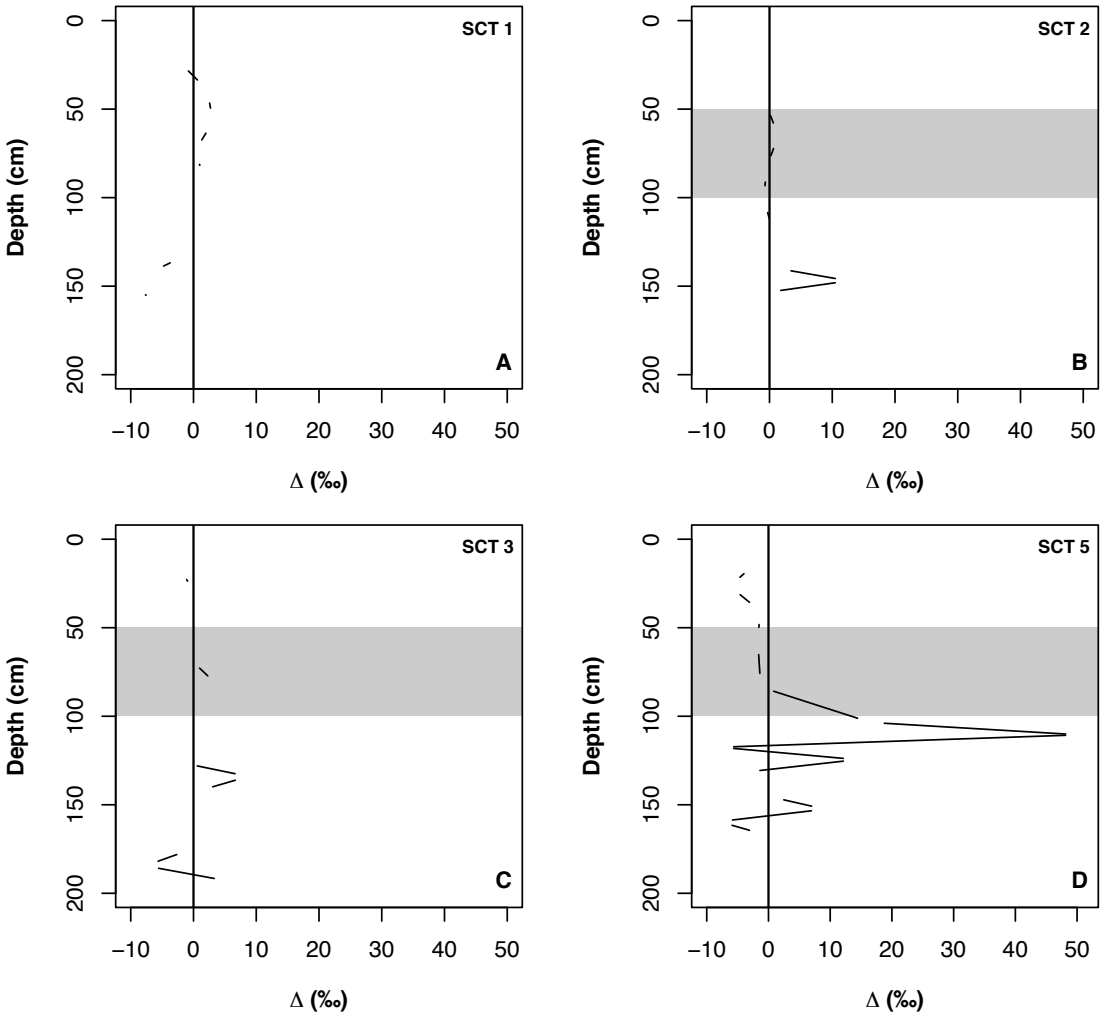

Figure 6 (a-d): Variation in the fractionation Δ for S isotopes with depth on the four terraces. Vertical lines indicate no fractionation. Negative values (to the left of the vertical lines) indicate that the products are depleted in ^{34}S compared to the substrate; conversely, positive values (to the right of the vertical lines) indicate that the products are enriched in ^{34}S compared to the substrate. The light gray areas indicate the location of the seasonal perched water table, after White et al. (2009). No seasonal perched water table has been observed on SCT 1.

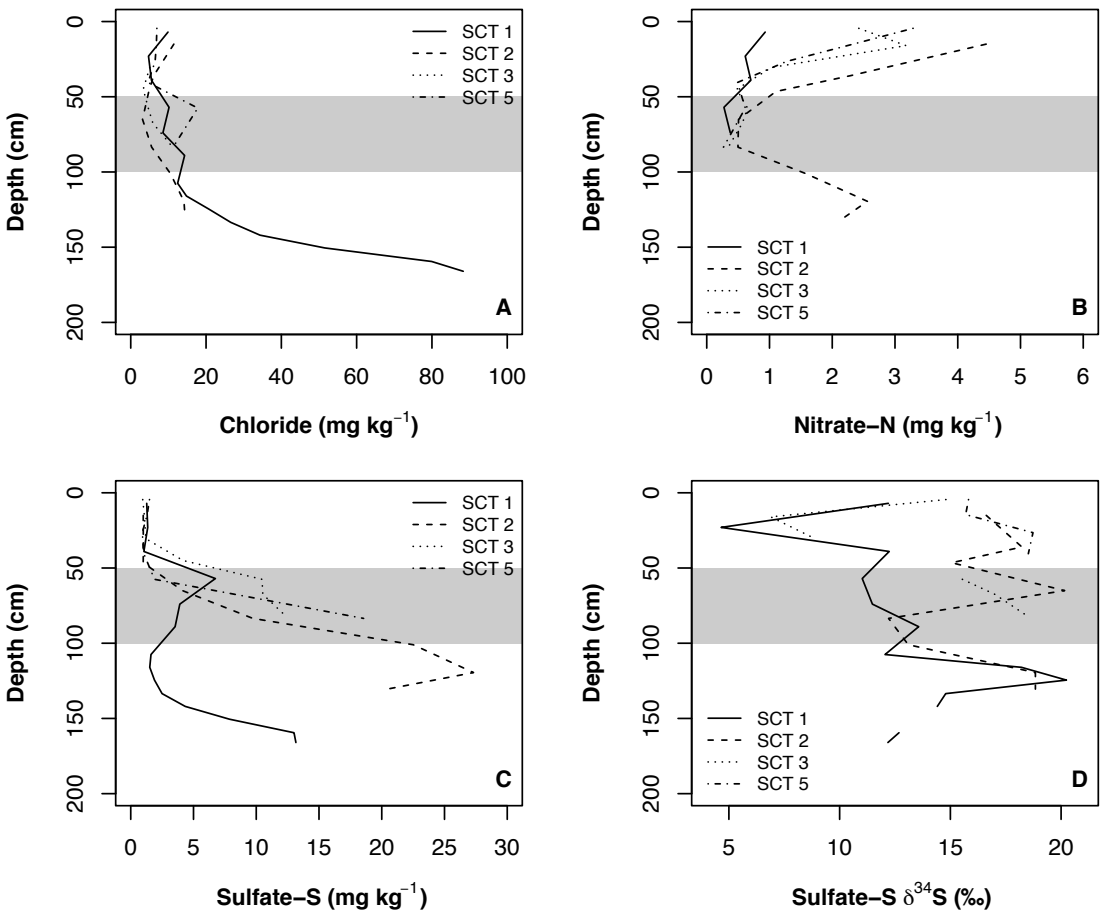

Figure 7 (a-d): Soil extractable anion chemistry versus depth on the Santa Cruz terraces: chloride (a), nitrate (b), sulfate (c) and sulfate S isotopes (d). The light gray areas indicate the location of the seasonal perched water table, after White et al. (2009).

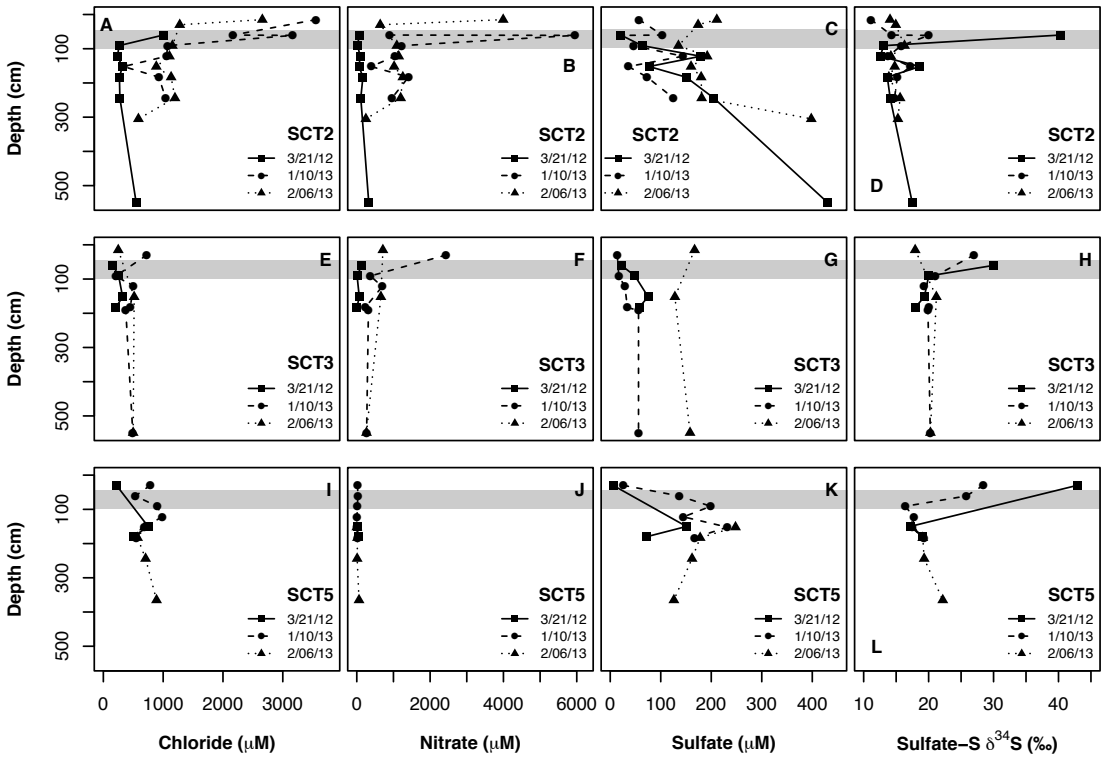

Figure 8 (a-l): Pore water chemistry versus soil depth on the three terraces at three different sampling times: chloride (a, e, i), nitrate (b, f, j), sulfate (c, g, k) and sulfate S isotopes (d, h, l). The light gray areas indicate the location of the seasonal perched water table, after White et al. (2009).

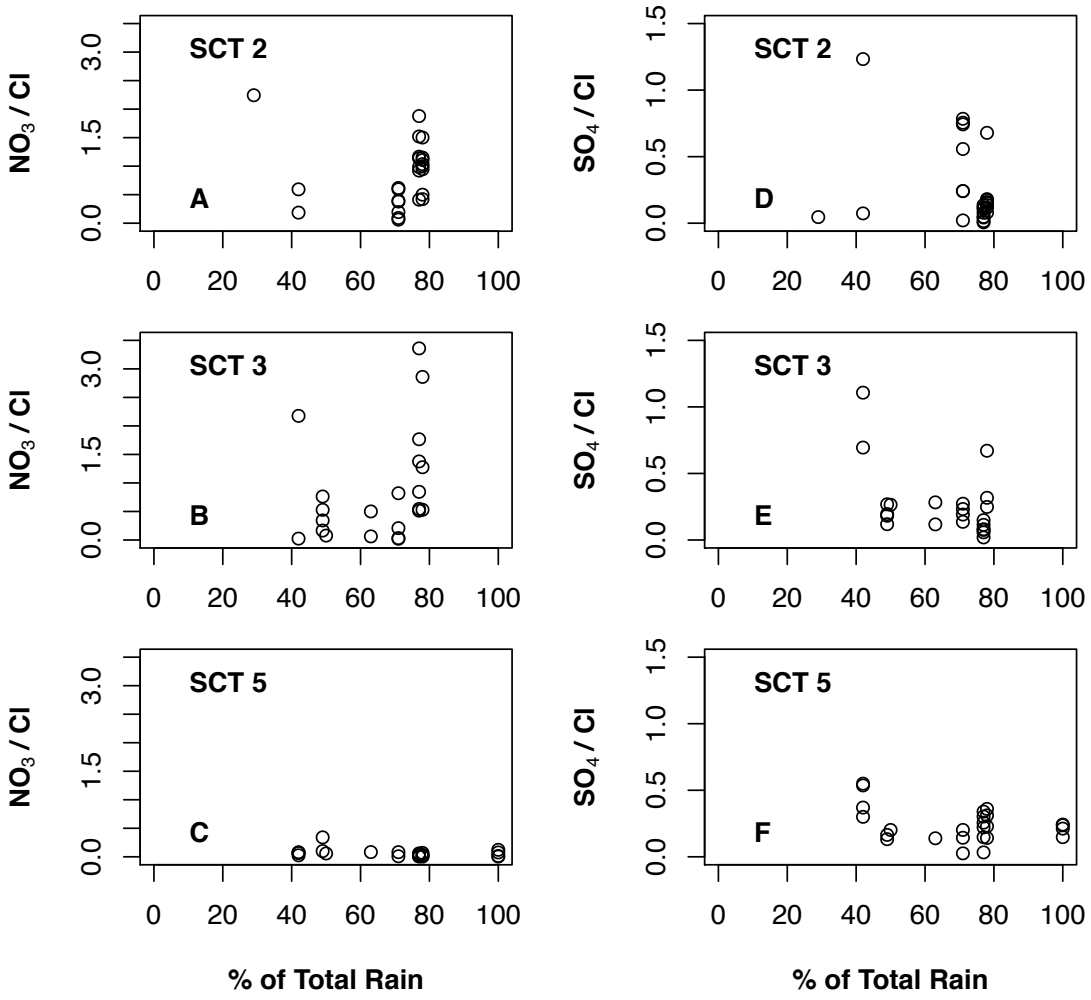

Figure 9: Ratios of nitrate and sulfate to chloride in pore water samples versus the % of total rain fallen during that rain season. % of total rain indicates the amount of rain that has occurred up to that sampling date since the beginning of the rain season, relative to the total amount of rainfall during that entire rain season. Rain season was considered October through May. Rainfall data from www.wunderground.com.

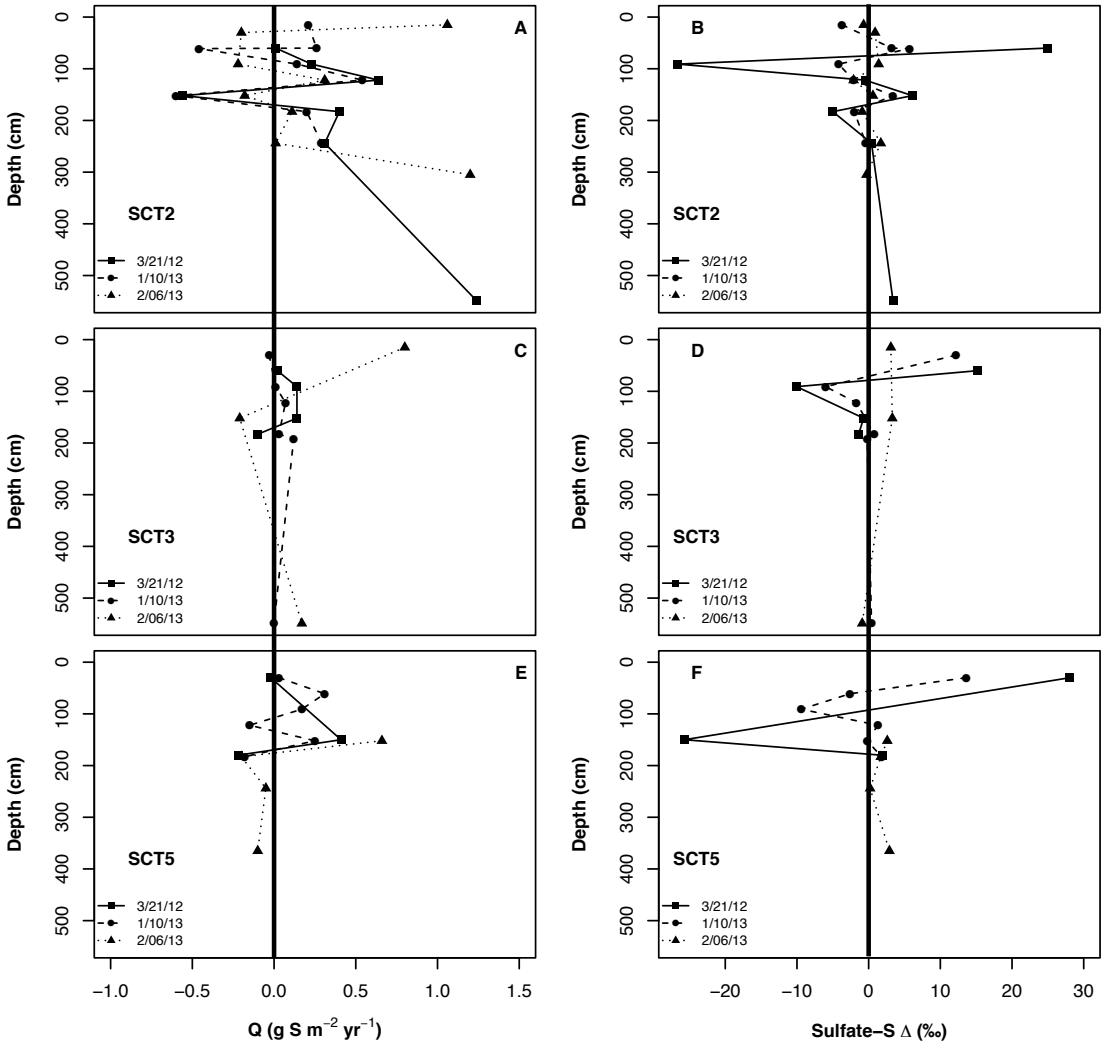

Figure 10 (a-f): The flux of pore water sulfate concentration and the change in sulfate S isotopes (Δ values) with soil depth.

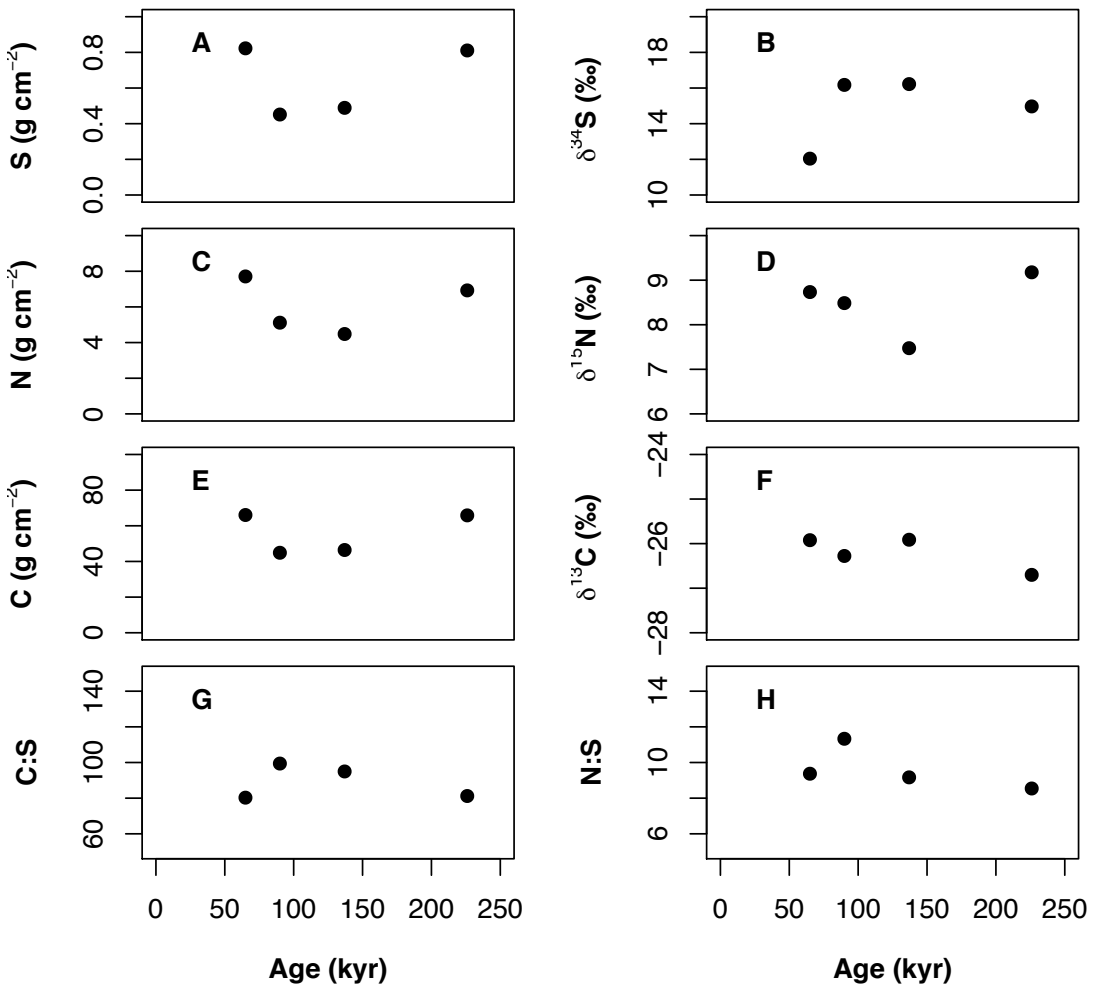

Figure 11 (a-h): Total soil S (a), N (c) and C (e) content, stable isotopes (b, d, and f), and C:S (g) and N:S (h) ratios in top 50 cm versus landscape age on the Santa Cruz terraces.

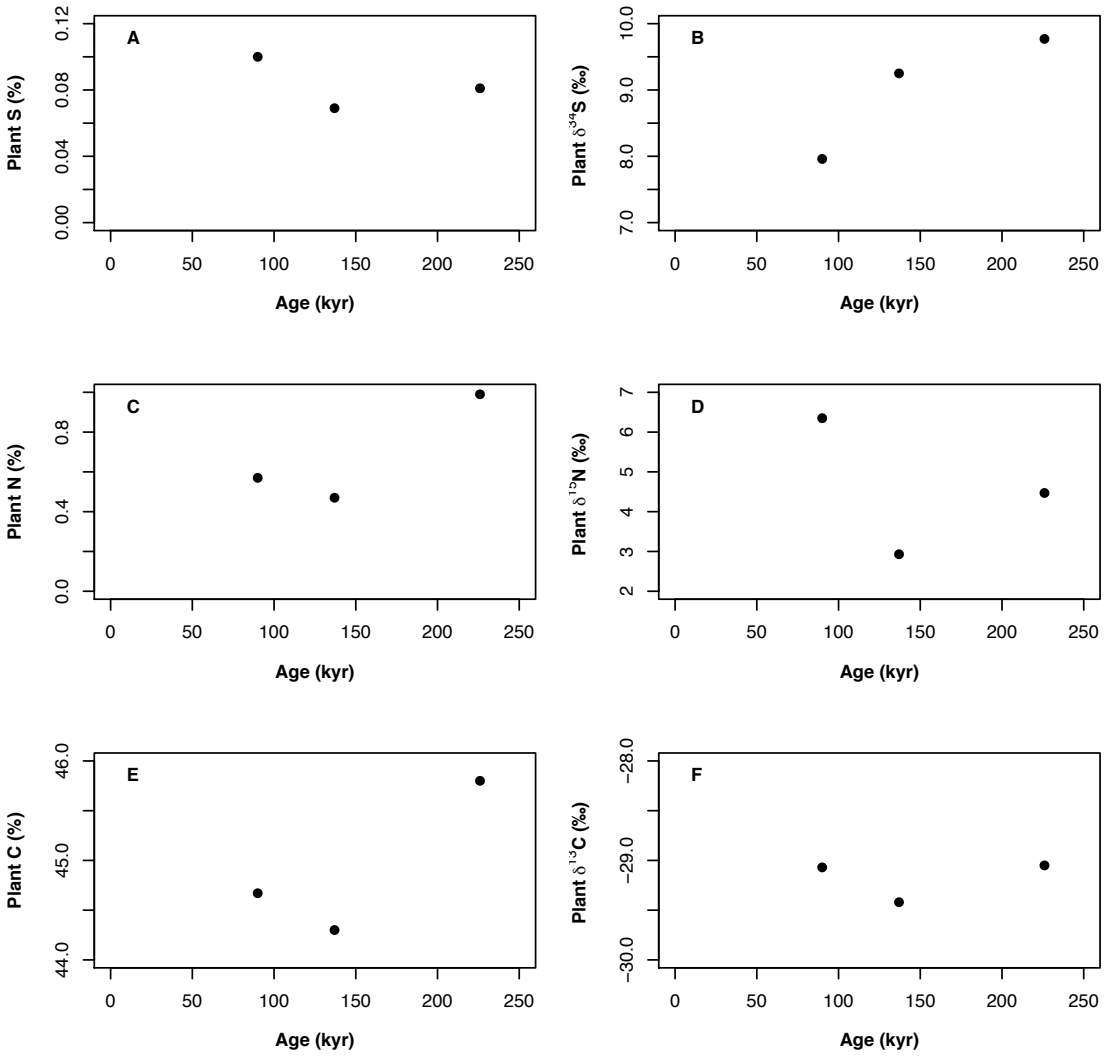

Figure 12 (a-f): Total S (a), N (c) and C (e) content and stable isotopes (b, d, and f) of vegetation versus landscape age on the Santa Cruz terraces.

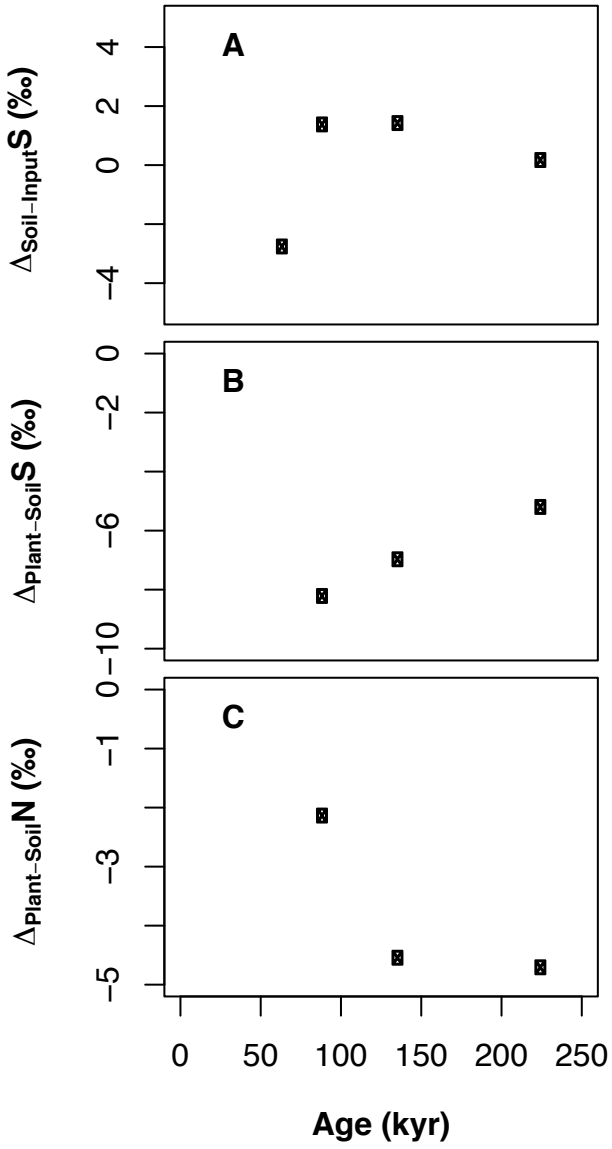

Figure 13 (a-c): The difference between S isotopes in soils and inputs (a) and S (b) and N (c) isotopes in vegetation and soils versus landscape age on the Santa Cruz terraces.

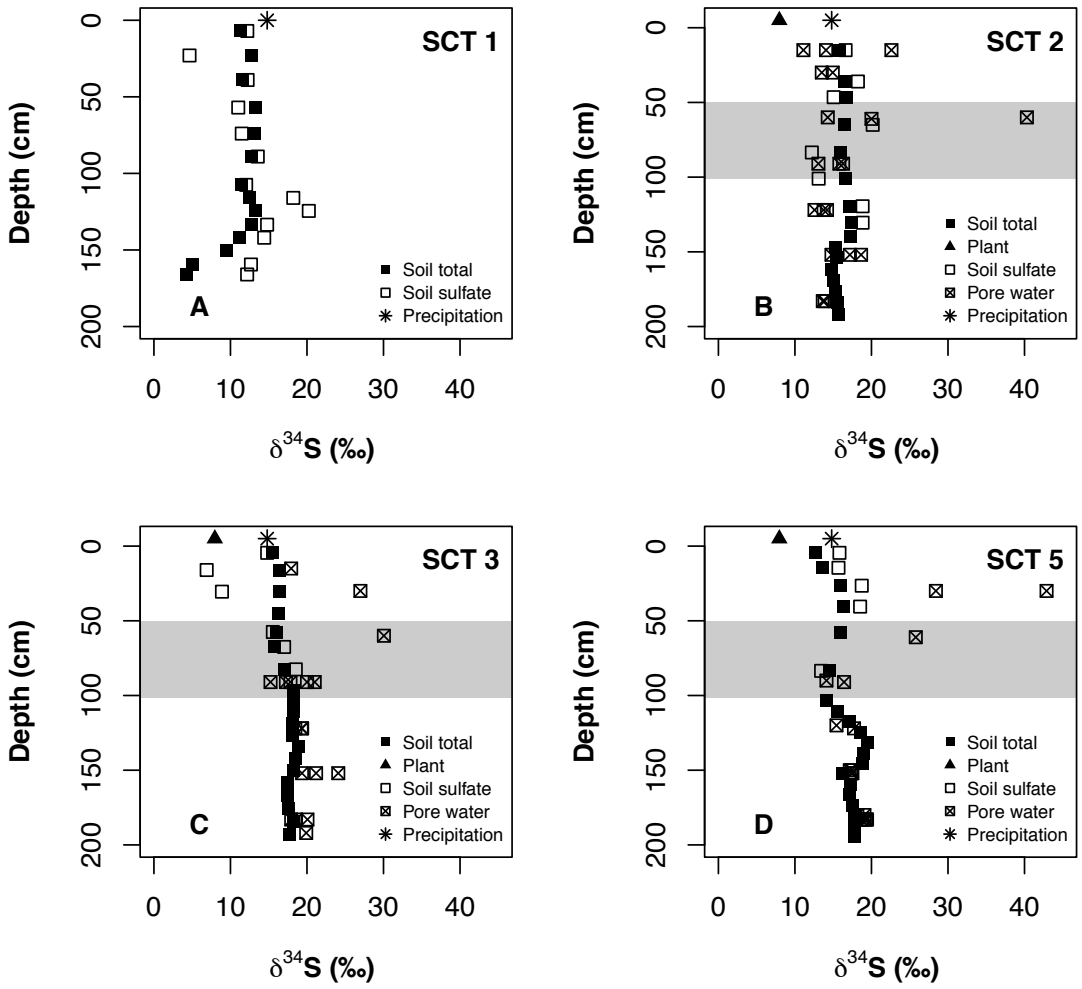

Figure 14 (a-d): $\delta^{34}S$ values in total soil and plant tissue, and in soil extracts, pore water and precipitation sulfate. The light gray areas indicate the location of the seasonal perched water table, after White et al. (2009). No seasonal perched water table has been observed on SCT 1.

Chapter 5

Conclusions

The goal of this thesis was to identify the main factors that control the terrestrial sulfur (S) cycle in pristine environments, and to compare the effects of these factors on S cycling to those on nitrogen (N) cycling. To this end, I measured S, N and carbon (C) concentration and stable isotope ratios in archived and newly collected soil and vegetation samples from 11 locations, as well as major anion concentration and sulfate $\delta^{34}S$ values in pore water and precipitation samples where available.

An unexpected finding of this research was that the cycling of N and S were decoupled to some extent. Average soil $\delta^{34}S$ and $\delta^{15}N$ values followed opposing trends with climate. Additionally, the trends in N (and C) concentration and stable isotope ratios with soil depth, in both a wet tropical forest and in a seasonal grassland with Mediterranean climate, could be explained by successive cycles of mineralization coupled with downward advective movement of organic matter. Unlike N and C, S concentration did not decrease with soil depth, and S isotopes indicated that other processes besides mineralization and advective transport controlled S cycling in these soils. This is surprising because N should be reduced before S during anoxic conditions. The apparent greater sensitivity of S to redox conditions suggested by these data may be because N is in greater biological demand in these ecosystems, which may lead to reduced fractionation for N compared to S isotopes during biotic processes. Additionally, the ability of S to undergo successive reduction-reoxidation steps can enhance the isotopic signal. Alternatively, denitrification could be inhibited if sulfides are present in these soils, though studies still need to determine whether they are indeed present.

My results showed that, out of all soil-forming factors, climate, and especially mean annual precipitation (MAP), elicits the greatest control on soil S. Globally, total soil S content generally increased with MAP, while soil and plant $\delta^{34}S$ values increased with both MAP and mean annual temperature (MAT). The difference between the $\delta^{34}S$ values of soils and atmospheric inputs also increased significantly, but weakly, with MAP, suggesting greater biological S isotope fractionation in wetter climates. The importance of rainfall was also evident at the two main sites of this study, Puerto Rico and Santa Cruz, where rainfall amount mediated the occurrence of dissimilatory bacterial sulfate reduction (DBSR). On average, plants were depleted in the heavy S isotope compared to soils, indicating fractionation during uptake, however the magnitude of this fractionation seemed to be controlled more by climatic conditions than by vegetation type. Topography only impacted S isotopes in low-lying topographic positions, close to streambeds, where waterlogging, and thus DBSR, was more common. Soil S, N and C content generally decreased downslope from ridgetops to riparian regions. Parent material did not seem to have a significant impact on soil S. Landscape age influenced S cycling primarily by changing soil hydrology. Additionally, input chemistry, which correlated with distance from coast, led to overall higher ecosystem $\delta^{34}S$ values near the coast compared to inland.

The dependence of S cycling in most ecosystems on climate and on the steady

supply of atmospheric S implies that S is particularly vulnerable to climate change, and especially to changes in rainfall patterns. A significant decrease in rain may result in lower soil S content and in reduced biological cycling and fractionation of soil S. Disturbances in vegetation cover may also accelerate S losses and decrease the soil organic S pool. The maps produced in Chapter 2 illustrate soil and plant $\delta^{34}S$ values for steady state soils, in the absence of anthropogenic disturbance. Available data however show that many of these regions deviate from the steady-state scenario due to anthropogenic influences.

Given the rate of global change and the extent of anthropogenic impact on soils, it is essential that research continues to explore the response of the terrestrial S cycle to environmental variables. New opportunities to further tease apart the controls on the S cycle enabled by this research include: (1) performing long-term measurements of S isotopes in inputs, soils and gaseous losses from soils in a variety of climates to better characterize the integrated isotope fractionation during ecosystem S loss, and its variation with climate; (2) measuring integrative litter inputs as opposed to folial $\delta^{34}S$ values in various regions to better constrain fractionation during plant S uptake, and its relationship to climate; (3) including distance to coast and to pollution centers in addition to climate in models of ecosystem $\delta^{34}S$ values; (4) studying S cycling on longer chronosequences, to determine if there is a significant impact of phosphorus availability; (5) adding more data points to this dataset to expand the global perspective; and (6) replicating these studies of S cycling in disturbed watersheds, to better understand the impact of land cover change on soil biogeochemical cycles. Such studies will continue to improve our understanding of the ecosystem S response to global change.